EVALUATION OF EXISTING AND NEW TEST CONFIGURATIONS FOR HEADED SHEAR STUDS

Omkar Ashok Tawade

Thesis submitted to the faculty of Virginia Polytechnic Institute and State University in partial fulfillment of the requirements for the degree of

Masters of Science
In
Civil Engineering

Matthew R. Eatherton, Chair
W. Samuel Easterling, Co-Chair
Carin L. Roberts-Wollmann

14th July 2023
Blacksburg, Virginia

Keywords: Headed shear stud, Composite beam, Push-out test, Shear Test, Single-sided Push-out Test

EVALUATION OF EXISTING AND NEW TEST CONFIGURATIONS FOR HEADED SHEAR STUDS

Omkar Ashok Tawade

Abstract

Composite beams are frequently used in building, combining a steel beam with either a concrete-filled steel deck or solid concrete slab. To ensure proper composite action, shear connectors, typically in the form of headed shear studs, are utilized. Traditionally, the strength assessment of these headed shear studs is made using empirical design specifications that are based on push-out tests, which have been widely conducted and standardized over the years. However, the standardized push-out tests have short-comings, such as uneven slab bearing, slab buckling, questions regarding the distribution of load to each stud, etc.

A study was conducted to evaluate and compare the existing push-out test setup with two alternative test setups. The study also aimed to examine the behavior of headed shear studs in composite beams having deck deeper the current allowable limit of 3 in., as specified by American Institute of Steel Construction (AISC) design specification. While the standard specification allows for steel decks with rib heights of up to 3 in., there are deck profiles deeper than 3 in. available in the market. Utilizing these deeper decks in composite beams offers several advantages, including faster and more cost-effective construction by reducing the number of beams required.

This research therefore found that a major challenge in creating an alternative test setup involves eliminating moment at the interface between the concrete-filled steel deck and the steel beam. This moment leads to tension in the headed shear stud/stud group closest to the actuator, thus affecting the shear strength of the headed shear studs. Further, these headed shear studs have significant strength when used with 3.5 in. decks but further research is necessary.

EVALUATION OF EXISTING AND NEW TEST CONFIGURATIONS FOR HEADED SHEAR STUDS

Omkar Ashok Tawade

General Audience Abstract

Composite beams are widely used in building construction, combining a steel beam with either a concrete-filled steel deck or a solid concrete slab. To ensure their proper function, shear connectors are used, typically in the form of headed shear studs. Traditionally, the strength of these shear studs is determined using standardized push-out tests, but these tests some challenges like uneven slab bearing, questions about even load distribution, etc.

In this study, the existing push-out test setup was evaluated and compared with two alternative setups. The behavior of headed shear studs in composite beams with deeper decks than the current allowable limit specified by design standards was also investigated. Using these deeper decks offers advantages such as faster and more cost-effective construction.

One major challenge in creating an alternative test setup was eliminating the moment at the interface between the concrete-filled steel deck and the steel beam. This moment caused tension in the headed shear stud closest to the actuator, impacting the overall shear strength of the studs. Additionally, it was found that these shear studs show promising strength when used with 3.5 in. decks, but more research is needed to fully understand their capabilities.

By exploring new test setups and considering deeper decks, this research contributes to improving the design and construction of composite beams, making them more efficient and reliable for future building projects.

Acknowledgments

I would like to extend my sincere gratitude to Dr. Matthew Eatherton for giving me the opportunity to work on this project and for his guidance throughout. I am also thankful to Dr. W. Samuel Easterling for his expertise and valuable advice. It has been a privilege to work with and learn from both of them. I am grateful to Dr. Carin Roberts-Wollmann for serving on my graduate committee. I would like to acknowledge the generous support of the American Institute of Steel Construction, the Steel Deck Institute, Canam Steel Corporation, Epic Metals, New Millennium, and Verco Decking, Inc. Their support has been instrumental in the success of this project. In-kind support was also provided by Epic Metals, New Millennium, and Infra metals. I would like to express my appreciation to the Steel Diaphragm Research Initiative coordinated by the Cold-Formed Steel Research Consortium. I am grateful to Dr. Benjamin Schafer and Dr. Jerome Hajjar for their valuable input before and during the research. I would like to acknowledge the assistance of Dr. David Mokarem, Garret Blankenship, and Brett Farmer in the Structures Laboratory. Their contributions have been invaluable. Finally, I want to express my heartfelt gratitude to my family and friends for their unwavering support and love throughout this journey. I sincerely appreciate the significant contributions of all the organizations and individuals involved in this project. Their collective efforts have advanced the knowledge and understanding of composite beams in construction.

Table of Content

List of Figures

List of Tables

1. Introduction

1.1 Composite Beams

A composite beam is a structural element typically consisting of a concrete slab attached to a steel beam. The composite beam thus can take advantage of the compressive strength of concrete and the tensile strength of steel. Composite beams possess high strength and ductility, and are economical to assemble and construct. A composite beam (Figure 1.1 and Figure 1.2) consists of a solid concrete slab or a concrete-filled steel deck over a wide flange steel beam with shear connectors to transfer loads between the two, so that they act together as a unified section. Perhaps, the most important elements of composite beams are the shear connectors. Shear connectors should have sufficient strength and ductility for composite action to take place. Headed shear studs are typical shear connectors used in these composite beams. The classification of composite beams as partially-composite or fully-composite depends on whether the shear connectors are designed to provide partial or full composite action, respectively, between the steel beam and the concrete slab.

Some of the advantages of composite beams are as follows:

1. Effective utilization of material properties with concrete in compression and steel in tension.
2. Stiffer elements causing less deflection.
3. More economical design by using shallower steel beam sections than non-composite beams.

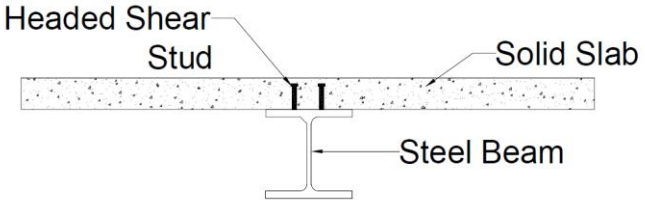

Fig. 1.1 Solid Slab Composite Beam

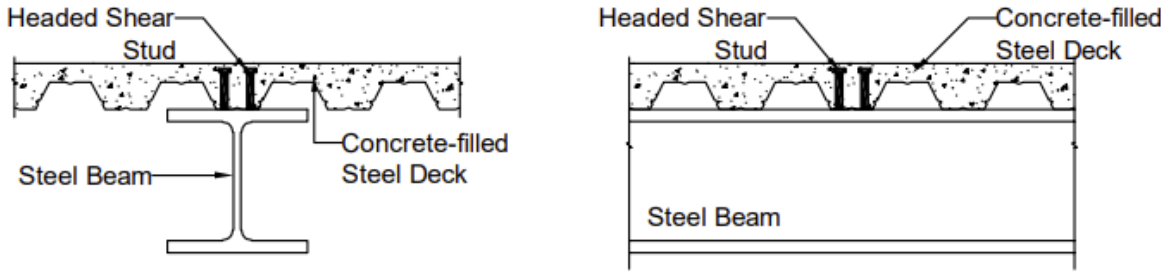

a) Deck Parallel b) Deck Perpendicular

Fig. 1.2 Concrete-Filled Steel Deck Composite Beam

Trapezoidal or dovetail deck profiles are typically used in steel buildings for composite beams as seen in Figure 1.3. Dovetail decks are advantageous as they allow hanging fixtures, pipes, and ceilings from their ribs and also are also considered aesthetically pleasing by some architects. A key advantage of trapezoidal decks are that they can be stacked or nested into one another and so are efficient to transport or store. Trapezoidal profiles of a given depth also use less material (steel coil width) than comparable dovetail profiles.

Trapezoidal deck Dovetail deck

Fig. 1.3 Typical Deck Profiles

1.2 Motivation for Research

The conventional push-out test, conducted using AISI S923-20 (2020), has some challenges. The push-out test specimen consists of two halves using composite slabs attached with headed shear studs to structural tees bolted together and placed in a vertically as seen in Figure 1.4(a). While testing, the headed shear studs in one of the slabs often fails first and so the results are biased towards the weaker slab. The test also suggests application of a normal load: a

perpendicular load less than or equal to 10 % of the applied axial load to discourage unrealistic failure modes where the slab separates from the beam. Unusual failure mode are observed these tets like slab cracking, which give unreliable headed shear stud strength. Achieving uniform bearing between the slabs and the floor is also challenging. Uneven bearing leads to uneven stress distribution at the interface, which results in rotational movements of the slabs as they strive to achieve even bearing. Also, after failure is observed in these tests, it is difficult to record slip between concrete and steel. To overcome all these challenges different test setups were evaluated. To reduce the bias toward weaker studs, eliminate rotation of the slab due to non-uniform bearing, and improve post-peak slip measurements, it is better to test only one slab at a time such as shown in the shear test setup of Figure 1.4(b). Evaluation of the shear test led to a modification which resulted in a single-sided push-out test (Figure 1.4(c)). This configuration was designed to have boundary conditions similar to the conventional push-out test. This single-sided push-out test will offer the same advantages as shear test over the conventional push-out test. A more detailed description of all the three test setups will be give latter in this document.

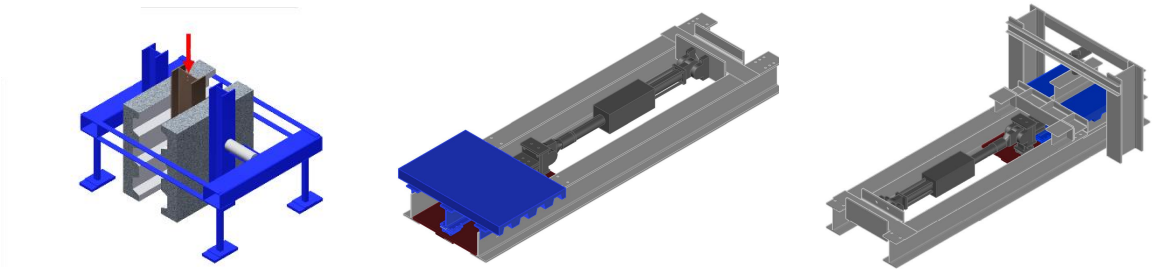

a) Push-out Test Setup b) Shear Test Setup c) Single-Sided Push-Out Test

Fig 1.4 Different test setup for headed shear studs

In addition to investigating alternative test configurations for headed shear studs, this study is also concerned with the behavior of headed shear studs with deeper steel decks. The AISC specification section I2c (AISC 2022) allows steel decks with rib heights up to 3 in. for these composite beams. This is because past tests were almost exclusively conducted using a maximum

of 3 in. deck for composite beam A review of past tests is provided in Chapter 2. Using deeper decks with composite beams has advantages and deeper decks such as 3.5 in. and 4 in. dovetail decks are already being produced, but aren't allowed to be used in composite beams. Utilizing deeper decks offers the advantage of achieving longer unsupported spans, resulting in reduced number of beams thereby enabling quicker construction and a cost-effective solution.

1.3 Scope

The objective of the research is to develop a test setup for headed shear studs in composite beams and to provide preliminary data about the applicability of 3.5 in. deep deck for composite beams. A total of 33 tests were conducted using three different test setups. To evaluate and understand the challenges of the conventional push-out test six tests were conducted. Further, a test setup was designed to mitigate the challenges of the conventional push-out test given in AISI S923-20. To eliminate the bias in data toward the weaker shear connectors of two slabs as tested in the conventional push-out test, eliminate rotation of the slab due to non-uniform bearing, and improve post-peak slip measurements only one slab is used in the proposed test setup. To avoid unusual limit states such as the slab cracking or rotation of the specimen the shear test had the specimen attached on the sides to the testing frame. With the shear test setup, it is also possible to record reliable post-peak behavior. The test frame was thus designed as a self-reacting frame which used an actuator to impart a shear load to the specimen. The testing procedure of the shear test setup was set to be monotonic and displacement controlled to understand the strength as well as the ductility of the headed shear studs. The test setup was assessed by conducting a total of 24 tests. Out of these, six tests were conducted in conjunction with the conventional push-out test for comparison purposes. The evaluation of the setup was based on several factors, including its ability to generate shear force on the headed shear stud while minimizing tension force, consistent failure

modes in headed shear studs of the specimen, exclusion of undesirable failure modes, and the recording of post-peak behavior. The setup was further modified to create a single-sided push-out test. To evaluate this modified setup, three additional tests were conducted.

These tests were also utilized to conduct a preliminary examination of the behavior of headed shear studs with 3.5 in. steel deck, both trapezoidal and dovetail, for their potential application in composite beams.

1.4 Thesis Organization

Chapter 1 gives an introduction to composite beams and discusses the motivation for the research. Also, the scope of research is laid out in the chapter.

Chapter 2 consists of a literature review explaining the composite action in composite beams and describing past research related to solid slab composite beams and the derivation of empirical equations. Further describing past research related to concrete-filled steel deck composite beam with the rib height less than 3 in. and some research about deeper deck i.e., rib height greater than 3 in. This chapter also briefly summaries the full-scale composite beam tests and challenges that come along while conducting conventional push-out test.

Chapter 3 summarizes the test setups used and gives information on the procedure; instrumentations used to collect data. It also discusses the test matrix and material test conducted.

Chapter 4 discuss the stress state of concrete around the headed shear studs in the different test setup evaluated and their correlation to the stress state in composite beams

Chapter 5 provides a discussion of the results from the tests conducted.

Chapter 6 gives conclusions discovered and summaries the scope of future work.

2. Literature Review

2.1 Composite Beam Action

Composite action is when a steel beam and the concrete-filled steel deck act as a single unit together as a composite beam section. The degree of composite action depends on how much the slip at the interface is minimized.

Considering a non-composite beam and slab under vertical load and neglecting the friction between the slab and beam, each carries a part of the load separately as seen in Figure 2.1(a). When subjected to positive moment, the slab deforms generating tension on the lower surface and compression of the upper surface and similar is the case of the steel beam. This creates a discontinuity in strain at the surface of contact between the slab and steel beam. Neglecting friction, only the vertical forces act between the slab and steel beam generating a relative slip between the two. When the slab and steel beam act compositely, horizontal forces develop at the contact surface causing the lower surface of the slab to compress and the top surface of the steel beam to elongate. When there is no composite action, each element resists the moment individually and the total resisting moment can be given a $\sum M = M_{slab} + M_{beam}$. It can be seen from the strain variation (Figure 2.1 (a)) there are two neutral axes, one at the center of gravity of the slab and one at the center of gravity of the steel beam. The horizontal slip resulting from the bottom of the slab in tension and the top of the beam in compression is also indicated in Figure 2.1(a). Further, when partial composite action takes place, the neutral axes move closer to each other, and also the horizontal slip is reduced. This partial interaction results in the partial development of compressive and tensile forces C' and T' in the slab and beam respectively and thus the resisting moment of the section would be increased by T'e' or C'e'. When full composite action is developed, no horizontal slip occurs and a linear strain diagram is generated with a single neutral axis. The neutral axis lies

between the center of gravity of the slab and the center of gravity of the steel beam. The compressive and tensile forces C" and T" are therefore larger than C' and T' respectively existing in partial interaction. The resisting moment thus for fully composite beam becomes $\sum M = T$"e" or C"e".

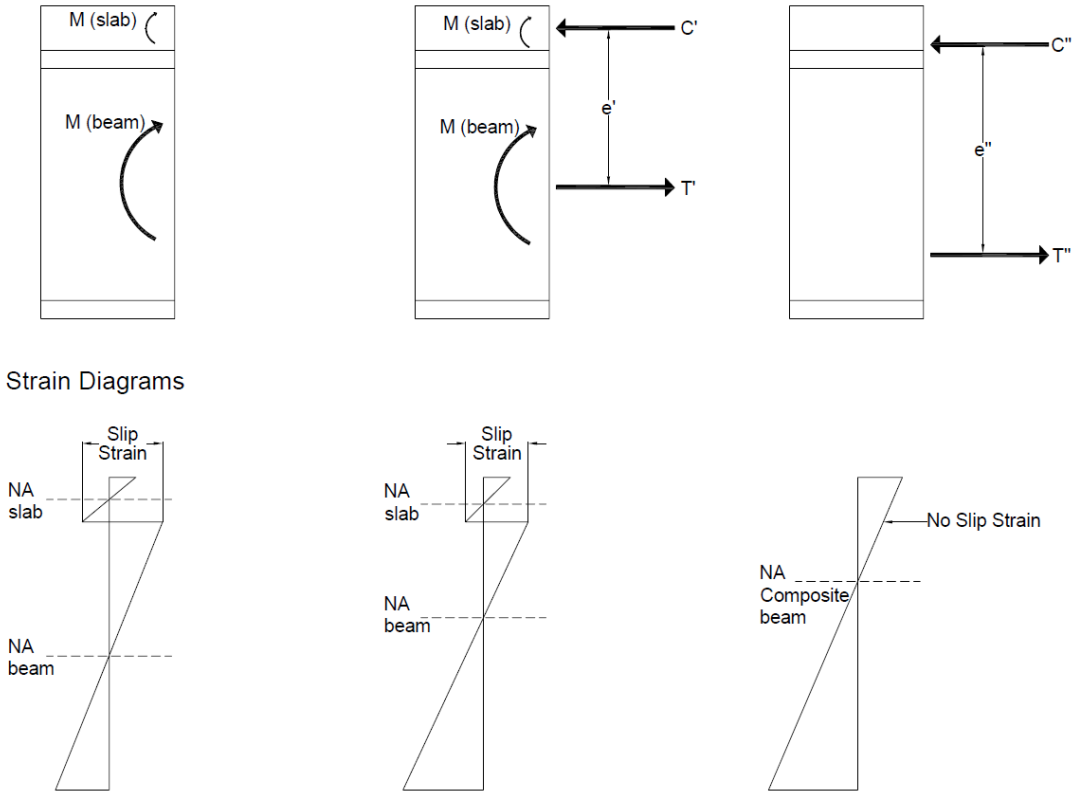

a) Non composite b) Partial composite c) Fully composite

Fig. 2.1 Strain variation in composite beams (Salmon & Johnson, 1996)

2.2 Shear Connectors

The horizontal shear developed between the concrete slab and the steel beam must be resisted for composite action. Mechanical shear connectors are therefore required to create substantive composite action. Headed shear headed shear studs and channel connectors are included in the AISC specification, but the most commonly used are the headed shear studs. For full composite action, the shear connectors must be stiff and this would require the connectors to be rigid. Also, considering a simply supported beam with a uniformly distributed load (Figure 2.2).

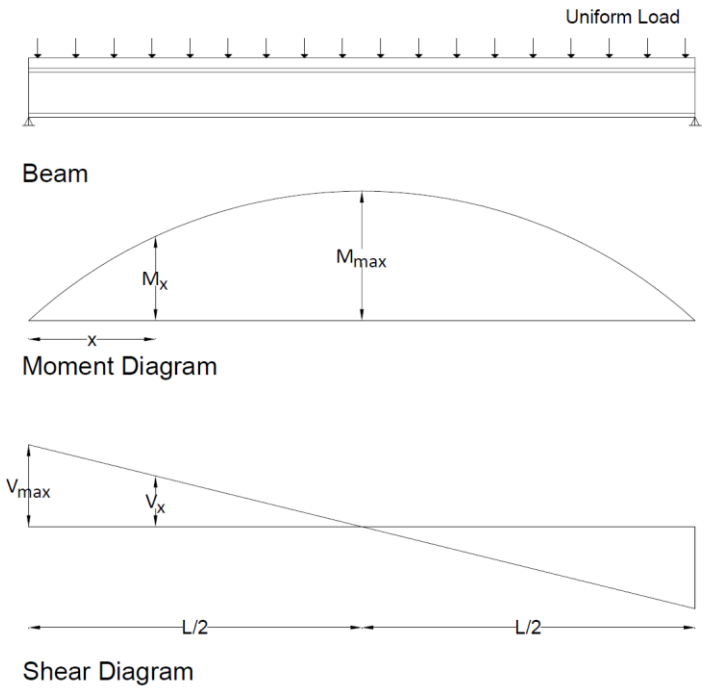

Fig. 2.2 Simply supported beam under uniform loading

Under elastic conditions the shear force at any point will vary from maximum at the supports to zero at midspan. So, it would require more shear connectors where the shear is high and fewer connectors where shear is low. This would lead to non-uniform distribution of headed shear studs which is not necessary as the ductility in stud connectors allow the load to spread evenly among all the headed shear studs. Thus, the connectors are required to transfer the maximum compressive force developed in the slab between the region of the zero moment and maximum moment. The nominal shear demand need not exceed the maximum compressive force the concrete can develop which is given by,

$$C = 0.85 f_c' b_{eff} d_c \tag{2.1}$$

Where:

f'_c = compressive strength of concrete

b_{eff} = effective slab width

d_c = depth of concrete in a concrete filled steel deck

or the maximum tensile force in the steel beam given by,

$$T = A_s F_y \tag{2.2}$$

Where:

A_s = cross − sectional area of the steel beam

F_y = yield strength of the steel beam

The nominal shear strength can be given by,

$$\sum Q_n = n\, Q_n \tag{2.3}$$

Where:

Q_n = strength of one stud

n = number of studs required between the point of maximum moment and zero moment

Thus, for full composite action

$$\sum Q_n = min\{C, T\} \tag{2.4}$$

When, $\sum Q_n < min\{C, T\}$ partial composite action takes place and the degree of composite action is defined as $\frac{\sum Q_n}{min\{C,T\}}$, this term is also sometimes defined as partial shear connection. The determination of this shear connector capacity is complex as the connectors deform under load and the surrounding concrete also crushes. The amount of deformation of a shear connector depends on many factors like its own shape and size, its location along the beam and the way the steel deck is been placed, etc. As a result, a number of research programs were undertaken to develop the strength of different types of shear connectors. The further literature review gives a brief about different research programs undertaken about headed shear studs as it is one of the widely used shear connectors in the industry.

2.3 Push-out Test for Headed Shear Connectors

The earliest form of composite beam included a solid slab over a steel beam with spiral or channel shear connectors for composite action before headed shear studs were used. The headed shear stud's popularity stems from the fact that it can be installed using a welding gun. The shear capacity of these headed shear studs in solid slabs was first evaluated by Viest (1956). Push-out tests were conducted for channel connectors and they gave good results in agreement with the beams test and so were used for headed shear studs as well. Viest (1956) conducted 12 Push-out tests each consisting of two solid slabs attached on either side of a wide flange steel beam with each test consists of four or eight headed shear studs. All headed shear studs were approximately 4 in. long after welding and the stud diameter varied from 0.50 to 1.25 in. The center-to-center stud spacing was either 2 in. or 4 in. All other parameters were held constant. Flanges were greased before the slabs were cast to prevent bond and to reduce the effect of friction during testing. A sharp drop in load vs residual slip curves was observed for small diameter headed shear studs. Load corresponding to the transition from small to large residual slip was determined by extrapolation and Viest (1956) considers the load as the "critical load, Q_{cr}". Viest (1956) defines residual slip as the slip recorded between the concrete slab and the wide flange section after removal for load in each load step. Slip can be defined as the amount of displacement of the concrete slab with respect to the steel section when shear load is applied. For large diameter headed shear studs, this procedure was difficult to follow as a sharp transition was not observed so the load corresponding to 0.003 in. residual slip was considered the "critical load, Q_{cr}".

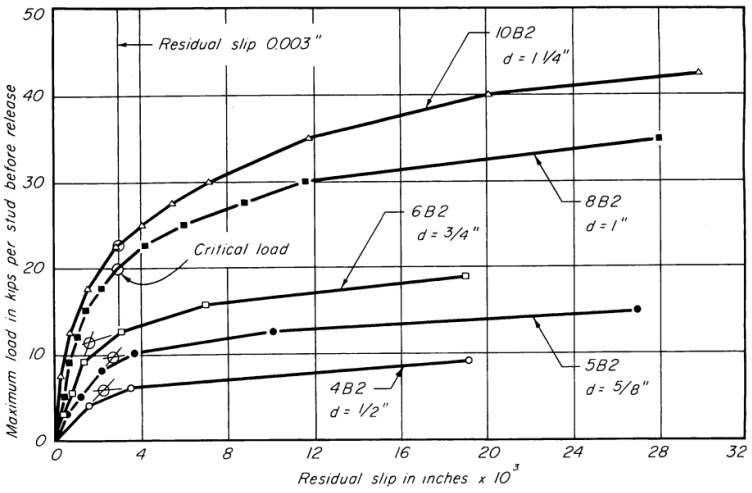

Fig. 2.3 Determination of Critical load by Viest (1956)

Tests also revealed that the load capacity of the headed shear studs was proportional to the square of the stud diameter for small diameters and linear increase in strength for large diameter headed shear studs. He saw no significant effect of stud spacing and a linear relationship between concrete compressive strength and stud capacity. The following equation for the critical load was proposed.

$$\text{for, d} < 1 \text{ in. } Q_{cr} = 5.25d^2 f_c' \sqrt{\frac{4000}{f_c'}} \tag{2.5}$$

$$\text{for, 1 in.} \leq \text{d} \leq 1\,{}^{1}\!/_{4} \text{ in } Q_{cr} = 5d f_c' \sqrt{\frac{4000}{f_c'}} \tag{2.6}$$

Where, $\text{d} = \text{stud diameter, in.}$

$f_c' = \text{concrete strength, psi}$

Further limitations were placed on the use of the above equation as follows,

The yield point of headed shear studs should at least be 50000 psi.

A lower limit of f_c' = 2500 psi and upper limit of f_c' = 5000 psi was suggested. For concrete with f_c' > 5000 psi yield safe value of f_c' = 5000 psi must be substituted.

All headed shear studs must be 4 in. or higher.

Viest (1956) also observed that the envelope of load vs slip curve for loading and unloading specimens were in good agreement with simple monotonic loading until failure specimens

Chin (1965) carried out solid slab push-out experiments in the same manner as Viest (1956), but with lightweight concrete with 1/2, 5/8, 3/4, and 7/8 in. diameter headed shear studs at lengths nearly four times the diameter. Similar to Viest (1956) he also observed that cyclic loading did not affect the load vs slip envelope and determined "useful load, Q_{uc}" the same way Viest determined "critical load, Q_{cr}". The failure was due to one or two headed shear studs shearing off in all specimens except the 7/8 in. diameter headed shear studs which failed by slab cracking and from failure it was evident that considerable plastic action occurred in headed shear studs. Further, it was observed that the square root variation with concrete strength given by Viest (1956) had good relation with the results and gave the following equation.

$$Q_{uc} = 6.5d^2 f_c' \sqrt{\frac{4000}{f_c'}} \tag{2.7}$$

where, $\mathrm{Q_{uc}} = \text{useful load, lb}$

$\mathrm{d} = \text{stud diameter, in.}$

$f_c' = \text{concrete strength, psi}$

However, it was observed that the ultimate headed shear stud capacity had no effect of the concrete strength and gave the following equation.

$$Q_u = 39.22d^{1.766} \tag{2.8}$$

where, $\mathrm{Q_u} = \text{ultimate stud capacity, lb}$

$\mathrm{d} = \text{stud diameter, in.}$

Lastly, Chin (1965) performed two beam tests and observed that the calculated ultimate loads for both beams using results of the push-out tests were close to the experimental values.

Davis (1967) conducted 20 half-scale solid slab push-out tests to understand the variation in stud configurations on the strength of headed shear connectors. All specimens used 3/8 in. diameter headed shear studs 2 in. long. He discovered that in a recommended specimen provided by the British code of practice CP 117: Part I:1965 (two headed shear studs set perpendicular to the direction of force) give 25% higher ultimate strength value than when the two headed shear studs are oriented parallel to the direction of loading. In addition, Davis (1967) discovered a linear relationship between longitudinal stud spacing and stud capacity, which Viest (1956) did not. Finally, he believes that ultimate strength improves with stud spacing at a faster rate for three headed shear studs per flange than for two headed shear studs per flange, with two headed shear studs orientated perpendicular to the applied force appearing to be the ideal arrangement.

Ollgaard et al. (1971) evaluated shear stud capacity by testing 48 small-scale push-out tests. These tests considered stud diameter (5/8 and 3/4 in.), number of headed shear studs per slab, type of concrete (normal weight and lightweight), and concrete properties (concrete strength, density, modulus of elasticity and split tensile strength). Two distinct failure mode i.e., Stud shearing and concrete crushing in the region of shear connectors were observed. It was also observed that the connector strength decreased (from 15 to 25%) when lightweight concrete was used. The cracks in the slabs were more numerous and larger in lightweight concrete than in normal weight concrete specimens. When compared the test results with Equation 2.9 given by Slutter and Driscoll (1965) which they modified from Viest (1965) it was observed that it did not account for the difference between normal and lightweight concretes so further performed regression analyses using logarithmic transformations.

$$Q_u = 37.45 A_s \sqrt{f'_c} \tag{2.9}$$

Where:

Q_u = ultimate stud capacity, kips

A_s = nominal area of the headed shear stud, in^2

f'_c = concrete compressive strength, ksi

The results also showed that the stud strength was primarily influenced by compressive strength and modulus of elasticity of concrete and cross-sectional area of headed shear studs played an important factor. Based on the following he gave an empirical equation (Equation 2.10) to determine the shear stud capacity in solid slab composite beams as

$$Q_u = 0.5 A_s \sqrt{f'_c E_c} \tag{2.10}$$

Where:

f'_c = concrete compressive strength, ksi

E_c = modulus of elasticity of concrete , ksi

A_s = nominal area of the headed shear stud, in^2

Further, it was observed unloading of the specimens did not affect the envelope of the curves, and the reloading was reasonably linear until the maximum load prior to unloading was reached which was also seen by Viest (1956) and Chin (1965). An empirical formula for the load-slip relationship of continuously loaded specimens was therefore given as follows,

$$Q = Q_u(1 - e^{-18\Delta})^{2/5} \tag{2.11}$$

Where:

Q = Load, kip

Δ = slip, in.

Hawkins and Mitchell (1984) conducted a total of 23 push-out test: 13 push-out specimens were tested monotonically, and 10 specimens were tested under reversed cyclic loading. The influence of the following variables: type of loading, presence of metal deck, deck geometry, and

deck orientation were tested with 10 solid slab specimens and 13 concrete filled metal deck (1½ in. or 3 in.). Each specimen had two ¾ in. diameter headed shear studs in each slab. Four distinct failure modes: stud shearing, concrete withdrawal, rib shearing, and rib punching were observed. Large elastic deformations and slips were observed in the specimens that failed in stud shearing. Such connections had a reversed cyclic shear strength that was roughly 17% lower than their monotonic strength. They also concluded that the empirical equation predicted by Ollgaard et al. (1971) very well predict the stud capacity for specimens with stud shear failure. The specimens that showed concrete pullout failure were very brittle. When compared to the responses of stud shearing failure specimens, there was a considerable drop in strength and ductility. For such failures, the reversed cyclic strength was around 29% lower than the monotonic strength. Hawkins and Mitchell (1984) thought the shearing force (stud capacity), can be thought of as the frictional force arising from the normal force (developed in the stud due to large slippage), and the coefficient of friction and gave the following equation

$$V_c = 5.4\sqrt{f_c'}A_c \tag{2.12}$$

Where:

$V_c = \text{Shear capcity due to concrete pullout failure, psi}$

$A_c = \text{area of concrete pullout failure surface, } in^2$

$f_c' = \text{concrete compressive strength, psi}$

The value of A_c was derived as the cone-shaped failure formed by the underside of the stud head and making a 45° angle with the vertical axis of the stud (Figure 2.4).

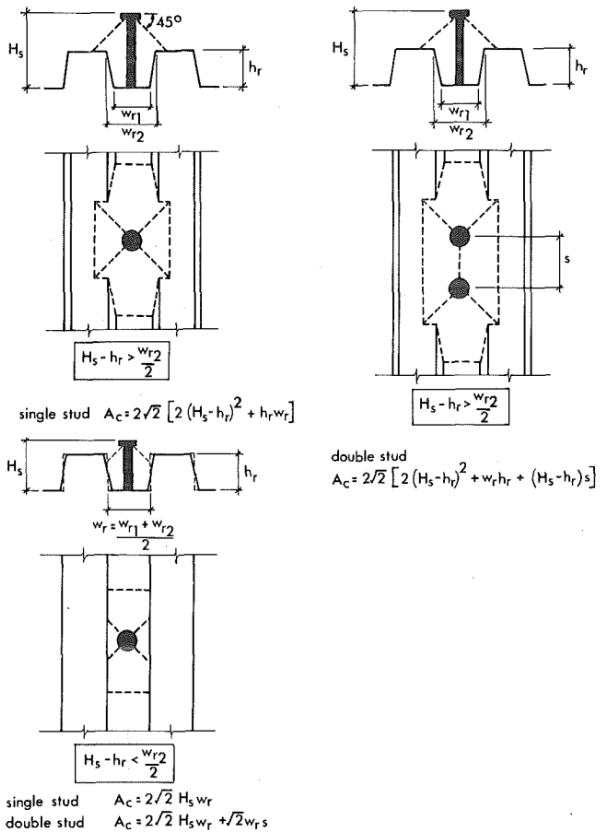

Fig. 2.4 Pull-out surface area (Hawkins and Mitchell (1984))

Further, Hawkins and Mitchell (1984) observed particularly in a narrow rib profile close to the edge of a slab that rib shearing failures are brittle that can become grave if headed shear studs are grouped together, they believed this failure may not have occurred if the test specimen had been wider. Also, if the headed shear studs had very little concrete cover in the direction of the applied load, rib punching failure.

Jayas and Hosain (1988) conducted 18 push-out tests. Five of the 18 push-out specimens had a solid slab, five had a metal deck parallel to the steel beam, and eight had a metal deck perpendicular to the steel beam. Their objective was to study headed shear studs in composite beam with ribbed metal deck perpendicular and parallel to a steel beam and the experimental parameters were longitudinal spacing and rib geometry. They tested 1.5 in. and 3 in. steel deck with headed shear studs 3/8 in. diameter and 3 in. long or ¾ in. diameter and 5 in. long.

The failure modes observed in these tests were shearing off of the headed shear studs, crushing of concrete adjacent to the stud cluster, longitudinal shearing of the concrete slab, stud pull-out together with a concrete wedge and rib shear. The first three failure modes were observed in solid slab and metal deck parallel to the steel beam specimens. Stud shearing occurred in specimens where stud spacing was more than 6d (six time the diameter of stud) and concrete related failure in specimens with closed spaced headed shear studs i.e., stud spacing approximately 6d. The stud shearing failure observed by the Jayas and Hosain (1988) were similar to Hawkins and Mitchell (1984) and Ollgaard et al. (1971). Concrete related failure led to the reduction in stud strength by 7% for solid slab and 14% for specimens with metal deck parallel to the steel beam. The failure area was similar to the pyramidal cone given by Hawkins and Mitchell (1984). Almost all specimens with perpendicular deck saw stud pull-out failure. This failure led to a drastic reduction in stud strength compared to solid slab specimens, approximately 40% reduction for specimens with wide rib ($W_r/h_r > 4$) and even more reduction for narrow rib ($W_r/h_r > 4$) deck profiles. The stud spacing had no effect on stud strength in these perpendicular deck specimens.

Jayas and Hosain (1988) saw that Hawkins and Mitchell (1984) equation underestimated the stud strength for 1.5 in. deck and overestimated for 3 in. deck. So proposed two different Equations 2.13 and 2.14 for each deck with the upper limit as Ollgaard et al (1971) Equation 2.9.

For 3 in. deck,

$$V_c = 0.35\lambda\sqrt{f_c'}A_c \leq Q_u \tag{2.13}$$

For 1.5 in. deck,

$$V_c = 0.61\lambda\sqrt{f_c'}A_c \leq Q_u \tag{2.14}$$

Where:

$V_c =$ Shear capcity due to concrete pullout failure, N

$f_c' =$ concrete compressive strength, MPa

$A_c =$ area of concrete pullout failure surface, mm^2 (Hawkins and Mitchell, 1984)

$Q_u =$ ultimate shear stud strength, N (Ollgaard et al, 1971)

$\lambda =$ factor which depends on the type of concrete

$= 1.0$ for normal density concrete

$= 0.85$ for semi low density concrete

$= 0.75$ for structural low density concrete

Further, Jayas and Hosain (1988) conducted four composite beam test which will be discussed later in the literature.

Robinson (1988) evaluated 17 push-out test simulating three distinct components of composite floor system: a) an interior beam (Steel deck perpendicular to the beam), b) a spandrel beam (Steel deck perpendicular to the beam at the edge), and c) a girder (Steel deck parallel to the beam). Steel deck 3 in. and 2 in. deep were used along with headed shear studs having ¾ in. diameter and 4.5 in. and 3.5 in. long respectively. Robinson (1988) observed that up to the first crack the load increased proportionally with the slip. The crack generated at the root of the concrete rib containing headed shear studs and then extended across the slab as the ultimate load was reached. The mode of failure for both the interior beam and spandrel beam specimens was ultimately cracking through the solid part of the concrete slab at the root of the concrete rib on both sides of the rib, but the average normalized ultimate shear capacities for spandrel type specimens were significantly lower. Comparing these test results with of perpendicular deck specimens with theoretical formula given by Grant et al. (1977) saw that the formula was conservative. Further comparing the specimens with pair of headed shear studs to that having a

single stud showed that the peak load performance of a pair of headed shear studs is only 1.3 time of that of a single stud which was also comparable to the formula given by Grant et al. (1977).

$$Q_{rib} = \frac{0.85}{\sqrt{N}}\left(\frac{H-h}{n}\right)\left(\frac{w}{h}\right)Q_{sol} \leq Q_{sol} \tag{2.15}$$

Where:

$Q_{rib} =$ strength of a stud in formed steel deck

$Q_{sol} =$ strength of a stud stud shear connector in a flat soffit slab (Ollgaard et al, 1971)

$H =$ height of stud shear connector

$h =$ height of rib

$N =$ number of headed shear studs in a rib

$w =$ average rib width

Robinson (1988) also saw that for girder type (steel deck parallel) relatively small edge distance of the stud in the concrete rib had no significant effect on the shear capacity and the ultimate strength were greater than for a single shear connector in solid slab. The failure mode for these types of specimens was stud shearing.

Later, Robinson (1988) tested two composite beams having degree of composite action of 0.25 and 0.26 with deck perpendicular to the steel beam and saw good agreement between the ultimate shear strengths obtained from the push-out tests and the ultimate shear strengths observed in the test. So, it was concluded that the comparable push-out specimens tested, having one lateral row of single or pairs of headed stud connectors, gave reliable values of ultimate shear strength.

Mottram and Johnson (1990) evaluated 35 push-out test using through-deck welded headed shear studs with normal and lightweight concrete. Three different types of steel deck were employed perpendicular to the steel beam, together with ¾ in. diameter headed shear studs 3.75 in. or 4.7 in. long. The results showed plastic deformation in the headed shear studs but indicated

that the strength was proportional to $f_{cu}^{0.27}$, f_{cu} is the cube strength of concrete. For lightweight concrete the 10% reduction for solid slab given in BS 5950: 'Part 3.1.' were slightly conservative. The resistance of headed shear studs was seen to be decreased by 6% when the stud spacing was reduced from 3 in. to 2 in. The headed shear studs placed in weak position had strength 35% lower to the headed shear studs placed in strong position. Within one steel trough, two headed shear studs placed diagonally were weaker than two headed shear studs placed in line, even though the latter were further apart. The strength per stud in a pair of headed shear studs per rib was less than for ribs with one stud, but this reduction was not greater than the 30%. Increasing the slab thickness by 0.75 in. and stud height by 1 in. increased the resistance by 19%. Mottram and Johnson (1990) also saw that the slip capacity for all specimen having one stud per rib was more than 0.3 in. but specimens having two headed shear studs per rib had the slip capacity less than 0.2 in. which concerned him. They also did a detailed comparison of the experimental results with the equation given by Grant et al. (1977) and the modified equation by Lawson (1989) and found that the modified equation by Lawson (1989) was more consistent with the test results which can be for the fact that equation accounted for the stud positions in the rib. The modified strength reduction factor (SRF) given by Lawson (1989) is as follows

$$SRF = \frac{0.75r}{\sqrt{N_r}}\left(\frac{H_s}{H_s + h_R}\right) \leq 1.0 \tag{2.16}$$

Where:

$r =$ factor to account for position of stud in rib

$=$ headed shear studs in central or strong position, r is the lesser of $\frac{b_0}{\mathrm{h}_R}, \frac{\mathrm{e}}{\mathrm{h}_R} + 1$ and 2.0

$=$ headed shear studs in weak position, r is the lesser or b_0/h_R and 2.0

$H_s =$ stud height

h_R = depth of deck

N_r = number of headed shear studs in a rib

b_0 = average rib width

e = distance between midheight of deck web and stud center in direction of loading

Lloyd and Wright (1990) conducted 42 push-out test to investigate the effects of amount and position of reinforcement and slab width and height. Tests were also conducted to investigate the effects of applying transverse loading to the slab during the test. The slab thickness of 4.5 in. along with 4 in. long ¾ in. diameter headed shear studs and normal weight concrete was chosen for all specimens. Five different slab width chosen ranged from 17 in. to 53 in. Three different wire mesh placed at different heights along the slab studied the effect of reinforcement to the stud strength. On few specimens prior to the application of the main load transverse moment was applied until a longitudinal crack appeared centrally along the specimen and this moment was then help constant throughout the test to stimulate the slab hogging over the beam.

Almost all the specimens saw minor horizontal and vertical cracks with concrete separating from the steel deck just prior to the ultimate load had reached. Further loading the specimen, the slab was seen to ride over the deck causing extensive distortion to the deck. A wedge-shaped cone of concrete (figure 2.5) around the stud was seen unlike the pyramidical cone seen by Hawkins and Mitchell (1984). Some specimens exhibited rib-shear failure wherein the concrete shears along a plane level with the upper flange of the deck. Specimens with parallel deck saw failure as a result of longitudinal shear along the rib or by stud shearing. Increasing the width of the specimens or the variation in reinforcement quantity and position appeared to have a little effect on the stud resistance. The application of transverse moment to a push-out test specimen appears to raise the ultimate connection capacity only marginally. Based on the observed wedge-shape cones Lloyd

and Wright (1990) gave an expression of the surface area of the cone to predict the connection strength.

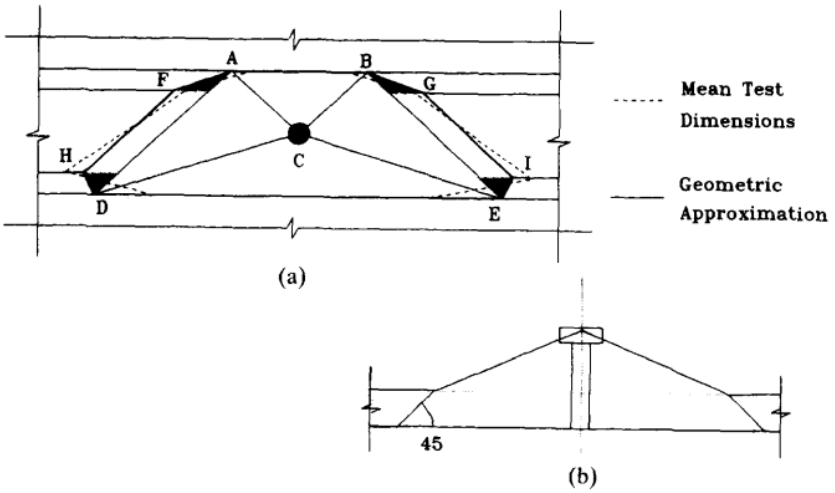

Fig. 23. (a) Wedged-shear-cone geometry; (b) centre-line section.

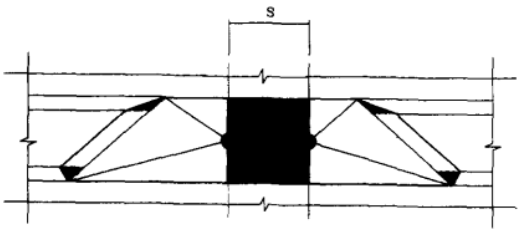

Fig. 24. Double-stud wedged-shear cone.

Fig. 2.5 Wedge-shear cone (Lloyd and Wright, 1990)

For single stud,

$$A_c(ss) = 2w_1\sqrt{w_1^2/_4 + h_p^2} + w_1\sqrt{w_1^2 + 2h_p^2} + 2w_2\sqrt{3D_p^2} \tag{2.17}$$

For double stud,

$$A_c(ds) = A_c(ss) + 2s\sqrt{w_1^2/_4 + h_p^2} \tag{2.18}$$

And the connection resistance can be given as

$$Q_k = \left(A_c\sqrt{f_{cu}}\right)^{0.34} \tag{2.19}$$

Lloyd and Wright (1990) also gave an expression of the rib-shear failure surface area that occurred in 17.7 in. wide specimens

For single stud,

$$A_{c_r}(ss) = w_1\sqrt{b^2/_4 + h_p^2} + b\sqrt{w_1^2/_4 + h_p^2} \tag{2.20}$$

For double stud,

$$A_{c_r}(ds) = w_1\sqrt{(b-s)^2/_4 + h_p^2} + (b-s)\sqrt{w_1^2/_4 + h_p^2} + 2s\sqrt{w_1^2/_4 + h_p^2} \tag{2.21}$$

When the rib-shear surface area is less than the wedge-shear cone surface area the failure modes changes from cone failure to rib-shear failure. The critical breadth of slab at which this occurs can be given by

For single stud,

$$b_{cr}(ss) = {A_c(ss)}\Big/{h_p^2\sqrt{w_1^2/_4 + h_p^2}} - {w_1}/{2h_p^2\sqrt{A_c(ss)^2 + 4h^2}} \tag{2.22}$$

For double stud,

$$b_{cr}(ds) = b_{cr}(ss) + s \tag{2.23}$$

Where:

A_c = Area of concrete

h_p = Projection height of stud $(h - D_p)$

w_1 = Overall trough width

D_p = Overall profile depth

s = stud spacing

f_{cu} = Characteristic concrete strength

b = Slab breadth

h = Overall stud height

Androustos and Hosain (1992) conducted 16 Push-out tests to study the stud behavior in narrow ribbed metal deck placed parallel to the steel beam. The effect of stud spacing on stud capacity was investigated. The spacing was varied from 6 times to 3 times the diameter of the headed shear studs. Two metal decks having the ratio of rib width to rib height (w_r/h_r) 0.78 and 1.485 were used with the overall concrete thickness of 6 in. and 4 in. respectively. Since the ratio w_r/h_r for both the deck was less than 1.5 they were termed as narrow ribbed metal decks. Companion solid slab specimens were also tested. 6 in. thick slab used 5 in. long ¾ in. diameter headed shear studs and 4 in. slab used 3 in. long 5/8 in. diameter headed shear studs. Androustos and Hosain (1992) observed five different failure modes namely longitudinal splitting of the concrete slab, combination of longitudinal splitting and stud shank shear, stud shank shear, cursing of the concrete rib and concrete shear. Stud spacing greatly affected the failure mode. Closely spaced stud specimens saw concrete related failure. for such specimens the strength increased proportionally as the spacing was increased. This similar trend was observed by Davies (1969). Further as the spacing increased stud shank shear became the predominant failure mode. The transition point appeared to be approximately 5d for 6 in. solid slabs and 6d for 4 in. solid slab.

Sublett (1992) conducted 36 push-out tests with three different deck geometries. Test variables were normal load application, stud position, slab thickness, deck rib geometry, and base member thickness. Test conducted by past researchers showed that during push-out test the concrete would tend to peel away from the specimens which caused premature failure in the push-out test and therefore poor relation to the full-beam test. Sublett (1992) therefore applied normal load ranging from 5% to 20% of the main load to understand its effect. It was also believed that the normal load closely models gravity loading of the full-scale beams. When comparing identical specimens which varied in the applied normal load Sublett (1992) saw transverse cracks when

20% normal load was applied and longitudinal cracks when only 5% normal load was applied. The stud strength increases as the normal load was increased. The load vs slip equation given by Ollgaard (1972) although derived from solid slab push-out test gave acceptable results when compared with the test results. Sublett (1992) also saw that the location of the stud in the flute of the metal deck impact the strength and stiffness of the headed shear studs. Strong position stud specimens observed longitudinal cracks which showed high concentration of compressive force at stud location and as result shear cone is developed whereas weak position stud specimens did not form longitudinal cracks and the concrete limits the size of the shear cone and the deck yields and fails. The weak position headed shear studs showed more ductility than the strong position headed shear studs. A linear relationship between the stud strength and the base metal thickness similar to Goble (1968) was also observed. Thin base members flanges rotated in the direction of reaction load with the headed shear studs remained perpendicular to the flange and the failure observed was ductile. When compared specimens having two headed shear studs per slab to one stud per slab good relation between the ultimate strength was observed indicating equal load distribution between headed shear studs. Increase in the flute increased the strength, an increase in ratio of rib width to height from 0.387 to 0.706 saw a 38% increase in stud strength owing to the fact that larger flute forms bigger concrete shear cone. Further Sublett (1992) compared the experimental results to the formulas given by Mottram and Johnson (1990) and saw that the test results were within 10% of the predicted strength as these equations considered the position of the headed shear studs in the rib unlike the design codes used during at that time.

Chandrasekar (1995) conducted a total of 104 push-out test in three phases on solid slab and wide ribbed metal deck ($W_r/h_r > 1.5$). The first phase was focused on to study the effects of transverse spacing and the staggered placement of headed shear studs on the shear capacity of

headed shear studs in both solid slab and wide ribbed deck specimens. Phase two focused on the effect of longitudinal spacing, compressive strength of concrete and transverse reinforcement on solid slab specimens while phase three focused on wide ribbed metal deck specimens to study the effects of longitudinal stud spacing and the rib width to height ratio (W_r/h_r). Chandrasekar (1995) observed 5 failure mode: shank shearing of headed shear studs, concrete splitting and crushing, combination of concrete crushing and stud shear, longitudinal splitting of concrete slabs, and concrete shear plane failure. Shear shank failure appeared in specimens having stud spacing relatively large and also large W_r/h_r ratio whereas concrete splitting and crushing occurred when headed shear studs spacing was relatively small and so the combination of both of this failure was seen somewhere in between when longitudinal stud spacing was 4.5 times the diameter of the stud. Longitudinal splitting of concrete was observed in specimens with a single row of headed shear studs and a single layer of welded wire mech as the only transverse reinforcement and concrete shear plane failure was predominant in specimens having 4 in. thick slab and 1.5 in. deck or 6 in. slab and 3 in. deck. The stud capacity increased as the transverse stud spacing was increased from 3d to 4d but further decreased as the spacing was increased to 5d for headed shear studs planed in line. For staggered position the stud capacity increased as the transverse spacing was increased. For 6 in. solid slab specimens the stud capacity increased as the longitudinal spacing was increased from 3d to 4.5d then slight increase until 6d and further no significant increase when spacing was 8d illustrating a transition point to a plateau region at approximately 5d was observed. Similar trend was observed for 4 in. solid slab specimen with the transition point at 4.5d. Observing these trend Chandrasekar (1995) carried out a least square regression analysis to give an equation for predicting ultimate load per stud in solid slabs as:

$$q_u = 0.47 s_t h \sqrt{f_c'} + 2.85 s_l d \sqrt{f_c'} + 0.15 A_{tr} f_y + 2.23 dh \sqrt{f_c'} \leq 0.8 A_{sc} F_u \quad (2.24)$$

Where:

s_t = transverse stud spacing

s_l = longitudinal stud spacing

d = stud diameter

h = stud height

f_y = yield strength of transverse reinforcement

f_c' = concrete compressive strength

A_{tr} = area of transverse reinforcement

A_{sc} = cross sectional area of stud

F_u = ultimate strength of stud

For 6 in. metal deck specimens Chandrasekar (1995) saw no plateau within the range of longitudinal spacing tested but seeing the trend expected a plateau slightly over 8d and for 4 in. metal deck specimens saw a plateau at around 6d. Following the same least square regression analysis procedure gave an equation for ultimate load per stud in wide ribbed metal decks as:

$$q_u = (11 s_l d - 0.82 s_l^2)\sqrt{f_c'} + 0.36 \frac{w_d}{h_d} dh\sqrt{f_c'} \leq 0.8 A_{sc} F_u \qquad (2.25)$$

$$3d \geq s_l \leq 6d$$

Where:

$\frac{w_d}{h_d}$ = rib width to rib height ratio

Lyons (1994), Lyons et al. (1996) conducted 48 push-out tests on solid slabs and 87 push-out using steel deck. The normal load apparatus developed by Sublett (1992) was adopted to more accurately simulate the behavior of shear connectors in a composite beam and the steel deck test specimens were identical to Sublett (1992) except the specimens were 2 ft. wide as recommended

by him to ensure that the premature failure caused by failure planes extending to the boundaries does not occur. The solid slab specimens were similar to Ollgaard (1971) that single stud grouping was used instead of two headed shear studs grouping and specimens were cast horizontally instead of vertical. ¾ in. stud diameter with ultimate strength of 67 ksi and 0.56 in. and 0.68 in. headed shear studs with 84 ksi ultimate strength were tested. The failure mode observed were stud shearing, stud rupture, concrete pull-out, rib punching, rib cracking, slab splitting and tee rotation. Solid slab specimens observed mainly stud shearing failure except a few which exhibited concrete pull-out failure. The specimens which failed in stud shearing saw that the connector strength depends on concrete strength. Lyons's (1994) relation was first observed by Viest (1956) and also by Slutter and Driscoll (1965). The strong position headed shear studs in steel deck specimens failed in stud shearing and concrete pull-out failure. Lyons (1994) saw no difference in the shape between a stud sheared from a sloid slab and the one which sheared from a metal deck slab. As the stud height was decreased the specimens exhibited concrete pull-out failure. The weak position headed shear studs in steel deck specimens exhibited rib-punching and observed a low ultimate strength compared to the strong position headed shear studs but extraordinary ductility. The strength of weak position headed shear studs increased if the strength of the steel deck increased. In staggered position headed shear studs if the headed shear studs weren't high enough concrete pull-out failure would occur or the headed shear studs saw rib punching/stud shearing and rib cracking failure. The concrete pull-out failure for staggered position headed shear studs was similar to strong position concrete pull-out. When the headed shear studs exhibited rib punching and stud shearing failure they acted independently as one stud in strong failing in stud shearing and other in weak position failing in rib punching. In rib cracking failure the headed shear studs behaved similar to rib punching/stud shearing failure until cracking of the rib occurred. Lyons

(1994) also observed that increase in the tensile strength adversely affects the stud performance. High strength headed shear studs (F_u = 84 ksi) fail at lower slip than standard strength headed shear studs (F_u = 67 ksi). Concrete strength and unit weight affects the ultimate strength of headed shear studs even if stud shearing failure occur and significant portion of the connection strength comes from the friction at the concrete-steel interface. Following the observation, Lyons (1994) recommended to not use cold working to increase the tensile strength of stud and consider the importance of friction at concrete-steel interface and steel deck strength for weak position headed shear studs. He also recommended to predict the stud strength based on each possible failure mode.

Joshnson and Yuan (1997a) carried out research to verify the existing design rules for stud shear. They analyzed 269 push-out tests from previous research and also carried out 34 new push-out tests. Comparing the 269 push-out tests with the rules that existed during that time Joshnson and Yuan (1997a) saw that the Eurocode method appeared to be the least safe with several test results below 70% of predicted strength and the Hanswille et al. (2004) method to be over conservative with all of the test results to be 1.5 times the predicted strength. While planning the 34 new push-out test Joshnson and Yuan (1997a) considered the parameters which had the most scare data in the previous researches. Analysis of all the tests i.e., 269 previous tests with the new 34 test they identified seven modes of failure. For push tests with perpendicular profiled sheeting, five failure modes were specified including stud shearing, rib punching, rib punching with stud shearing, rib punching with concrete pull-out, and concrete pull-out. Joshnson and Yuan (1997a) then gave a detailed theoretical model for each failure mode (Johnson and Yuan, 1997b) which is discussed below.

For stud shearing the equation was given from Eurocode (Equation 2.26),

$$P_{rs} = 0.37A_s(f_c E_{cm})^{0.5} \leq 0.8A_s f_u \quad (2.26)$$

Where:

$P_{rs} =$ shear strength of stud in a solid slab

$f_u =$ ultimate strength of stud

$E_{cm} =$ modulus of elasticity of concrete

$f_c =$ cylinder strength of concrete

$A_s =$ cross sectional area of stud

Strength for other modes of failure was defined as

$$P_r = k_t P_{rs} \tag{2.27}$$

Where:

$P_{rs} =$ shear strength of stud

$k_t =$ reduction factor

$$k_t = \frac{\eta + \lambda(1 + \lambda^2 - \eta^2)^{0.5}}{1 + \lambda^2} \leq 1.0 \tag{2.28}$$

For concrete pull-out failure (CP) with one stud in favorable or central position,

$$\eta_{cp} = \frac{0.56 v_{tu} h^2 \left(b_o - \frac{h}{4}\right)}{h_p N_r P_{rs}} \leq 1.0 \tag{2.29}$$

$$\lambda_{cp} = \frac{e_r T_y}{h_p P_{rs}} \tag{2.30}$$

If $h > 2h_p$, use $h = 2h_p$ and the failure mode is shank shear (SS)

For rib punching failure (RP),

$$\eta_{rp} = \frac{1.8\left(e_f + h - h_p\right) t f_{yp}}{P_{rs}} \leq 1.0 \tag{2.31}$$

$$\lambda_{rp} = \frac{e T_y}{2 h_p P_{rs}} \tag{2.32}$$

The stud in unfavorable position (u) is considered to fail by rib punching for combined rib punching and concrete pull-out failure (RPCP) of headed shear studs in slabs with two headed shear studs positioned in series or diagonally in a rib. The stud on the favorable side (f) is anticipated to fail due to concrete pull-out. The combined resistance is calculated by adding the resistances of the two headed shear studs.

$$\eta_u = \frac{(e_f + h - h_p)tf_{yp}}{P_{rs}} \leq 1.0 \tag{2.33}$$

$$\lambda_u = \frac{eT_y}{2h_pP_{rs}} \tag{2.34}$$

$$\eta_f = \frac{0.56v_{tu}h^2\left(e + s_t - \frac{h}{4}\right)}{h_pP_{rs}} if\ 0.75h \leq (e + s_t) \tag{2.35}$$

$$\eta_f = \frac{v_{tu}(e + s_t)^2\left(0.75h - \frac{(e + s_t)}{3}\right)}{h_pP_{rs}}\ if\ 0.75h > (e + s_t) \tag{2.36}$$

$$\lambda_f = \frac{eT_y}{h_pP_{rs}} \tag{2.37}$$

If $h>2h_p$, use $h = 2h_p$ and the failure mode is combination if rib punching and shank shear (RPSS)

Where:

$v_{tu} = 0.8f_{cu}^{0.5} \leq 5$, shear strength of concrete

$h =$ height of stud

$b_o =$ average width of deck trough

$h_p =$ height of steel deck

$N_r =$ number of headed shear studs per rib

$e_r =$ distance from center of stud to nearest rib wall

for favorable position stud,

$T_y \cong 0.8A_s f_u$, yield tensile strength of stud

$f_{cu} =$ cube strength of concrete

$e_f =$ distance from center of headed shear stud to nearer rib wall for unfavorable position

$t =$ thickness of steel deck

$f_{yp} =$ yield strength of steel deck

Kim et al. (2001) conducted three push-out test to determine the behavior of ½ in. stud shear connectors welded through-deck in a composite slab and provide specific data to develop a numerical mode. The effect of profiled steel deck, width of the specimen and different loading conditions were studied. They also discussed the concrete pull-out failure observed in the tests. The specimens used ½ in, diameter and 2.5 in. long headed shear studs and 1.5 in. deep steel deck. The measured concrete pull-out failure area observed was 30% higher than suggested by Hawkins and Mitchell (1984) and 41% less than that suggest by Lloyd and Wright (1990). The pull-out strengths predicted using the formulae proposed by Hawkins and Mitchell (1984), Jayas and Hosain (1987), and Lloyd and Wright (1990) overestimate approximately twice as large as those observed in the tests.

Further numerical analysis was caried out to develop a finite element model for the push-out specimens. The model simulated concluded that inclusion of profiled sheeting in the linear analysis led to increase in the strength, the concrete crack pattern was in good agreement with the test and the main failure mode for the FE analysis was concrete pull-out and it did not show the yielding of the headed shear studs even though they were given non-linear material properties.

To study the effect of friction, normal force, stud position, concrete strength and stud properties on stud strength, Roddenberry (2002) carried out 24 solid slab push-out test and 93

composite slab push-out tests Stud diameter ranged from 3/8 in. to 7/8 in. and deck heights of 2 in. or 3 in. for most of the specimens and 4.5 in. and 6 in. for three specimens each. It was observed that the flange thickness has no significant effect to stud strength. Few solid slab specimens had steel metal placed between the concrete slab and steel beam eliminating steel/concrete interface friction. These specimens saw a reduction in stud strength that those which had the steel/concrete interface. It was therefore believed that the use to steel deck composite slab had less stud strength that solid slab due to reduction in the frictional component. Appling a 10% normal load of the shear load increased the stud strength by 14% to when no normal load was applied. The normal load appeared to increase the frictional resistance of the beam/slab interface. The specimens having headed shear studs in strong position in 2 in. and 3 in. deck had stud shearing failure, a few had weld failure and it was unknown as if the failure started a concrete pull-out. The specimens having headed shear studs in strong position in 2 in. deck with a normal force of 20% of the applied shear load had the highest strengths and believed to exhibit concrete pull-out failure. The specimens having headed shear studs in weak position in 2 in. and 3 in. deck all had rib punching failure. A few specimens having deep deck saw average strength of headed shear studs to be $0.28A_sF_u$ for 4.5 in. deck and $0.21A_sF_u$ for 6 in. deck. These strengths were less 50% of the stud strength used in typical decks and therefore not efficient for use in composite floors. Roddenberry (2002) found to attain reliable welds for 7/8 in. diameter headed shear studs and many for these specimens failed due to weld defects but comparing the reliable specimens it was found the average stud strength of 7/8 in. headed shear studs was much less than that of 3/4 in. headed shear studs. Further analysis of the test conducted by herself, Lyons (1994), Sublett (1992) gave a new strength prediction model as.

For headed shear studs in 2 in. and 3 in. deck with $\frac{d}{t} \leq 2.7$,

$$Q_{sc} = R_p R_n R_d A_s F_u \tag{2.38}$$

$R_p = 0.6$ for $e_{mid-ht} \geq 2.2$ in. (strong position headed shear studs)

$= 0.6$ for $e_{mid-ht} \leq 2.2$ in. (weak position headed shear studs)

$= 0.52$ for staggered position headed shear studs

$R_n = 1.0$ for one stud per rib or two headed shear studs in staggered position

$= 0.85$ for two headed shear studs per rib

$R_d = 1.0$ for all strong position headed shear studs

$= 0.88$ for 22 gauge deck (weak headed shear studs)

$= 1.0$ for 20 gauge deck (weak headed shear studs)

$= 1.05$ for 18 gauge deck (weak headed shear studs)

$= 1.11$ for 16 gauge deck (weak headed shear studs)

For headed shear studs in 1 in. and 1 1/2 in. deck with $\frac{d}{t} \leq 2.7$,

$$Q_{sc} = R_n 3.08 e^{0.048 A_s F_u} \tag{2.39}$$

$R_n = 1.0$ for one stud per rib

$= 0.85$ for two headed shear studs per rib

For headed shear studs in 2 in. and 3 in. deck with $\frac{d}{t} > 2.7$,

$$Q_{sc} = R_p R_n R_d A_s F_u - 1.5\left(\frac{d}{t} - 2.7\right) \tag{2.40}$$

For headed shear studs in 1 in. and 1 1/2 in. deck with $\frac{d}{t} > 2.7$,

$$Q_{sc} = R_n 3.08 e^{0.048 A_s F_u} - 1.5\left(\frac{d}{t} - 2.7\right) \tag{2.41}$$

Where:

$A_s =$ Cross − sectional area of stud

$F_u =$ Ultimate tensile strength of the stud

Hicks and Couchman (2004), Hicks and Couchman (2006), Smith and Couchman (2010), Hicks and Smith (2014), Hicks and Odenbreit (2017) conducted a multiple push-out test and full beam test program from 2004 to 2017. These tests were conducted along with finite element modelling. The main objective was to study and standardize push-out test and its correlation to full-beam test along with understanding the various paraments effecting the stud strength. Hicks and Couchman (2004) recognized that the drafting committee for British code of practice for composite construction identified variable to be considered as the number of headed shear studs to be present per slab, the size and quality of concrete slab and amount of steel reinforcement and size of steel member to be used. A standardized specimen configuration was latter given as BS 5950-3 1990 without comment on the need to modify it when profiled steel sheeting was employed (Figure 2.6).

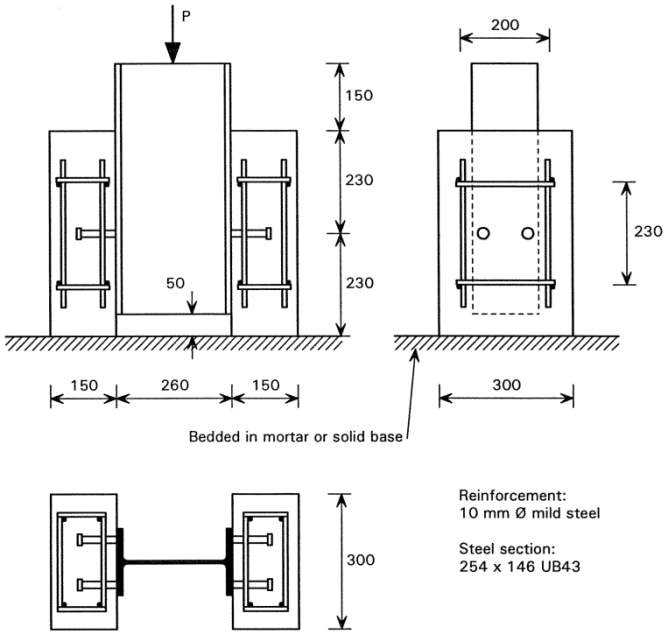

Fig. 2.6 Standard push test specimen according to BS 5950-3 1990

These specimens were criticized by Johnson and Anderson (1993) to be very small and having a tendency to split longitudinally. So, later the Eurocode 4 (EN 1994-1-1 2204) made significant changes to the standard push-out test (Figure 2.7) compared to the British standards as to increase the slab size to 25.6 x 23.6 in., increase in reinforcement and flange width of the steel section and providing connectors at two levels in each slab and a few others. Hicks and Couchman (2004) push-out specimens were identical to Johnson and Yuan 1997 except the edge trim (used to create the formwork for the slabs) was removed for few specimens. They saw that the absence of edge significantly lowered stud resistance and slip capacities. Further they created an FE model for composite beam calibrated with the two-beam test to confirm that the slip capacity of shear connectors in composite beam appeared to be in excess of 0.25 in. required by Eurocode 4.

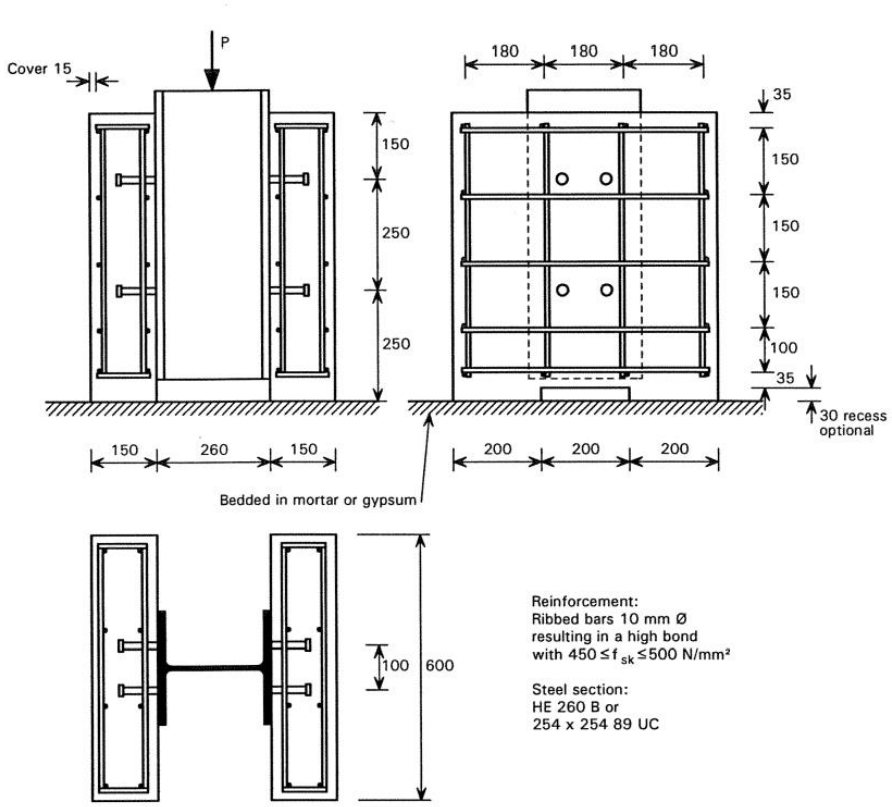

Fig. 2.7 Standard push test specimen according to Eurocode 4 (EN 1994-1-1 2004)

Further in Hicks (2006), reported the results of 24 push-out tests and 2 full beam tests and found that the specimens with two headed shear studs per rib gave a consistently lower ratio of experimental resistance to predicted resistance than those with one stud per rib, irrespective of the stud layout this was latter attributed as the effect of artificial ‘back-breaking’ (discussed latter in the literature) failure mode. Comparing the full-beam test results to the companion push-out test it was found that the peak resistance in push-out test is compatible with the plateau of load vs slip curve of the headed shear studs in the beam specimens but the slip measured in the push-out test was well below the slip measured in full-beam test. The slip in the push-out tests were lower than what was required by the Eurocode 4 to consider the connection as ductile. The resistance of a single stud back calculated from the full-beam results showed that the Eurocode 4 was overly conservative and the characteristic slip capacity outperformed the ductility requirements by a factor of two. The stud strength and slip for single headed shear studs in beam outperform the push test results (45% and 269% respectively) but for a pair of headed shear studs, the strength value agrees with the push test.

Smith and Couchman (2010) conducted 27 push-out test to investigate the effect of mesh position, transverse spacing, number of headed shear studs per rib and slab depth on the stud resistance in deck perpendicular to the steel beam. The test was performed on a “new push rig” (Figure 2.8) which applied a transverse load to the faces of the test specimen to prevent the specimen from splitting or spreading away from the beam. The slip capacity of the headed shear studs exceeded the minimum ductile requirement by Eurocode 4 which weren’t seen in Hicks (2006). They further saw that two headed shear studs per rib gave only 16% more strength than a single stud per rib and three headed shear studs per rib had a similar performance to two headed shear studs per rib. Increase in the transverse spacing had a small effect on the total area of the

failure surface and so a small increase in the stud resistance. Increase in the slab depth increased the stud resistance and positioning the mesh on top of the deck instead of top of the slab saw an improvement of stud resistance by 31%.

Hicks and Smith (2014) performed one full-beam test and six companion beam tests for 2 or 3 headed shear studs per rib and also saw that the resistance of three headed shear studs per rib was no better than two headed shear studs per rib. The push-out test was performed on the improved standard push test (Figure 2.8), which reflected the conditions that exist in a real beam more closely. Hicks and Smith (2014) felt that the reason for the poor performance in push-out tests was due to the absence of the compression force at the interface between the concrete and the flange of the steel section, which exists in real composite beams and so the loading system consists of two vertical jacks applying the longitudinal shear force, accompanied with two horizontal jacks applying a lateral force, which is uniformly distributed over the face of the test slabs through a grillage of W sections. This introduction of the transverse loading was similar to the 'new push rig' of Smith and Couchman (2010) except that the transverse loading was more uniformly distributed over the slab.

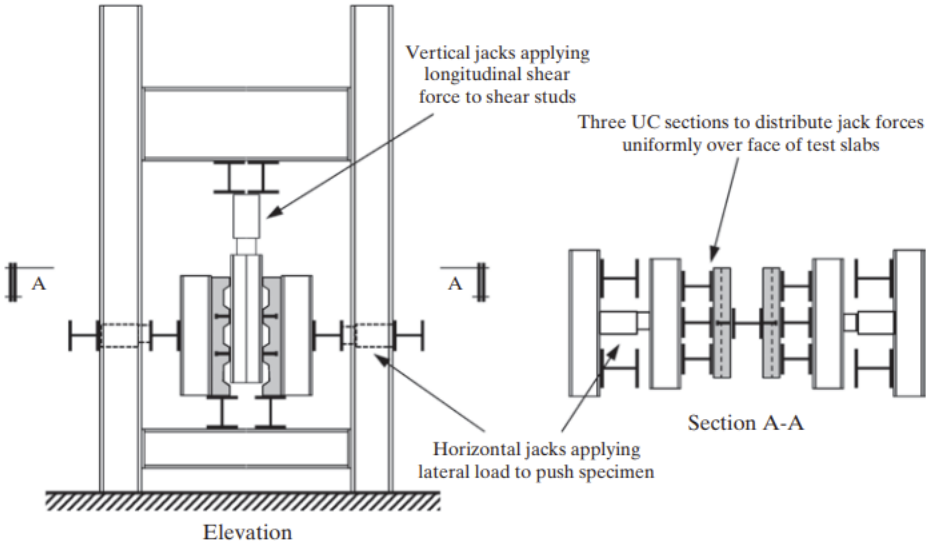

Fig. 2.8 Improved standard push test (Hicks and Smith (2014))

Hicks at al. (2017) showed that modifying the push test through the introduction of a normal force to the face of the test slabs provides comparable load-slip performance to that encountered within a beam and proposed test setup modification (Figure 2.9) in Eurocode 4 for headed stud connectors welded with trapezoidal profiled sheeting.

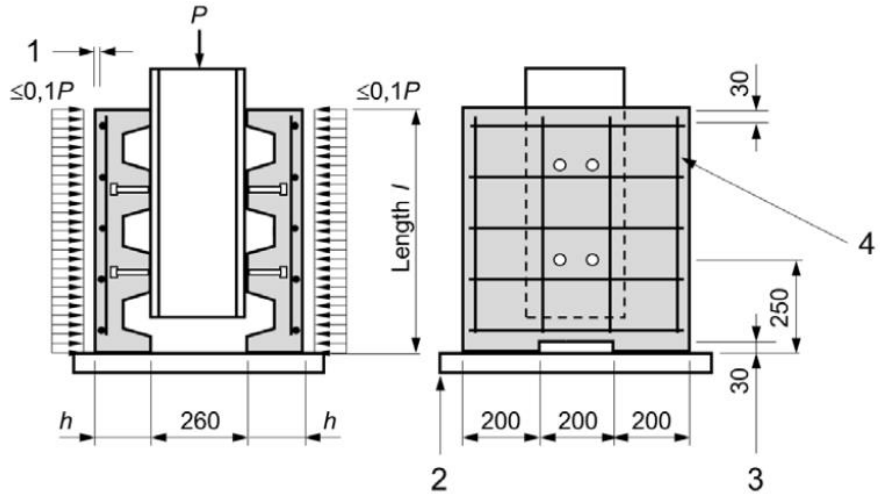

1 cover 15 mm
2 bedded in mortar, gypsum or similar
3 recess optional
4 reinforcement:
ribbed bars with $450 \leq f_{sk} \leq 550$ MPa
steel section: HE 260 B or 254 x 254 x 89 kg. UC

Fig. 2.9 Proposed test specimen for headed stud connectors welded within trapezoidal profiled sheeting (Hicks and Couchman (2004))

Veljkovic and Johansson (2004) carried push-out test to study the residual static resistance of stud shear connectors. The specimens were standard push-out specimens given in Eurocode 4 except that the concrete slabs were placed on rollers and a steel tie was placed in the bottom of the specimen to measure horizontal forces between the slabs. The loading was cyclic with a constant load range of $0.2P_R$ and a peak load of $P_{max} = 0.6P_R$ with different number of cycles and the loaded to failure under displacement control. P_R is the stud strength observed for the companion push-out test under monotonic loading. it was observed that the strength of headed shear studs reduced at all states of fatigue loading and concluded that the maximum load applied to the headed shear

studs does not affect fatigue damage but increasing the maximum load reduces the fatigue life. Observing the results and the from previous test conducted by Oehlers (1990) and Hanswille at al. (2004) Veljkovic and Johansson (2004) assumed a linear decrease in the residual strength and gave the following equation for 7/8 in. headed shear studs.

$$P_{res} = P_R\left(1 - \frac{N}{E_a}\right) \tag{2.42}$$

Where P_R is the static resistance of the stud, N is the number of cycles and E_a is the asymptotic endurance which is a theoretical parameter as a point where the failure envelop (assuming to be linear) crosses the N (number of cycle) axis. Further they also did a preliminary FE study for assessment of the mechanical model for residual static strength.

Fan and Liu (2014) and Sun at al. (2019) also conducted few monotonic and cyclic loading test on shear headed shear studs. Both studied the presence of profiled sheeting, the direction of the steel sheeting and the loading patterns. Fan and Liu (2014) used 2 in. trapezoidal and closed deck profiles. Sun et al. (2019) also used a 2 in. dovetail deck in addition to the two above. The specimens were in accordance of Eurocode 4. Companion monotonic test were also conducted for each cyclic specimen tested. The monotonically loaded specimens were loaded under force control until an evident reduction in stiffness was noted in the load-slip relationship. At this point, the specimen was loaded in displacement control until failure. In cyclic specimens the lateral displacement of slab was constrained and loaded was subjected to one cycle, in force control, at each 30%, 60%, and 90% of the elastic capacity determined from the monotonic test. This was followed by further cyclic loading. Fan and Liu (2014) observed stud shearing and rib shear failure modes while Sun at el. (2019) observed concrete pull-out, stud weld rupture and rib shearing failure mode. Both saw that the type and orientation of steel deck effected the stud strength. Fan and Lui (2014) saw very little difference in transverse and parallel sheeting for closed type deck

but for trapezoidal the resistance of transverse rib was less than parallel rib. Sun et al. (2019) observed degradation of shear capacity in the latter cycles with large slip. Concrete pull-out failure was primarily observed in open and monotonically loaded dovetail profile specimens, stud weld rupture in closed profile specimens and rib shearing with stud shearing in cyclically loaded dovetail specimens. Under cyclic loading the envelope response was similar to the monotonic response initially but degraded quickly as deformations increased. Energy dissipation characteristics did not vary significantly between specimens.

Hirama et al. (2017) did a comprehensive literature review focusing on slab type, failure mode, and large-diameter headed stud from existing 1002 push-out test results. Hirama et al. (2017) performed regression analysis and saw the apparent variation depending of slab type and failure mode but the shear test tended to increase as the total cross-sectional area of the stud shaft increased. Further analyzing only solid slab specimens for stud failure and concrete failure Hirama et al. (2017) saw that the shear strength was 1.023 times the tensile strength for stud failure and 0.915 times for concrete failure and thus believed that for solid slabs the shear stud strength can practically be taken as the tensile strength of the stud. The number of results for steel deck specimens were small and so Hirama et al. (2017) classified the results based on stud diameter rather than the failure mode. While analyzing the results with steel deck having headed shear studs with diameter less than 1 in., they observed that the shear strength of cutting type (deck parallel) is slightly lower than solid slab and of cross type (deck perpendicular) showed a different tendency and lesser than solid slabs from which it was concluded that the concrete volume surrounding the headed shear studs affect its strength. The limited results of headed shear studs having diameter greater than 1 in. showed that the shear strength with solid slabs tended to gradually decease per evaluation by headed stud tensile strength.

Konrad et al. (2020) summarized a new approach for the shear resistance of headed shear studs in profiled steel sheeting in perpendicular orientation to the steel beam. This new approach was first given in Konrad (2011) based on the mechanical model given by Lungershausen. Lungershausen defined four load bearing mechanisms for headed stud connectors in solid slabs (Figure 2.10).

A. The compression strut at the welding collar
B. Bending of the shank including the associated vertical force
C. The horizontal component of the normal force in the stud
D. Friction forces between the concrete and steel surfaces

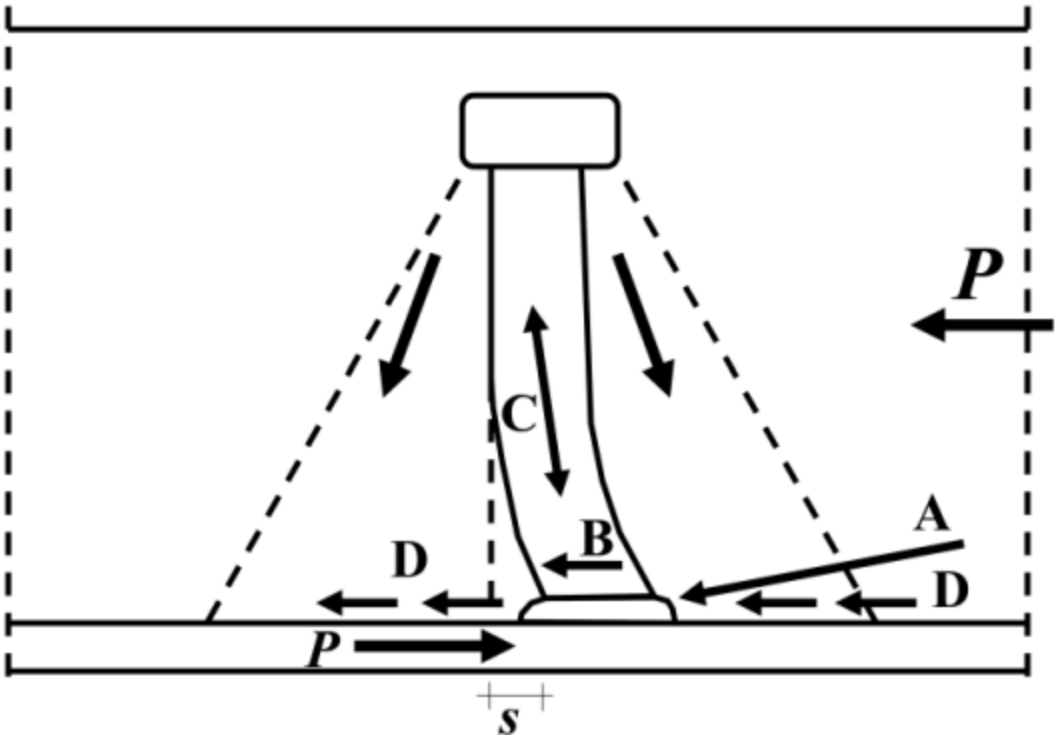

Fig. 2.10 load bearing mechanisms for headed stud connector given by Lungershausen

The compression force acting on weld collar (mechanism A) was determined as the product of reduced horizontally projected weld collar area and increased concrete compressive strength. The shank bending (mechanism B) was determined based on a cantilever structural system and

thus the shear force was obtained by multiplied by the concrete pressure in front of the stud shank by the length of equivalent structural system with plastic moment resistance of the shank assumed as the upper limit. The horizontal component of the stud's normal force (mechanism C) results from the anchorage of the head in the surrounding concrete and depends on the slip occurring at the base and the axial force in the shank when reaching the maximum load. Summing up these load bearing components of each mechanism and few simplifications two equations were given for headed shear connections in solid slab

Shear resistance of headed stud connector for concrete failure

$$P_{m,c} = 39.85 A_{w,eff} f_{c,cyl}^{2/3} + 3.75 d^2 f_{c,cyl}^{1/3} f_u^{1/2} \tag{2.43}$$

Shear resistance of headed stud connector for steel failure

$$P_{m,s} = 39.85 A_{w,eff} f_{c,cyl}^{2/3} + 0.59 f_u d^2 \tag{2.44}$$

Where:

$A_{w,eff} =$ effective projected weld collar area, mm^2

$f_{c,cyl} =$ uniaxial cylinder concrete compressive strength N/mm^2

$f_u =$ tensile strength of stud shank N/mm^2

$d =$ shank diameter of headed stud, mm

These equations were further extended to increase the scope of usage as,

$$P_{Rd,c} = \left[326 A_{w,eff} \left(\frac{f_{ck}}{30\ N/mm^2} \right)^{2/3} + 220 d^2 \left(\frac{f_{ck}}{30\ N/mm^2} \right)^{2/3} \left(\frac{f_{uk}}{500\ N/mm^2} \right)^{1/2} \right] \frac{1}{\gamma_v} \tag{2.45}$$

$$P_{Rd,c} = \left[313 A_{w,eff} \left(\frac{f_{ck}}{30\ N/mm^2} \right)^{2/3} + 240 d^2 \left(\frac{f_{uk}}{500\ N/mm^2} \right)^{1/2} \right] \frac{1}{\gamma_v} \tag{2.46}$$

Where:

$A_{w,eff} =$ effective projected weld collar area, mm^2

$f_{ck} =$ uniaxial characteristic concrete compressive strength, N/mm^2

$f_{uk} =$ characteristic tensile strength of stud shank, N/mm^2

$\gamma_v =$ partial factor $= 1.25$

Provided $20\ N/mm^2 \leq f_{ck} \leq 100\ N/mm^2$, $f_{uk} \leq 740\ N/mm^2$ and $16\ mm \leq d \leq 25\ mm$.

Further a new reduction factor was determined, based on the equation developed from various individual results depending of the position of headed shear studs and other various dependencies which were compared with push-out test. 17 push-out tests were carried out by Konrad et al. (2009) to investigate the influence of position of stud in the rib and influence of embedment depth on stud strength. They observed that the rib shearing and concrete breakout failure had the same cause of the maximum concrete pressure being exceeded in front of the stud base. Headed shear studs in weak position had low strength than strong and centrally positioned headed shear studs. A numerical analysis found that as the embedment depth increased the stud strength increase up the value of $h_{sc}/h_p = 1.56$ (ratio of stud height to steel deck), a value greater than that does not lead to any further increase. Further the reduction factors were summarized and the following equations was given for headed stud in steel deck in perpendicular position.

$$P_{Rd,Tr} = kP_{Rd,c} \leq P_{Rd,s} \tag{2.47}$$

For diameter $d \leq 22mm$ (pre-punched) and $16\ mm \leq d \leq 22mm$ (through-welded)

1. Pre-punched profiled steel sheeting or through-deck welded headed shear studs with sheeting thickness t < 0.75 mm

$$k = k_n \left[k_e 0.038 \left(\frac{b_m}{h_p} \right) + 0.597 \right] \leq 1 \tag{2.48}$$

2. Welded-through headed shear studs with steel sheeting thickness t ≥ 0.75 mm and e ≥ 55 mm

$$k = k_n k_{tr} \left[k_e 0.042 \left(\frac{b_m}{h_p} \right) + 0.663 \right] \leq 1 \tag{2.49}$$

3. Welded-through headed shear studs with e < 55 mm

$$k = k_n \left[0.317 \left(\frac{b_m}{h_p} \right) + 0.06 \right] \leq 0.8 \tag{2.50}$$

Where:

b_m = width of ribs, mm

h_p = height of profiled steel sheeting , mm

k_n = factor for number of headed shear studs

= 1.0 if $n_r = 1$

= 0.8 if $n_r = 2$

k_e = factor for position of stud in rib

= 1 if $55 \leq e \leq 100mm$

= 2 if $e \geq 100mm$

e = distance between headed stud and profiled steel sheeting in load direction, mm

k_{Tr} = factor to account for geometry of profiled steel sheeting

= 1.25 re − entrant steel sheeting

= 1.00 open steel sheeting

Eggert et al. (2017) compared the Eurocode 4 and the equations given by Konrad (2011) with the push-out test results and saw that a wide difference between the two calculation approaches when using modern deck profiles with a narrow rib. (Konrad, 2011) slightly underestimates the test results which is safe and conservative. They saw 22% increase when

through-deck welding was used instead of headed shear studs welded directly on the flange of the steel beam. The reduction factors by Konrad were found to be more realistic for open deck profiles. The stud strength according to Konrad is proportional to $\sqrt{f_c^{2/3}}$ which gives a 11% increase from 40 N/mm^2 to 46 N/mm^2 which fitted well with the measured 11% seen in the test results.

2.4 Push-out Test for Headed Shear Connectors in Deeper Decks

The above section has given us a brief about the research on push-out conducted on composite beam with steel deck up to deck height of 3 in. since all these past researches focused on decks with a maximum height of 3 in. the existing design equation restrict the use of deck with height more than 3 in. for composite beam. However as mentioned in the scope of the research decks with height more than 3 in. are already been manufactured and offer advantages a few researchers investigated the resistance of shear headed shear studs in deeper decks.

Ottenbreit and Nellinger (2017) predicted mechanical model of shear stud resistance in composite beam with deep steel deck. They observed a concrete cone failure mode rather than a pure shear failure in composite beams with deep decks. The concrete cone failure mode was observed in combination with the load bearing capacity of the shear stud by formation of one or two plastic hinge. This hinge mechanism was developed by Lungershausen. Ottenbreit and Nellinger (2017) developed a new equation on mechanical models of formation of concrete cone in bending and stud in bending which are explained below.

The assumed the concrete cone to be pinned at the bottom of the steel deck and fixed in the concrete above the steel deck and the load to spread under the shear stud in each direction making an angle of 40° giving the concrete width $w=2.4h_{sc}$. The moment resistance of the cone was given as follows.

$$W = 0.4h_{sc}\frac{b_{max}^3}{b_{top}} \tag{2.51}$$

Where:

h_{sc} = height of steel stud

b_{max} = maximum width of the deck rib max

b_{max} = width of the top deck rib max

Further the relative slip between the concrete and steel section leads to the bending of the headed shear studs forming one or two plastic hinge which was given by the following equation

n_y = number of plastic hinge

= 1 for $h_A \leq 2d\sqrt{n_r}$

= 2 for $h_A > 2d\sqrt{n_r}$

With the first hinge always forming at the bottom of the stud just above the weld and the second hinge forming at the distance $h_s = \beta h_{sc}$ from the bottom where β is 0.45 for trapezoidal deck and 0.41 for re-entrant deck and the plastic bending resistance of the stud to be

$$M_{pl} = \frac{1}{6}(f_{uk}d^3) \tag{2.52}$$

Where:

f_{uk} = tensile strength of shear headed shear studs

d = stud diameter

based on these two mechanical model the Ottenbreit and Nellinger (2017) gave the loadbearing capacity of the shear headed shear studs

$$P_{Rd,1} = 0.9\left[\frac{0.85f_{ctm}W}{h_p n_r} + \frac{n_y M_{pl}}{h_s - {}^{d}/_{2}}\right]\frac{1}{\gamma} \tag{2.53}$$

Where:

f_{ctm} = concrete tensile strength as defined in EN 1992

W = moment of resistance of concrete cone

n_r = number of headed shear studs per rib

n_y = number of yield hinges

h_p = height of steel sheeting

M_{pl} = plastic bending resistance of shear stud

To account for the possibility of pure shear failure the Ottenbreit and Nellinger (2017) gave the following equation

$$P_{Rd,2} = 0.6\left[f_{uk}\frac{\pi d^2}{4}\right]\frac{1}{\gamma} \tag{2.54}$$

Where:

γ = factor of safety according to EN 1994 − 1 − 1 = 1.25

The stud resistance was therefore given as

$$P_{Rd} = min\left(P_{Rd,1}, P_{Rd,2}\right) \tag{2.55}$$

The Ottenbreit and Nellinger (2017) compared these equations with 211 test results and saw that the 201 failed due to concrete cone and shear stud bending and 10 failed in pure shear and concluded that equation developed based on Lungershausen mechanical model governs for most cased and it is important to consider all important parameters of observed failure modes.

Albarram et al. (2017) conducted a FE study to understand shear connection behavior in narrow (b_o/h_p<1.5) and deep concrete filled steel decks. He modelled 54 push-out test specimens for decks in perpendicular positions having 4 in. and 5.75 in. deep decks to understand the effect of various parameters like rib geometry, stud layout, slab reinforcement and slab depth. Through his results, he saw that the stud capacity with narrow and deep decks were almost 65% of that from

traditional deck geometries. The narrow geometry having less concrete was found to be the main reason. Any increase in the concrete volume above the deck i.e increasing the slab dept or reinforcing the slab above the deck didn't increase the stud capacity. Further, he proposed to place headed shear studs in alternative ribs in the push-out specimens and saw an increase in strength by 20%. Using a special wire mesh reinforcement in the narrow rib region around the headed shear studs saw a 24% increase in strength by suppressing the concrete damage. Reinforcing the rib region also saw higher ductility than the traditional specimens. Albarram et al. (2017) further compared these results with AISC predicted strength equations and found out that these equations overpredicted the strength for deep deck profiles with the average $P_{FE}/P_{AISC} = 0.79$. He also noticed that for concrete strength higher than 3 ksi the steel failure side of the equation governed. These equations also didn't consider the geometries of steel deck as considered in Eurocode.

2.5 Challenges with Push-out Tests

With many push-out test being conducted by different researchers for the past two decades, researchers faced challenges while conducting these tests and have been modifying these standardized tests.

As seen above Hicks and Couchman (2004)) proposed a modified Push-test for Eurocode. When Hicks (2017) conducted push-out test on specimens having trapezoidal steel deck sheeting he saw the wedge-shaped portion of concrete separating when loads were applied which was called as the concrete pull-out failure. During this failure mode there was a significant axial tension force being generated in the headed shear studs. Approximately 30% of longitudinal force (van der Sanden, 1996). Due to this tension and the rotation of the headed shear studs the concrete slab use to separate from the steel decking. He then compared these results with similar full-scale beam test and saw that the slips measured in the push-out test were lower than the full-beam test which

concluded that the behavior of the headed shear studs in the push-out test weren't similar to the full-beam test. He modified the push-test by introducing a normal force to be applied uniformly to the face of the test slab. This normal force to be 10% of the applied shear force gave comparable results to the full beam test as seen by Rodenberry (2002). Hicks also observed an artificial back breaking of the specimen (Figure 2.11), which was due to the stud in the last rib at the top causing rotation and giving rise to a horizontal crack. To eliminate his pre-mature failure, he proposed to keep the top rib of the specimen without headed shear studs.

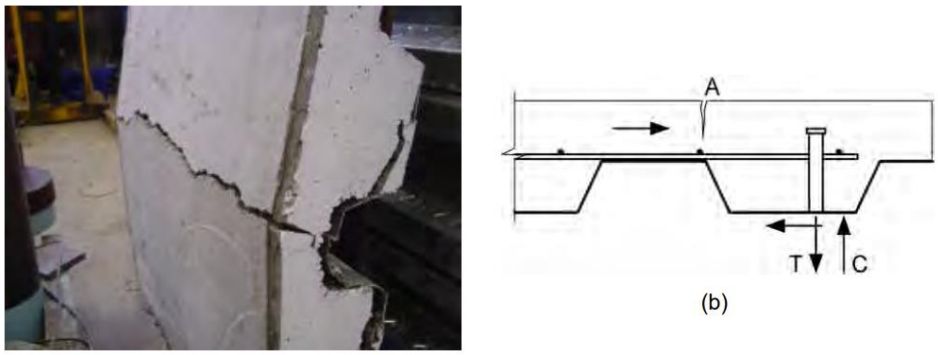

Fig. 2.11 Back-breaking of the specimen due to internal forces causing rotation of the last rib of the specimen. (Hicks, 2017)

The most recent push-out being conducted at Virginia Tech as a part of the concrete filled deck diaphragm research by Raul Avellaneda (personal communication) saw few challenges. The test specimen being vertical it is important the specimens to have even bearing on the ground, uneven bearing of the specimens can pollute the slip measurements which can hamper the results. Normal force is often required which according to the AISI S923-20 should be a maximum of 10% of the applied longitudinal load. The result is often biased towards the weakest stud. As while giving the results, we assume all headed shear studs failed at the same time and shear stud strength is given by total applied load divided by the number of headed shear studs Q = P/n. Often one of the headed shear studs fails first then the rest. The specimens being vertical the compression stresses in the specimens causes slab bucking (Figure 2.12) similar to the back breaking seen by

Hicks (2017). Often the post-peak behaviors are polluted (Figure 2.14 and 2.15), as any one headed shear studs fails in one slab the test setup rotates (Figure 2.13) and further given unreliable slip measurements.

Fig. 2.12 Slab Buckling (Avellaneda, personal communication)

Fig. 2.13 Slab Rotation (Avellaneda, personal communication)

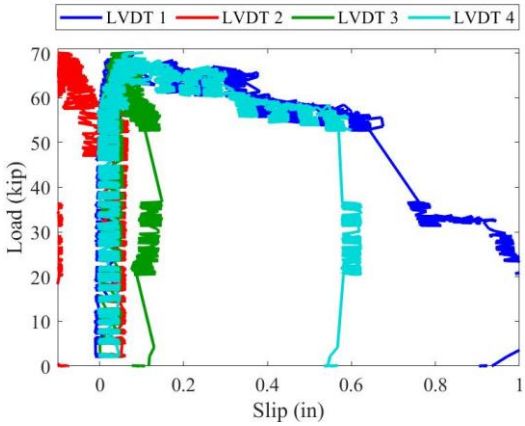

Fig. 2.14 Negative slip measurements (red) due to uneven bearing (Avellaneda, personal communication)

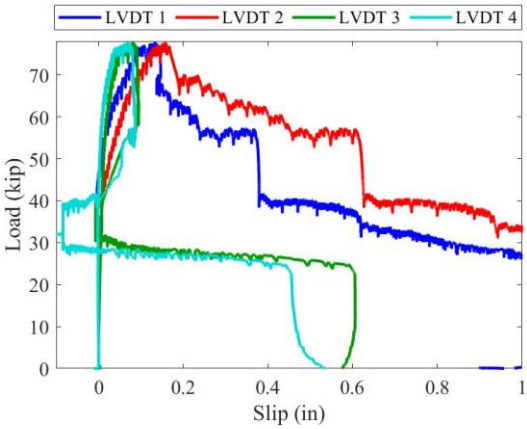

Fig. 2.15 Unreliable slip measurements (light blue and green) after 1st stud failure (Avellaneda, personal communication)

2.6 Different Test Setup

Apart from the conventional push-out test few researchers conducted test on different setup to evaluate the shear strength of the headed shear studs in a composite beam. These setups have a single slab placed horizontally instead of the two slabs bolted together vertically like the conventional push-out test.

Van der Sanden (1996) developed a new push test setup where a single headed stud was tested in a composite slab. He tested 23 push tests on this setup. The setup had intricate details with. The specimen was a steel deck paced on a steel plate to which the stud was welded through the deck and latter reinforcement was placed before concrete casting. A typical specimen used by the Van der Sanden (1996) is shown in Figure 2.16.

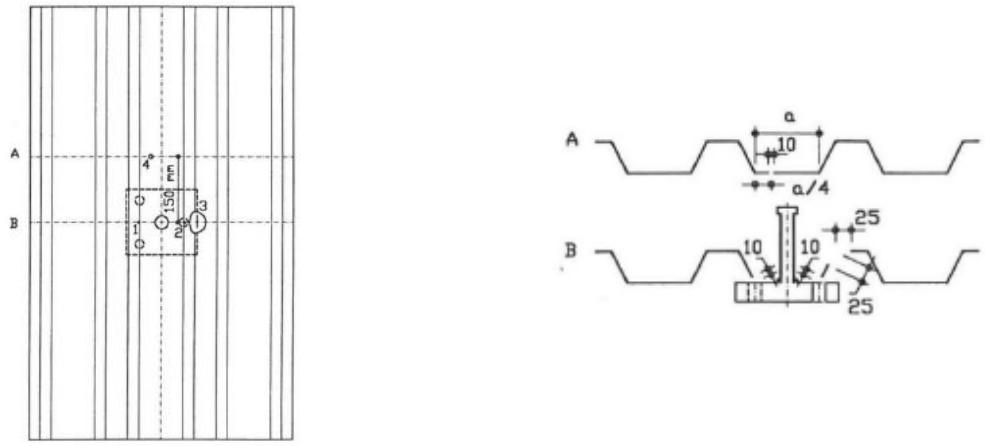

Fig. 2.16 Typical Test Specimen by Van der Sanden (1996)

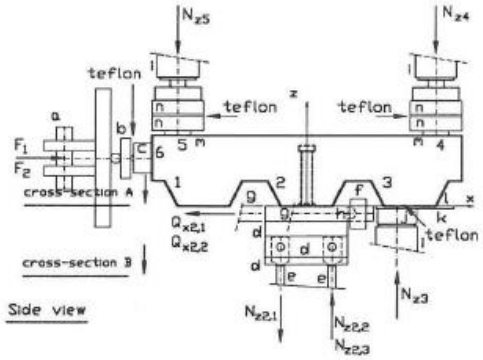

Fig. 2.17 ‘New’ Push Test setup (Van der Sanden (1996))

These specimens were then placed in the loading frame which was made of several parts which the Van der Sanden (1996) described as supports from 1 to 6 as shown in Figure 2.17. There was no support at Support 1. Support 2 was just below the steel plate on which the stud was welded. It transferred the shear force and the normal force. Support 3 consisted of a load cell to measure the normal load. Support 4 and 5 were identical and also consisted of load cell to measure the normal load. Whereas support 6 was the loading apparatus which consisted of two hydraulic jacks which imparted concentrated load and the further arrangement transferred these concentrated loads to the specimen as distributed loads. The loading was displacement controlled.

Hicks and McConnel (1996) undertook a series of push-out tests aimed at investigating the impact of different boundary conditions at the base of specimens on the strengths of shear connectors. The primary objective was to gain insights into the behavior of these connectors in various loading scenarios. A Single-sided push-out test configuration (Figure 2.18) to evaluate individual slabs was developed. Four distinct boundary conditions were examined during the experimentation process:

a) Two-directional roller bearing was employed at the interface of the reaction floor, facilitating unrestricted movement in both lateral (x) and normal (y) directions.

b) One-directional roller was utilized at the interface, allowing movement solely in the lateral (x) direction.

c) A standard German-style push-out specimen was prepared, wherein the base of the specimen was recessed and securely embedded in dental plaster placed directly on the strong floor.

d) Similar to c) without the recess adhering to British code specifications.

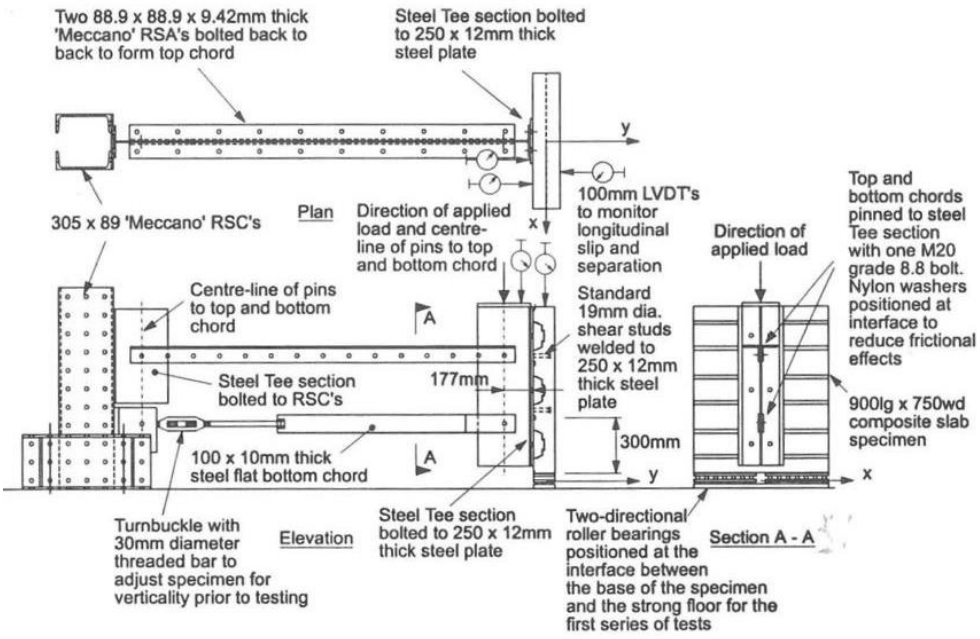

Fig 2.18 Single-sided Push-out Test setup by Hicks and McConnel (1996)

To compare the Single-sided Push-out test and conventional test setups, two specimens were subjected to testing in accordance with the British code. The failure modes observed in both the Single-sided Push-out test and the conventional test were found to be identical, demonstrating that the lateral bracing system in the former effectively mitigated any adverse effects arising from eccentric loading. Further, to understand influence of boundary conditions, specimens with a two-directional roller base (boundary condition (a)) exhibited ultimate strengths that led both the Eurocode and British code to overestimate the true strengths. However, conclude that such two-directional roller base conditions did not precisely replicate the loading conditions experienced in a composite beam, as seen the separation between the slab and the deck. Specimen with a one-directional roller (b) boundary condition also resulted in overestimations of strengths according to Eurocode 4 and the British code. Nonetheless, this overestimation was of a lesser magnitude when compared to the first (a) boundary condition. This can be attributed to the restriction imposed on the specimen and consequently reducing the separation between the slab and the deck. Next, comparing specimens with boundary conditions (c) and (d), both of which exhibited favorable

agreement with the British code, with specimen with boundary condition (d) displayed a strength 10% higher than that of (c). Lastly while investigating the effect of added reinforcement Hicks and McConnel (1996) observed the specimen with boundary condition (b) gave similar results identical specimen with boundary condition (c). This concluded that the friction force present between the slab and floor played a significant role in enhancing the strength of the specimens. The magnitude of this friction force relied on the specific conditions of the floor where the specimens were tested. This variability in the floor conditions across different laboratories thus explaining the wide range of data scatter observed in previous tests. Therefore, it was suggested the implementation of a one-directional roller (boundary condition b) during testing. This approach aimed to eliminate the influence of the friction force, thus ensuring that the data obtained would be more reliable and comparable across different experimental setups.

Chan et al. (1985) conducted 42 tests on a horizontal setup to understand the behavior of headed shear studs in a stub girder system to observer the effect of prying action of concrete due to shorter length of available concrete slab. Chan et al. (1985) also studied the behavior of headed shear studs in relation to parameters such as the concrete flute length, transverse reinforcement, stud size and configuration and method of stud installation. The setup used in shown in Figure 2.18.

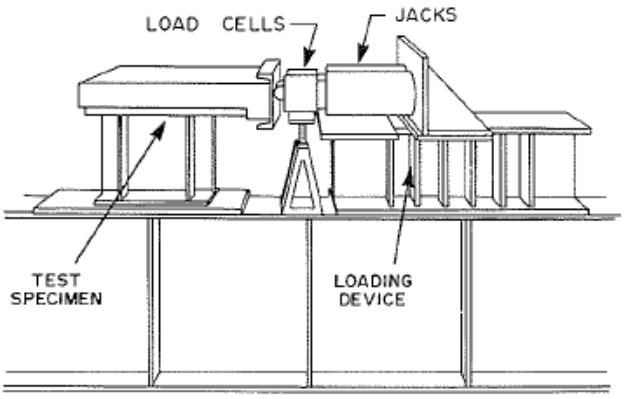

Fig. 2.19 Test Setup by Chan at al. (1985)

The stud assemblage (specimen) was attached to a rolled I section which acted as the test bed which also held the loading setup. The loading assembly consisted of two Enerpac hydraulic rams operated against a rigid support subjecting all specimens to a symmetrical two-point loading. To measure the applied shear load, a pre calibrated load cell was placed between each ram and the specimen. Vertical uplift and slip of the concrete were measured by three mechanical dial gauges and slab rotation was measured by water-bubble type clinometer placed on the concrete slab at the location of first stud. As seen in the Figure 2.18 the specimen consisted a concrete block with no deck in the front few lengths for equal distribution of force similar to the specimens in push-out test to have full bearing on the ground. Chan et al. (1985) saw the increasing the overhang length (length ahead of the stud) increased the prying action and thus reduced the stud strength. Transverse reinforcement slightly increased the stud capacity and welding the headed shear studs through the deck was better the stud welded directly to the flange.

Lam (2000) developed a new similar horizontal (Figure 2.19) setup as Chan at el. (1985) to determine the shear strength of headed shear studs in composite beam with precast concrete hollow cored floor slabs. The setup consisted of a 254 x 254 x 73 UC (I shaped steel section) on which the loading apparatus as well as the specimens was set. The test specimens each consisted of four 23.5 in. wide x 31.5 in. long prestressed hollow core units (hcu) with single row of pre-welded headed shear studs to the same 254 x 254 x 73 UC section. Horizontal load was applied by two hydraulic jacks and spreader beam was used to produce uniform distribution of load on the specimen. A single load cell was used to measure the applied load. Linear voltage displacement transducers (LVDTs) measured strains in the tie bars as well as horizontal slippage between the slab and the beam at the specimen's end.

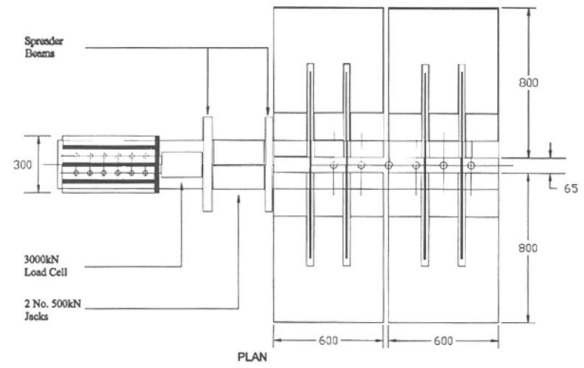

Figure 3 Plan of proposed push off test

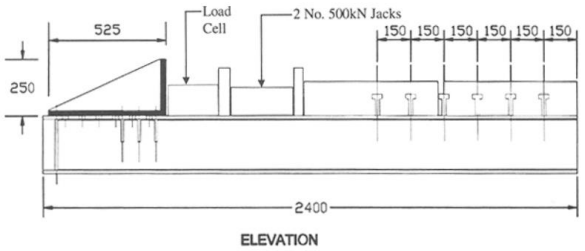

Fig. 2.20 Test setup by Lam (2000)

Lam (2000) said the advantages of this setup over the convention push-out test were that this setup could be used for other type of slabs and different shear connectors, the possibility of weaker slab failing first in the conventional setup is eliminated as the new setup uses one slab per specimen. The friction force between the base of the slab and floor is eliminated. He also verified the new setup with conventional setup and saw the results were compatible.

Lowe et al. (2014) carried out a finite element analysis for understanding the failure mode at the shear stud-concrete connection. He modeled half of the composite beam specimen which would accurately represent the full test specimen. The setup (Figure 2.20) was a modified version of Gillies et al. (2006). The load was applied to the I beam form one side and the concrete was held against a reaction beam on the other side. This created slight eccentricity in shear transfer but it was found to have negligible effect on stud strength and strength. They believed that the advantage of this configuration is that there is only one interface where slip might occur, as

opposed to two in a standard push-off test. When the behavior moves from linear to nonlinear in a conventional push off-test, the force distribution in each contact is unknown, and acceptable data cannot be derived after nonlinear behavior is recognized.

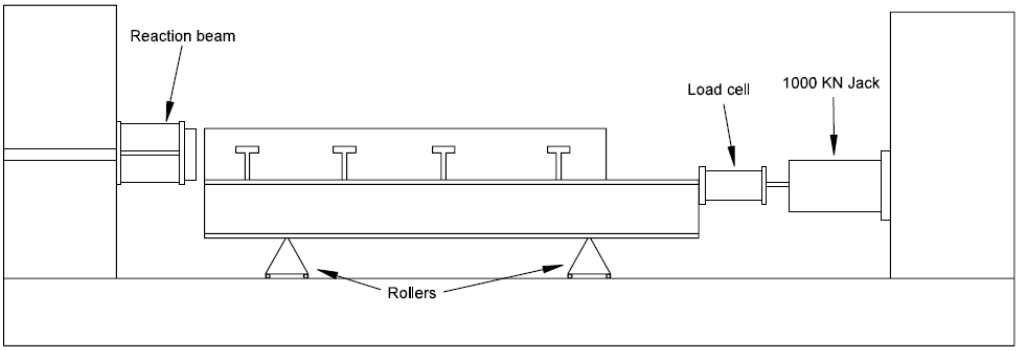

Fig. 2.21 Test setup used by Lowe at al. (2014)

Briggs et al. (2021) used a horizontal push-out test setup (Figure 2.22) to explore the cyclic behavior and strength of the composite concrete-filled steel deck diaphragm system. This test design differs from conventional pushout test arrangements in that it contains four sets of studs along the length as opposed to the typical one or two studs. This made it possible to conduct a more in-depth analysis of the distribution of shear transfer throughout the length as a result of cyclic loading, as would be observed in a collector in a diaphragm. The gravity loading was also applied with a actuator in a more controlled manner as opposed to hydraulic jack in a conventional test setup. The specimen beam was supported by three rollers and the concrete slab was restrained laterally as seen in Figure 2.22. The two horizontal actuator one at each edge of the specimen acted anti-symmetrically to impart the monotonic or cyclic loading. The vertical actuator applied the normal load equal to 10% of predicted shear load of the specimen.

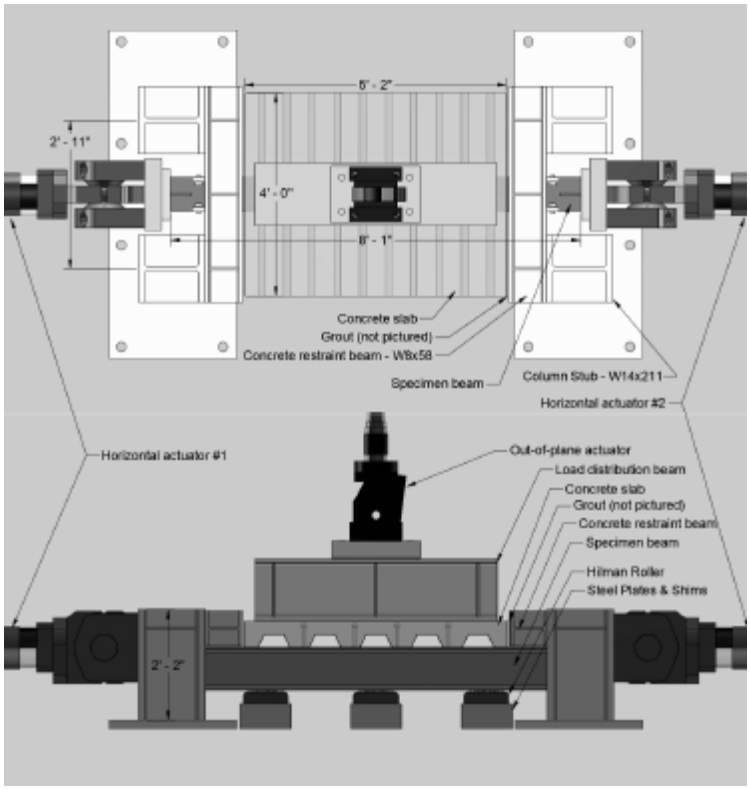

Fig. 2.22 Push-out test setup by Briggs et al. (2021)

Ernst et al. (2010) and Ernst (2006) introduced a horizontal one-sided push-out test, as depicted in Figure 2.23 of their work. The test setup comprised a vertical test frame with two horizontal actuators, responsible for applying the load to the loading beam. This loading beam was responsible for transmitting the applied load to the sliding steel section. To facilitate horizontal movement while preventing vertical uplift, the sliding steel section was positioned on two Teflon sliding bearings. For the experimental configuration, the specimen was affixed to the sliding section using a pre-hold connection plate. The end restrains were designed to load a specific area of the slab, simulating the concrete compression zone or the recess typically found in standard Eurocode 4 specimens (Figure 2.7). To ensure uniaxial support, the horizontal force was transferred to a hardened steel plate via five rollers. Considering the eccentric loading, vertical movement was restricted by four steel plates—two on each flange—that were securely bolted to

the transverse beam. If required, these vertical restraints could be removed to investigate the effects of uplift on shear connectors

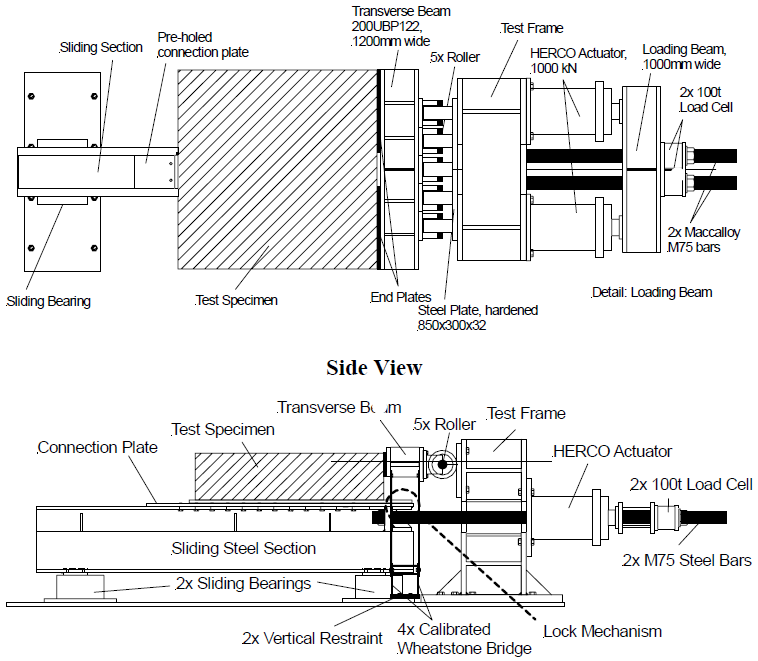

Fig. 2.23 Horizontal Push-out test rig by Ernst (2006), Ernst et al. (2010)

2.7 Full Beam Composite Test

Even though tests are conducted to understand the behavior of headed shear studs in shear using the conventional push-out test or any other setup. These need to be validated by full-scale beam test to accurately corelate the behaviors observed in these tests to depict the real-life composite beams. This section summaries some of the full-scale composite beam test conducted by research in the past.

Robinson (1967) carried out 15 Full scale beam tests having cellular deck configuration to study influence of different rib proportions on the failure modes and load capacity of the beams. He used rib heights caring from 1.5 in. to 3 in. with concrete over deck 1.5 in thick. The beams varied from 90 in. to 166.5 in. long with two-point loading. Comparing the results of beams having deck removed before loading to ones having deck, he saw that the deck significantly contributes

to the strength and stiffness of the connections causing spreading of the yield zone. He also saw that the strength of the beams was proportional to the square of the width and inversely proportional to the square root of the height of the cellular rib geometry. There was no significant difference in the behaviors of the beams due to difference in diameter and spacing of the headed shear studs. None of the beam failed due to stud shearing. All beams failed due of inadequate shear connection. Crushing or spalling of the concrete occurred in some instances but was a secondary effect occurring after large deformations, and was confined to the region of the load points.

Fisher (1970) discovered that for rib heights up to 1.5 in., there is no appreciable drop in beam stiffness in the working load range as long as the compressive stress block does not reach below the top of the rib corrugation. The rib height had no significant effect on the ultimate flexure capacity too. But the beams with 3 in. rib height didn't develop the predicted ultimate capacity. The flexure capacity of the beam reduces as rib height increases due to a reduction in shear connection strength. Robinson (1967) relation of rib geometry to the strength of the beams matched with his results too except for specimens having Lightweight concrete. The reduction in the strength of beams having Lightweight concrete was proportional to the square root of the ratio of the moduli of elasticity of lightweight to normal weight concrete. The ratio of rib width to the rib height effected the strength of the shear connectors which in turn effected the flexure capacity. Based on the observation the Fisher (1970) gave the following equation for the shear stud strength for rib height up to 3 in as.

$$Q_{rib} = 0.5\frac{w}{h}Q_{sol}\sqrt{\frac{E_{cl}}{E_{cn}}} < Q_{sol} \tag{2.56}$$

where, Q_{rib} = strength of a stud in formed metal rib deck

Q_{sol} = AISC allowable horizonatal shear load in ASTM C33 agregates

$\frac{w}{h}$ = Ratio of rib width to rb height

$\frac{E_{cl}}{E_{cn}}$ = Ratio of moduli of elasticity of lightweight to normal weight concrete.

Further, depending on the rib height and the depth of the concrete compression block he gave provisions for flexure capacity calculations of the beam. Continuing the study Grant at al. (1977) conducted 17 Full scale beam tests having lightweight concrete, ¾ in. dia. Shear headed shear studs. The beams varied in ratio of rib width to rib height from 1.5 to 2. Most beams were designed for 80% partial shear connections and a few below 50%. The beams were 24ft. or 32 ft simply supported. Four-point loading was used. All of the test beams had maximum deflections ranging from 8 to 22 in. The creation of a plastic hinge near the midspan in all of the beams allowed for such enormous deflections. The final strength of individual connection groups varied greatly, as seen by the connector force vs slip curves of one beam. However, all displayed ductile behavior, allowing for force redistribution across the slab and hence a ductile composite beam. This force redistribution allows the beam's average connection capacity to be predicted. The equation given by Fisher (1970) was inadequate for rib height of 3 in. and conservative for rib height of 1.5 in. and so a new equation was given (eq. 2.55). Fisher (1970) also stated that by assuming that the slab force acts at the mid-depth of the solid component of the slab above the ribs rather than the centroid of the concrete stress block, the flexural capacity of a composite beam with formed steel deck can be evaluated more precisely and conservatively.

McGarraugh and Baldwin (1971) also conducted 6 composite beam tests with two different types of lightweight concrete along with a theoretical analysis to study the effects of degree of shear connection and modular ratio of concrete to steel. The beams were either designed to have 50% shear connectors to ensure shear connector failure or have adequate shear connectors. Loading was applied with four independent hydraulic rams. For beams with 50% shear connectors

equal quarter-point deflections were used to control the loading whereas the beams with adequate shear connectors were loaded to their working load and sustained for the test period. Based on the results compared with the theorical analysis McGarraugh and Baldwin (1971) concluded that composite beams with lightweight concrete is as effective as normal weight concrete and their behavior can be predicted with satisfactory accuracies with theoretical analysis. Also, the design procedures for normal weight concrete may be utilized to select the beam cross section for lightweight concrete based on the lightweight concrete's actual modular ratio.

Jayas and Hosain (1989) conducted four full scale composite beam tests to study the failure modes for simply supported composite beans and verify the push-out test conducted by Jayas and Hosain (1988). All specimen used 3 in. deck with total slab thickness of 6 in. have ¾ in dia shear headed shear studs 5 in. long. Three beams were around 13.5 ft long and one beam was 6.25 ft long. 13.5 ft long beam first tested had a width of 4 ft which observed rib shear failure and so the width was increased to 6.9 ft for the next two beams having a length on 13.5 ft. Each beam was mounted on roller supports and two rams operated by a single hydraulic pump applied the load to the beam with help of spreader beams. Concrete pull-out failure was observed in all the beams except for the rib shearing observed in the first beam. A linear relationship was observed between load and deflection up till the initiation of the cracks around the headed shear studs. The predicted flexure capacity calculated considering the shear strength of the headed shear studs in concrete pull-out failure were in good agreement with the test results. Further comparing two beams identical except for the headed shear studs spacing due to variation in deck geometry Jayas and Hosain (1989) saw that the stud capacity in concrete pull-out failure is a function of deck geometry and stud layout. Also, the effective stiffness calculated using CSA CAN3-S16.1-M84 was reliable when predicted and test deflections were compared.

Easterling at al. (1993) conducted four composite beam tests to understand the headed shear studs in strong vs the weak position and also compared then with the then AISC LRFD specifications equations. All four beams had a length on 30 ft. with 3 in. steel deck and 6 in. total slab thickness having ¾ in. dia. 5 in. long shear headed shear studs. The specimens only different in the position of the headed shear studs. Four-point loading system was used. The beams with headed shear studs in strong or alternate strong and weak position remained elastic up to 0.6 of predicted moment strength while the beam with headed shear studs in weak position remailed elastic up to 0.4 of predicted moment strength. Strong position headed shear studs failed by forming concrete shear cones or shearing off in the shank. Weak position headed shear studs failed by punching through the deck rib with no major shear cone in the concrete or shearing in the stud shank. The stud strengths were comparable to the push-out test conducted by Easterling at al. (1993) previously, but weren't comparable with the then AISC equations.

Nie at al. (2008) conducted composite beam tests to understand the variation in strength with respect or the degree of composite action, behaviors of continuous composite beams and simply supported beams under negative bending. The series of simply supported beams under positive bending varied in the degree of shear connection from 0.25 to 1.85. These beams saw a linear elastic behavior before the bottom fiber of the steel beam yielded. For beams with degree of shear connection more than 0.5 full strength of concrete achieved with sufficient ductility of the headed shear studs but for beams with degree of shear connection less than 0.5 the rupture od headed shear studs governed the strength of the beams. For simply supported beams with negative bending Nie at al. (2008) saw the longitudinal strain of reinforcement and the steel above the yield strain with some buckling of the steel web at failure loads. They also observed the cracks to be coinciding with the trough spacing of the steel decks. For continuous beams Nie at al. (2008) saw

three stages in the load vs deflection curves. First the linear behavior until no cracking in the negative bending region, second with the initiation of cracks in the negative bending region continued to the steel at the critical location began to yield and third the nonlinear behavior with the steel beginning to yield and significant moment redistribution.

Ranzi et al. (2009) conducted 2 full scale composite beam tests. The beams were 26.5 ft long, 6.5 ft wide simply supported. It has 3 in. Trapezoidal deck with total slab thickness of 5 in. One beam having one stud per rib and other having two headed shear studs per rib having degree of shear connection of 0.39 and 0.48 respectively. The shear headed shear studs were 3/4 in. diameter and 4.5in. in height. The beams were tested by applying 16-point loads. The Beam with 0.39 degree of shear connection was first tested at 20 days age of concrete and then again reloaded at 27 days age of concrete while the other beam was tested just at 27 days age of concrete. The beams tested on two different days shows similar behavior with their concrete compressive strength also not varying significantly. The second beam shows significant beam displacement along the beam length indicating a ductile behavior. The moment capacities calculated with Eurocode EC4 underestimated the beam strength and showed ductile response even though the degree of shear connection were less than 0.5.

2.8 Current AISC Provision for Headed Shear Studs in Composite Beam

The AISC 360(2022) gives provision to calculate the strength of the headed shear studs as,

$$Q_n = 0.5A_{sa}\sqrt{f'_c E_c} \leq R_g R_p A_{sa} F_u \tag{2.57}$$

$A_{sa} = \text{cross} - \text{sectional area of steel headed shear studs}, in.^2$ f'_c

$= \text{conrete compressive strength, ksi}$

$E_c = \text{modulus of elasticity of concrete, ksi}$

$F_u = \text{specified minimum tensile strength of steel headed shear studs, ksi}$

$R_g = 1.0$ one headed shear stud welded in deck rib with deck perpendicular to the beam

or any number of headed shear stud welded in directly to the beam

o*r a*ny number of headed shear stud welded in deck rib with deck parallel to the beam with rib width to rib depth ≥ 1.5

$= 0.85$ two headed shear stud welded in deck rib with deck perpendicular to the beam

or one headed shear stud in deck rib with deck parallel to the beam with rib width to rib depth ≥ 1.5

$= 0.70$ three or more headed shear stud welded in deck rib with deck perpendicular to the beam

$R_p = 0.75$ headed shear stud welded directly to the beam

or headed shear stud welded in deck rib with deck perpendicular to the beam with $e_{mid-ht} \geq 2\ in.$

$R_p = 0.60$ headed shear stud welded in deck rib with deck perpendicular to the beam with $e_{mid-ht} < 2\ in.$

2.9 Summary

Composite beams with headed shear studs as shear connectors have been extensively studied in the past literature. The evaluation of these shear studs has often involved the use of push-out tests, which have been employed since several decades. The initial utilization of push-out tests can be traced back to Viest (1956), and subsequent researchers have employed them to gain insights into the behavior of headed shear studs in composite beams, alongside full-scale beam tests. Over time, modifications and standardization efforts have been made to enhance the representation of actual composite beam behavior in push-out tests. Nevertheless, the complexity associated with the test setup poses challenges that can occasionally affect the test results.

Consequently, some researchers have explored alternative test setups to evaluate the performance of headed shear studs, finding comparable results to those obtained from full composite beam tests. This study aims to address the challenges encountered in conventional push-out tests and proposes the development of a new test setup. The primary objective of this new setup is to overcome some of the limitations of push-out tests, while simultaneously representing the stress states in the concrete surrounding headed shear studs in composite beams. By doing so, a more comprehensive evaluation of the behavior of headed shear studs can be achieved.

Further, In the current provisions of the AISC (American Institute of Steel Construction) code, the strength prediction for headed shear studs permits the use of a steel deck with a maximum height of 3 in. This limitation is a result of previous research that primarily focused on composite beams utilizing decks with a maximum height of 3 in. Unfortunately, there are limited research conducted on composite beams with decks deeper than 3 in. However, 3.5 in. and 4 in decks are already been manufactured and utilizing these deeper decks in composite beams could potentially reduce erection time and costs. However, due to the lack of comprehensive investigation in this area, there exists a research gap that needs to be addressed. Consequently, a preliminary investigation has been undertaken to study composite beams with 3.5 in. decks.

3. Test Setup and Instrumentation

Chapter 2 highlights that most testing programs on shear stud strength in composite beams have focused on a steel deck with a maximum rib height of 3 in. using the conventional push-out testing frame. This study aimed to assess the current test setup and develop a new setup to address the challenges identified in the literature during push-out testing. Additionally, the AISC Specification (AISC 2022) permits a maximum rib height of 3 in. for steel decks in composite beams and so a preliminary investigation was conducted to examine the feasibility of using 3.5 in. steel decks in composite beams.

3.1 Test Matrix

The testing program consists of a total of 33 specimens with 11 specimen groups as seen in Table 3.1. The first two rows in the test matrix shows two test groups using a conventional push-out test setup (AISI S923-20), while the remaining rows except the T3.0A-4N-W-SS are run using the shear test setup described further in this chapter. The shear test setup was further evaluated and single-sided push-out test setup was developed as tested in group T3.0A-4N-W-SS.

Table 3.1 Test Matrix

Group	No. of Specimen	Test setup	Deck[2] Profile	f'_c,[1] ksi	Stud Configuration
D3.5A-3N-C-PO	3	Push-Out	DT1	3NW	Centered
D3.5A-3N-2S-PO	3	Push-Out	DT1	3NW	Two studs
T3.5A-3N-S-ST	3	Shear	TZ1	3NW	Strong
T3.5A-3N-W-ST	3	Shear	TZ1	3NW	Weak
T3.5A-3N-2ST-ST	3	Shear	TZ1	3NW	Two Staggered
D3.5A-3N-C-ST	3	Shear	DT1	3NW	Centered
D3.5A-3N-2S-ST	3	Shear	DT1	3NW	Two studs
D3.5B-3N-S-ST	3	Shear	DT2	3NW	Strong
D3.5B-3N-W-ST	3	Shear	DT2	3NW	Weak
T3.0A-3N-W-ST	3	Shear	TZ2	3NW	Weak
T3.0A-4N-W-SS	3	Single-sided Push-out	TZ2	4NW	Weak

Note:
1. 3NW: 3ksi Normal weight concrete; 4NW: 4ksi Normal weight concrete
2. For deck notation refer to Table 3.2

The two groups D3.5A-3N-C-PO and D3.5A-3N-2S-PO using the push-out test will help to give a correlation with groups D3.5A-3N-C-ST and D3.5A-3N-2S-ST which consist of a similar deck and stud configuration, but use the shear test setup. Further running tests on the shear test setup and identifying the challenges with the new setup it was modified and T3.0A-4N-W-SS group was run on the single-sided push-out test setup. Test groups T3.0A-3N-W-ST and T3.0A-4N-W-SS used 3 in. trapezoidal deck and will be used to understand the new test setup and how well it relates to past literature.

The group notation used in the test matrix describes the variables selected and in the following order: deck type (D for dovetail and T for trapezoidal); deck height in inches; deck manufacturer (A or B); nominal concrete compressive strength in ksi; type of concrete (N for normalweight or L for lightweight); stud configuration (see Figure 3.1 for options); and test setup (PO for push-out test setup, ST for shear test setup and SS for single sided push-out test setup).

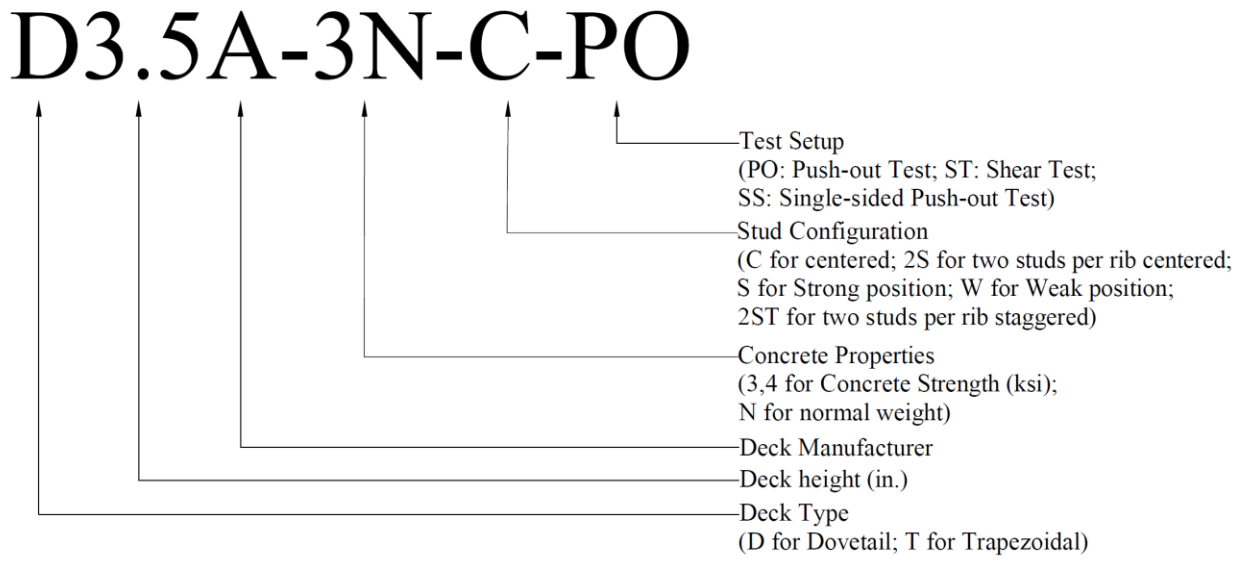

Fig. 3.1 Specimen Notation

3.2 Push-out Test Setup

The experimental setup was in accordance to AISI S923-20 (Figure 3.2). The two groups D3.5A-3N-C-PO and D3.5A-3N-2S- PO used the push-out test. This set of total six specimens are used to compare to the shear test setup. A downward force using a hydraulic ram bearing on a swivel plate was applied to the steel section and the base of the specimen was supported by two elastomeric pads to encourage that the load was level and evenly distributed creating a shear force in the headed shear connectors. The steel section consists of two WT's bolted together. Using two WT's one for each slab of the specimen allowed horizontal casting of the specimens. Using a hydraulic ram and yoke, a normal load (10% of the applied axial force) was applied to the test specimens.

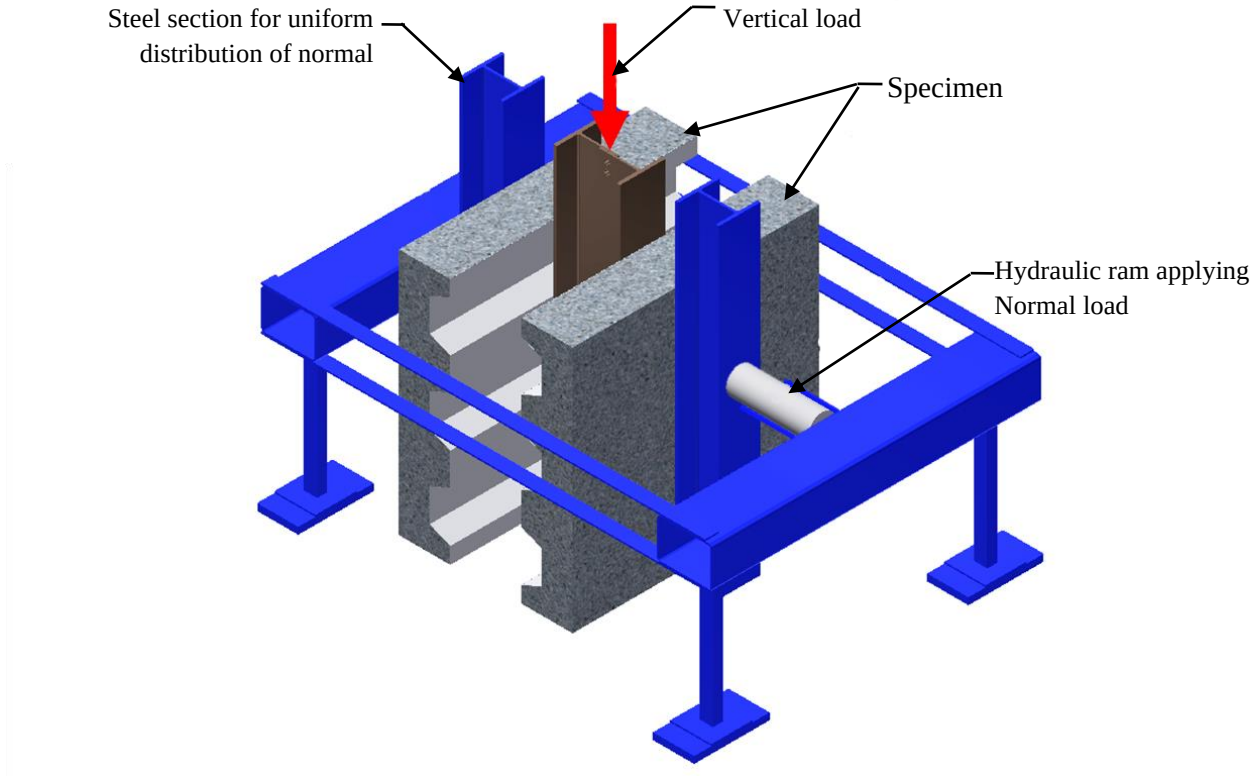

Fig. 3.2 Push-Out Test Experimental Setup

3.3 Shear Test Setup

The setup consists of two side beams as part of the self-reacting frame using W 18 x 86, which are attached on one end to a reaction block consisting of a W 14 x 120, with bolted connection. The two W 18 x 86 were coped (Figure 3.4 (b)) to attach WTs of the specimen. The reaction block hosts the servo-controlled hydraulic actuator with capacity of 110 kips and was shored up with wooden supports. Loading was introduced by the actuator pulling the W 12 x 50 of the specimen thus testing the headed shear studs welded to it. The use of one slab specimen than the two slabs in the push-out test will reduce the bias in the data. Attaching the specimen to the side eliminates the need to provide the even bearing required in the push-out test. This will also eliminate undesirable failure modes like the back-breaking (buckling) of the slab and rotation of the setup.

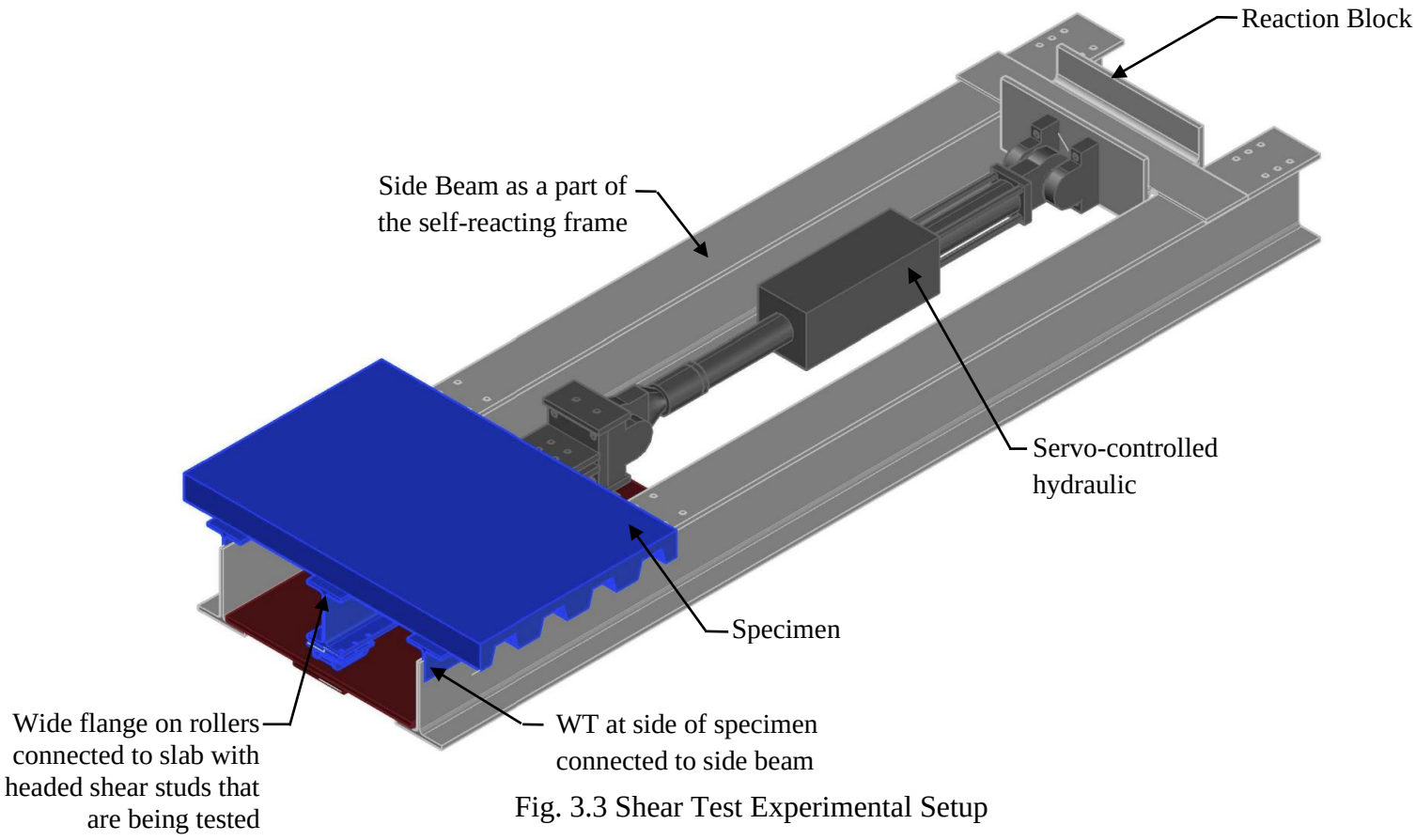

Fig. 3.3 Shear Test Experimental Setup

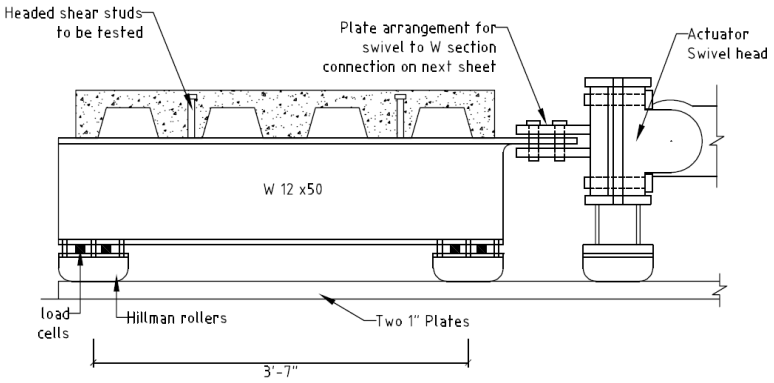

a) Section at the center of the specimen

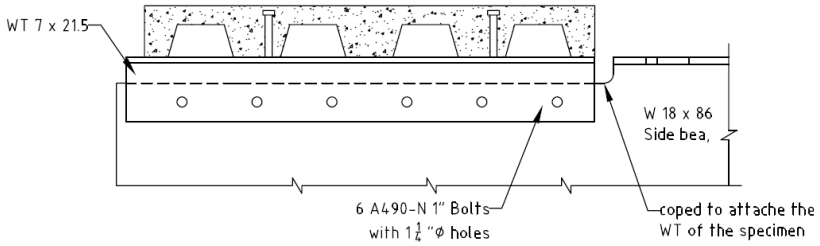

b) Section at the end of the specimen

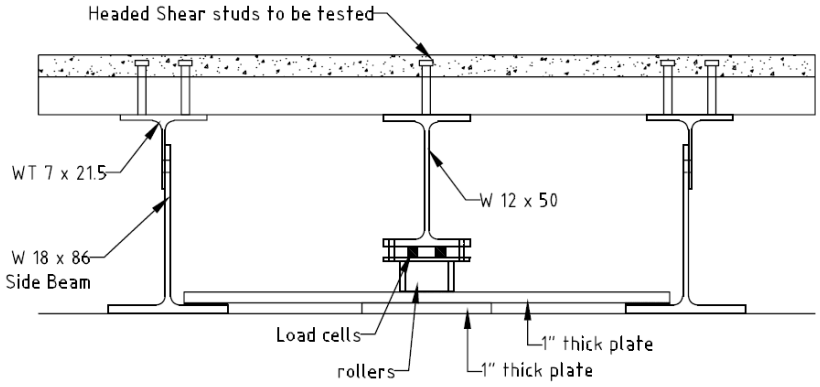

c) End view of the setup

Fig 3.4 Setup to specimen connection details

3.4 Single-sided Push-out Test Setup

The setup was altered based on the shear test setup described in Section 3.3. However, some modifications were made to accommodate the desired experimental conditions. The main components of the modified setup include a side beam, a reaction block positioned at the back, and a servo-controlled actuator used to apply the shear force. To encourage even concrete bearing, a W section arrangement was incorporated at the front of the setup. This arrangement helps distribute the load evenly across the concrete surface. In addition to the above modifications, a separate steel frame was introduced and placed on top of the specimen. This steel frame was connected to the strong floor and utilized an Enerpac jack to apply a normal load on the specimen. By applying a normal force in this manner, the boundary conditions created in the setup resemble those typically encountered in conventional push-out tests described in Section 3.2.

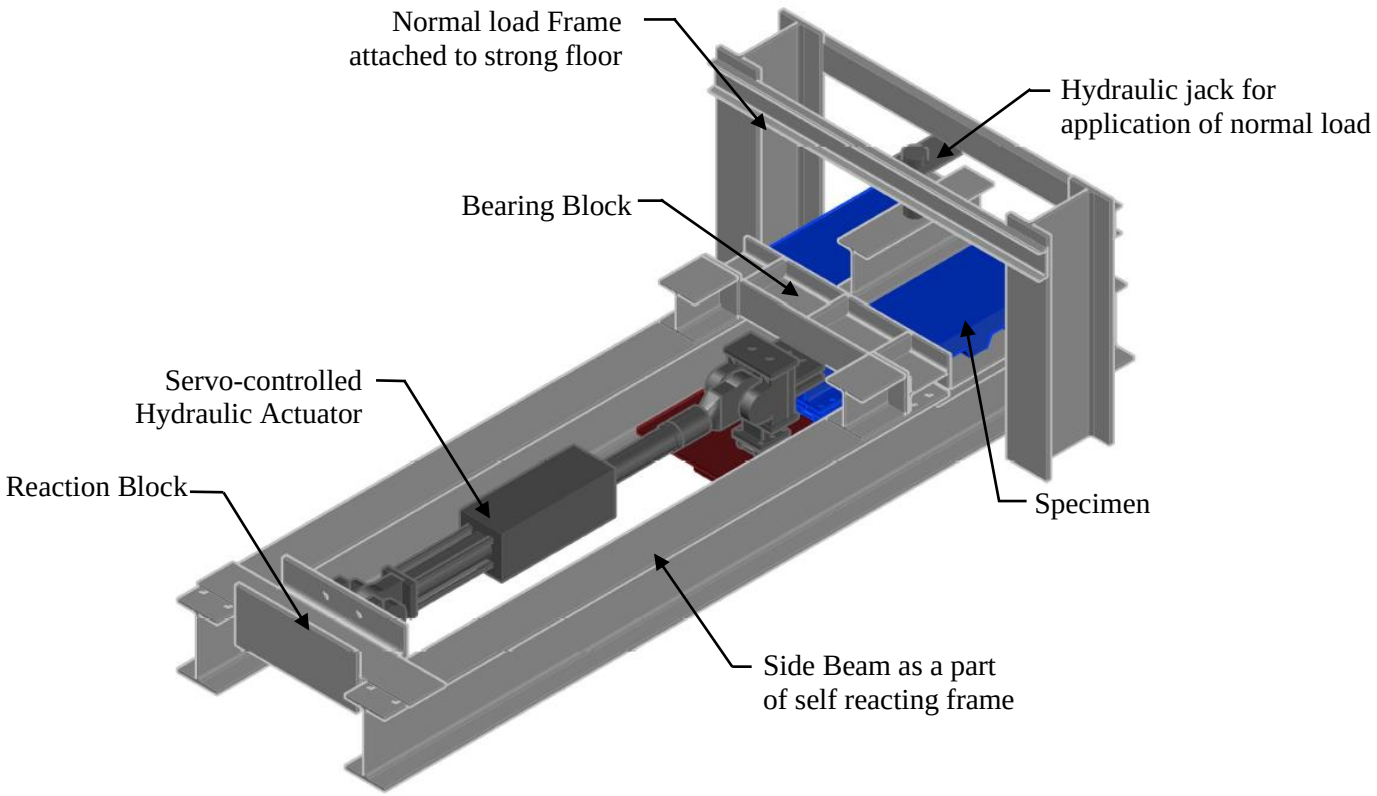

Fig. 3.5 Single-sided Push-out Test Experimental Setup

3.5 Specimens

The different steel decks and stud configuration used in these specimens are shown in Table 3.2 and Figure 3.6 respectively. For the DT1 profile, both centered studs and two studs per rib centered positions were employed. This configuration was feasible because there was no stiffener present in the center of the rib. Other profiles, namely DT2 and TZ2, featured a stiffener at the center of the rib, and hence, the strong, weak, and two studs staggered positions were tested with these profiles. As for the TZ1 profile, it was specifically manufactured for the study, as a 3.5 in. trapezoidal deck are not produced. It was assumed that the TZ1 profile would possess a stiffener at the center of the rib if it were to be further manufactured for construction use and so strong, weak and two stud staggered configurations were employed.

Table 3.2 Deck Profiles

Deck Notation	Deck Name	Profile
DT1	EPICORE EC3.5	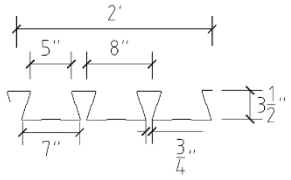
DT2	Versa-Dek 3.5LS	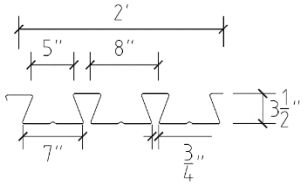
TZ1	-	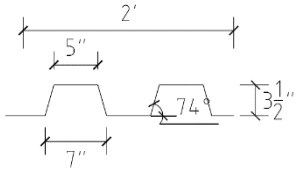
TZ2	W3-36 Formlok	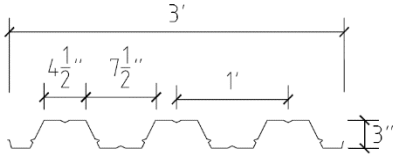
Note: The TZ1 were manufactured specifically as 3.5 in. Trapezoidal deck isn't being produced		

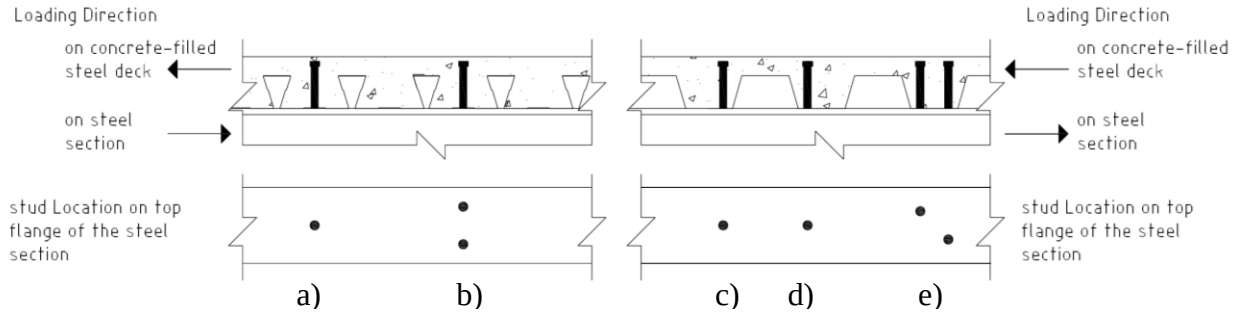

Fig. 3.6 Stud configurations
a) centered b) two studs centered c) weak position d) strong position e) staggered

3.5.1 Push-out Test Specimen

Specimens consist of two 38 in. x 48 in. concrete-filled steel deck slabs each attached to a WT 6 x 17.5, 4 ft 8 in. long. The steel deck was oriented perpendicular to the beam. Headed shear studs with nominal ultimate strength, f_u = 65 ksi and ¾ in. diameter were used. To avoid slab buckling, No.5 rebars were used one on each side of the slab. In accordance with the AISC Specification (AISC 360) minimum height of studs above the deck, 5 in. long headed shear studs were used with a total concrete thickness of 5.5 in. Two or four headed shear studs were welded to each WT 6 x 17.5 based on the configuration of centered or two headed shear studs per rib. Each of the two half specimens i.e., 38 in. x 48 concrete-filled steel decks attached to WT 6 x 17.5 were attached with a bolted connection.

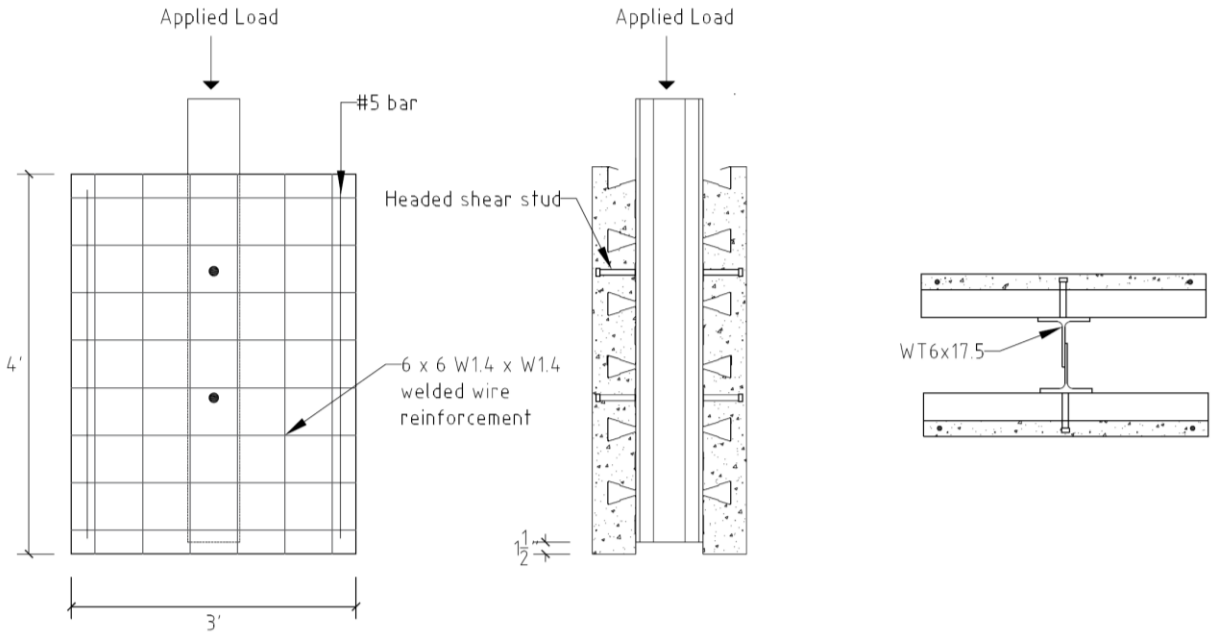

Fig. 3.7 Typical Push-out Test Specimen

3.5.2 Shear Test Specimen

All specimens consist of a 48 in. x 72 in. concrete-filled steel deck except for 3in. trapezoidal deck consisting of 36 in. x 72 in. concrete-filled steel deck this is because 3 in. trapezoidal deck had a coverage of 36 in. and each specimen consisted of one deck sheet while other decks used had a coverage of 24 in. so two sheets were used. Each specimen had two WT7x21.5 attached at the sides and a W12x50 at the center. The decks were oriented perpendicular to beam. Each of the two WT7x21.5 was attached to W18x86 with the bolted connection. The W12x50 was coped at the front end and a loose bolted connection was made with the plate arrangement that was attached to the actuator swivel. Headed shear studs with nominal ultimate strength, f_u = 65 ksi and ¾ in. diameter were used. One or two No.5 rebars were used as tension chord (Figure 3.8(a) and Figure 3.9(a)) to avoid flexure failure and one No.5 rebars were used on both side of specimen to avoid transverse cracking in the specimen. In accordance with the AISC Specification (AISC 360) minimum height of studs above the deck, 4.5 in. and 5 in. long headed shear studs were used with a total concrete thickness of 5 in. and 5.5 in for 3 in. and 3.5 in steel

decks respectively. For 3.5 in. steel deck specimens 6 headed shear studs were welded to each WT7x21.5, whereas for 3 in. trapezoidal decks 4 headed shear studs were welded to each WT7x21.5 according to the specimen dimensions. Two or four headed shear studs were welded to W12x50 to be tested based on stud configuration. The W12x50 were placed on two rollers to allow lateral translation.

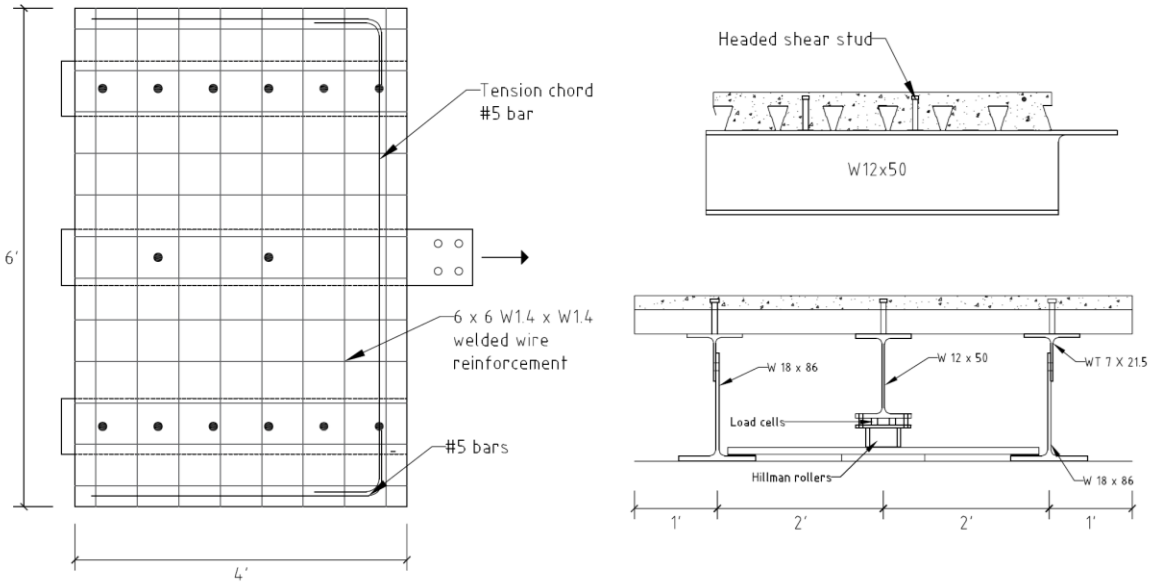

Fig. 3.8 Typical Shear Test Specimen with 3.5 in. steel deck

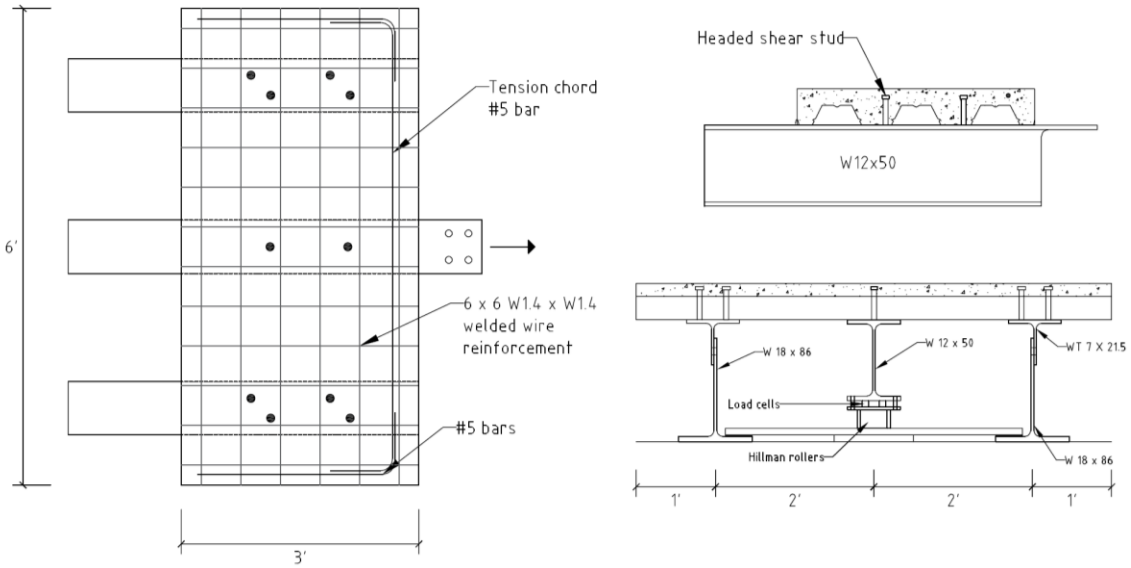

Fig. 3.9 Typical Shear Test Specimen with 3.0 in. steel deck

3.5.3 Single-sided Push-out Test Specimen

The specimen group T3.0A-4N-W-SS which was ran using the Single-sided Push-out test setup consisted of 36 in. x 48 in. concrete-filled steel deck with a W12x50 at the center on which the headed shear studs welded. The W12x50 was coped at the front end and a loose bolted connection was made with the plate arrangement that was attached to the actuator swivel while testing Headed shear studs with nominal ultimate strength, f_u = 65 ksi and ¾ in. diameter were used. The total slab thickness of 7.5 in. was chosen as according to standard 2 hr. fire rating and two No.5 bars were used on both sides of the specimens to avoid any slab buckling during testing.

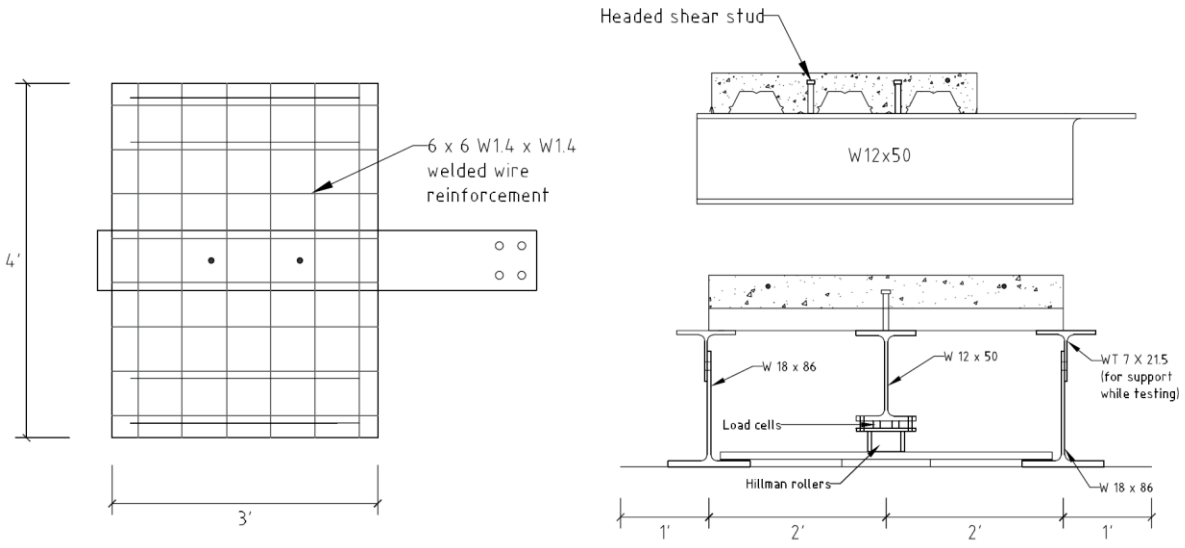

Fig. 3.10 Typical Single-side Push-out Test Specimen

3.6 Instrumentation Setup

3.6.1 Push-out Test

The specimens had four Linear variable differential transducers (LVDT) used to measure the slip between the concrete and the WT's. Prior to concrete pouring, 1 in. diameter holes were made in the steel deck 5 in. away on both sides of the shear headed shear studs. Concrete self-anchor screw was first drilled through a small wooden piece and then anchored into the concrete (Figure 3.12). It was made sure that the wooden piece isn't held against the WT's web. The LVDT's spring-loaded tip was then made in contact with the wooden piece and were attached to the WTs with the help of a magnetic fixture (Figure 3.12) to get the relative slip. A 250-kip capacity load cell was used to measure the load applied at the top of the WT and a 25-kip capacity load cell was used to measure the applied normal load. Four string potentiometers were attached to one of slab as shown in Figure 3.11 to four of the specimens to measure slab buckling which was seen during testing of the initial specimens.

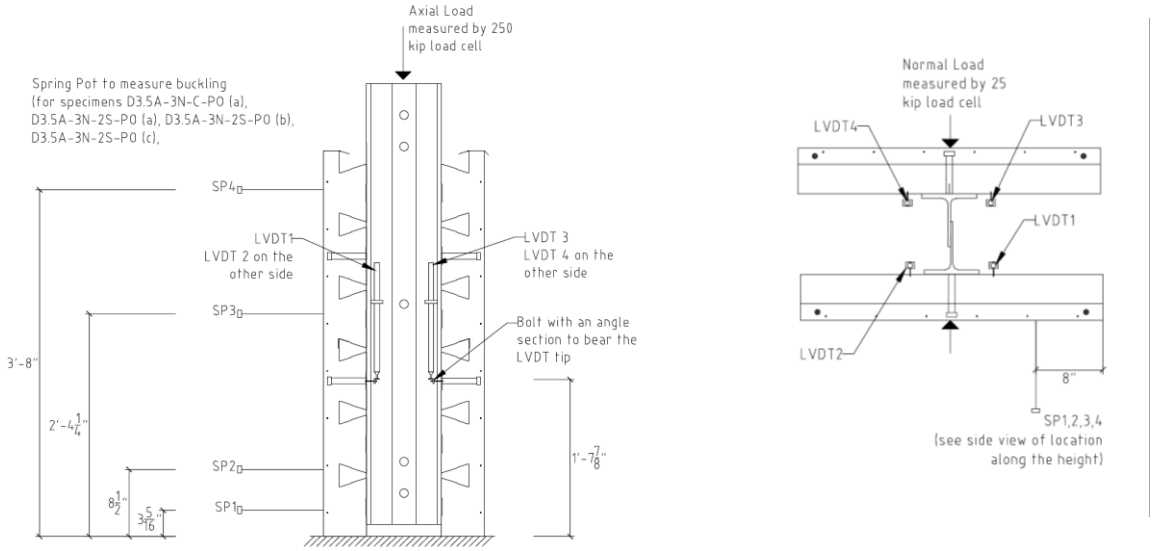

a) Side view b) Plan view

Fig. 3.11 Push-out Test Instrumentation Setup

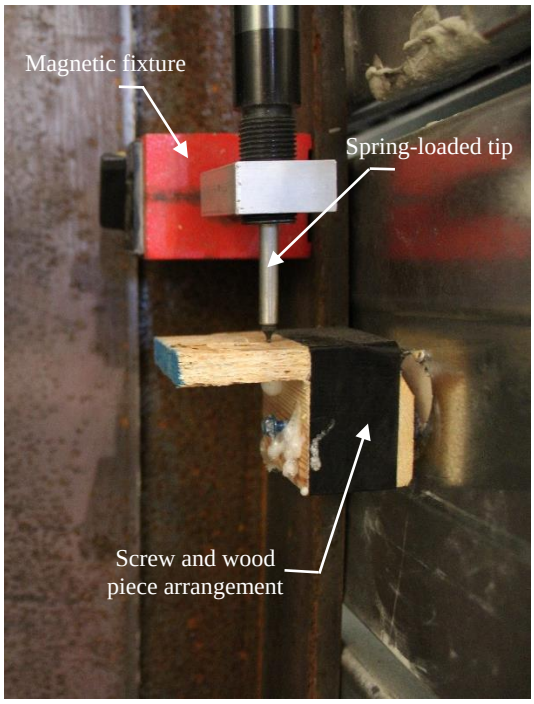

Fig. 3.12 LVDT arrangement in Push-out Test

3.6.2 Shear Test

Figure 3.13 shows the two LVDT's used to measure slip between the concrete and the W section. Prior to concrete pouring, 1 in. diameter holes were made in the steel deck 5in. away on both sides of the shear headed shear studs. A hole was then first drilled in the concrete and a screw was then anchored into the concrete (Figure 3.14). It was made sure that the bolt wasn't touching the steel deck. The LVDT's spring-loaded tip was then made in contact with the angle section attached to the screw and the LVDT was attached to the WTs with the help of a magnetic fixture (Figure 3.14) to get the relative slip. The actuator had an inbuilt load cell which was used to measure the load generated due to the applied displacement. Three load cells each having a capacity of 10 kips were sandwiched between each roller and the W section as seen in Figure 3.13 to measure the normal load generated. Four string potentiometers were used to measure rotation of the specimen or concrete uplift. These string potentiometers were attached to a reference beam that was supported on the ground. Two string potentiometers were connected to the W section with

a magnet and two string potentiometers were connected to the concrete slab with screws drilled into the slab. Each of the string pots connected to the W section and concrete slab was on either side of the specimen as seen in Figure 3.13.

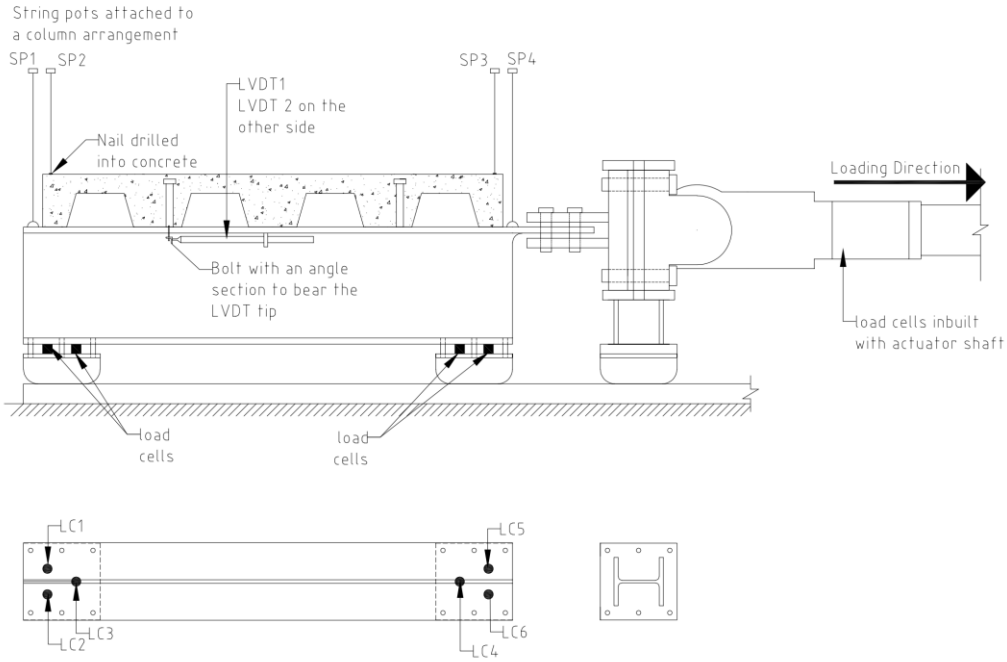

Fig. 3.13 Shear Test Instrumentation Setup

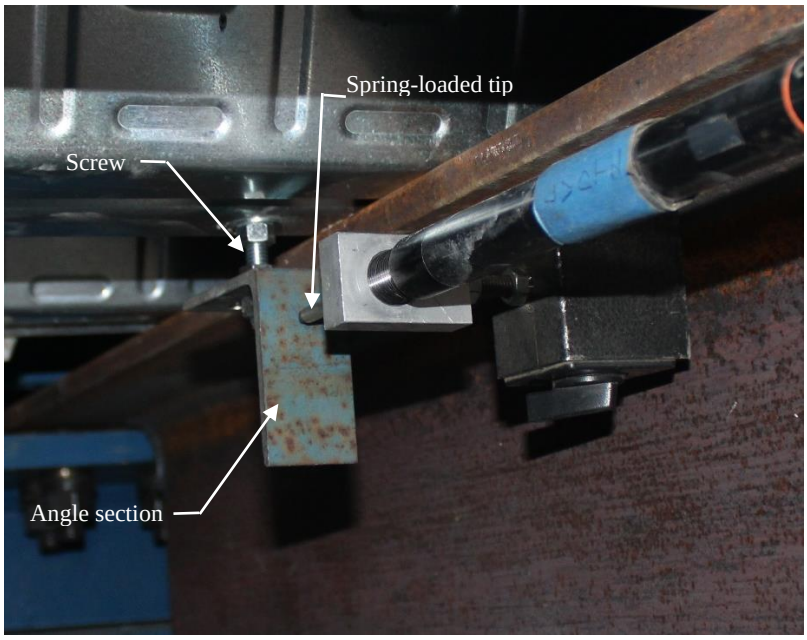

Fig. 3.14 LVDT arrangement in Shear Test

3.6.3 Single-sided Push-out Test

Figure 3.15 shows the specimen have two LVDT's used to measure the slip between the concrete and the W section same as the shear test instrumentation in Figure 3.14. The actuator had an inbuilt load cell which was used to measure the load generated due to the applied displacement. Three load cells each having a capacity of 10 kips same as the shear test instrumentation were sandwiched between each roller and the W section as seen in Figure 3.15 to measure the applied normal load. Four string potentiometers were used to measure any buckling in occurring in the specimen. These string potentiometers were attached to a reference beam that was supported on the ground. The string pots were connected to concrete slab with a help of screws drilled into the slab at 14in. interval leaving 3 in. from the back edge of the slab. They were attached off-center of the specimen as the normal load spreader beam was at the center. They were attached at 10 in from the east edge of the slab.

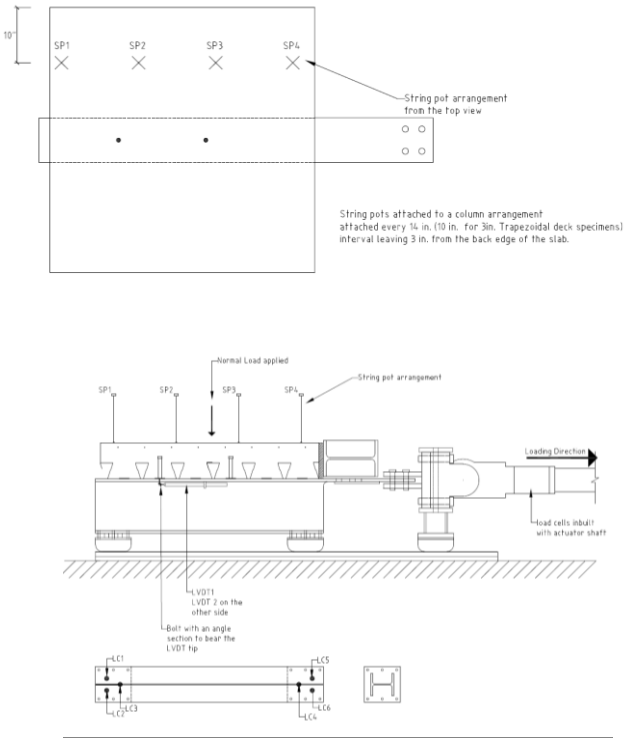

Fig. 3.15 Single-sided push-out test Instrumentation Setup

3.7 Specimen Fabrication

3.7.1 Push-out Test

Wooden framework was created as shown in Figure 3.16 to keep the WT in place. Further, four steel pour stops were attached to the deck with self-tapping screws. The steel deck attached with pour stops was then placed on the flange of the WT in such a way leaving a 1.5 in. gap between the end of the deck and one edge of the WT to allow the slip during testing. The headed shear studs were then welded through the deck to the flange of the WT using a stud welding gun. Holes for the LVTD arrangement were drilled. Two No.5 bars were placed one on each side as shown in figure 3.10 to avoid the slab cracking during testing. These bars had 1 in. concrete cover from the top. Further 6x6 W1.4 x W1.4 welded wire reinforcement was placed having 0.5 in concrete cover from the top. This wire mesh was used to limit shear cracks in concrete. The 0.5 in. cover was so chosen that it is outside the anchorage zone of the shear headed shear studs. After that, the concrete was cast, covered, and moist-cured for 28 days. The pour stop was removed from the slabs, and each pair of corresponding slabs was bolted together via the web of the WTs.

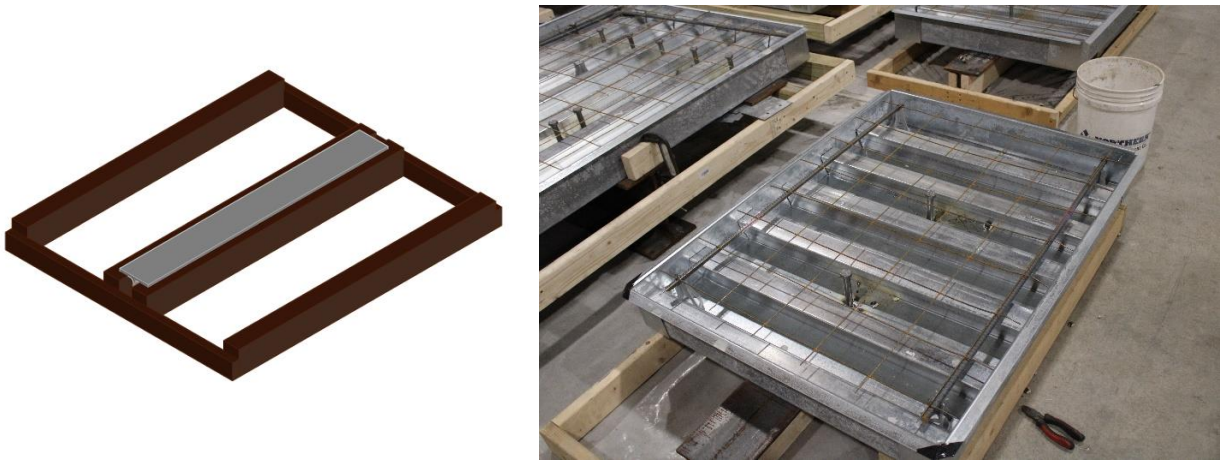

Fig. 3.16 Push-out Specimen Fabrication Framework

3.7.2 Shear Test

A wooden framework was created as shown in Figure 3.11 to keep the two WTs in place and the W section was placed centered in the framework Further, the steel deck was placed on the flange of the WTs and the W section and the pours stops were attached. Holes for the LVTD arrangement were drilled. Two No.5 bars were placed one on each side as shown in Figure 3.11 to avoid transverse cracking. To avoid flexure failure, tension chords were placed on the front side of the specimens. One or two No.5 bars were used as the tension chords based on the specimen configurations. These bars had 1 in. concrete cover from the top similar to push-out specimens. Further 6x6 W1.4 x W1.4 welded wire reinforcement was placed having 0.5 in concrete cover from the top for the same reasons as for push-out specimens. After that, the concrete was cast, covered, and moist-cured for 28 days. The pour stop was removed from the slabs before testing.

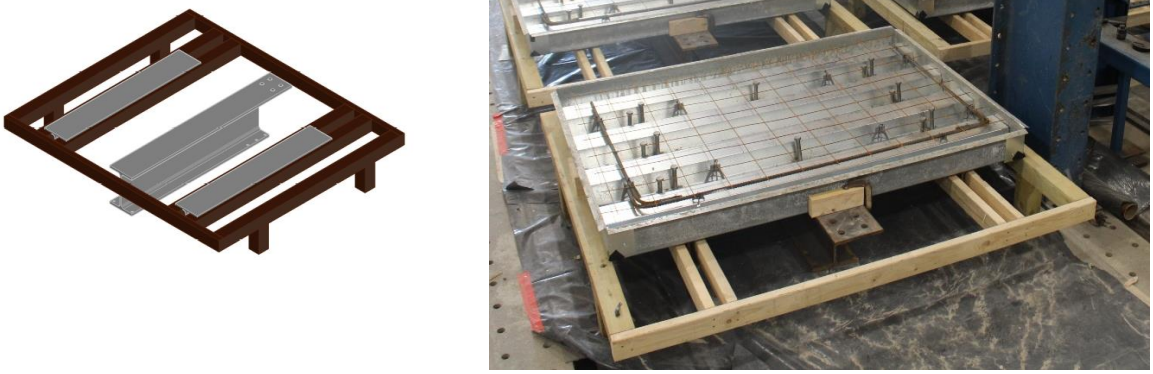

Fig. 3.17 Shear Test Specimen Fabrication Framework

3.7.3 Single-sided Push-out Test

The same wooden frame as for shear test specimens were used with the W section placed as the center. Further, the steel deck was placed on the flange of the W section and the pours stops were attached. Two No.5 bars have a concrete cover of 1.5in. were placed on each side of the

specimen to avoid the slab cracking during testing and 6x6 W1.4 x W1.4 welded wire reinforcement was placed having 1 in concrete cover from the top. After that, the concrete was laid, covered, and moist-cured for 28 days. The pour stop was removed from the slabs before testing.

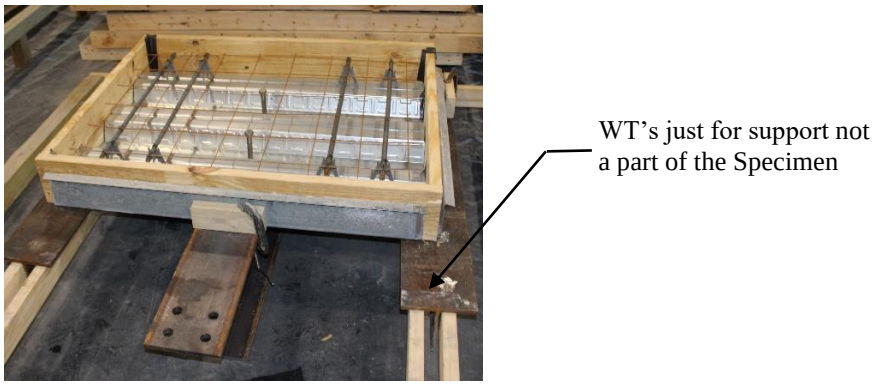

Fig. 3.18 Single-sided push-out test Specimen Fabrication Framework

3.8 Testing Procedure

3.8.1 Push-out Testing Procedure

The procedure followed while testing each push-out specimen is given below. The procedure is in accordance with AISI S923-20.

- Pre-load of 5% of predicted axial load or 2 kips which ever was smaller was applied for the specimen and held for 5 min.
- The axial load was increased in increments of 2 kips per 30 seconds and simultaneously normal load was applied equally to 10% of the applied axial load.
- Conformation that an equal load is being applied on both slabs was seen by comparing the slip measurements for each slab. If the slip in one slab exceeded 15% then the other slab before reaching 10% of the expected peak load. The specimen was unloaded and aligned as needed.
- Loading was carried out until 80% of the expected peak load was achieved.

- After attaining 80% of the load. Deformation control was implemented, where loading was applied in such a way that the average slip increment does not exceed 0.050 in. within the 30 seconds interval of load application.
- Load was continued until the load dropped below 30% of peak load or at least 1 in. slip was recorded.
- Failure mode was recorded.

3.8.2 Shear Testing Procedure

The procedure that was followed while testing each shear test specimen is summarized below. Monotonic displacement-controlled loading was implemented

- Pre-load of 5% of predicted peak load was applied for the specimen and held for 5 min.
- Displacement control loading was implemented. A rate of 0.05 in/min loading was applied until the expected peak load was reached.
- Once the failure mode was observed, loading was carried out until the shear load was below 10 kips and constant for a while.
- Failure mode was recorded.

3.8.3 Single-sided Push-out Testing Procedure

The procedure that was followed was similar to shear test and is summarized below. Monotonic displacement-controlled loading was implemented

- Pre-load of 5% of predicted peak load was applied for the specimen and held for 5 min.
- Displacement control loading was implemented. A rate of 0.05 in/min loading was applied until the expected peak load was reached.
- A normal load equal to 10% of the shear load generated was applied simultaneously for specimen T3.0A-4N-W-SS (b) only.

- Once the failure mode was observed, loading was carried out until the shear load was below 10 kips and constant for a while.
- Failure mode was recorded.

3.9 Materials

The properties of steel deck, headed shear studs, steel sections and reinforcement used are summarized below. All decks used were gauge 20 (0.0358 in. nominal thickness) satisfying ASTM A653. The shear headed shear studs were ¾ in. diameter, satisfying ASTM A29 with a nominal tensile strength of 65 ksi. Specimens were cast in batches as mentioned in Table 3.3

Table 3.3 Specimen Batches

Batch 1	D3.5A-3N-C-PO		D3.5A-3N-2S-PO
	D3.5A-3N-C-ST		D3.5A-3N-2S-ST
Batch 2	T3.5A-3N-S-ST	T3.5A-3N-W-ST	T3.5A-3N-2ST-ST
	D3.5B-3N-S-ST	D3.5B-3N-W-ST	T3.0A-3N-W-ST
Batch 3	T3.0A-4N-W-SS		

Table 3.4 presents an overview of the material properties of the concrete mix. Table 3.5 provides a summary of the concrete cylinder tests conducted according to ASTM C39 for each batch of castings. However, since it was challenging to perform cylinder tests daily, the concrete properties for specimens tested on days when cylinder tests were not conducted were estimated through interpolation. The concrete properties for each specimen are outlined in Table 3.6.

Table 3.4 Concrete Mixture Properties (per cubic yard)

Batch	1	2	3
Cast Date	12/19/2022	03/08/2023	05/08/2023
Cement (lbs)	412	412	445
Fly Ash (lbs)	137	137	148
Coarse Aggregate #78 (lbs)	1709	1709	-

Coarse Aggregate #68 (lbs)	-	-	1768
Fine Aggregate Natural Sand (lbs)	560	560	638
Fine Aggregate Manmade Sand (lbs)	898	898	679
Water (lbs)	310	310	269
Water to Cement Ratio	0.565	0.565	0.454

Table 3.5 Concrete Cylinder Test Results

Days	Batch 1		Batch 2		Batch 3	
	Compressive Strength (psi)	Unit weight (lb/ft^3)	Compressive Strength (psi)	Unit weight (lb/ft^3)	Compressive Strength (psi)	Unit weight (lb/ft^3)
3	2220	146.1	-	-	-	-
7	-	-	3050	146.1	3490	-
14	-	-	3310	145.7	3920	142.8
21	3210	145.3	3640	145.7	-	-
23	-	-	-	-	4190	142.0
25	3270	145.7	-	-	-	-
28	3450	145.7	-	-	4340	142.0
29	-	-	3760	145.7	-	-
31	3560	144.8	-	-	-	-
33	-	-	4190	144.8	-	-
35	-	-	4190	144.8	-	-
37	-	-	4230	144.8	-	-
50	4000	144.8	-	-	-	-
52	4070	144.8	-	-	-	-

Table 3.6 Concrete Properties

Specimen		Compressive Strength (psi)	Unit weight (lb/ft^3)
D3.5A-3N-C	a	3270	145.7
	b	3450	145.7
D3.5A-3N-2S	a	3560	144.8
	b	3560	144.8
	c	3560	144.8
D3.5A-3N-C-PO	b	4000	144.8
	c	4000	144.8
D3.5A-3N-2S-PO5	a	4070	144.8
	b	4070	144.8
	c	4070	144.8

D3.5B-3N-W	a	3550	145.7
	b	3550	145.7
	c	3600	145.7
D3.5B-3N-S	a	3600	145.7
	b	3715	145.7
	c	3715	145.7
T3.0A-3N-W	a	3730	145.7
	b	3750	145.7
	c	3750	145.7
T3.5A-3N-W	a	3760	145.7
	b	3760	145.7
	c	4190	145.8
T3.5A-3N-S	a	4190	145.8
	b	4190	145.8
	c	4190	145.8
T3.5A-3N-2ST	a	4210	145.8
	b	4210	145.8
	c	4210	145.8
T3.5A-4N-W-M	a	4190	142.0
	b	4190	142.0
	c	4190	142.0

Tension tests were performed on steel decks, WT6x17.5 and W12x40 on which test headed shear studs were welded, rebars and wire mesh used for reinforcement according to ASTM E8. Table 3.7, 3.8, 3.9 and 3.10 summarizes the results. Three specimens were tested for each material and detailed results of the same are in Appendix C

Table 3.7 Steel Deck Properties

Deck	Yield Stress, f_y (ksi)	Ultimate Stress, f_u (ksi)	Elongation, (%)
DT1	57.6	68.3	25.5
DT2	64.5	71.0	20.4
TZ1	56.0	66.9	25.9
TZ2	63.4	84.1	19.1

Table 3.8 Structural Steel Properties

Steel Section (Heat number)	Yield Stress, f_y (ksi)	Ultimate Stress, f_u (ksi)	Elongation, (%)
WT 6 x 17.5 (556446)	53.8	69.8	26.5
W 12 x 40 (558710)	55.5	72.6	26.8

W 12 x 40 (558712)	56.9	73.2	25.3
Note: W 12 x 40 steel had two heat specification and so both were tested			

Table 3.9 Rebar Properties

Rebar	Yield Stress, f_y (ksi)	Ultimate Stress, f_u (ksi)	Elongation, (%)
No.5_1	64.0	105.1	14.7
No.5_2	78.3	97.8	14.0
No.5_3	60.6	98.2	16.4

Table 3.10 Welded Wire Reinforcement Properties

Rebar	Yield Stress, f_y (ksi)	Ultimate Stress, f_u (ksi)	Elongation, (%)
6 x 6 W1.4 x W1.4	114.5	128.6	2.5

Shear tests were performed on the bare headed shear studs to understand their fracture properties and are summarized below in Table 3.11. The tests were conducted with the following fixture arrangement shown in Figure 3.19.

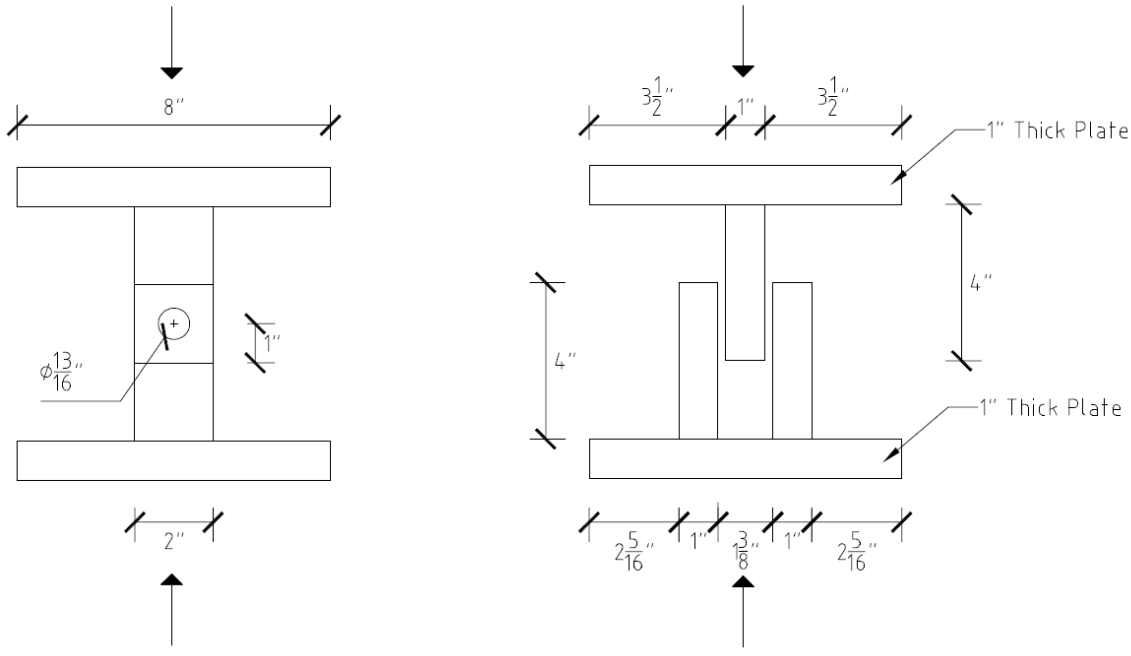

Front view Side view

Fig 3.19 Shear Fixture for Headed Shear Studs

Table 3.11 Headed Shear Studs Properties

Headed Shear Studs (3/4 in. Dia)	Ultimate Stress, f_u (ksi)	Shear Strength, V_e (kip)	V_e/A_sF_u
S3L 3/4 X 4-7/8 MS	75.2	21.67	0.65
S3L 3/4 X 5-3/16 MS	74.0	22.34	0.69
S3L 3/4 X 5-7/8 MS	78.3	22.05	0.64
Note: The f_u values are taken from the mill certificates provided by the manufacturer			

Fig. 3.20 Shear Test on Headed Shear Studs

Further to check the weld quality of headed shear studs bend test was performed according to AWS D1.1 (2010). Here the Headed shear studs were welded through a piece of a steel deck on a Steel section with the same heat setting as used for the headed shear studs welded while fabrication of the specimens. The weld was allowed to cool and then with the help of a hollow pipe, the studs were bend to approximately 30°. The weld didn't fracture concluding the weld was strong. Figure 3.21 shows the bend headed shear studs.

Fig. 3.21 Bent test on headed shear studs.

4. Stress States of Concrete around Headed Shear Studs

This chapter explains the stress state of concrete around the headed shear studs in the specimens using different test setups and how they correlate with the concrete stress state in a composite beam

4.1 Concrete Stress State in a Composite Beam

In a composite beam, the shear force between the W section and the concrete-filled steel deck is primarily generated by the effect of gravity loading. This gravitational force induces bending in the composite beam, generates shear forces at the interface between the two components resulting in a slip between the W section and the slab. To illustrate this concept, let's focus on a specific section of the beam, as depicted in Figure 4.1.

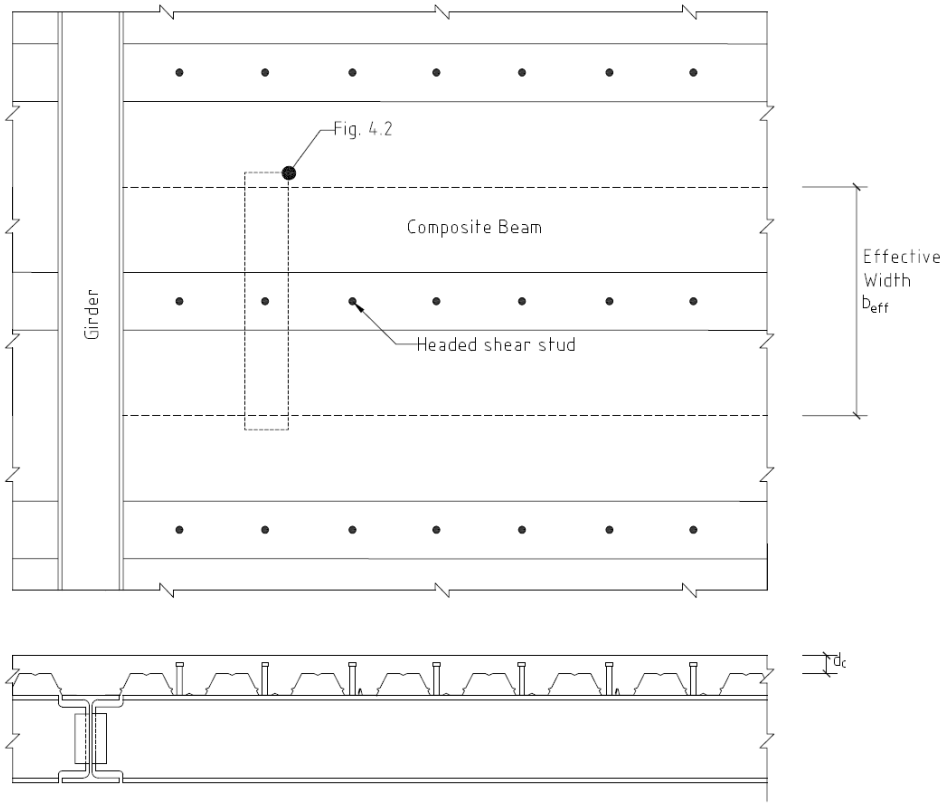

Fig. 4.1 Composite beam

Assuming the following:

- Stresses in the slab are uniform across the entire effective width, b_{eff}.
- There is no stress transferred at the edge of the effective width.
- The stress is idealized as a uniform stress distribution over the depth of the concrete over the deck, dc.
- The effective width is symmetric about the composite beam

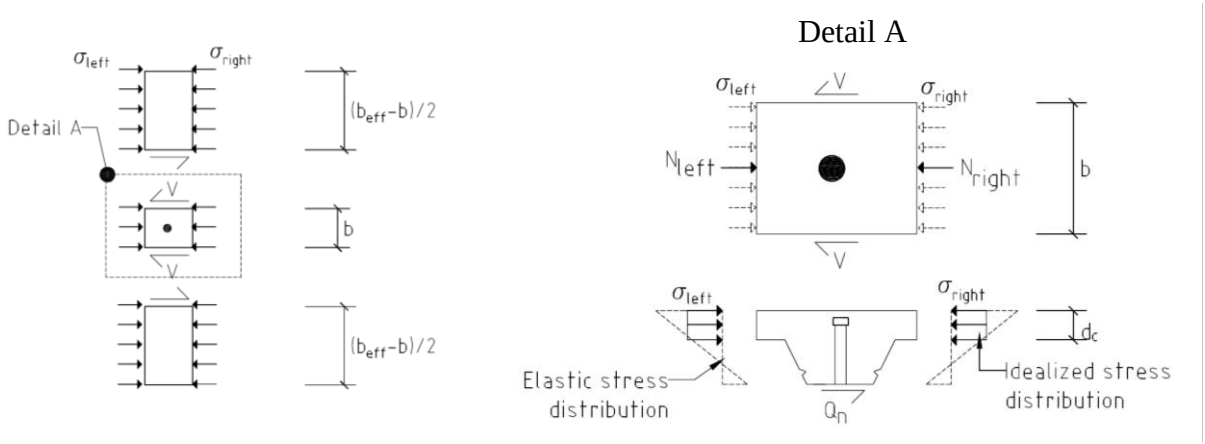

a) Effective width b) Portion around headed shear stud

Fig. 4.2 Stresses around the headed shear studs (composite beam)

In a composite beam, the presence of a moment causes compression in the slab near the stud. This compression is characterized by opposing stresses, σ_{left} and σ_{right}, as shown in the Figure 4.2. The magnitude of this compression can be determined by calculating the sum of the stud forces between the specific location being considered and the end of the beam. It's important to note that the magnitude of compression varies along the length of the beam. The shear load in the stud, represented by Q_n, is distributed to the concrete slab in two ways. Firstly, through the difference in axial compression stress (σ_{right} - σ_{left}) and secondly, through shear flow to the rest of the effective width, resulting in a shear force V acting on both sides of the composite beam.

For effective specimen design, it is valuable to understand the contribution of the stud force associated with the difference in axial stress and the portion associated with the shear force V. This

knowledge helps in determining the appropriate design parameters and optimizing the performance of the composite beam. So, summing the horizontal forces in the longitudinal direction of the composite beam over the full effective width we get,

$$\sigma_{right} d_c b_{eff} - \sigma_{left} d_c b_{eff} = Q_n \tag{4.1}$$

$$\sigma_{right} - \sigma_{left} = \frac{Q_n}{d_c b_{eff}} \tag{4.2}$$

Where,

d_c = total concrete depth

b_{eff} = effective width of the slab

Further considering a small width b the slab around the headed shear studs. The Axial forces N_{left} and N_{right} are the resultant longitudinal forces in Figure 4.2(b) and given as,

$$N_{left} = \sigma_{left}\, b\, d_c \tag{4.3}$$

$$N_{right} = \sigma_{right}\, b\, d_c \tag{4.4}$$

Summing the horizontal forces in the longitudinal direction of the composite beam for the portion of slab around the studs considered in Figure 4.2 (b).

$$2V + \left(N_{right} - N_{left}\right) - Q_n = 0 \tag{4.5}$$

Substituting Equations 4.3 and 4.4 in Equation 4.5

$$2V + \left(\sigma_{right} - \sigma_{left}\right) b\, d_c = Q_n \tag{4.6}$$

Substituting Equations 4.2 in Equation 4.6

$$\frac{2V}{Q_n} = 1 - \frac{b}{b_{eff}} \tag{4.7}$$

Substituting Equations 4.7 in Equation 4.5

$$\frac{N_{right} - N_{left}}{Q_n} = \frac{b}{b_{eff}} \tag{4.8}$$

Note that the concrete width b considered influenced the amount of force coming from axial and shear force in the concrete around the headed shear studs. Understanding the distribution of forces in a composite beam is crucial for specimen design. In the given context, where a specimen with a width of 3 ft is intended to represent a composite beam with 10 ft beam spacing and effective width, the analysis reveals that 70% of the load should be applied as shear on the sides of the specimen, while 30% should be applied as compression. This information describes how the forces should be applied to the specimen to more accurately represent real composite beams. By appropriately considering these factors in the specimen design, it becomes possible to replicate the real-world behavior of composite beams and ensure that the testing accurately reflects their performance under different loading conditions. This aids in enhancing the reliability and applicability of test results for composite beam structures.

4.2 Concrete Stress State in Push-out Specimen

Chapter three shows that a push-out specimen consists of two slabs bolted together with the WTs. The specimen is then set on the strong floor and the load is applied to the WTs'. Assuming the slabs have a uniform bearing on the strong floor when subjected to loading and each headed shear stud reaches its shear strength Q_n, both the slabs being identically cast will bear an equal load. Considering a push-out specimen subjected to an axial load of $2NQ_n$, where N is the number of studs per slab as seen in Figure 4.3.

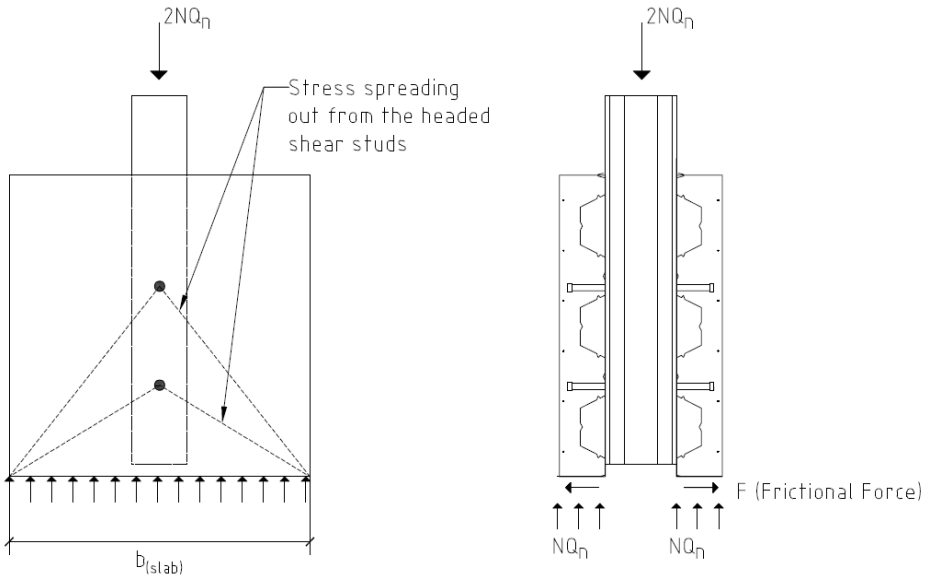

Fig. 4.3 Forces in a push-out specimen

For the compression stress to be uniform along the bottom edge of each slab of width b_{slab}, the stresses should spread in a triangular portion as seen in Figure 4.3. From this it can be observed that there are no shear forces acting on the sides of the specimen. Instead, force is introduced solely through longitudinal force generating compressive stresses around the headed shear studs. This differs from how load is introduced to the concrete around a headed shear stud in a composite beam, as demonstrated in the earlier subsection. In the composite beam, both shear forces and longitudinal forces contribute to the stress state around the stud (Figure 4.2). Furthermore, it is important to note that the push-out specimen slab, as depicted in Figure 4.3, is not subjected to any net compression stress. This means that there is no downward force acting on the top edge of the slab, which contrasts with the stress state in a composite beam where the net compressive force is given by $\sigma_{right} - \sigma_{left}$.

Further, seeing at the free body diagram of each slab (Figure 4.4) in a push-out test the loading in each slab is eccentric which causes the slabs to rotate which is counteracted with the help of the applied normal load. depending upon the geometry of the specimen this applied normal

i.e., 10% of the axial force may or not be enough to avoid the rotation and buckling of the slab which is further seen in Chapter 5

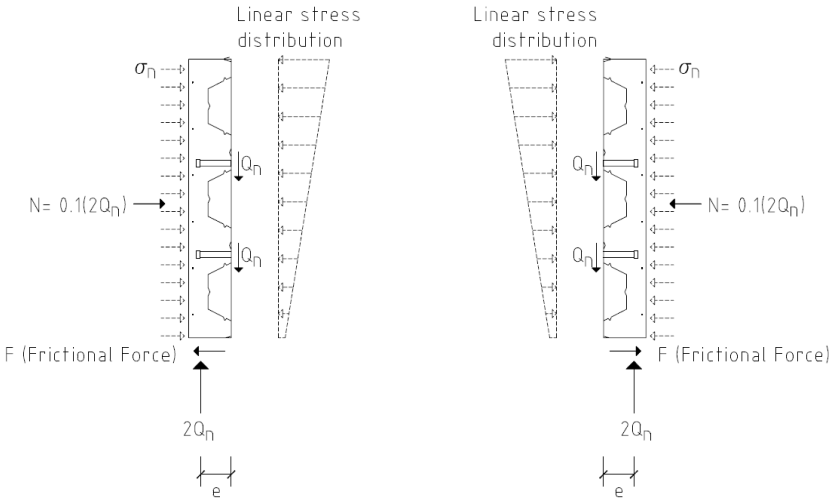

Fig. 4.4 Free body diagram of each slab in a push-out test

4.3 Concrete Stress State in Shear Test Specimen

Now, consider a shear test specimen (Figure 4.5) that is applied with a shear load of NQ_n where N is the number of headed shear stud each reaching their shear strength Q_n.

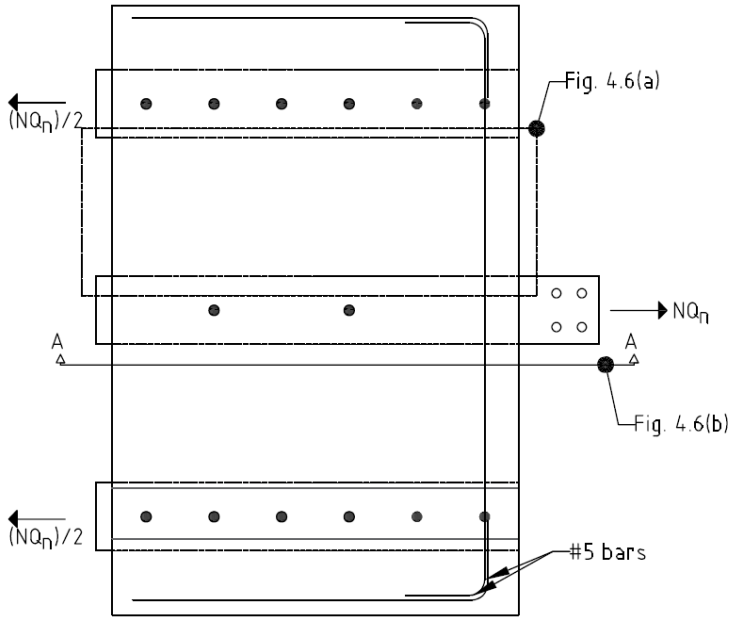

Fig. 4.5 Forces in a shear test specimen

Each WT of the specimen is bolted to the side beam of the self-reacting frame in under axial load NQ_n /2 which is being transferred to the concrete with the help of the headed shear studs welded on them. Assuming each stud transfers equal shear force to the concrete.

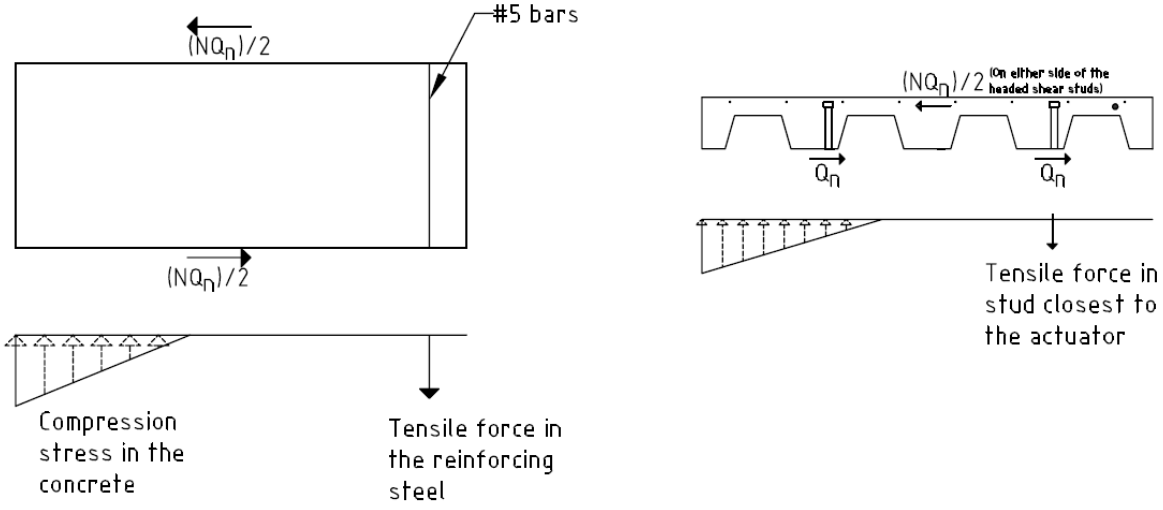

a) Plan view b) Section AA

Fig. 4.6 Stresses in concrete around the stud (Shear Test)

In the test setup, the load is primarily transferred to the shear studs through shear forces coming from the sides rather than longitudinal axial forces. This stress state resembles similar behavior observed in composite beams (Figure 4.2), where shear forces play a significant role.

Further, one of the challenges encountered in the test setup, as illustrated in Figure 4.6(a), is the development of lateral tension stresses in the slab around the stud closest to the actuator as the beam tends to act as deep beam with support at the location where the WTs are bolted with the shear load at the center creating bending. To minimize cracking associated with these stresses, reinforcing steel (No.5 bar) was strategically placed along the edge of the slab nearest to the actuator. The calculations of these reinforcements are provided in Appendix E. This reinforcement helps to mitigate the adverse effects of the tension stresses on the slab. Another issue identified, as shown in Figure 4.7(b), is the eccentricity between the longitudinal load applied to the slab and the interface between the slab and the steel beam. Initially, it was assumed that the stiffness of the

4 ft span of the concrete-filled steel deck slab would be sufficient to resist the upward force exerted at the edge of the slab nearest to the actuator. However, the subsequent test results discussed in the following chapter revealed that the stud closest to the actuator experienced a tension force, indicating that the assumption about the slab's stiffness was incorrect.

4.4 Concrete Stress State in Single-sided Push-out Test Specimen

The single-sided push-out test was created in such a way to have similar boundary conditions as in a push-out test specimen. So, the stresses in concrete around headed shear suds are going to be similar as that in each slab of the push-out test. The concrete edge nearest to the actuator is borne similar to the push-out specimens sat on the strong. For the compression stress to be uniform along that edge of each slab of width b_{slab}, the stresses should spread in a triangular portion as seen in Figure 4.7.

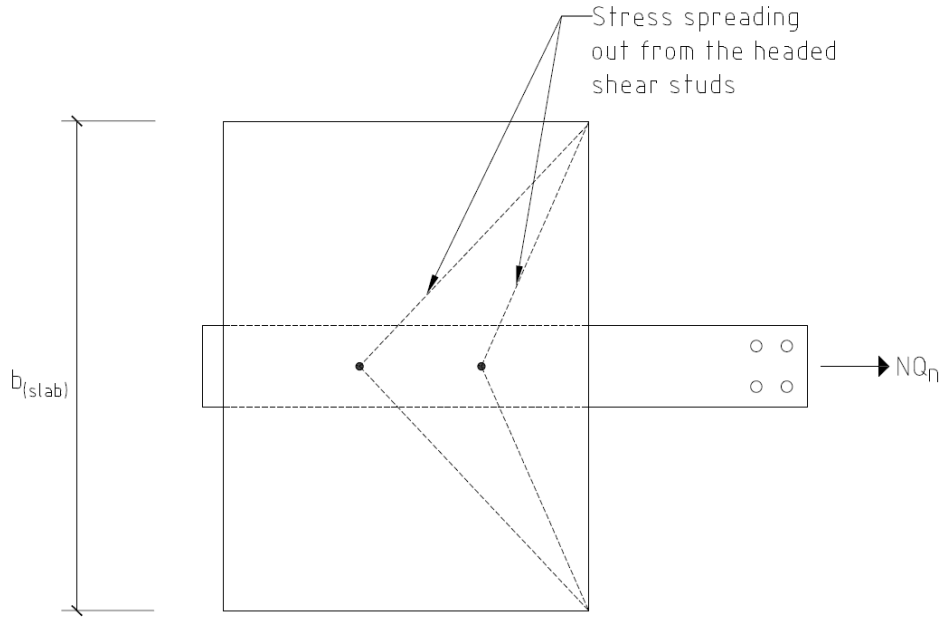

Fig 4.7 Stresses around the headed shear studs (Single-sided push-out test)

Similar to the push-out specimen the loading in these specimens is also eccentric causing the specimens to rotate giving rise to normal reaction which would be measured by the load cells below the specimens. The influence of this eccentricity has been evaluated in Chapter 5

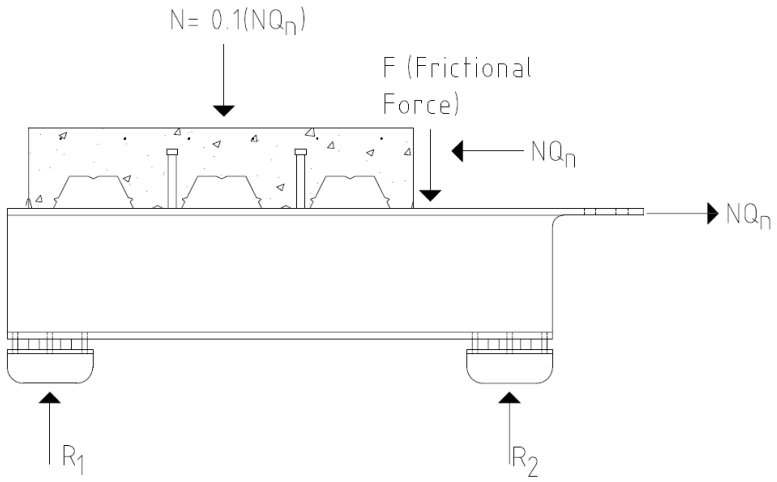

Fig. 4.8 Free body diagram of modified shear specimen

5. Results

This chapter summarizes the results of all the tests conducted comparing them with the current AISC provisions (Eq. 2.58) and those given by Rambo-Roddenberry (2002) (Eq. 2.39). Further, it evaluates the different test setups described in Chapter 3 analyzing the test results and documenting the challenges.

5.1 General Overview

A total of 33 tests were performed to assess, compare and evaluate the different test configurations including the push-out test setup, shear test setup, and single-sided push-out test setup. Among these tests, six were conducted using the conventional push-out test, 24 were carried out using the shear test setup, and three were performed using the single-sided push-out test setup. American Institute of Steel Construction (AISC) and the equation developed by Rambo-Roddenberry (2002) are applicable for deck heights up to 3 in. However, to facilitate the use of deeper decks, it is necessary to determine their applicability with these provisions. Table 5.1 presents a summary of all the test results. The first two groups of specimens were tested using the conventional push-out test, while the last group of tests employed the single-sided push-out test setup. All other specimens were evaluated using the shear test setup.

Table 5.1 Results

Specimen		Test setup	f'_c (psi)	w (pcf)	f_u (ksi)	Q_E[1] (kip)	Slip at peak (in.)	Failure Mode[2]
D3.5A-3N-C-PO	b	Push-out	4000	144.8	74.0	20.02	0.105	SS/RS
	c	Push-out	4000	144.8	74.0	19.05	0.130	SS/RS
D3.5A-3N-2S-PO[3]	a	Push-out	4070	144.8	74.0	11.57	-	SS/RS
	b	Push-out	4070	144.8	74.0	11.52	-	SS/RS
	c	Push-out	4070	144.8	74.0	15.75	-	SS/RS
D3.5A-3N-C-ST	a	Shear	3270	145.7	74.0	19.40	0.135	SS
	b	Shear	3450	145.7	74.0	20.80	0.098	SS
D3.5A-3N-2S-ST	a	Shear	3560	144.8	74.0	14.80	0.036	SS
	b	Shear	3560	144.8	74.0	14.25	0.061	SS
	c	Shear	3560	144.8	74.0	14.60	0.039	SS/CC
D3.5B-3N-W-ST	a	Shear	3550	145.7	74.0	11.27	0.105	SS
	b	Shear	3550	145.7	74.0	13.34	0.084	SS
	c	Shear	3600	145.7	74.0	13.10	0.010	SS
D3.5B-3N-S-ST	a	Shear	3600	145.7	74.0	16.36	0.033	SS
	b	Shear	3715	145.7	74.0	16.96	0.075	SS
	c	Shear	3715	145.7	74.0	17.68	0.067	SS
T3.0A-3N-W-ST	a	Shear	3730	145.7	75.2	12.00	0.115	SS/DP
	b	Shear	3750	145.7	75.2	11.02	0.070	SS/DP
	c	Shear	3750	145.7	75.2	11.93	0.176	SS/DP
T3.5A-3N-W-ST	a	Shear	3760	145.7	74.0	12.08	0.051	DP
	b	Shear	3760	145.7	74.0	12.83	0.049	SS*
	c	Shear	4190	145.8	74.0	12.12	0.042	SS*
T3.5A-3N-S-ST	a	Shear	4190	145.8	74.0	18.23	0.024	SS
	b	Shear	4190	145.8	74.0	17.86	0.056	CC/SS
	c	Shear	4190	145.8	74.0	18.20	0.027	SS
T3.5A-3N-2ST-ST	a	Shear	4210	145.8	74.0	12.14	0.013	SS/CC
	b	Shear	4210	145.8	74.0	11.05	0.004	SS
	c	Modified Shear	4210	145.8	74.0	12.14	0.032	SS
T3.0A-3N-W-SS[4]	a	SS push-out	4190	142	78.3	14.46	0.769	DP
	b	SS push-out	4190	142	78.3	12.18	0.027	SS/DP
	c	SS push-out	4190	142	78.3	12.09	0.279	SS/DP

Note: 1. Q_E: Experimental Load per stud

2. Failure modes: SS: Stud Shearing, CC: Concrete cone, RS: Rib Shear, DP: Deck Punching

SS*: Shows deck bulging in the start but at peak Stud shearing

3. D3.5A-3N-2S-PO to be redone due to buckling of slab not giving correct slip measurements

4. T3.0A-4N-W-SS (b) was carried out with an application of a normal force while (a) and (c) weren't.

The failure modes observed are described below:

Stud shearing (SS): The shear stress at the critical section of the stud reaches a level where the stud's shank fractures. The failure surface was mostly seen on the base metal. This failure mode is typically seen in headed shear studs in strong position.

Concrete cone (CC): This failure more happens when the compressive forces applied to the concrete surrounding the headed shear stud reach a critical level. The stress concentration at the base of the stud creates a cone-shaped failure pattern in the concrete, causing it to break and spall.

Rib shear (RS): This concrete failure is cause when the prying of the headed shear studs is sufficient to cause transverse cracks at in the concrete at the deck height. This failure mode occurs usually when the width of the specimens is small so that concrete cone isn't able to form.

Deck punching (DP): This is a typical failure mode of headed shear studs in weak position. Where the small portion of concrete between the headed shear studs and deck crushes, causing the decks to bulge first and then tear.

Stud shearing with deck bulging (SS*): This failure mode was observed in headed shear studs in weak position with 3.5 in trapezoidal deck. Where initially deck bulging was seen indicating of deck punching however at peak stud shearing was seen.

5.2 Evaluating the Conventional Push-out Test

5.2.1 Test Result of the Conventional Push-out Test

The results of push-out test are shown in Table 5.2 and the load vs slip plots in Figure 5.1. Predicted strength are calculated using AISC provisions (Equation 2.57) and that given by Rambo-Roddenberry (2002) (Equation 2.38). Results of D3.5A-3N-C-PO (a) were polluted and therefore aren't considered.

Table 5.2 Push-out Test Results

Specimen		f'_c (psi)	w (pcf)	f_u (ksi)	Q_{AISC}[1] (kip)	Q_{RR}[2] (kip)	Q_E[3] (kip)	Q_E/Q_{AISC}		Q_E/Q_{RR}		Slip at peak (in.)	Failure Mode[4]
D3.5A-3N-C-PO	b	4000	144.8	74.0	24.42	22.14	20.02	0.82	0.80	0.90	0.88	0.105	SS/RS
	c	4000	144.8	74.0	24.42	22.14	19.05	0.78		0.86		0.130	SS/RS
D3.5A-3N-2S-PO	a	4070	144.8	74.0	20.76	18.82	11.57	0.56	0.62	0.61	0.69	-	SS/RS
	b	4070	144.8	74.0	20.76	18.82	11.52	0.55		0.61		-	SS/RS
	c	4070	144.8	74.0	20.76	18.82	15.75	0.76		0.84		-	SS/RS

Note: 1. QAISC: AISC Predicted Load per stud 2. QRR: Predicted Load per stud by Rambo Rodenberry
3. QE: Experimental Load per stud
4. SS: Stud Shearing RS: Rib Shear

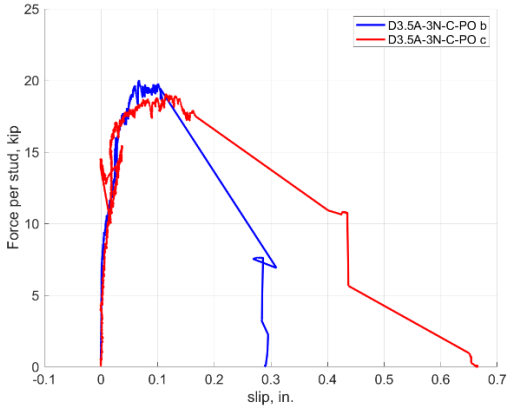

a) D3.5A-3N-C-PO

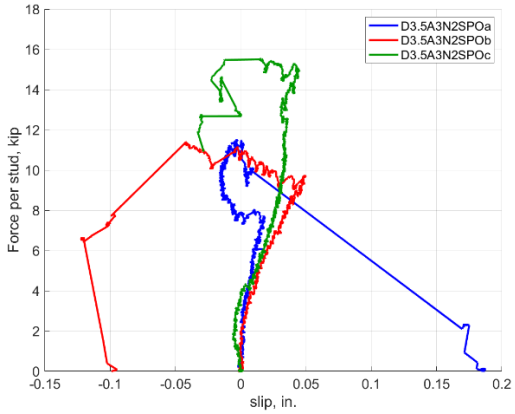

a) D3.5A-3N-2S-PO

Fig. 5.1 Load vs Slip plots for Push-out test

All specimens had a 3.5 in. Dovetail deck with a 2 in. concrete cover above the deck. These specimens had single or two headed shear studs welded through the deck, positioned at the center of the rib. During the initial loading of these specimens, rib shear cracks in one or both slabs were observed at approximately 68% to 84% of the maximum load achieved. As the loading continued,

the headed shear stud/s in one of the two slabs failed with a loud noise. The normal load was maintained at around 10% of the applied axial force. When the slabs exhibited signs of buckling, the normal load tended to increase without manually increasing pump pressure and had to be adjusted by reducing the pump pressure to maintain it at 10% of the applied axial load. All of these specimens displayed transverse cracks.

For specimens with single stud positions centrally per rib (D3.5A-3N-C-PO) exhibited transverse cracks during the early stages of loading, typically occurring at around 30% to 45% of the peak load (Figure. 5.2). As the loading continued, both slabs of the specimen showed rib shear cracks at approximately 68% to 84% of the peak load (Figure. 5.3). Additionally, both specimens experienced some buckling, which was monitored using a string potentiometer arrangement in D3.5A-3N-C (c). The strength of a single headed shear stud per rib was measured to be 19.5 kips. This represents approximately 80% of the strength predicted by the AISC equation. This discrepancy may be attributed to the fact that the AISC provisions were originally developed based on past tests involving trapezoidal profiles and were limited to deck heights of up to 3 in. However, the tests conducted in this study utilized a 3.5 in. dovetail profile, which could lead to a lower strength due to the deck's geometry and increased height. The failure mode observed was stud shearing with the failure plane in the base metal (Figure. 5.4). East slab showed stud shearing with the headed shear studs being severed, while the west slab had the headed shear studs intact.

a) D3.5A-3N-C-PO (b)

b) D3.5A-3N-C-PO (c)

Fig. 5.2 Transverse cracks in D3.5A-3N-C-PO

a) D3.5A-3N-C-PO (b)

b) D3.5A-3N-C-PO (c)

Fig. 5.3 Rib shear cracks in D3.5A-3N-C-PO

a) D3.5A-3N-C-PO (b)

b) D3.5A-3N-C-PO (c)

Fig. 5.4 Stud Shear Failure in D3.5A-3N-C-PO

For Specimens with two headed shear studs positioned centrally per rib (D3.5A-3N-2S-PO) showed strength of a single headed shear stud per rib to be 13.0 kips on average. However, the peak load was associated with slab buckling and therefore the measured strength is not indicative of the strength of the headed shear studs. This buckling also polluted the slip measurements (Figure 5.1(b)) which is explained in the next subsection 5.2.2. These tests would need to be redone with a thicker slab and/or reinforcing steel to prevent this undesirable failure mode.

5.2.2 Challenges with the Conventional Push-out Test

While conducting these push-out tests, challenges were encountered, some of which are explained in section 2.4 of this dissertation. This section will briefly summarize all the challenges encountered while conducting the push-out test as part of this research.

Firstly, the push-out test has two slabs, and the strength of the headed shear stud is given as,

$$Q_n = \frac{P}{n} \tag{5.1}$$

Where,

Q_n = Strength of a headed shear studs

P = Peak applied axial force recorded in the push-out test for the specimen

n = total number of headed shear studs tested in the push-out test for the specimen

Mostly the headed shear studs in one of the slabs fail while there is no failure seen in the other slab. The peak load recorded at this time is then divided by the total number of headed shear studs in the specimen. This results in the strength being biased to the weakest headed shear stud in either slab. All five push-out specimens tested saw stud shearing in one of either slabs of the specimen.

Secondly, all load is transferred through compression along one edge of the slab that causes buckling. To record the buckling of the specimen four string potentiometers were attached along the height of the specimen as seen in Figure 5.5. The out of plane displacements for the east slab of the specimens can be seen in Figure. 5.6.

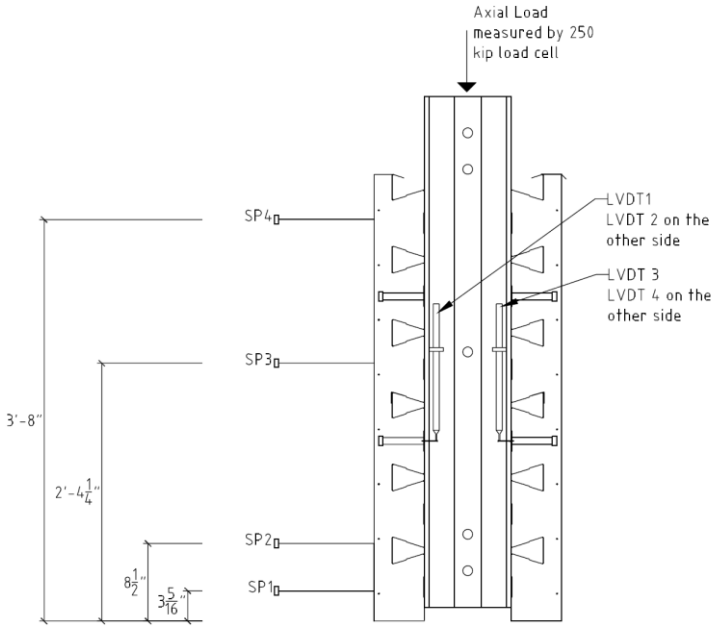

Fig. 5.5 String Potentiometer arrangement for Push-out specimens

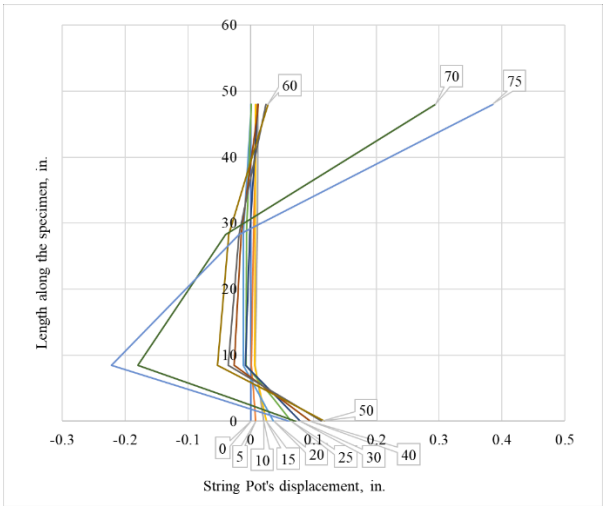

D3.5A-3N-C-PO (c)

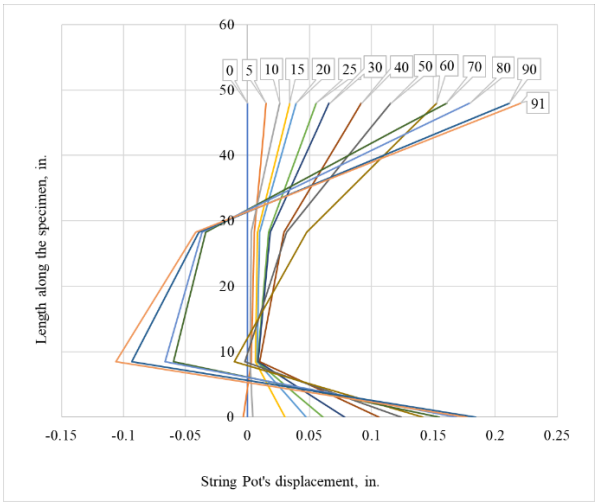

D3.5A-3N-2S-PO (a)

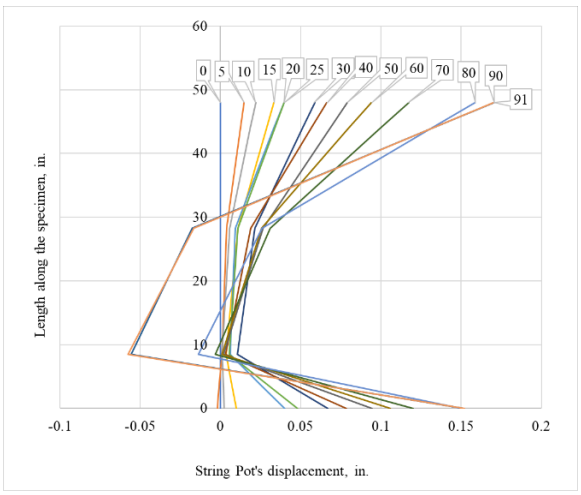

D3.5A-3N-2S-PO (b)

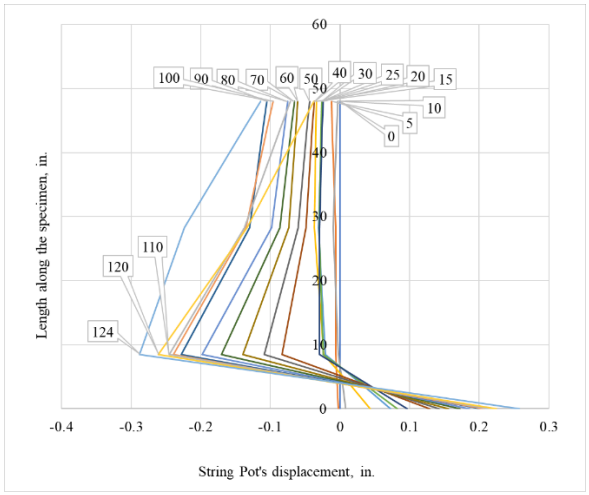

D3.5A-3N-2S-PO (c)

Fig 5.6 East Slab Buckling of the push-out specimens

Each curve represents the buckling shape of the specimen at the instance of the applied axial load, P shown by the call out of each curve. As we can see the specimen buckles as the axial load is applied. This cause transverse cracking similar to the so-called “back-breaking failure” observed by Hicks (2017). Further, due to the buckling of the slabs (Figure 5.7) the slip measure tends to get polluted. As the slab buckles the attachment for the LVDT tend to rotate causing the slip measurements to measure a negative slip (Figure 5.8) which pollute the slip measurements. Figure 5.9 shows the LVDT’s measuring negative slip thus polluting the slip measurements.

Fig 5.7 Slab Buckling in Push-out Specimens

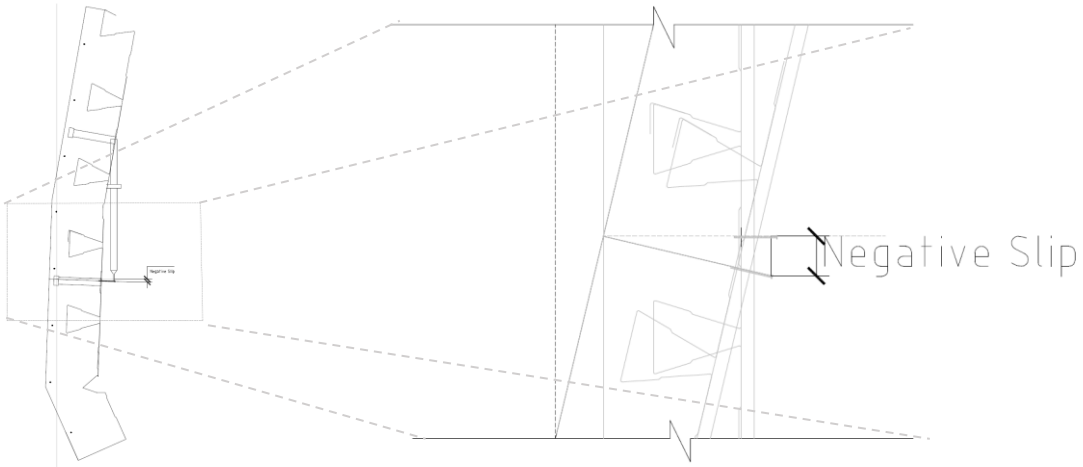

Fig. 5.8 Slab buckling causing negative slip

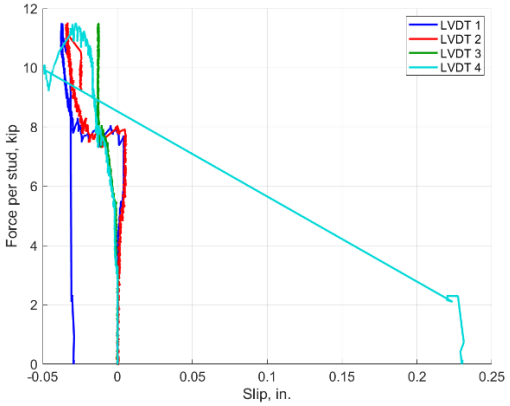

D3.5A-3N-2S- PO (a)

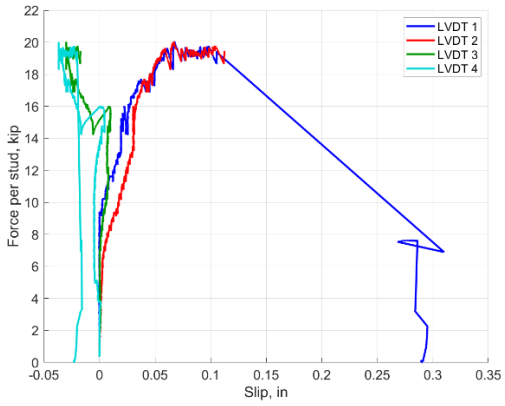

D3.5A-3N-C-PO (b)

Fig. 5.9 Buckling of slab polluting the slip measurements

Additionally, when one of the headed shear studs fails, there is a noticeable spike in slip measurements, as illustrated in Figure 5.9. Moreover, the slip increases for certain LVDTs located on the failing slab, while it decreases for others as the load is gradually reduced. Selecting the appropriate LVDT measurements to capture post-peak behaviors often involves subjective decisions, making it challenging to accurately capture such behaviors.

Uniform bearing of the specimen on the ground is crucial for reliable test results. Uneven bearing can lead to additional rotation of the specimen, introducing variability in the test outcomes. To address this, it may be necessary to adjust the slabs by shimming or resetting them to achieve

a more uniform bearing. However, this process can be challenging. Alternatively, a high strength grout can be used between the slab and the floor to ensure uniform bearing, although this method is time-consuming. If uniform bearing is not achieved, the slabs may experience relative movement, which can impact the accuracy of LVDT measurements and potentially influence the test results.

5.3 Evaluating the Shear Test Setup

5.3.1 Overview of Shear Test Results

The results of push-out test are shown in Table 5.3. Predicted strength are calculated using AISC provisions (Eq. 2.58) and that given my Rambo-Roddenberry (Eq. 2.39). The first two specimen groups D3.5A-3N-C-ST and D3.5A-3N-2S-ST are the companion specimen to the Push-out test specimens D3.5A-3N-C-PO and D3.5A-3N-2S-PO respectively. These specimen groups were used to see how well the shear test compares to the conventional push-out test which is briefly explained in section 5.3.2. More specimens having 3.5 in. dovetail and 3.5 in. trapezoidal deck profiles with different stud configurations were investigated having a nominal 3 ksi normal weight concrete. Results of D3.5A-3N-C-ST (c) were polluted and therefore aren't considered.

Table 5.3 Shear Test Results

Specimen		f'_c (psi)	w (pcf)	f_u (ksi)	Q_{AISC}[1] (kip)	Q_{RR}[2] (kip)	Q_E[3] (kip)	Q_E/Q_{AISC}		Q_E/Q_{RR}		Slip at peak (in.)	Failure Mode[4]
D3.5A-3N-C-ST	a	3270	145.7	74.0	22.44	22.14	19.40	0.86	0.88	0.88	0.91	0.135	SS
	b	3450	145.7	74.0	23.36	22.14	20.80	0.89		0.94		0.098	SS
D3.5A-3N-2S-ST	a	3560	144.8	74.0	20.76	18.82	14.80	0.71	0.70	0.79	0.77	0.036	SS
	b	3560	144.8	74.0	20.76	18.82	14.25	0.69		0.76		0.061	SS
	c	3560	144.8	74.0	20.76	18.82	14.60	0.70		0.78		0.039	SS/CC
D3.5B-3N-W-ST	a	3550	145.7	74.0	19.54	15.63	11.27	0.58	0.64	0.72	0.80	0.105	SS
	b	3550	145.7	74.0	19.54	15.63	13.34	0.68		0.85		0.084	SS
	c	3600	145.7	74.0	19.54	15.63	13.10	0.67		0.84		0.010	SS
D3.5B-3N-S-ST	a	3600	145.7	74.0	24.11	22.14	16.36	0.68	0.70	0.74	0.77	0.033	SS
	b	3715	145.7	74.0	24.42	22.14	16.96	0.69		0.77		0.075	SS
	c	3715	145.7	74.0	24.42	22.14	17.68	0.72		0.80		0.067	SS

T3.0A-3N-W-ST	a	3730	145.7	75.2	19.85	15.88	12.00	0.60	0.59	0.76	0.73	0.115	SS/DP
	b	3750	145.7	75.2	19.85	15.88	11.02	0.56		0.69		0.070	SS/DP
	c	3750	145.7	75.2	19.85	15.88	11.93	0.60		0.75		0.176	SS/DP
T3.5A-3N-W-ST	a	3760	145.7	74.0	19.54	15.63	12.08	0.62	0.63	0.77	0.79	0.051	DP
	b	3760	145.7	74.0	19.54	15.63	12.83	0.66		0.82		0.049	SS*
	c	4190	145.8	74.0	19.54	15.63	12.12	0.62		0.78		0.042	SS*
T3.5A-3N-S-ST	a	4190	145.8	74.0	24.42	22.14	18.23	0.75	0.74	0.82	0.82	0.024	SS
	b	4190	145.8	74.0	24.42	22.14	17.86	0.73		0.81		0.056	CC/SS
	c	4190	145.8	74.0	24.42	22.14	18.20	0.75		0.82		0.027	SS
T3.5A-3N-2ST-ST	a	4210	145.8	74.0	18.68	16.93	12.14	0.65	0.63	0.72	0.70	0.013*	SS/CC
	b	4210	145.8	74.0	18.68	16.93	11.05	0.59		0.65		0.004*	SS
	c[6]	4210	145.8	74.0	18.68	16.93	12.14	0.65		0.72		0.032	SS

Note: 1. Q_{AISC}: AISC Predicted Load per stud 2. Q_{RR}: Predicted Load per stud by Rambo Rodenberry

3. Q_E: Experimental Load per stud

4. SS: Stud Shearing CC: Concrete cone RS: Rib Shear DP: Deck Punching

SS*: Shows deck bulging in the start but at peak Stud shearing

Where there are two failure mode, the 1st failure mode is for front and second for back stud/stud group

6. T3.5A-3N-2ST c used modified shear test setup

5.3.2 Comparison between the Conventional Push-out Test and Shear Test Setup

The D3.5A-3N-C-ST and D3.5A-3N-C-PO specimens featured a 3.5 dovetail deck with a single headed shear stud per rib, welded at the central position. The shear test arrangement yielded a strength of 20.1 kips per stud for the headed shear stud, while the conventional push-out test resulted in a strength of 19.5 kips per stud. Both tests exhibited a peak slip of approximately 0.12 in., as depicted in Figure 5.10. The load versus slip curves for both test setups displayed a close match with each other. Furthermore, both tests exhibited shear shearing at the base metal as the failure mode. These findings suggest that the shear test setup was capable of producing comparable results to the push-out test setup.

In the case of groups D3.5A-3N-2S-ST and D3.5A-3N-2S-PO, both specimens featured a 3.5 dovetail deck with two headed shear studs per rib, welded at the center position. The shear test setup resulted in a headed shear stud strength of 14.6 kips per stud, with a peak slip of 0.05 in. However, in the conventional push-out test, a strength of 12.30 kips per stud was obtained.

Unfortunately, the peak load and slip measurements for the D3.5A-3N-2S-PO groups were compromised due to slab buckling during testing, as described in section 5.2.2. As a result, a comparison between these test groups was not possible.

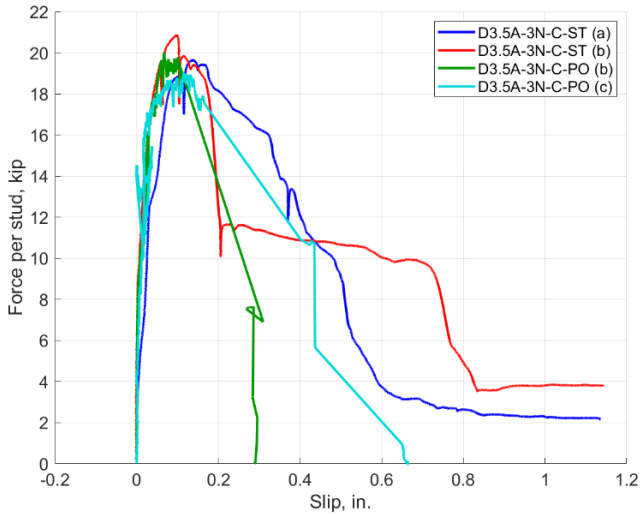

Fig. 5.10 Force vs Slip comparing the test setups

In the shear test setup, both specimens (D3.5A-3N-C-ST (a) and (b)) did not exhibit any cracks on the surface of the slab, except for negligible flexure and transverse cracks at the peak loads (Figure 5.11 (a)). These cracks were minimal and did not affect the strength of the headed shear studs. The specimens also experienced slight bulging of the deck before reaching peak loads (Figure 5.11 (b)). The failure mode observed in the shear test setup was stud shearing, with the failure plane occurring in the base metal for both specimens.

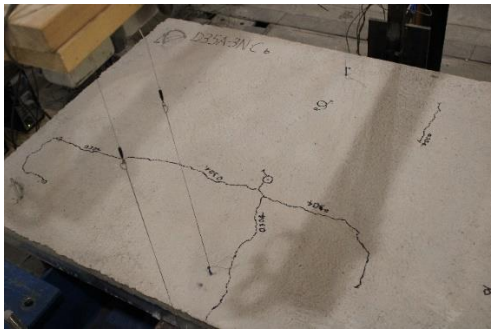

a) Cracking patten for D3.5A-3N-C (b)

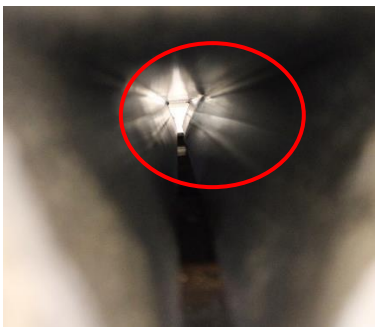

b) Deck budging in front of the headed shear stud

Fig 5.11 Behavior of Shear Test Specimens

5.3.3 Challenges with the Shear Test Setup

The correlation between the shear test and the previously explained push-out test initially gave the impression that the shear test was successfully capturing the behavior in push-out tests. However, subsequent testing conducted on additional specimens revealed some peculiar findings. Specifically, the headed shear studs exhibited different failure modes within the same specimen, which was unexpected. Additionally, the behavior of the traditional 3 in. trapezoidal deck with headed shear studs in a weak position did not align with the anticipated results based on existing literature. These observations indicate potential challenges with the test setup and the need for further investigation to understand and address these discrepancies.

The T3.0A-3N-W specimen group, which had a 3 in. trapezoidal deck with headed shear studs in the weak position the exhibited a strength of 11.65 kips per headed shear stud, which corresponds to approximately 60% of the strength predicted by the AISC equation. also, the behavior for headed shear stud in weak positions did not resemble past literature. Figure 5.12 illustrates the push-out test results for a headed shear stud in weak position (specimen D36 W64-7N6-2) conducted by Rambo-Roddenberry (2002) and T3.0A-3N-W (a) conducted on shear test. In D36 W64-7N6-2, the peak load was sustained for a significant amount of slip before reaching failure. On the other hand, when examining T3.0A-3N-W (a), it was observed that the peak load was achieved with very little slip and drops early. This disparity in behavior occurred because one of the studs failed in stud shearing, while the other experienced deck punching as the primary failure mode. In the T3.0A-3N-W specimen group, all three specimens consistently exhibited a failure mode where the headed shear stud nearest the actuator sheared and the one farthest to the actuator experienced deck punching. It is worth noting that a typical failure mode associated with weak position studs, is deck punching rather than stud shearing.

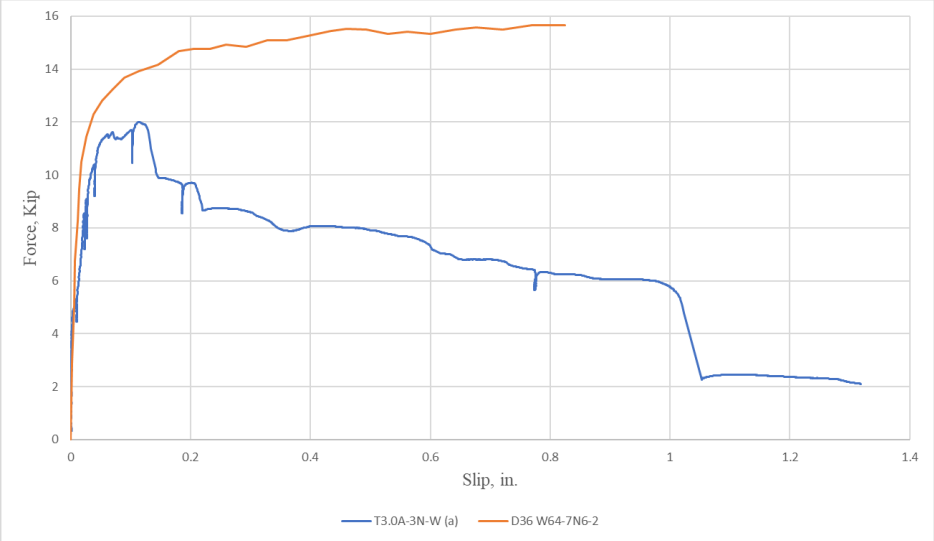

Fig 5.12 Force vs Slip plot of headed shear studs in weak position

Upon further investigation into the discrepancies, it was discovered that the specimens experienced moments during loading, leading to the development of axial forces in the two-headed shear stud/stud groups. Particularly, the front headed shear stud/stud group primarily experienced tension along with the shear force, resulting in the headed shear studs failing at lower capacities. The eccentric loading of the specimen, as depicted in Figure 4.6 (b) created the moment, which is evident from the unequal normal forces and the concrete uplift at the front and back as seen in Figure 5.13. The consistent failure of the front-headed shear stud first, attributed to its exposure to both tension and shear forces, further supports this observation.

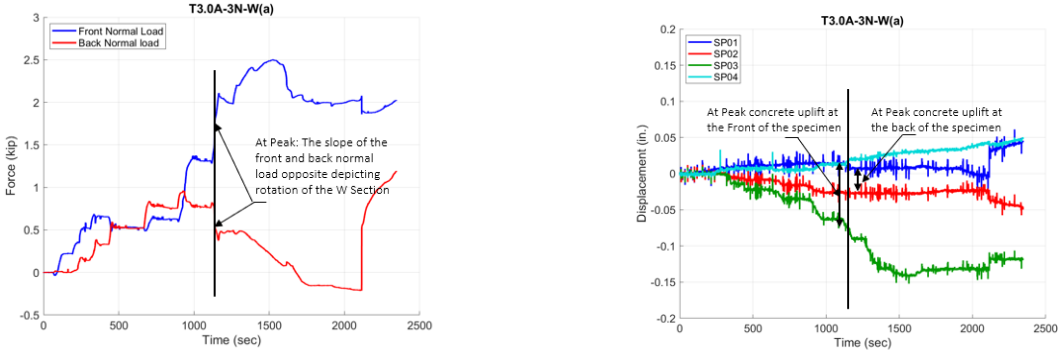

a) Plot of normal load vs time b) Plot of string potentiometers vs time

Fig. 5.13 Evidence of specimen rotation

5.3.4 Preliminary Observations Regarding 3.5 in. Deck

The specimens that had single headed shear studs in strong position showed a consistent occurrence of stud shearing, except for one case where a concrete pull-out failure was observed in one of the two headed shear studs. On average, the headed shear studs in strong positions had a strength of 17.55 kips, which accounted for 72% of the predicted strength based on the guidelines provided by AISC. The shear surface typically occurred at the base metal, as depicted in Figure 5.14.

a) View from below the deck a) on the W section

Fig. 5.14 Typical shearing failure

In the case of single headed shear studs in weak position the average strength was measured to be 12.19 kips, which accounted for 62% of the predicted strength based on AISC guidelines. When headed shear studs were in dovetail profiles, they exhibited stud shearing failure similar to the strong position, with minimal or no bulging observed on the deck in front of the shear studs. On the other hand, when trapezoidal deck profiles were used, two failure modes were observed: deck punching and stud shearing along with deck bulging. The headed shear studs in trapezoidal decks which saw stud shearing initially saw deck bulging, but eventually transitioned to shearing at peak load.

a) Deck punching failure at peak load

a) After lifting the specimen

Fig. 5.15 Typical deck punching failure

Fig. 5.16 Stud shearing failure with deck bulging

For two headed Shear studs in staggered position: The average strength of the headed shear studs in weak position was 11.78 kips which were 63% of the predicted strength given by the provisions in AISC. The headed shear studs showed stud shearing and concrete cone failure.

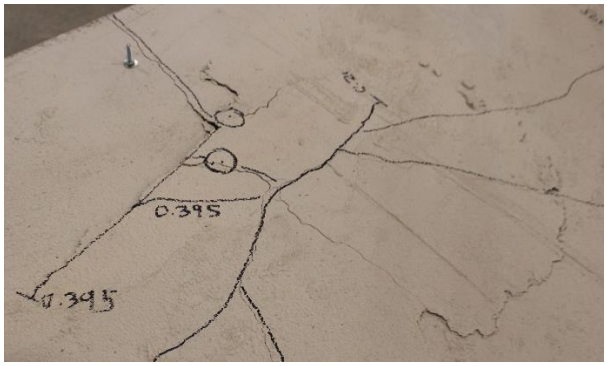

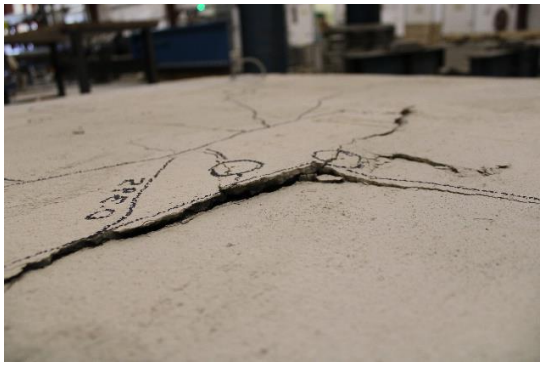

Fig. 5.17 Concrete cone failure

Load vs slip curves for all the specimen groups tested are shown in Figure 5.18 and 5.19. Figure 5.18 shows the curves with headed shear studs in strong, weak and two staggered positions

in 3.5 in trapezoidal deck while Figure 5.19 shows curves with headed shear studs in strong, weak, centered and two studs centered positions in 3.5 dovetail deck profile.

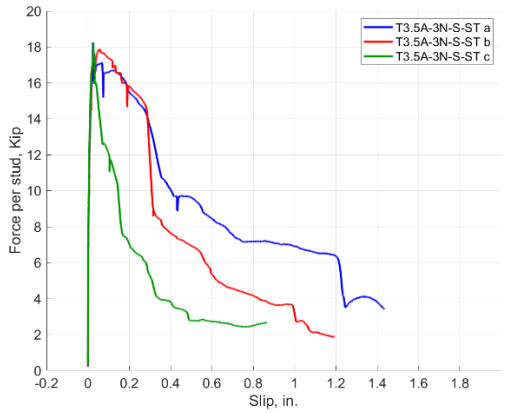

a) T3.5A-3N-S-ST

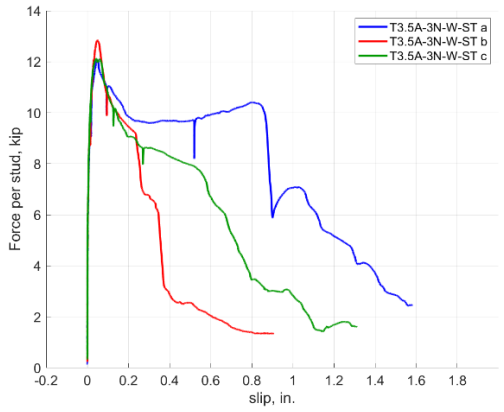

b) T3.5A-3N-W-ST

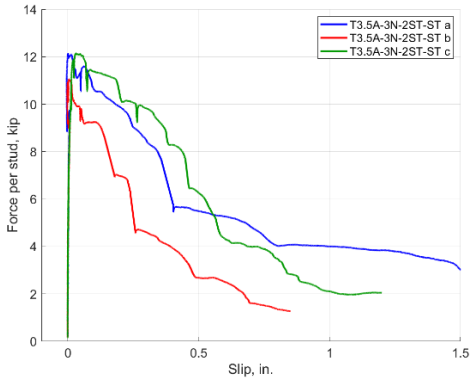

c) T3.5A-3N-2ST-ST

Fig. 5.18 Load vs Slip curves for 3.5 in. Trapezoidal deck Specimen

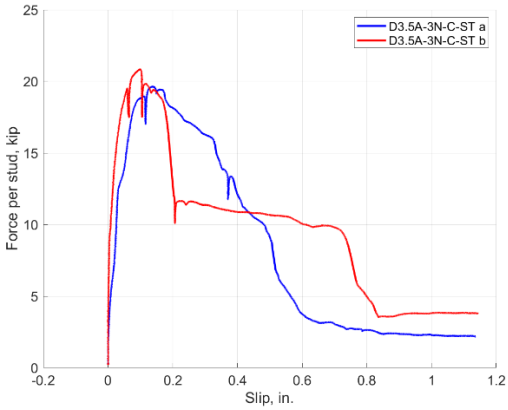

a) D3.5A-3N-C-ST

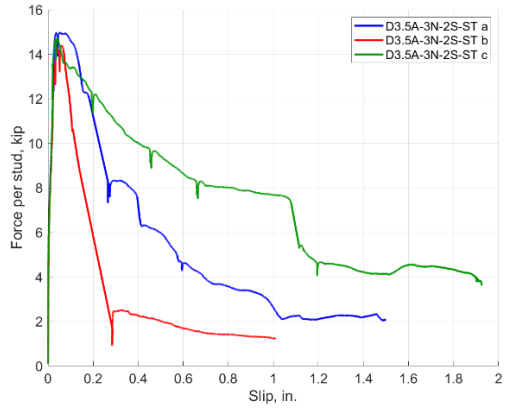

b) D3.5A-3N-2S-ST

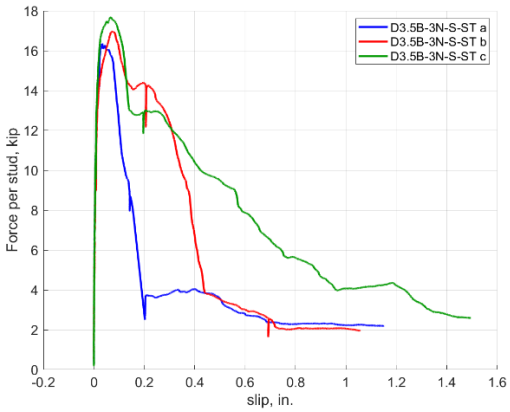

c) D3.5B-3N-S-ST

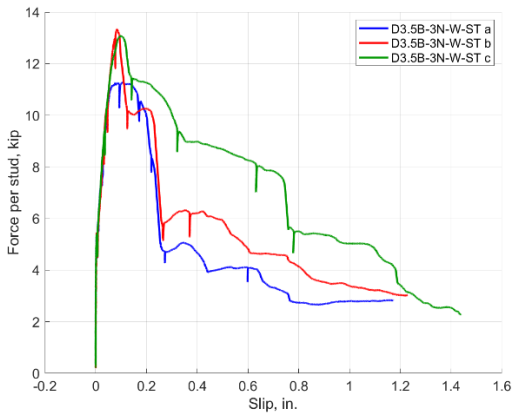

b) D3.5B-3N-W-ST

Fig. 5.19 Load vs Slip curves for 3.5 in. Dovetail deck Specimen

The average measured shear strength per stud, ranging between 63% and 74% of the predicted strength using the AISC 360 provision, indicates a deviation from the expected values. Considering the challenges highlighted in the Section 5.33, it is likely that certain groups experienced lower strength results due to these issues. Based on these findings, it may be necessary to consider a reduction factor for the shear strength of headed shear studs in the 3.5 in. deck. However, it is crucial to conduct further testing to gain a deeper understanding of the underlying factors causing the deviations and to validate the need for a reduction factor.

5.3.5 Modified Shear Test

To address these challenges, a solution was proposed to modify the test setup. The concept involved introducing restraints on the slab to prevent rotational movement of the specimen. This modification aimed to eliminate the axial forces experienced by the headed shear studs. The solution involved incorporating two steel frames, as depicted in Figure 5.20, to create the necessary restraints and counteract rotational movement during the test.

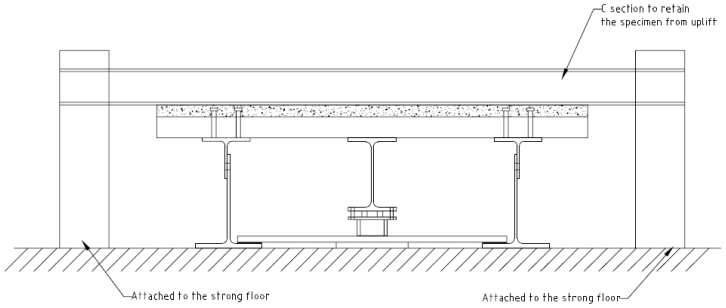

a) Steel frame to restrain from uplift

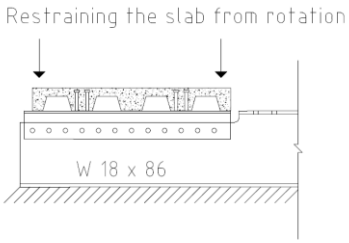

b) side view

c) Actual restrain arrangement

Fig. 5.20 Shear test setup with retrained from uplift

Despite implementing the restraints in the test setup, the generation of axial forces persisted, and the strengths of the headed shear studs remained similar to those without the restraints, as demonstrated in the plot shown in Figure 5.18. The test involved using a 3.5-inch trapezoidal deck with two staggered positioned studs. The peak load observed with the restraints was 12.1 kips per headed shear stud, while without the restraints, it was slightly lower at 11.1 kips. Both scenarios reached the peak load at a similar amount of slip and exhibited comparable post-peak behavior, as depicted in Figure 5.21. The uplift of concrete was also seen showing the specimen was still rotating some amount.

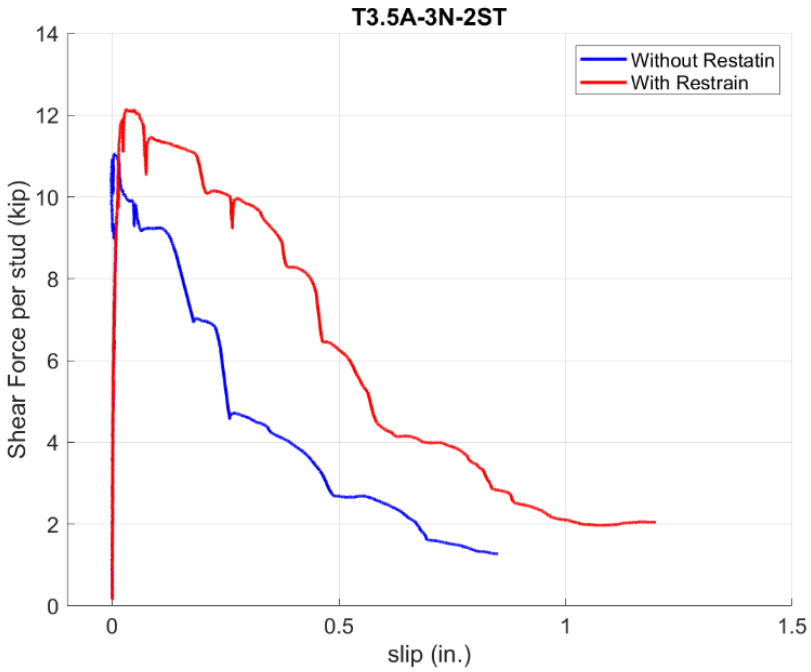

Fig 5.21 Plot of Force vs Slip for T3.5A-3N-2ST

5.4 Evaluation of Single-sided push-out test

5.4.1 Single-sided push-out test Results

One specimen group having 3 in. Trapezoidal deck with headed shear studs in weak position was tested on the single-sided push-out test setup. This group was so chosen as the typical behavior was known and could be compared with past literature and specimen group T3.0A-3N-W. The results of single-sided push-out test are shown in Table 5.4. Predicted strength are calculated using AISC provisions (Eq. 2.58) and that given my Rambo-Roddenberry (2002) (Eq. 2.39).

Table 5.4 Single-sided push-out test Results

Specimen		f'_c (psi)	w (pcf)	f_u (ksi)	Q_{AISC}[1] (kip)	Q_{RR}[2] (kip)	Q_E[3] (kip)	Q_E/Q_{AISC}		Q_E/Q_{RR}		Slip at peak (in.)	Failure Mode[4]
T3.0A-3N-W-M[5]	a	4190	142	78.3	20.67	17.92	14.46	0.70	0.62	0.81	0.72	0.769	DP
	b	4190	142	78.3	20.67	17.92	12.18	0.56		0.68		0.027	SS/DP
	c	4190	142	78.3	20.67	17.92	12.09	0.58		0.67		0.279	SS/DP

Note: 1. Q_{AISC}: AISC Predicted Load per stud 2. Q_{RR}: Predicted Load per stud by Rambo Rodenberry

3. Q_E: Experimental Load per stud

4. SS: Stud Shearing, DP: Deck Punching

5. T3.0A-4N-W-M (b) was carried out with an application of a normal force while (a) and (c) weren't.

T3.0A-4N-W-SS (a) and (c) were tested without application of external normal load and the normal reaction was recorded while specimen (b) was tested with an application of normal load approximately equal to 10% of shear load and the normal reaction was recorded. These are shown in Table 5.5.

Table 5.5 T3.0A-4N-W-M specimen results at peak load

Specimen		At peak load						
		Q_E, Kip	Slip, in.	Front Normal reaction, Kip	Back Normal reaction, kip	Total Normal reaction, Kip	Normal Force applied, Kip	Normal/Shear, %
T3.0A-4N-W-M	a	14.46	0.769	-0.01	3.21	3.21	-	11.09
	b	12.19	0.027	-0.60	3.82	3.13	2.06	12.85
	c	12.09	0.279	0.27	4.48	4.74	-	19.62

The single-sided push-out testes were compared with similar tests conducted by Avellaneda et. al (2023) (3/7.5-4-N-NF-W1) and Rambo-Roddenberry (2002) (D36 W64-7N6-2) on a push-out test frame. From the plot in Figure 5.20, it is observed that specimen T3.0A-4N-W-SS (a) reached a peak load of 14.5 kips per stud, holding the load for a significant amount of slip until failure occurred with deck punching at 0.769 in. of slip. This behavior is similar to the specimens 3/7.5-4-N-NF-W1 and D36 W64-7N6-2, which peaked at 15.7 kips and 15.0 kips with slip measurements of 0.789 in. and 0.850 in., respectively. However, specimens T3.0A-4N-W-M (b) and (c) did not correlate as closely with 3/7.5-4-N-NF-W1 and D36 W64-7N6-2. These

specimens experienced stud shearing failure in the headed shear stud nearest to the actuator, followed by deck punching in the headed shear stud farthest to the actuator. This failure mode is similar to what was observed in specimen T3.0A-3N-W-ST tested on the shear test setup.

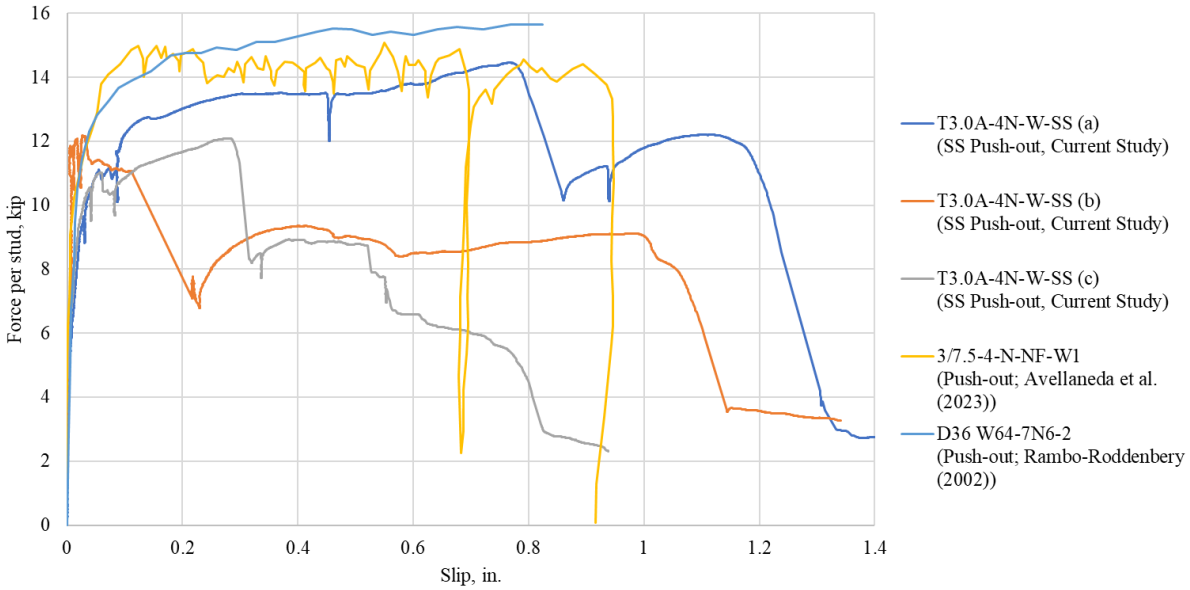

Fig. 5.22 Force vs slip plot

The behavior of T3.0A-4N-W-SS (b) and (c) being similar to the test ran on the shear test says the specimen still experience rotation as this setup also imparts load eccentrically and so there is need to eliminate this rotation causing the headed studs to fail at lower strength due to them being imparted with both axial and shear load. The recommendation for this has been given in the following section.

The axial forces generated can be approximately calculated using the interaction equation given by Nelson (1984). The relation of shear and tension loading on an embedded headed shear stud is given as; For full embedment i.e., the when the anchor embedment length is in the range of 8 to 10 times the shank diameter.

$$\left(\frac{P_u}{P'_u}\right)^{\frac{5}{3}} + \left(\frac{S_u}{S'_u}\right)^{\frac{5}{3}} \leq 1 \tag{5.2}$$

And for partial embedment,

$$\left(\frac{P_u}{P_{uc}}\right)^{\frac{5}{3}} + \left(\frac{S_u}{S_{uc}}\right)^{\frac{5}{3}} \leq 1 \tag{5.3}$$

Where:

P_u = Applied tension load

S_u = Applied Shear load

P'_u = Tensile capacity of the anchor = $0.9A_sF_s$

S'_u = shear capacity of the anchor = $0.9 \text{ x } 6.6\text{x}10^{-3}A_sf'_cE_c^{0.44} \leq 0.9A_sF_s$

P_{uc} = ultimate concrete tesnile capacity = $0.475CL_e(L_e + D_h)\sqrt{f'_c} \leq 0.85A_sF_s$

S_{uc} = Concrete shear capacity of the anchor = $5.66\text{x}10^{-3}A_sf'^{0.33}_cE_c^{0.44} \leq 0.85A_sF_s$

All the headed shear studs used had the embedment length less than 8 times the shank diameter the interaction equation, Equation. 5.3 was used. Since this equation were derived for solid slab, the ratios of S_u/S_{uc} were substituted with Q_E/Q_{AISC} and further the ratio of tensile force generated to the tensile capacity of the headed shear studs in concrete filled steel deck was calculate in Table 5.6. The tensile force ranges from 62% to 73% of its capacity which is a significant amount to lower the shear strength of these headed shear studs.

Table 5.6 Tensile Force Results

Specimen		Q_{AISC}[1] (kip)	Q_E[2] (kip)	Q_E/Q_{AISC}	P_u/P_{uc}[3]
T3.0A-4N-W-SS	a	20.67	14.46	0.70	0.62
	b	20.67	12.18	0.59	0.73
	c	20.67	12.09	0.58	0.73

Note: 1. Q_{AISC}: AISC Predicted Load per stud
2. Q_E: Experimental Load per stud
3. P_{uc}: Ultimate concrete tensile capacity
P_u: Tensile load generated
Pu/Puc: ratio of tensile force generated to the tensile capacity of the headed shear studs

5.4.2 Recommendations

The issue of rotation does not exist is push-out specimen as seeing at the free body diagram of each slab (Figure 4.4) because a couple is formed between the friction force and the compression force between the WT and the slab that counter acts the moment and the headed shear studs are mostly in shear force with little to no tensile force acting on them. This couple between the friction and compression force does not exist in single-sided push-out specimen because the rollers act like a spring support and thus there is a deformation incompatibility as seen in Figure 5.24.

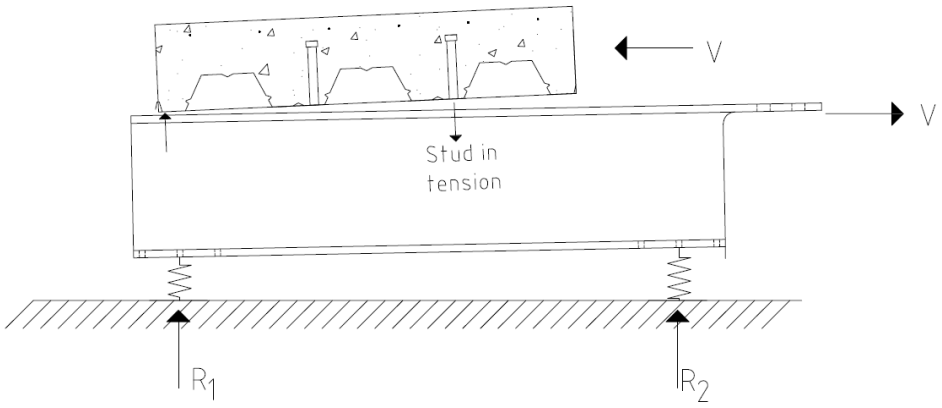

Fig. 5.24 Free body diagram the slab

To overcome this challenge, the rotation causing uplift of the slab on side closest to the actuator it needs to be restricted. The conventional push-out test, the push-out test by Briggs et. al (2021), the setup by Ernst (2006) restrains the out of plane translation at the bearing edge. This restrained should be introduced in this single-sided push-out test to get consistent results. This could be achieved by having an angle section on the bearing block which would bear as well as restrain any uplift of the slab. Also, a normal force should be applied, approximately 10% of the shear load.

6. Conclusions and Future Work

The purpose of this research was to assess and comprehend the difficulties involved in the conventional push-out test and subsequently develop and evaluate new test setups. Additionally, a preliminary investigation was conducted on the behavior of 3.5 in. deep decks in composite beams. A total of thirty-three tests were performed using three different test setups to evaluate the strength of headed shear studs. Two tests one each from the push-out and shear test setup were polluted and weren't considered. Six tests were carried out using the conventional push-out test setup to gain an understanding of the challenges associated with it and to observe the impact of using a 3.5 in. deck in composite beams. Furthermore, twenty-four tests were conducted using the shear test setup, which aimed to mitigate some of the challenges observed in the push-out test. However, certain challenges were still encountered, necessitating further modifications to the test setup. These tests also provided insights into the behavior of composite beams with 3.5 in. deep decks. Additionally, a single-side push-out test was developed, and three tests were performed using 3.0 in. trapezoidal decks to investigate the test setup and make comparisons with previous literature.

6.1 Push-out Test Setup

In the course of conducting the conventional push-out tests, a series of five experiments were considered out using a 3.5 in. dovetail deck configuration, with either one or two headed shear studs positioned at the center. These tests were conducted in accordance with the guidelines specified in AISI S923-20. However, several challenges were encountered during the test procedure, including:

- Bias in test results towards the weaker stud in either slab: All five conducted tests exhibited failure of the headed shear studs in one of the two slabs. It is important to note that the strength

of the headed shear stud (Q_n) is determined by the formula $Q_n = P/n$, where P represents the peak applied axial load and n denotes the total number of headed shear studs tested.

- Slab buckling impacting test accuracy: The recorded out-of-plane displacement of the slab indicated buckling behavior caused by the concentration of load transfer along one edge of the slab. This buckling phenomenon resulted in rotational movement of the LVDTs (Linear Variable Differential Transformers), leading to the recording of negative slip measurements and consequently affecting the accuracy of the test results. Additionally, transverse cracks were observed, which further influenced the strengths of the headed shear studs.
- Limitations in post-peak behavior data: Following the failure of one of the headed shear studs, erratic slip measurements were observed. Some measurements exhibited spikes, while others showed negative values, making it challenging to obtain reliable data on the behavior of the studs after reaching their peak strength.
- Difficulty in achieving uniform bearing on the ground: Ensuring a perfectly uniform bearing of the specimens on the ground proved to be a challenging and time-consuming task. Uneven bearing can result in additional specimen rotation, introducing variability in the test outcomes.
- These challenges highlight the limitations and complexities associated with the conventional push-out tests for headed shear studs and emphasize the need for alternative test setups or modifications to mitigate these issues and improve the accuracy and reliability of test results.

Further, the preliminary study on 3.5 in. deck showed that the strength of one headed shear stud per rib was 19.5 kips, while the strength for two headed shear studs per rib was 12.95 kips. These strengths were found to be unconservative compared to the current AISC provisions, with deviations of 20% and 38% respectively. The lower strength observed for one headed shear stud per rib can be attributed to the fact that the AISC provisions were originally developed based on

tests involving trapezoidal profiles and were limited to deck heights of up to 3 in. In contrast, the tests conducted here used a 3.5 in. dovetail deck configuration. However, the strength of the headed shear studs at 12.95 kips for two studs per rib was significantly low. This can be attributed to the observed buckling of the slab during testing, which adversely affected the measured slip values as well.

6.2 Shear Test Setup

To address the challenges encountered in the conventional push-out test, a shear test setup was developed as an alternative approach. The main objectives of this setup were as follows:

- Reduction of data bias: Unlike the push-out test that involves two slabs, the shear test setup utilized a single slab configuration. This modification aimed to minimize bias in the test results, as the failure of headed shear studs in one slab would no longer skew the data towards the weaker slab.
- Reliable slip measurement: The shear test setup employed a displacement-controlled loading method, which facilitated more accurate slip measurements both before and after reaching the peak load. This approach aimed to overcome the difficulties associated with slip measurement encountered in the push-out test.
- Elimination of uneven bearing and undesirable failure modes: The shear test setup addressed the challenge of achieving uniform bearing on the ground by eliminating the need for such bearing altogether. This modification helped mitigate rotational movements and variability in test data caused by uneven stress distribution. Additionally, it eliminated the occurrence of undesirable failure modes observed in the push-out test.

- Removal of the normal force requirement: Unlike the push-out test, the shear test setup did not require the application of a normal load, reducing the potential for unrealistic failure modes where the slab separates from the beam.

Five tests were conducted using the shear test setup in conjunction with the push-out test as companion tests. The results demonstrated a similar trend in the strengths obtained, with values of 20.10 kips in the shear test compared to 19.5 kips in the push-out test for a single headed shear stud per rib in the center position. The load versus slip curves exhibited close similarity between the two test setups, and the failure modes observed were also consistent. However, due to the compromised slip measurements observed in the push-out test with two headed shear studs per rib, a direct comparison with the shear test results could not be made.

In order to establish a correlation with existing literature, three specimens with a 3 in. trapezoidal deck configuration were tested using the modified test setup. These specimens were designed with headed shear studs positioned in the weak location. The test results revealed a consistent failure mode in which the headed shear stud closest to the actuator experienced stud shearing, while the stud farther away underwent deck punching. Surprisingly, the peak load was reached at a very low slip value. This observed failure mode differed from the typical behavior of headed shear studs in the weak position, which typically exhibit deck punching as the primary failure mode with the peak load sustained over a significant amount of slip. Additionally, the strengths of the specimens were lower than expected. Further investigation uncovered that the eccentricity in loading created moments within the specimens, leading to the development of tensile forces in the headed shear studs. Consequently, the lower strength values observed in these tests were attributed to the fact that the headed shear studs were subjected to both shear and tensile forces.

6.3 Single-sided Push-out Test Setup

To eliminate the axial forces in the headed shear studs, the test setup was modified to align with the boundary conditions of the conventional push-out test. This modification involved bearing the concrete filled steel deck on a bearing block instead of attaching the specimen to the side beams with the WTs. Additionally, a frame was introduced to accommodate a hydraulic jack, which would apply a normal load on the specimen during testing. This new setup aimed to replicate the conditions of the push-out test hoping to eliminate the axial forces in the headed shear studs.

Three tests were performed using 3 in. trapezoidal decks and headed shear studs in weak positions. The average strength obtained from these tests was 12.91 kips, which was found to be unconservative when compared to the AISC provisions. The behavior of one of the tests aligned well with the findings of previous literature, while the behavior of the other two tests did not match as closely. It was observed that the specimens still exhibited rotation during testing, resulting in the development of tensile forces within the specimen due to the eccentric loading in shear. To address this issue, a proposal was put forth to apply the normal force as close to the actuator side as possible, and to apply the normal force less than 10% of the predicted shear force before the start of the test to compress the rollers thus voiding lateral deformation eliminating the generation of axial forces in the headed shear studs.

6.4 Preliminary Observations Regarding 3.5 in. Deck

Tests conducted using a 3.5 in deck revealed headed shear stud strengths of 17.55 kips, 12.19 kips, and 11.78 kips for the strong, weak, and two staggered configurations, respectively. These strengths were found to be unconservative compared to the current AISC provisions, ranging from approximately 63% to 75% of the predicted strength. Given the challenges faced

during testing, it is important to conduct further investigations to identify the factors contributing to these deviations and to determine the necessity of a reduction factor.

6.5 Recommendation for Future Work

The suggested modification for the single-sided push-out test involves applying the normal load and keeping it approximately 10% of the predicted shear force prior to the test and also adding an angle section to the bearing block which would help to restrain vertical uplift of the specimen. This adjustment aims to enhance the rigidity of the boundary conditions by compressing the roller supports and restricting concrete uplift. By doing so, the specimen's rotation will be prevented, effectively avoiding the development of tensile forces in the headed shear studs. Tests should be carried out to evaluate this configuration.

To further investigate the behavior of headed shear studs in composite beams with 3.5 in. decks, additional tests should be carried out. Once these tests are completed, the findings can be validated through a full-beam test. This approach will provide a thorough understanding of the performance of headed shear studs in composite beams using 3.5 in decks.

References

AISC 360 (2022). *Specification for Structural Steel Buildings*, (AISC 360). American Iron and Steel Institute.

AISI S923 (2020). Test Standard for Determining the Strength and Stiffness of Shear Connections of Composite Members. (AISI S923). American Iron and Steel Institute

Viest, I. M. (1956). Investigation of Stud Shear Connectors for Composite Concrete and Steel T-Beams. *ACI Journal Proceedings*, *52*(4). https://doi.org/10.14359/11655

Davies, C. (1967). Small-scale push-out test on welded stud shear connectors. *Concrete (London)*, *1*(9), 311–316.

Ollgaard, J. G., Slutter, R. G., & Fisher, J. W. (1970). Shear Strength of Stud Connectors in Lightweight and Normal-Weight Concrete. *AISC Engineering Journal, American Institute of Steel Construction*, 55–64.

Hawkins, N. M., & Mitchell, D. (1984). Seismic Response of Composite Shear Connections. *Journal of Structural Engineering-Asce*, *110*(9), 2120–2136. https://doi.org/10.1061/(asce)0733-9445(1984)110:9(2120

Jayas, B. S., & Hosain, M. U. (1987). Behavior of headed studs in composite beam: push-out test. University of Saskatchewan manuscript, Saskatoon, Canada.

Robinson, H. (1988). Multiple stud shear connections in deep ribbed metal deck. *Canadian Journal of Civil Engineering*, *15*(4), 553–569. https://doi.org/10.1139/l88-076

Mottram, J. T., & Johnson, R. P. (1990). Push tests on studs welded through profiled steel sheeting. *The Structural Engineer*, *68*(10), 187–193.

Lloyd, R., & Wright, H. (1990). Shear connection between composite slabs and steel beams. *Journal of Constructional Steel Research*, *15*(4), 255–285. https://doi.org/10.1016/0143-974x(90)90050-q

Androutsos, C., & Hosain, M. U. (1992). Composite Beams with Headed Studs in Narrow Ribbed Metal Deck. *Composite Construction in Steel and Concrete II*, 771–782.

Sublett, C. N. (1991). Strength of Welded Headed Studs in Ribbed Metal Deck on Composite joists. MS Dissertation, Virginia Tech

Chandrasekar, G. (1995), Headed Stud Shear Connectors in Solid Slabs and in Slabs with Wide Ribbed Metal Deck, MS Dissertation, University of Saskatchewan.

Lyons, J. C., Easterling, S. W., & Murray, T. M. (1996), Strength of Headed Shear Studs in Cold-formed Steel Deck. *International Specialty Conference on Cold-Formed Steel Structures. 3.*

Lyons, C. J. (1994), Strength of Welded Shear Studs, MS Thesis, Virginia Tech

Johnson, R. P., & yuan, H. (1998). Existing Rules and New Tests for Stud Shear Connectors in Troughs of Profiled Sheeting. *Proceedings of the Institution of Civil Engineers - Structures and Buildings*, *128*(3), 244–251. https://doi.org/10.1680/istbu.1998.30458

Kim, B., Wright, H. D., & Cairns, R. (2001). The behaviour of through-deck welded shear connectors: an experimental and numerical study. *Journal of Constructional Steel Research*, *57*(12), 1359–1380. https://doi.org/10.1016/s0143-974x(01)00037-2

Rambo-Roddenberry, M., Lyons, J. C., Easterling, W. S., & Murray, T. M. (2002). Performance and Strength of Welded Shear Studs. *Composite Construction in Steel and Concrete IV*. https://doi.org/10.1061/40616(281)40

Rambo-Roddenberry, M. (2002). Behavior and Strength of welded Stud Shear Connectors, Ph.D. Dissertation, Virginia Tech.

Hicks, S., & Couchman, G. (2006). The Shear Resistance and Ductility Requirements of Headed Studs Used With Profiled Steel Sheeting. *Composite Construction in Steel and Concrete V*. https://doi.org/10.1061/40826(186)48

Hicks, Stephen. (2007). Resistance and ductility of shear connection: Full-scale beam and push tests.https://www.researchgate.net/publication/256537047_Resistance_and_ductility_of_shear_connection_Full-scale_beam_and_push_tests

Smith, A., & Couchman, G. (2010). Strength and ductility of headed stud shear connectors in profiled steel sheeting. *Journal of Constructional Steel Research*, *66*(6), 748–754. https://doi.org/10.1016/j.jcsr.2010.01.005

Hicks, S. J., & Smith, A. L. (2014). Stud Shear Connectors in Composite Beams that Support Slabs with Profiled Steel Sheeting. *Structural Engineering International*, *24*(2), 246–253. https://doi.org/10.2749/101686614x13830790993122

Hicks, S. J., Ciutina, A., & Odenbreit, C. (2017). Development of New Push Test for Eurocode 4. *Proceedings of the Eighth International Conference on Composite Construction in Steel and Concrete*, 62-73

Veljkovic, M., & Johansson, B. (2006). Residual Static Resistance of Welded Stud Shear Connectors. *Composite Construction in Steel and Concrete V*. https://doi.org/10.1061/40826(186)49

Fan, J. S., & Liu, W. (2014). Tests on Shear Studs Using Profiled Steel Sheeting Subjected to Cyclic Loading. *Applied Mechanics and Materials*, *578–579*, 196–200. https://doi.org/10.4028/www.scientific.net/amm.578-579.196

Hirama, C., Ishikawa, T., & Hisagi, A. (2017). 08.21: Shear strength of headed stud push-out tests: Comprehensive literature review focusing on slab type, failure mode, and large-diameter headed stud. *Ce/Papers, 1*(2–3), 2013–2022. https://doi.org/10.1002/cepa.246

Eggert, F., & Kuhlmann, U. (2017). Influence of The Composite Action on The Load Bearing and Deformation Behavior of Composite Beams with Profiled Steel Sheeting *Proceedings of the Eighth International Conference on Composite Construction in Steel and Concrete,* 310-321

Sun, Q., Nie, X., Denavit, M. D., Fan, J., & Liu, W. (2019). Monotonic and cyclic behavior of headed steel stud anchors welded through profiled steel deck. *Journal of Constructional Steel Research*, *157*, 121–131. https://doi.org/10.1016/j.jcsr.2019.01.022

Konrad, M., Eggert, F., Kuhlmann, U., & Schorr, J. (2020). New approach for the design shear resistance of headed studs in profiled steel sheeting with ribs transverse to supporting beam. *Steel Construction*, *13*(4), 252–263. https://doi.org/10.1002/stco.202000018

Odenbreit, C., & Nellinger, S. (2017). Mechanical model to predict the resistance of the shear connection in composite beams with deep steel decking. *Steel Construction*, *10*(3), 248–253. https://doi.org/10.1002/stco.201710029

Albarram, A., Qureshi, J., & Abbas, A. (2017). Behaviour of Headed Stud Connectors in Composite Beams with Very Deep Profiled Sheeting. *Advances in Structural Engineering and Mechanics (ASEM17), 28 August 2017–1 September 2017*.

Avellaneda, R. (2022). Experimental Evaluation of Concrete Filled Steel Deck Diaphragms for Seismic Actions, Ph.D. Dissertation, Virginia Tech.

Avellaneda, R et al. (2023). Pushout Test Data for Headed Shear Studs Associated with Diaphragm Testing Program, Report No. CE/VPI-ST-23/03, Virginia Tech.

Van der Sanden, P. G. F. J., (1996), The Behaviour of a Headed Stud Connection in a 'New' Push Test Including a Ribbed Slab Test: Background report, *BKO-report 96-16.*

Hicks, S. J., & McConnel, R. E. (1996). The Shear Resistance of Headed Studs used with Profiled Steel Sheeting. *Composite Construction in Steel and Concrete III*, 325–338

Chan, T. W. K., Rezansoff, T., Hosain, M. U. (1984). Behavior of Headed Studs in Stub-Girder Stub Assemblages. University of Saskatchewan manuscript, Saskatoon, Canada.

Lam, D. (2002). New Test for Shear Connectors in Composite Construction. *Composite Construction in Steel and Concrete IV*. https://doi.org/10.1061/40616(281)35

Lowe, D. J., Das, R., Clifton, G. C., & Navaranjan, N. (2014). Characterisation of the Shear Stud-Concrete Connection Using Finite Element Analysis. *Applied Mechanics and Materials*, *553*, 570–575. https://doi.org/10.4028/www.scientific.net/amm.553.570

Briggs, N.E., Avellaneda-Ramirez, R.E., Coleman, K., Schafer, B.W., Eatherton, M.R., Easterling, W.S. and Hajjar, J.F. (2023), Cyclic Behavior of Composite Connections in Composite Floor Diaphragms. Ce/papers, 6: 566-577. Https://doi.org/10.1002/cepa.1937

Ernst, S., Bridge, R. Q., & Wheeler, A. (2010). Correlation of Beam Tests with Pushout Tests in Steel-Concrete Composite Beams. *Journal of Structural Engineering*. https://doi.org/10.1061/(ASCE)0733-9445(2010)136:2(183)

Ernst, S. (2006). Factors Affecting the Behaviour of the Shear Connection of Steel-Concrete Composite Beams, Ph.D. Dissertation, University of Western Sydney

Robinson, H. (1967). Tests on Composite Beams with Cellular Deck. *Journal of the Structural Division*, *93*(4), 139–164. https://doi.org/10.1061/jsdeag.0001725

Fisher, J. W. (1970). DESIGN OF COMPOSITE BEAMS WITH FORMED METAL DECK. *Engineering J, Am Inst Steel Constr*.

Grant, J. A., Fisher, J. W., & Slutter, R. G. (1977). COMPOSITE BEAMS WITH FORMED STEEL DECK. *Engineering Journal*, *14*(1). https://trid.trb.org/view/52850

McGarraugh, J. B, & Baldwin, J. W. (1971). Lightweight Concrete-on-Steel Composite Beams. *AISC Engineering Journal*, 90–98.

Jayas, B. S., & Hosain, M. U. (1987). Behavior of headed studs in composite beam: Full-size Test. University of Saskatchewan manuscript, Saskatoon, Canada.

Eastering, W. S., Gibbings, D. R., Murray, T. M., (1993). Strength of Shear Studs in Steel Deck on Composite Beams and Joists, *Engineering Journal, American Institute of Steel Construction, Vol. 30*, 44-55.

Nie, J., Fan, J., & Cai, C. (2008). Experimental study of partially shear-connected composite beams with profiled sheeting. *Engineering Structures*, *30*(1), 1–12. https://doi.org/10.1016/j.engstruct.2007.02.016

Ranzi, G., Bradford, M., Ansourian, P., Filonov, A., Rasmussen, K., Hogan, T., & Uy, B. (2009). Full-scale tests on composite steel–concrete beams with steel trapezoidal decking. *Journal of Constructional Steel Research*, *65*(7), 1490–1506. https://doi.org/10.1016/j.jcsr.2009.03.006

Al-deen, S., Ranzi, G., & Vrcelj, Z. (2011). Full-scale long-term and ultimate experiments of simply-supported composite beams with steel deck. *Journal of Constructional Steel Research*, *67*(10), 1658–1676. https://doi.org/10.1016/j.jcsr.2011.04.010

Appendix A: Test Setup Detailed Drawings

A1: Shear Test Setup

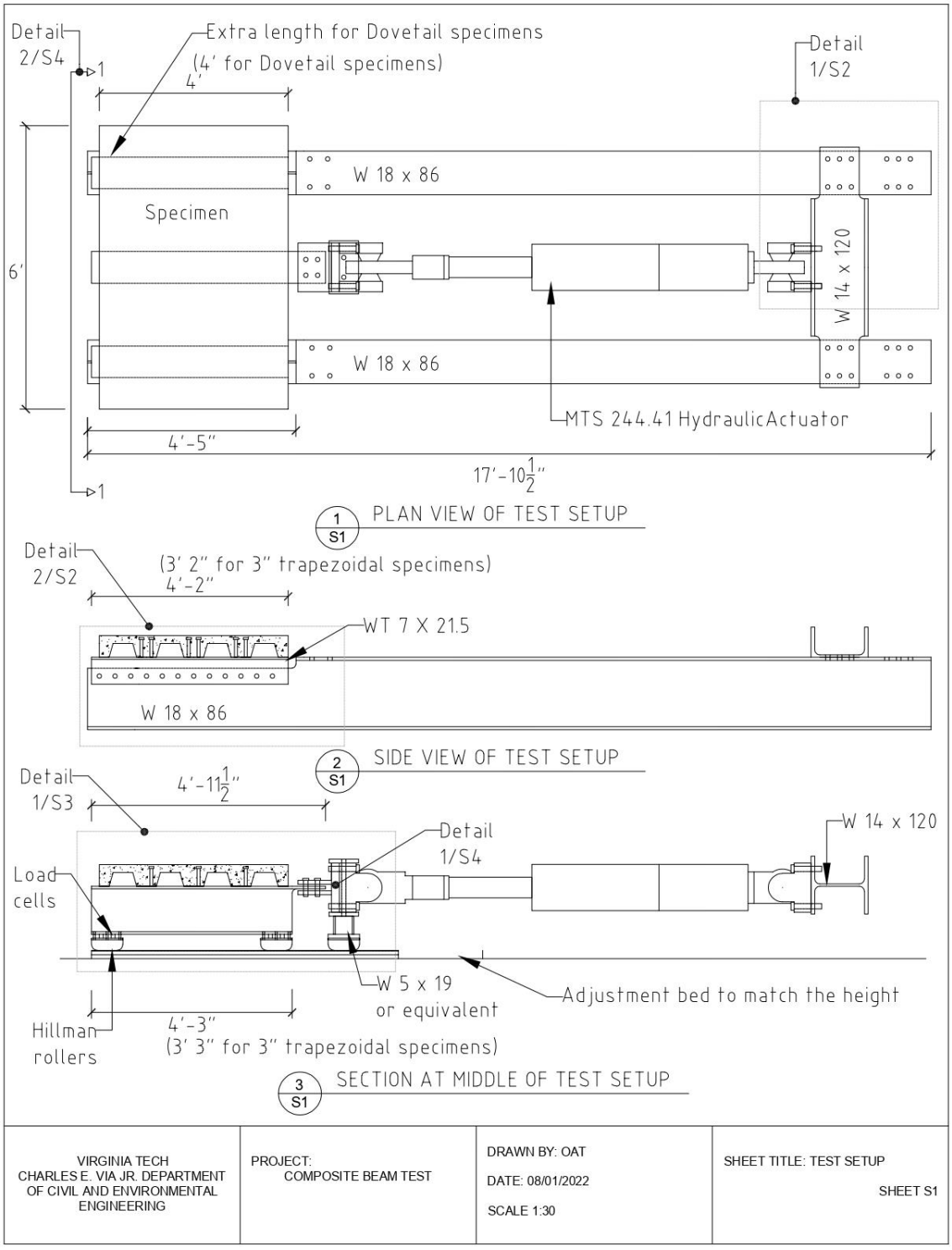

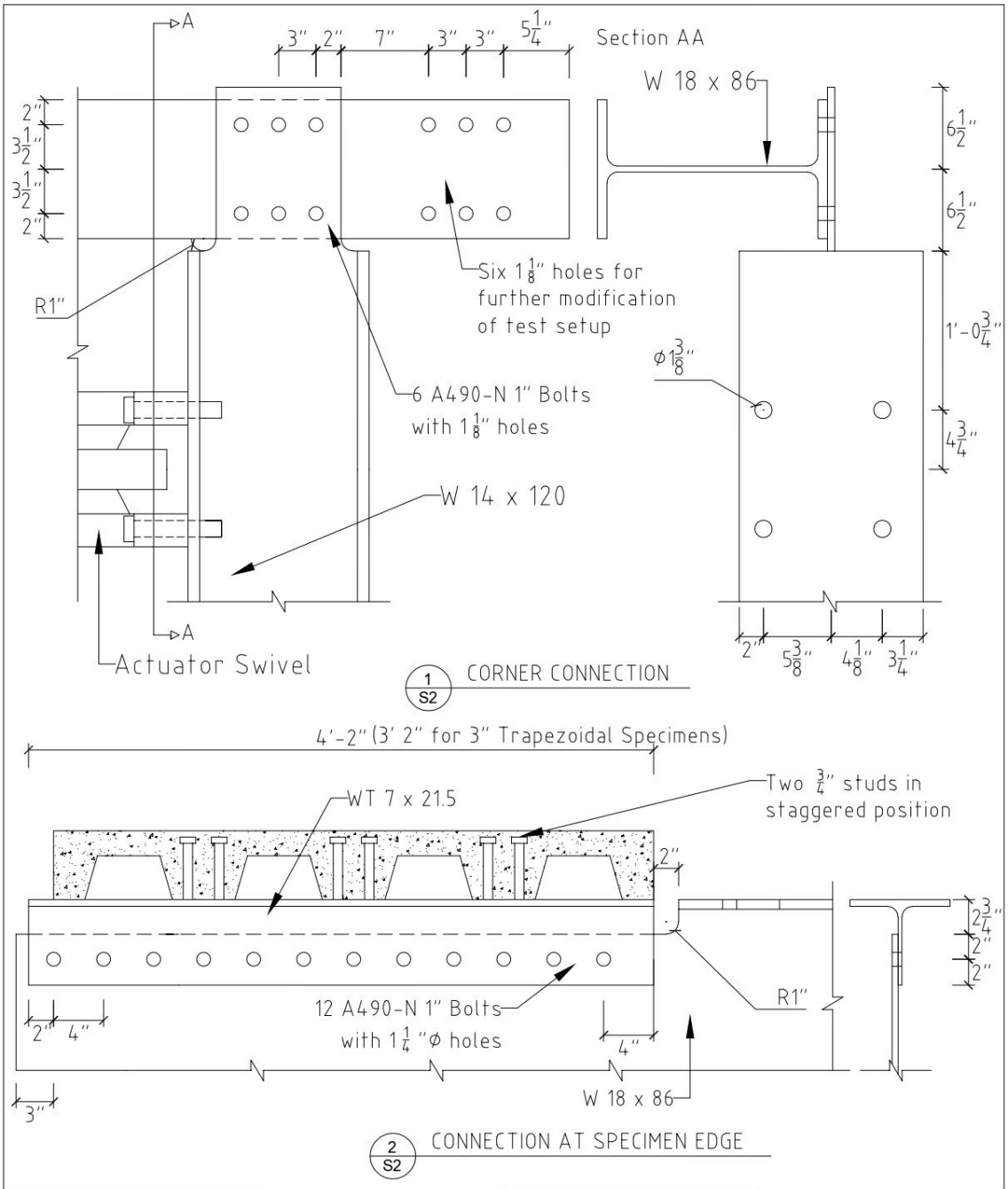

VIRGINIA TECH CHARLES E. VIA JR. DEPARTMENT OF CIVIL AND ENVIRONMENTAL ENGINEERING	PROJECT: COMPOSITE BEAM TEST	DRAWN BY: OAT DATE: 08/01/2022 SCALE 1:10	SHEET TITLE: CONNECTION DETAILS SHEET S2

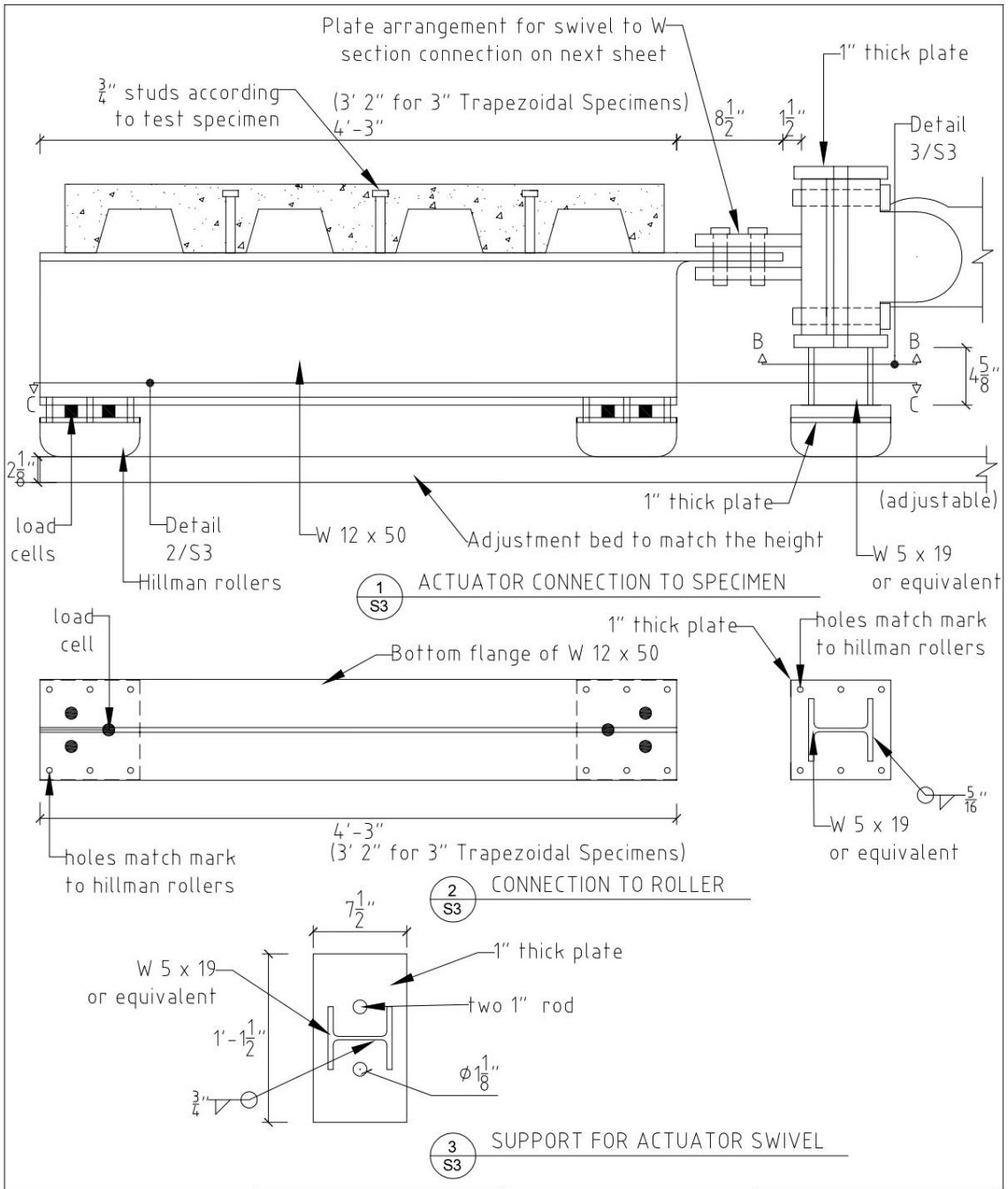

VIRGINIA TECH CHARLES E. VIA JR. DEPARTMENT OF CIVIL AND ENVIRONMENTAL ENGINEERING	PROJECT: COMPOSITE BEAM TEST	DRAWN BY: OAT DATE: 08/01/2022 SCALE 1:10	SHEET TITLE: CONNECTION DETAILS SHEET S3

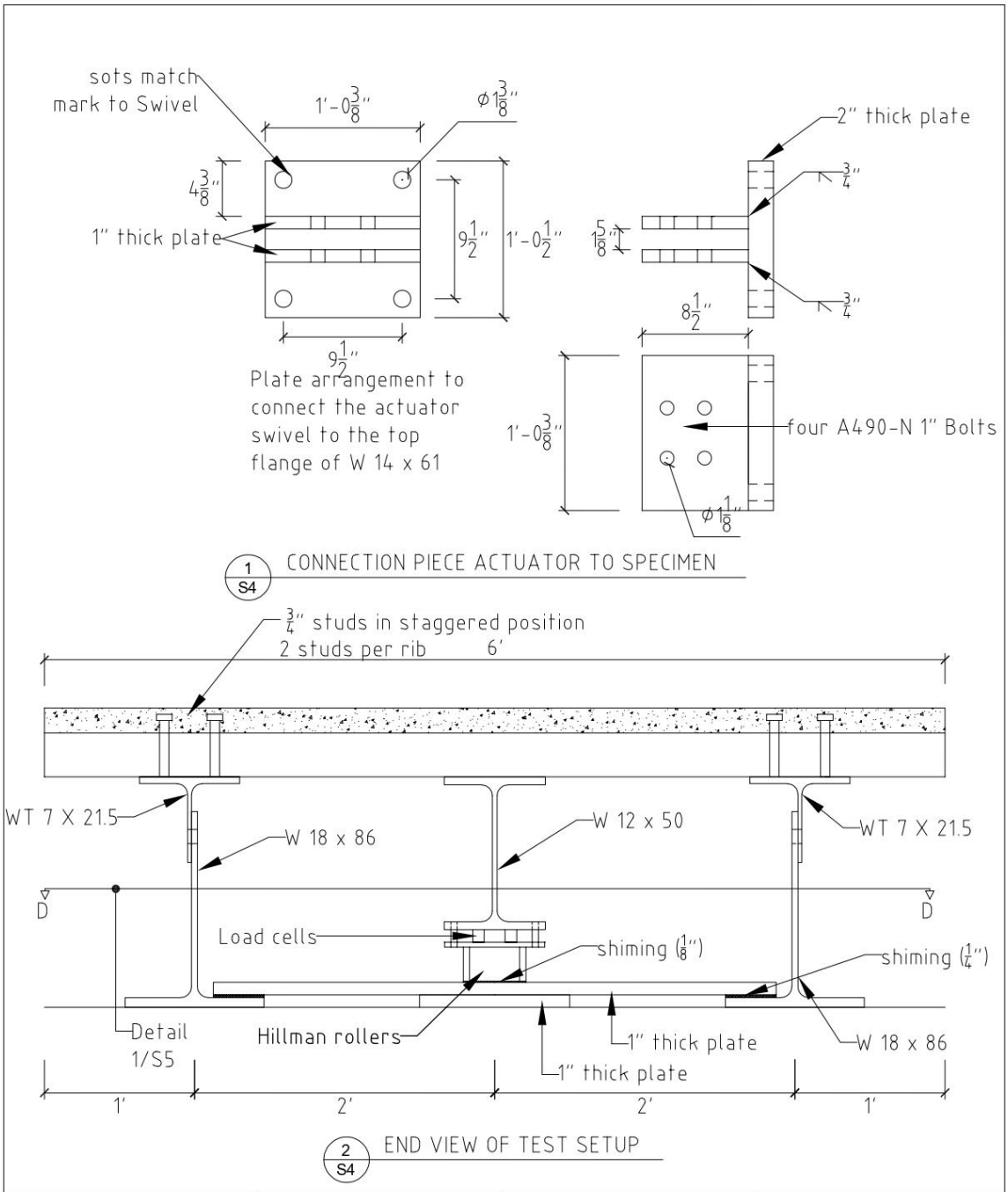

VIRGINIA TECH CHARLES E. VIA JR. DEPARTMENT OF CIVIL AND ENVIRONMENTAL ENGINEERING	PROJECT: COMPOSITE BEAM TEST	DRAWN BY: OAT DATE: 08/01/2022 SCALE 1:10	SHEET TITLE: CONNECTION DETAILS SHEET S4

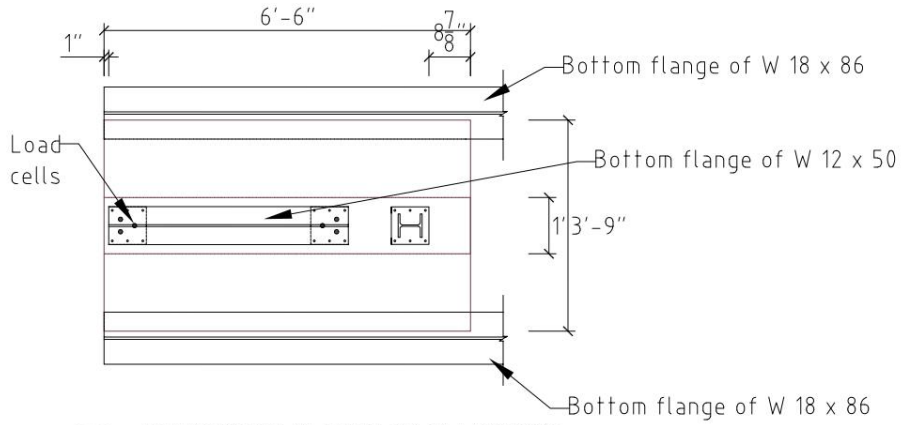

1 S5 ADJUSTMENT PLATES BELOW SPECIME

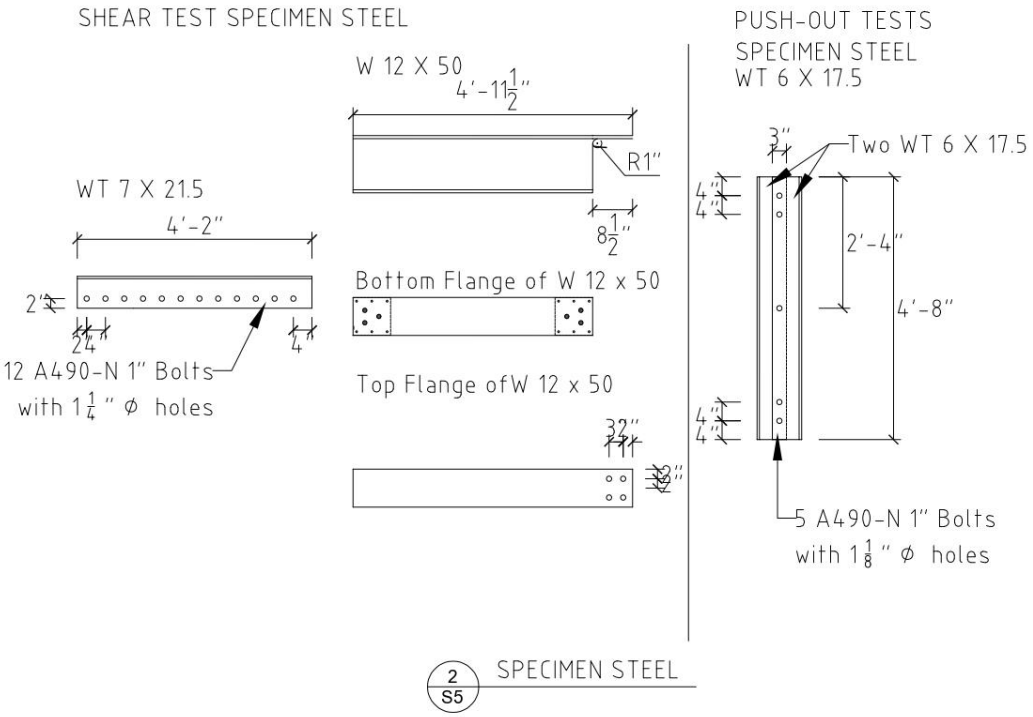

2 S5 SPECIMEN STEEL

VIRGINIA TECH CHARLES E. VIA JR. DEPARTMENT OF CIVIL AND ENVIRONMENTAL ENGINEERING	PROJECT: COMPOSITE BEAM TEST	DRAWN BY: OAT DATE: 08/01/2022 SCALE 1:30	SHEET TITLE: PLATE ARRANGEMENT & SPECIMEN STEEL SHEET S5

A2: Single-sided Push-out Test Setup

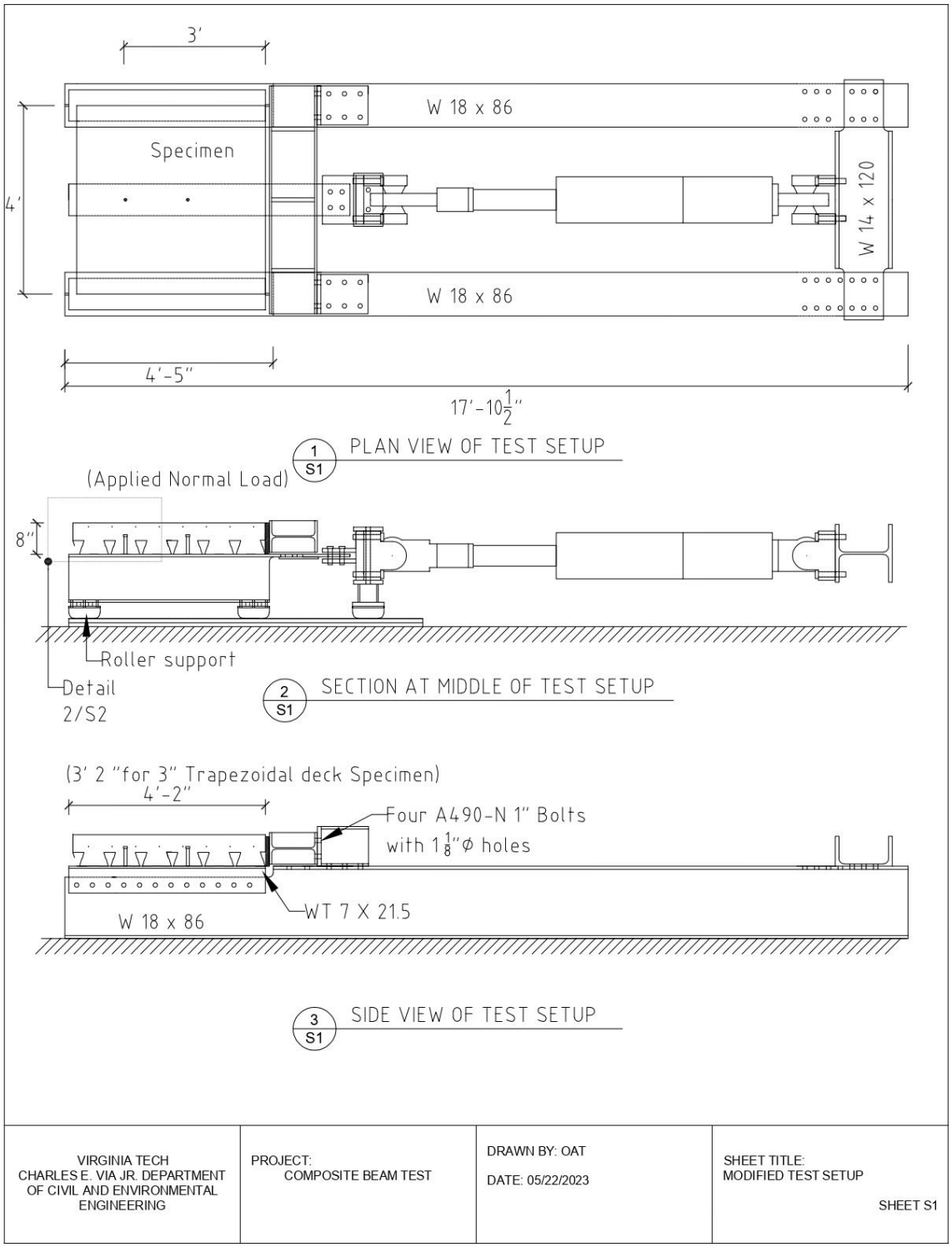

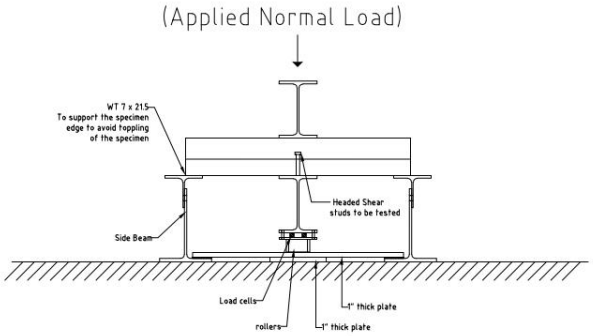

1 S2 END VIEW OF TEST SETUP

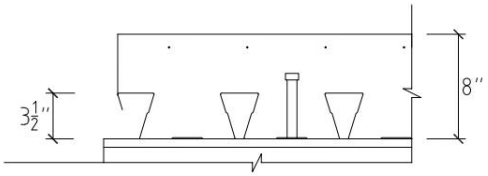

2 S2 SPECIMEN DETAIL

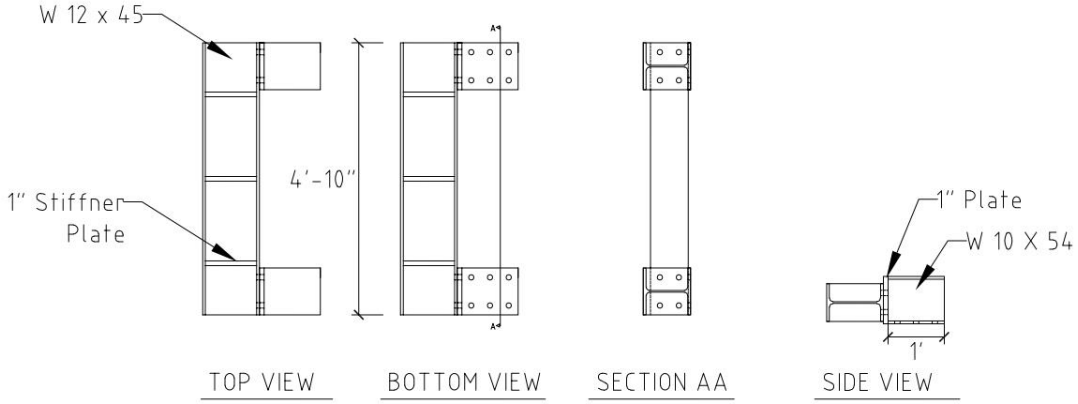

3 S2 W SECTION FOR CONCRETE BEARING

VIRGINIA TECH CHARLES E. VIA JR. DEPARTMENT OF CIVIL AND ENVIRONMENTAL ENGINEERING	PROJECT: COMPOSITE BEAM TEST	DRAWN BY: OAT DATE: 05/22/2023	SHEET TITLE: MODIFIED TEST SETUP SHEET S2

Appendix B: Specimen Details

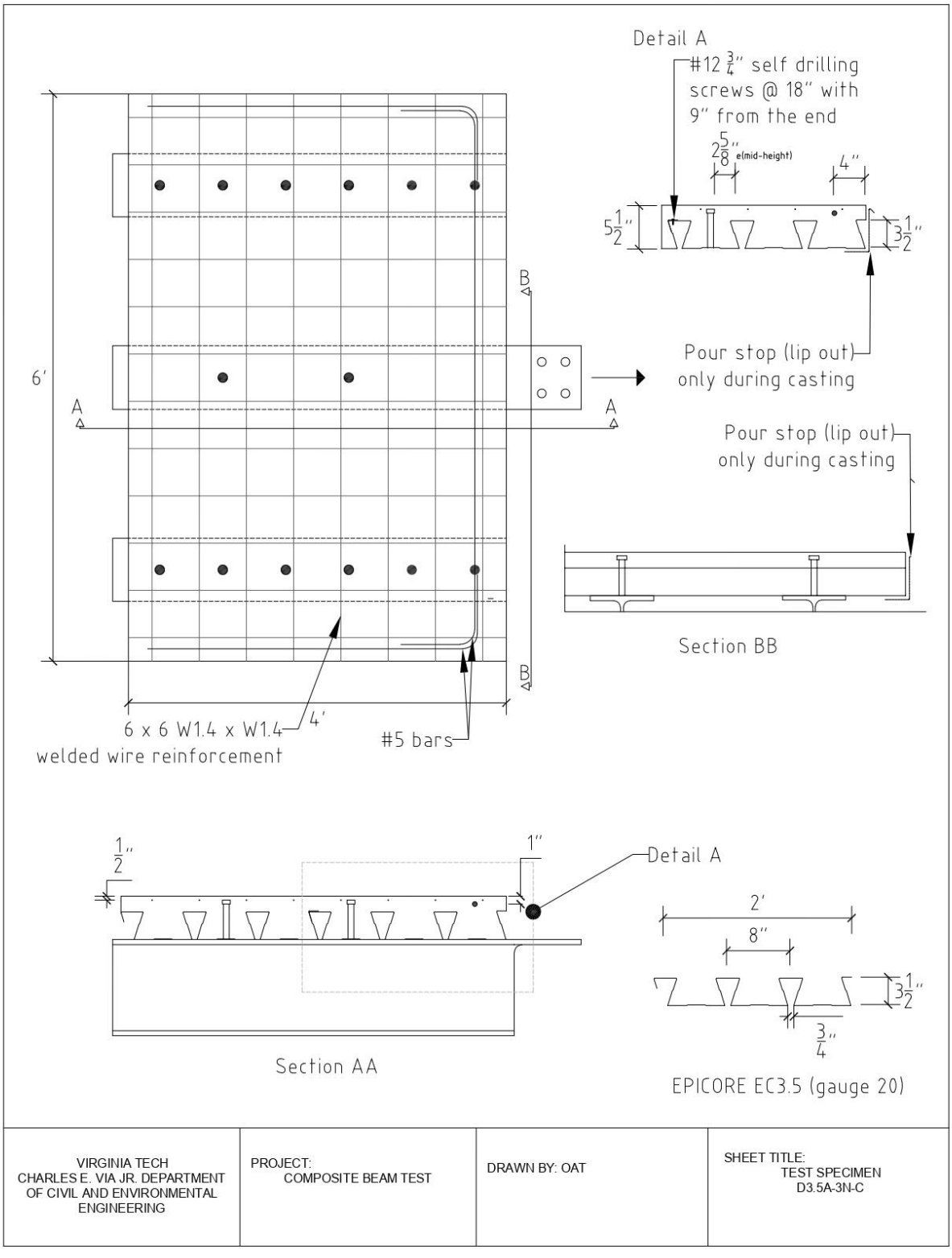

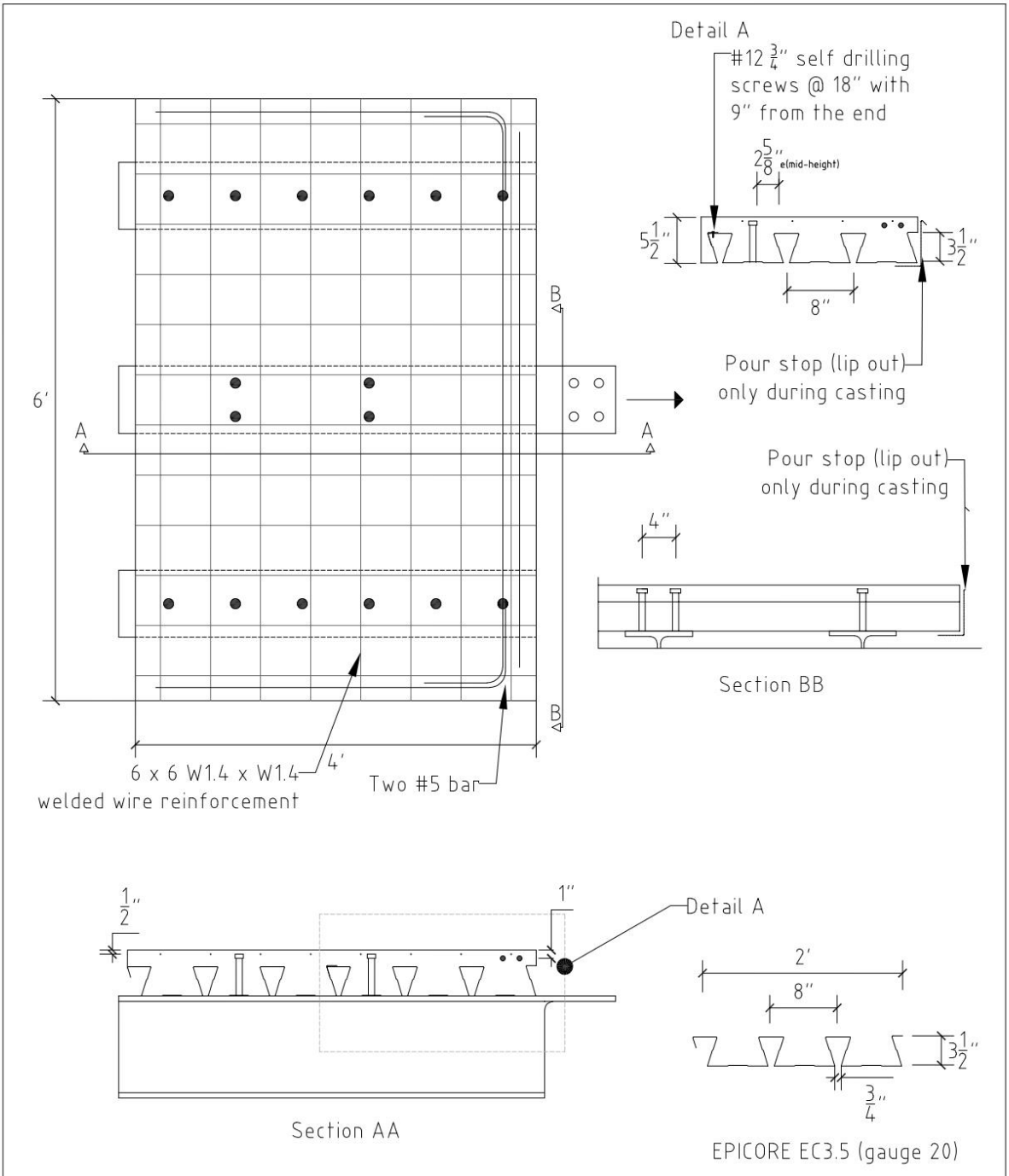

VIRGINIA TECH CHARLES E. VIA JR. DEPARTMENT OF CIVIL AND ENVIRONMENTAL ENGINEERING	PROJECT: COMPOSITE BEAM TEST	DRAWN BY: OAT	SHEET TITLE: TEST SPECIMEN D3.5A-3N-2S

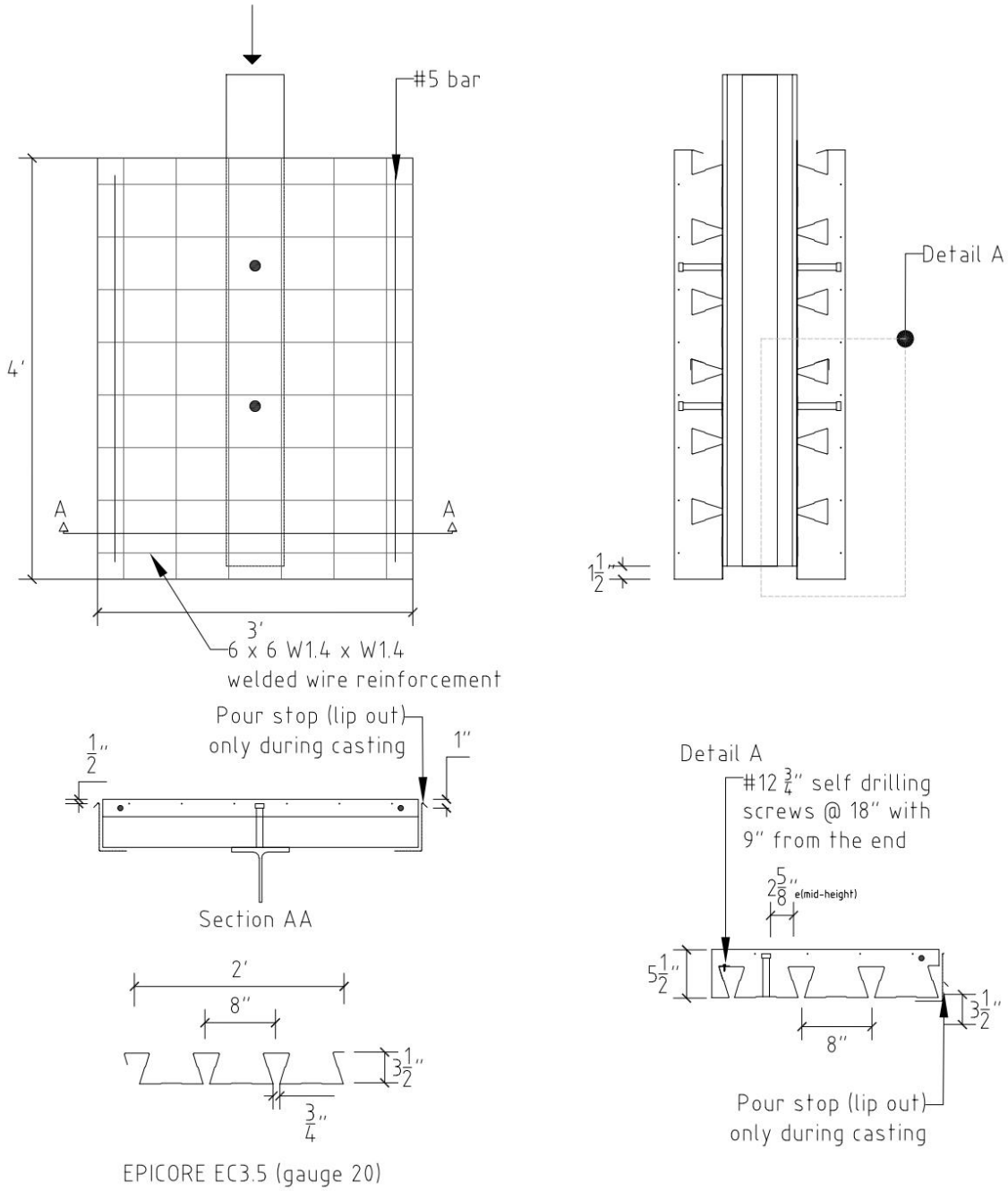

VIRGINIA TECH CHARLES E. VIA JR. DEPARTMENT OF CIVIL AND ENVIRONMENTAL ENGINEERING	PROJECT: COMPOSITE BEAM TEST	DRAWN BY: OAT	SHEET TITLE: TEST SPECIMEN D3.5A-3N-C-PO

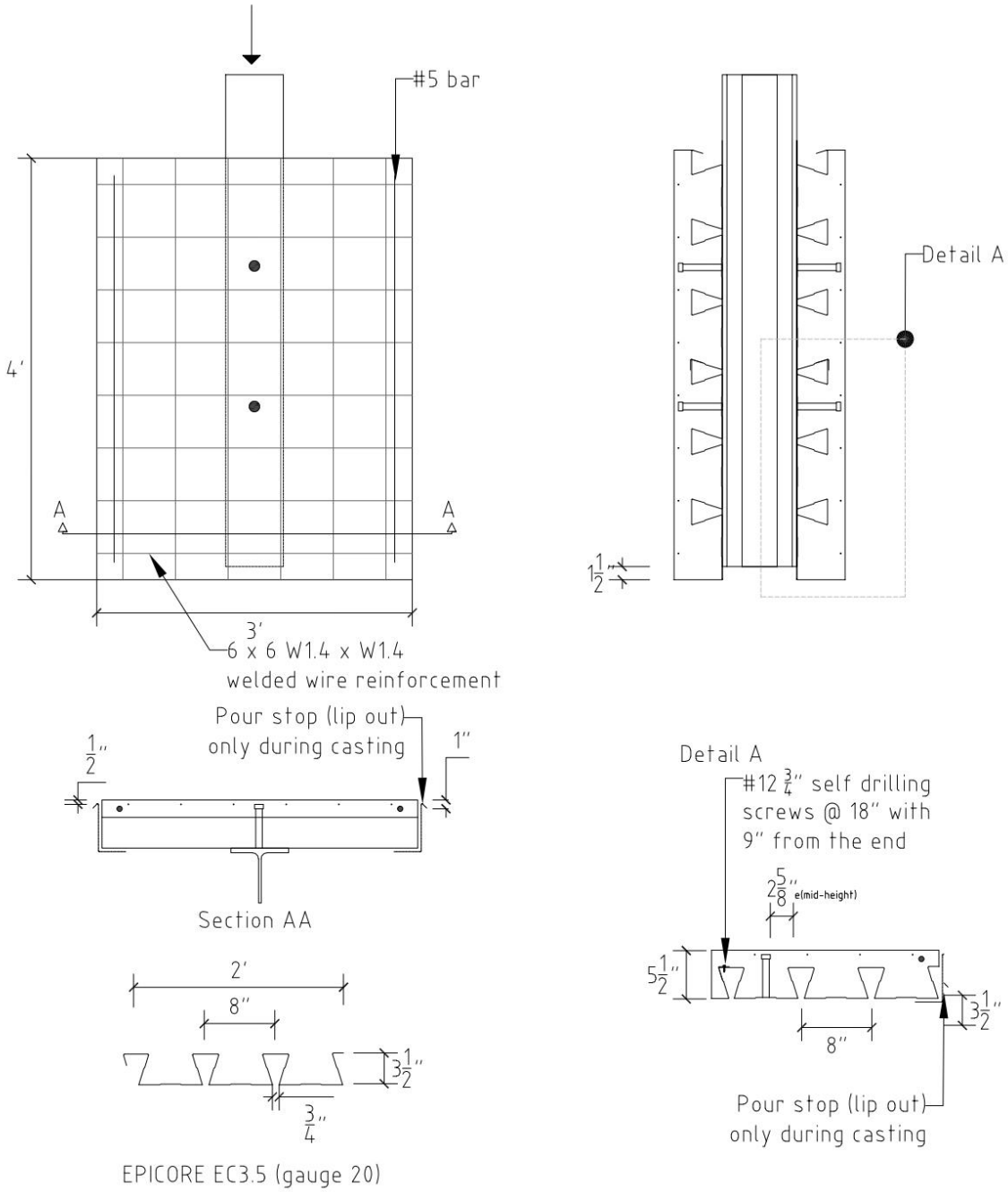

VIRGINIA TECH CHARLES E. VIA JR. DEPARTMENT OF CIVIL AND ENVIRONMENTAL ENGINEERING	PROJECT: COMPOSITE BEAM TEST	DRAWN BY: OAT	SHEET TITLE: TEST SPECIMEN D3.5A-3N-C-PO

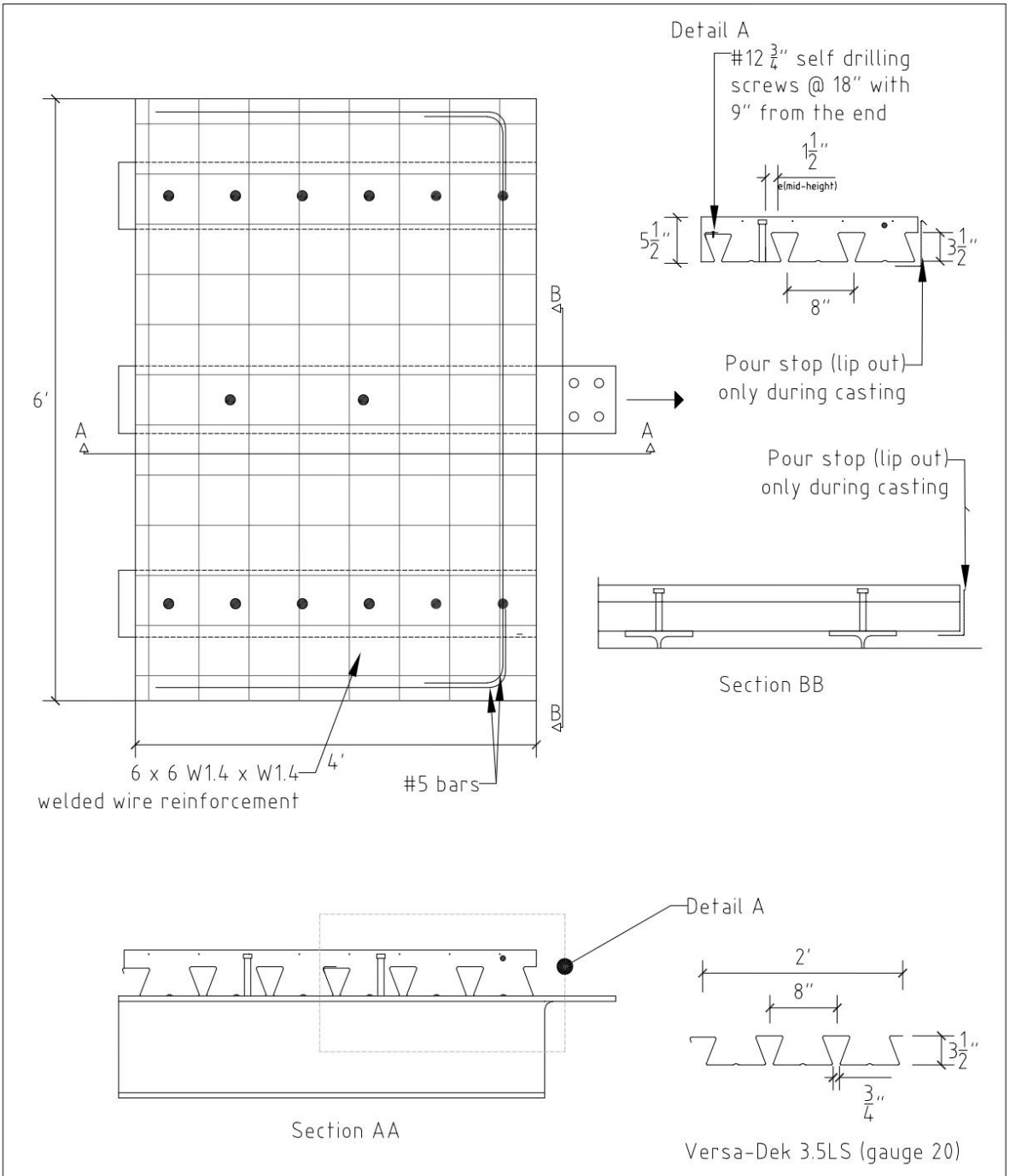

VIRGINIA TECH CHARLES E. VIA JR. DEPARTMENT OF CIVIL AND ENVIRONMENTAL ENGINEERING	PROJECT: COMPOSITE BEAM TEST	DRAWN BY: OAT	SHEET TITLE: TEST SPECIMEN D3.5B-3N-W

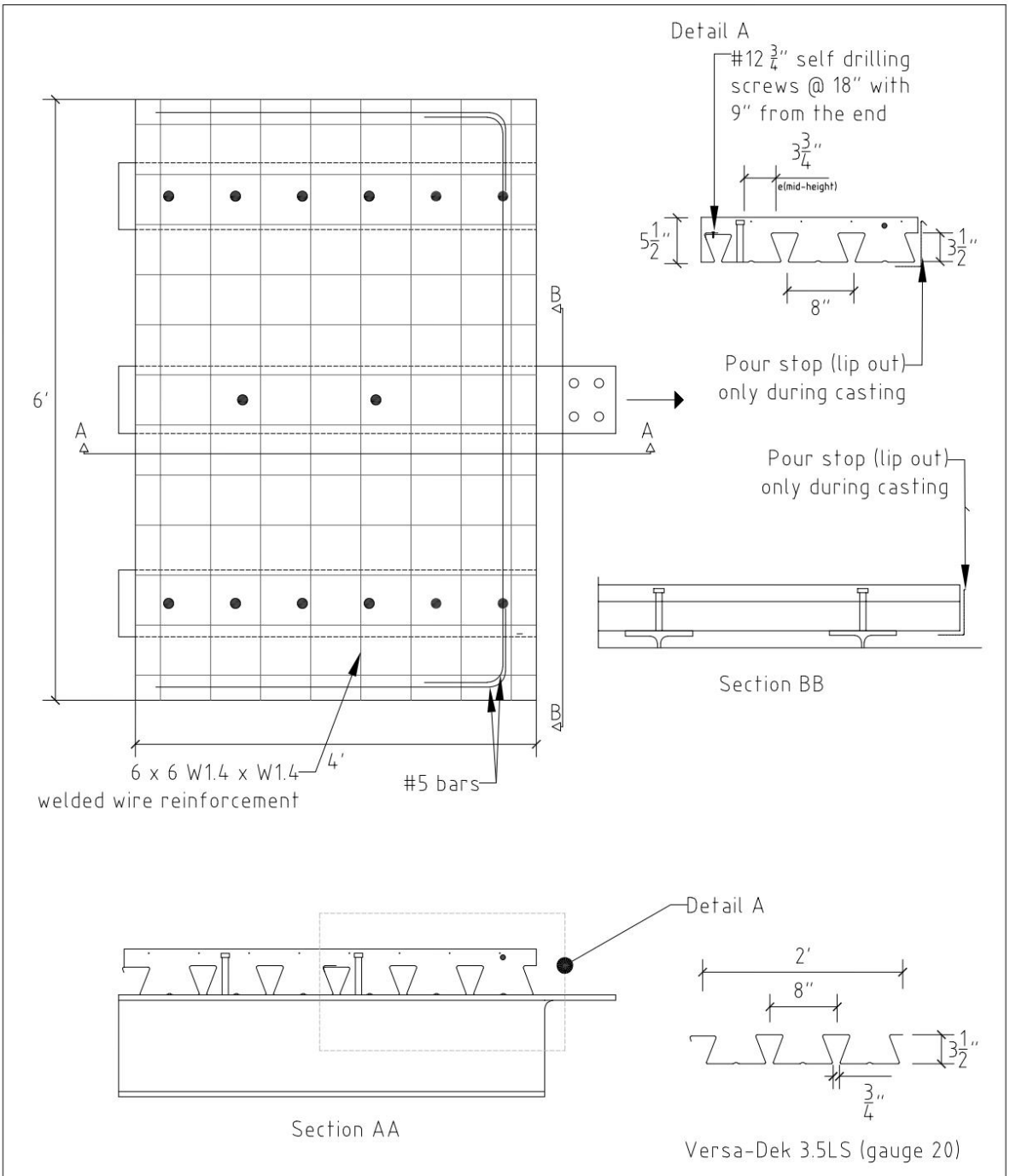

VIRGINIA TECH CHARLES E. VIA JR. DEPARTMENT OF CIVIL AND ENVIRONMENTAL ENGINEERING	PROJECT: COMPOSITE BEAM TEST	DRAWN BY: OAT	SHEET TITLE: TEST SPECIMEN D3.5B-3N-S

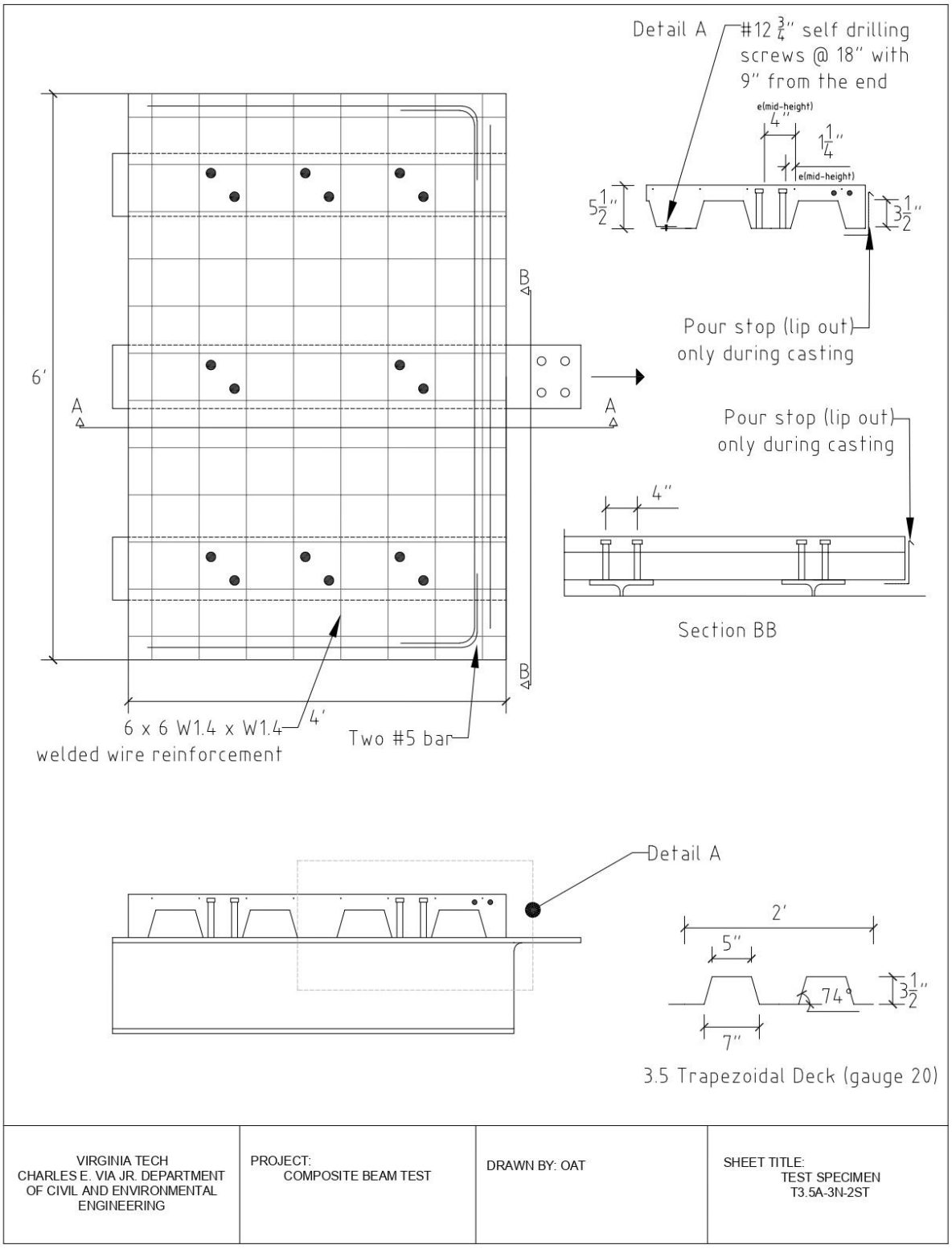

VIRGINIA TECH CHARLES E. VIA JR. DEPARTMENT OF CIVIL AND ENVIRONMENTAL ENGINEERING	PROJECT: COMPOSITE BEAM TEST	DRAWN BY: OAT	SHEET TITLE: TEST SPECIMEN T3.5A-3N-2ST

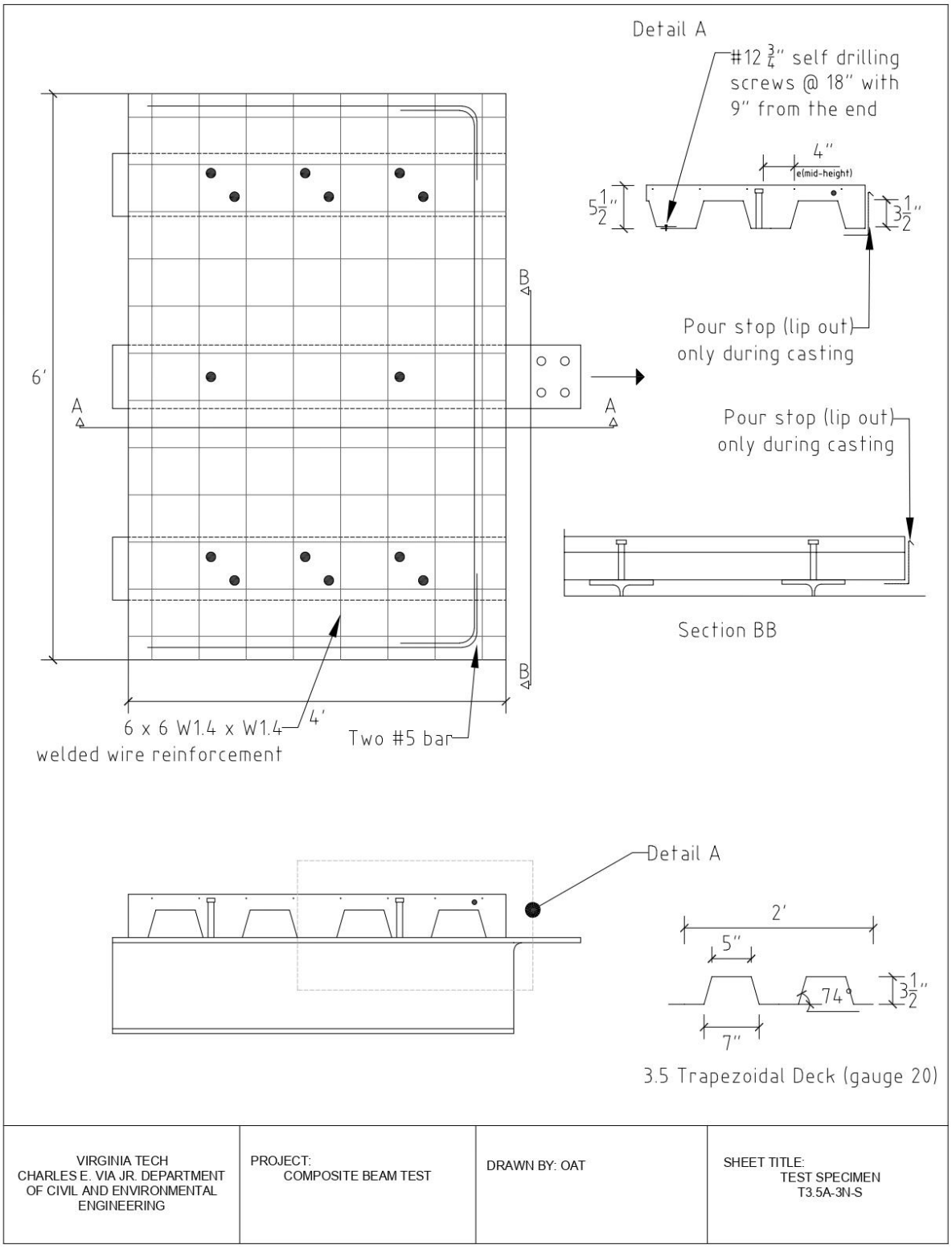

VIRGINIA TECH CHARLES E. VIA JR. DEPARTMENT OF CIVIL AND ENVIRONMENTAL ENGINEERING	PROJECT: COMPOSITE BEAM TEST	DRAWN BY: OAT	SHEET TITLE: TEST SPECIMEN T3.5A-3N-S

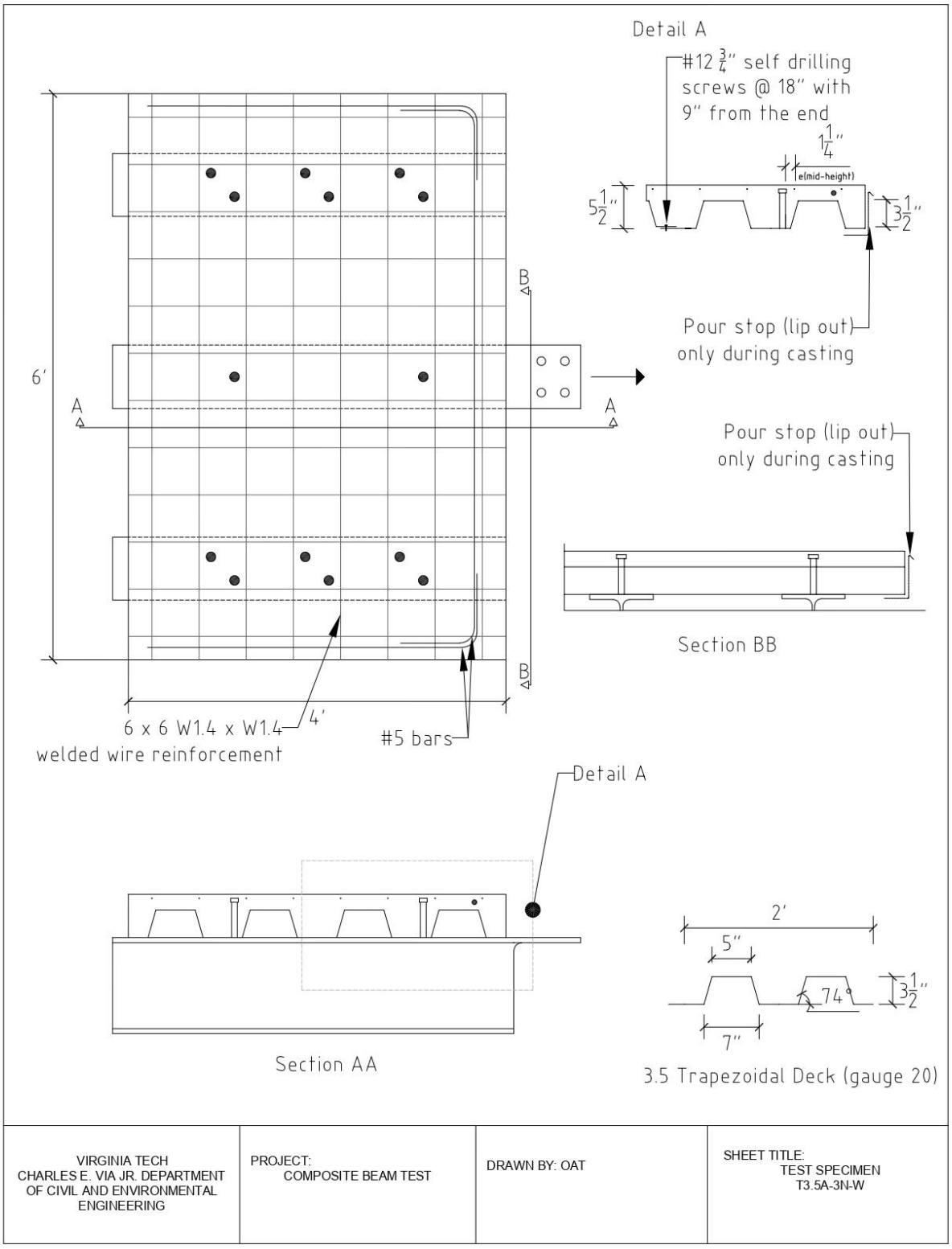

VIRGINIA TECH CHARLES E. VIA JR. DEPARTMENT OF CIVIL AND ENVIRONMENTAL ENGINEERING	PROJECT: COMPOSITE BEAM TEST	DRAWN BY: OAT	SHEET TITLE: TEST SPECIMEN T3.5A-3N-W

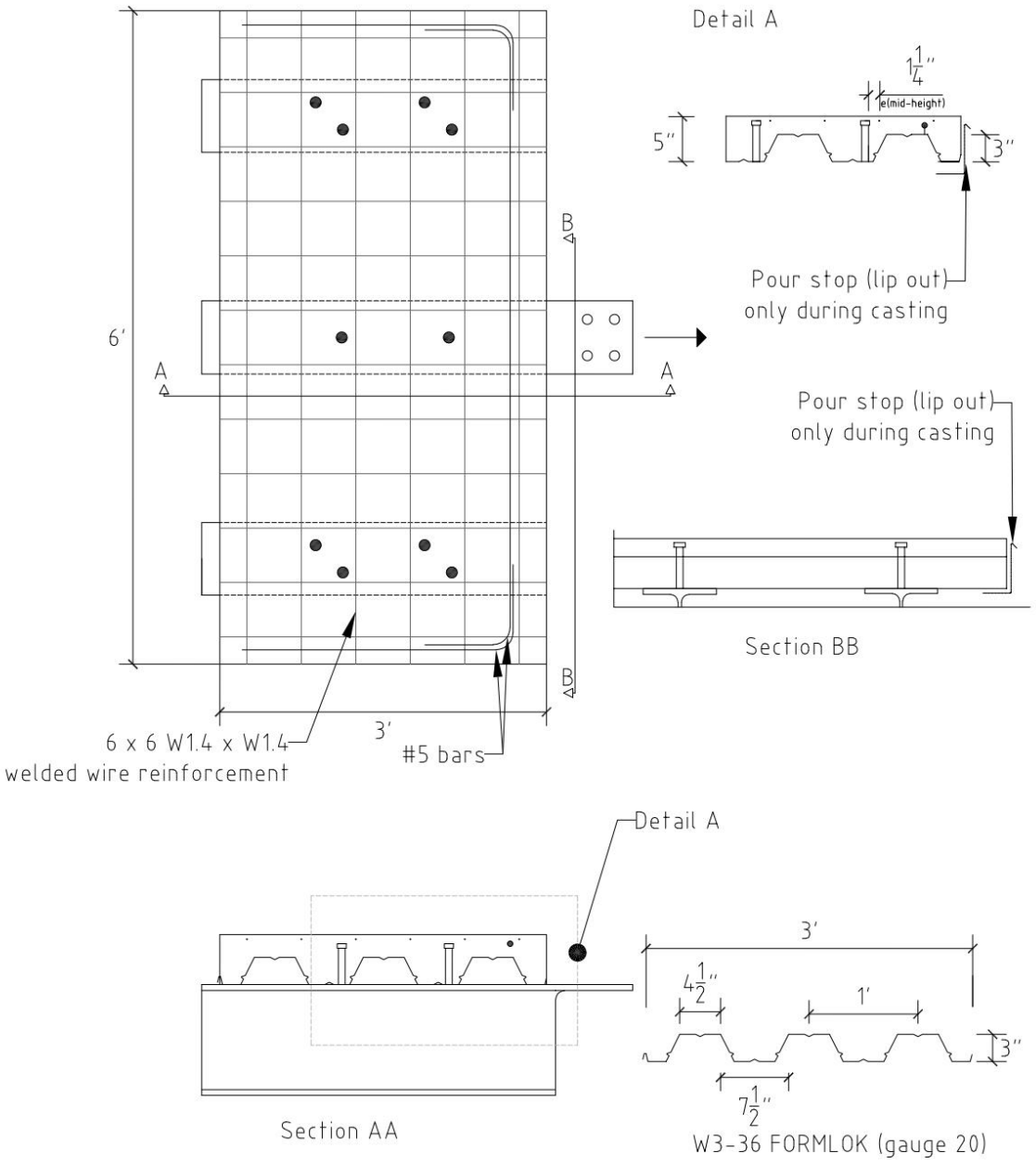

VIRGINIA TECH CHARLES E. VIA JR. DEPARTMENT OF CIVIL AND ENVIRONMENTAL ENGINEERING	PROJECT: COMPOSITE BEAM TEST	DRAWN BY: OAT	SHEET TITLE: TEST SPECIMEN T3.0A-3N-W

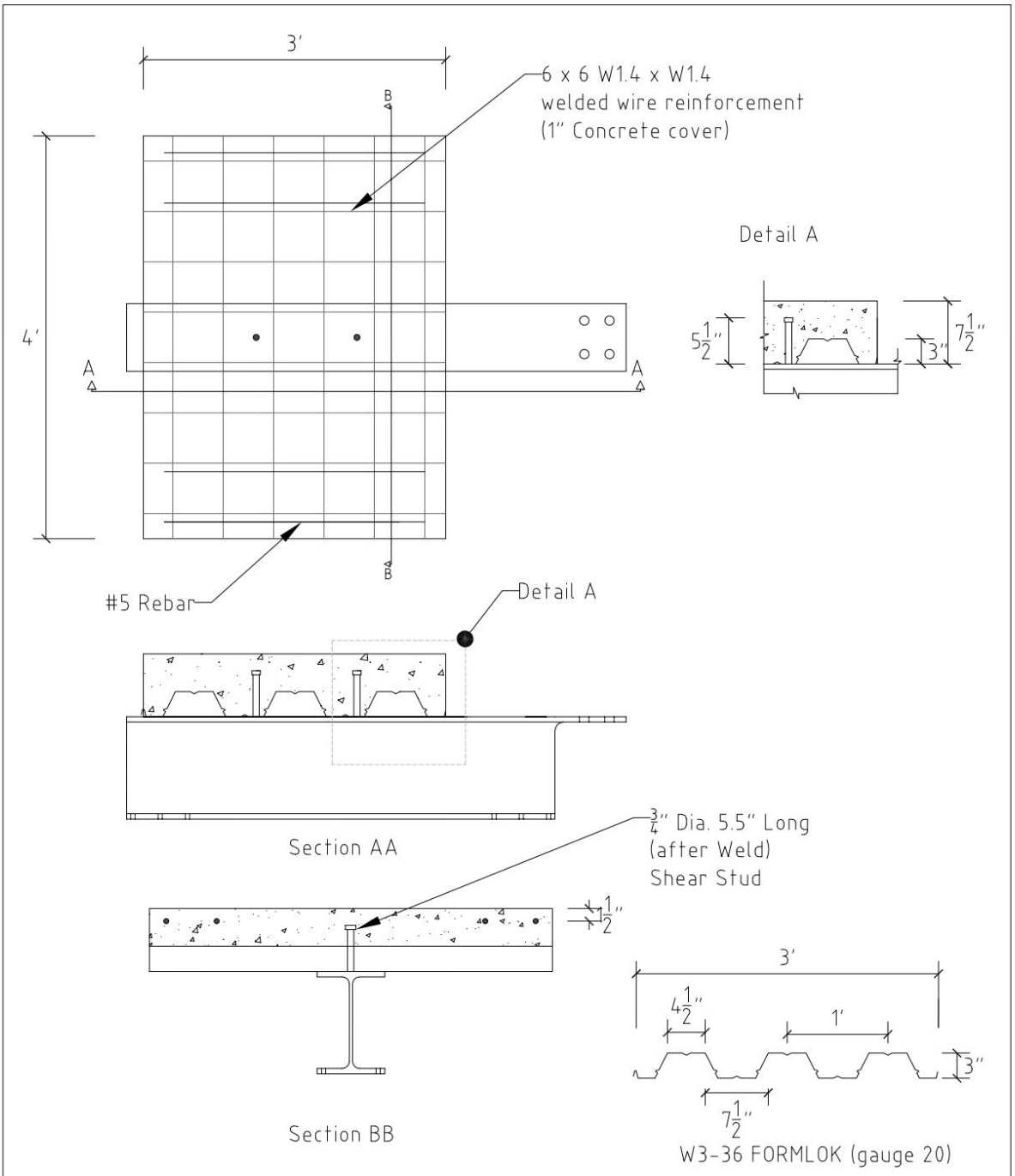

VIRGINIA TECH CHARLES E. VIA JR. DEPARTMENT OF CIVIL AND ENVIRONMENTAL ENGINEERING	PROJECT: COMPOSITE BEAM TEST	DRAWN BY: OAT	SHEET TITLE: TEST SPECIMEN T3.0A-4N-W-M

Appendix C: Material Testing

C.1 Steel Reinforcement

No.5 Rebar

Table C.1 No.5_1 Rebar Properties

	Modulus of Elasticity, E (ksi)	Yield Stress, f_y (ksi)	Ultimate Strength, f_u (ksi)	Elongation, in./in. (%)
S1	29465	65.6	106.3	13.8
S2	26245	64.7	106.7	15.2
S3	32257	61.8	102.4	15.2
Average	29322	64.0	105.1	14.7

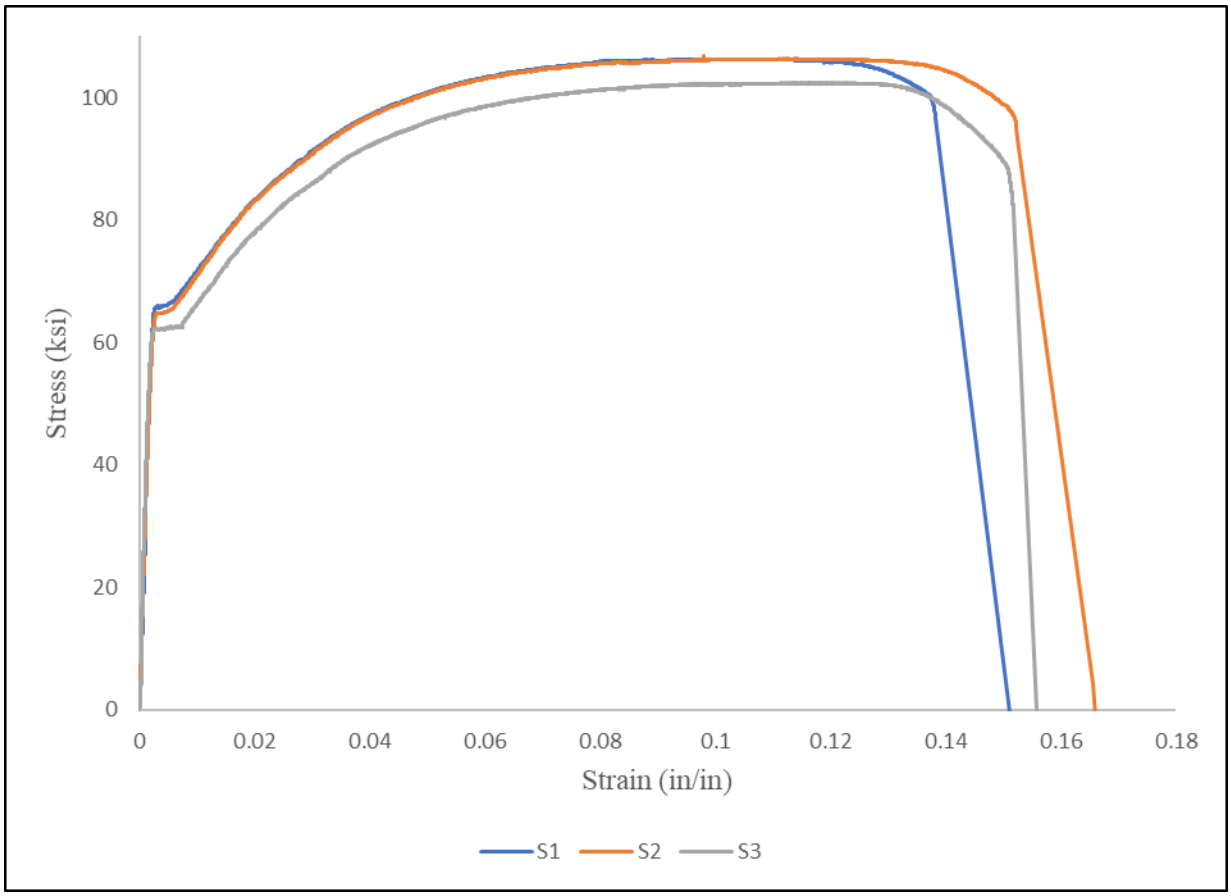

Fig. C.1 Stress-Strain Plots for Steel Reinforcement (No.5_1 Bars)

Table C.2 No.5_2 Rebar Properties

	Modulus of Elasticity, E (ksi)	Yield Stress, f_y (ksi)	Ultimate Strength, f_u (ksi)	Elongation, in./in. (%)
S1	27920	78.2	98.1	14.1
S2	25473	78.3	97.9	13.7
S3	28705	78.3	97.6	14.3
Average	27366	78.3	97.8	14.0

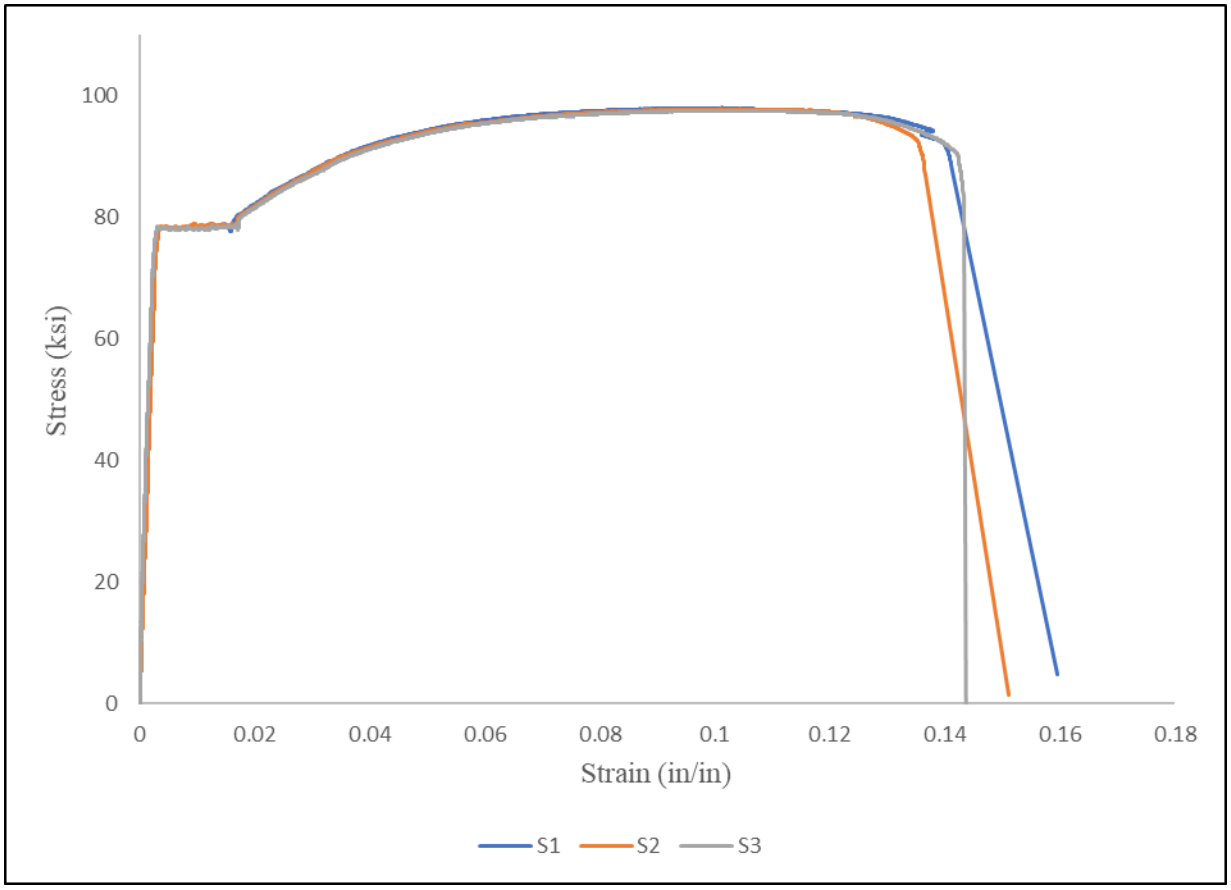

Fig. C.2 Stress-Strain Plots for Steel Reinforcement (No.5_2 Bars)

Table C.3 No.5_3 Rebar Properties

	Modulus of Elasticity, E (ksi)	Yield Stress, f_y (ksi)	Ultimate Strength, f_u (ksi)	Elongation, in./in. (%)
S1	61292	60.7	98.7	16.0
S2	27902	60.6	98.6	16.7
S3	32726	60.6	97.4	16.4
Average	40640	60.6	98.2	16.4

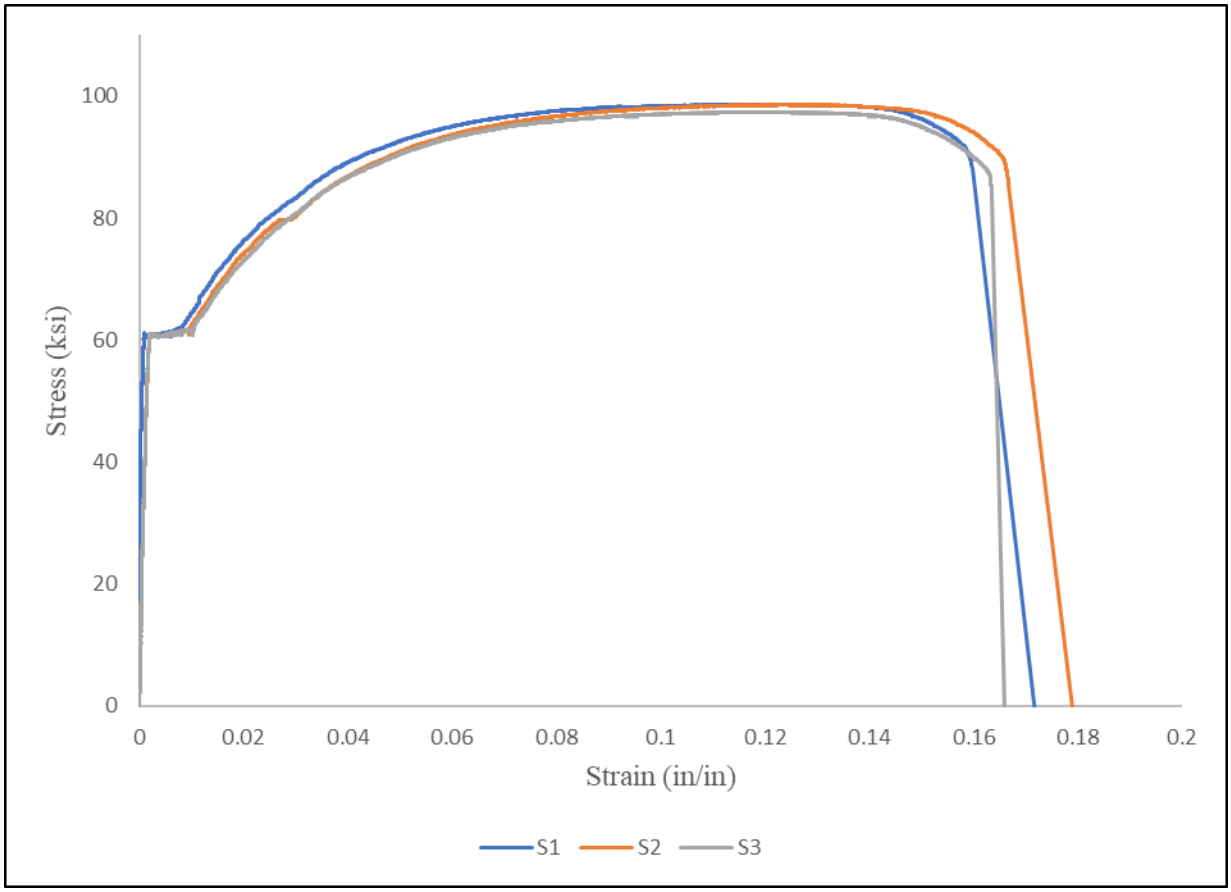

Fig. C.3 Stress-Strain Plots for Steel Reinforcement (No.5_3 Bars)

6 x 6 W1.4 x W1.4 Welded Wire Reinforcement

Table C.4 Welded Wire Fabric Properties

	Modulus of Elasticity, E (ksi)	Yield Stress, f_y (ksi)	Ultimate Strength, f_u (ksi)	Elongation, in./in. (%)
S1	38743	105.0	120.0	2.7
S2	45108	128.5	144.6	2.3
S3	43783	110.1	121.2	2.6
Average	42545	114.5	128.6	2.5

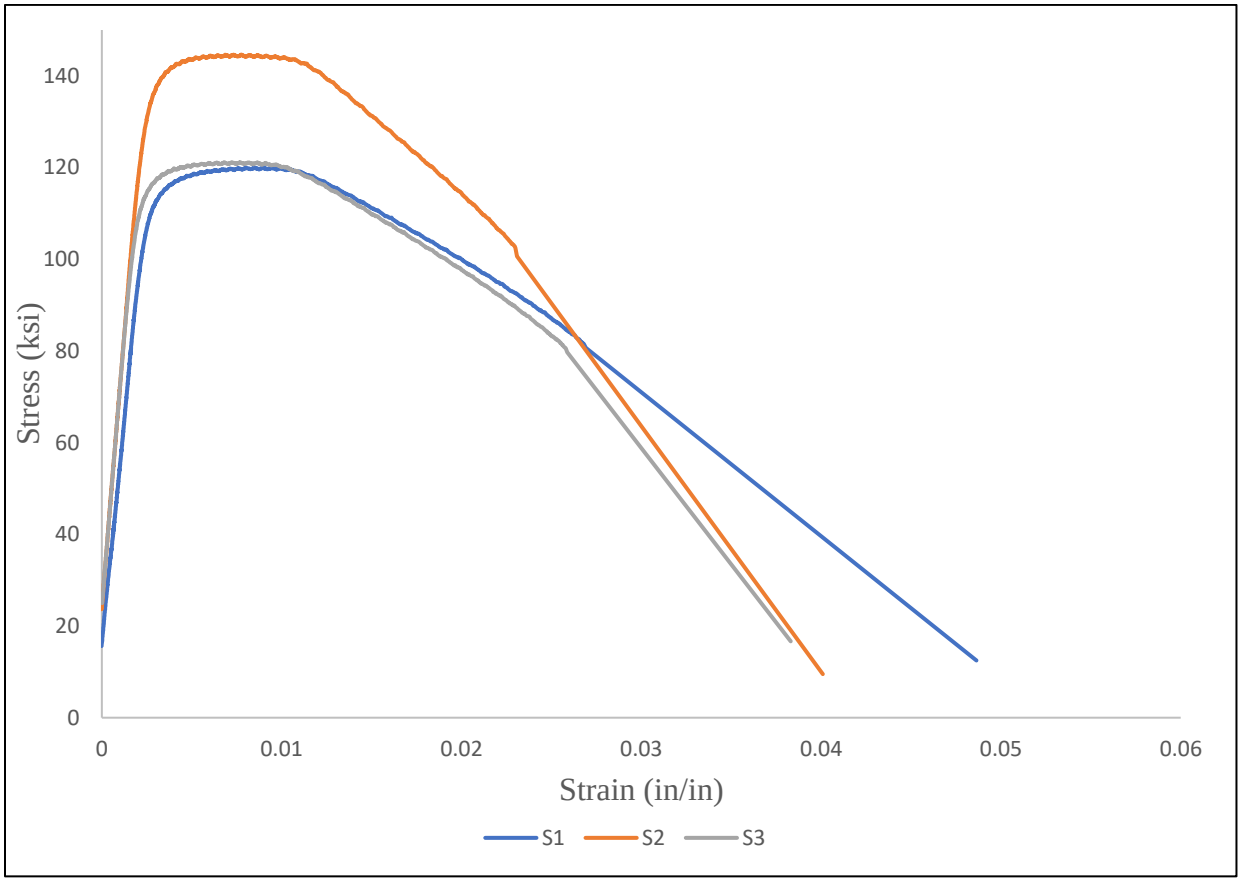

Fig. C.4 Stress-Strain Plots for Welded Wire Fabric (6x6 W1.4 x W1.4)

C.2 Specimen Steel

W 12 x 50

Table C.5 W 12 x 50 (558710) Properties

	Modulus of Elasticity, E (ksi)	Yield Stress, f_y (ksi)	Ultimate Strength, f_u (ksi)	Elongation, in./in. (%)
S1	36275	54.1	71.8	25.6
S2	29893	54..8	73.1	27.7
S3	33384	57.7	72.8	26.1
Average	33184	55.5	72.6	26.5

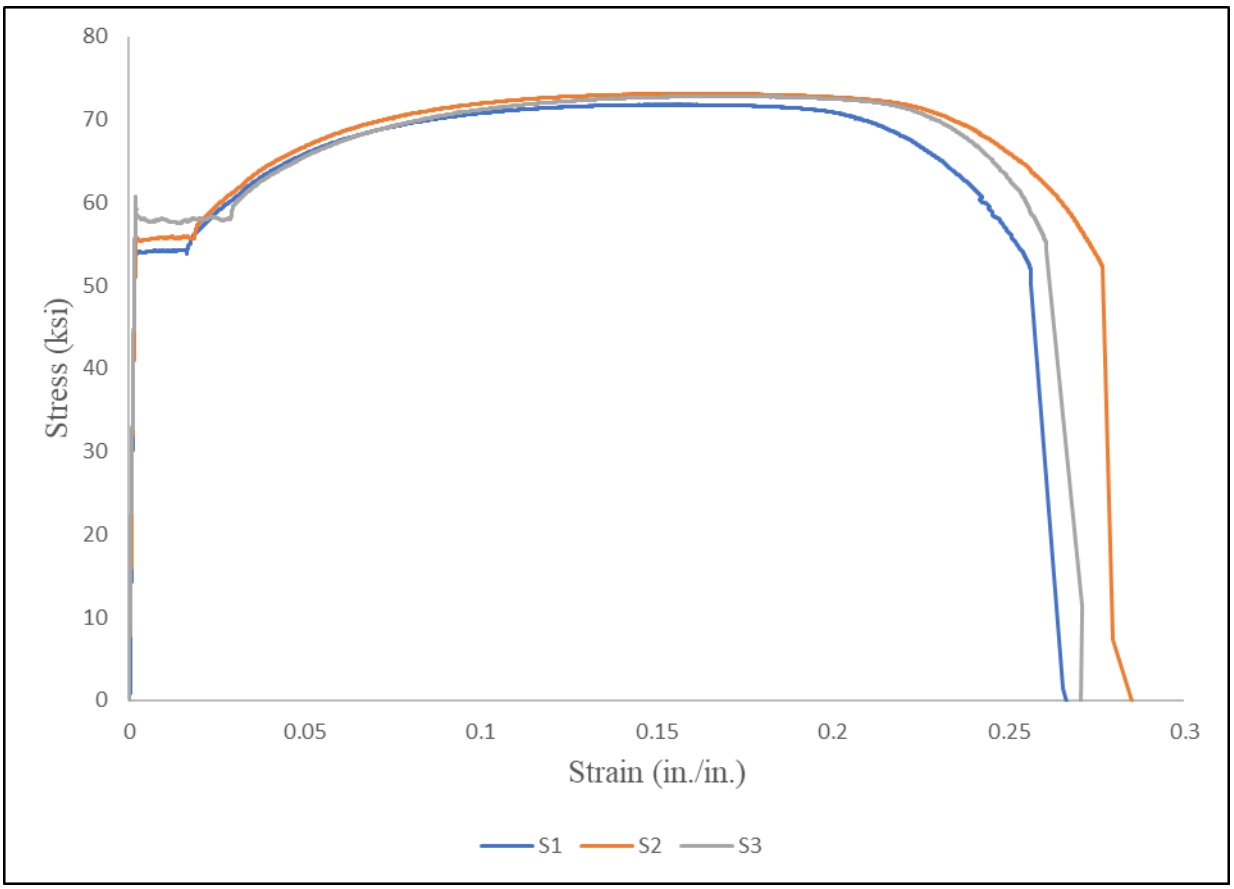

Fig. C.5 Stress-Strain Plots for W 12 x 50 (558710)

Table C.6 W 12 x 50 (558712) Properties

	Modulus of Elasticity, E (ksi)	Yield Stress, f_y (ksi)	Ultimate Strength, f_u (ksi)	Elongation, in./in. (%)
S1	35634	55.9	72.4	28.1
S2	37260	55.3	72.6	26.8
S3	31978	59.5	74.6	25.4
Average	34957	56.9	73.2	26.8

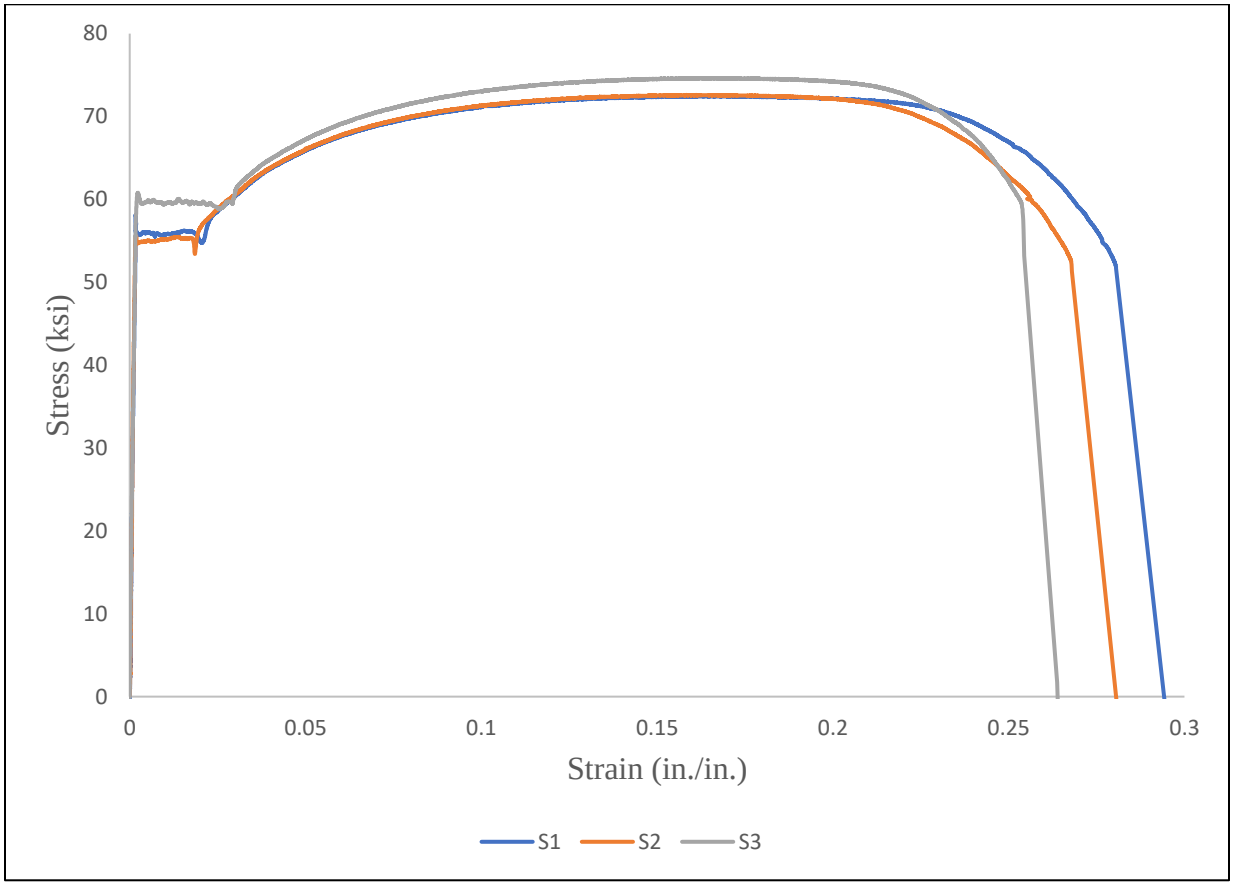

Fig. C.6 Stress-Strain Plots for W 12 x 50 (558712)

WT 6 x 17.5

Table C.7 WT 6 x 17.5 Properties

	Modulus of Elasticity, E (ksi)	Yield Stress, f_y (ksi)	Ultimate Strength, f_u (ksi)	Elongation, in./in. (%)
S1	34247	54.2	68.5	27.1
S2	25167	53.2	69.3	25.7
S3	36668	54.0	71.7	23.2
Average	32027	53.8	69.8	25.3

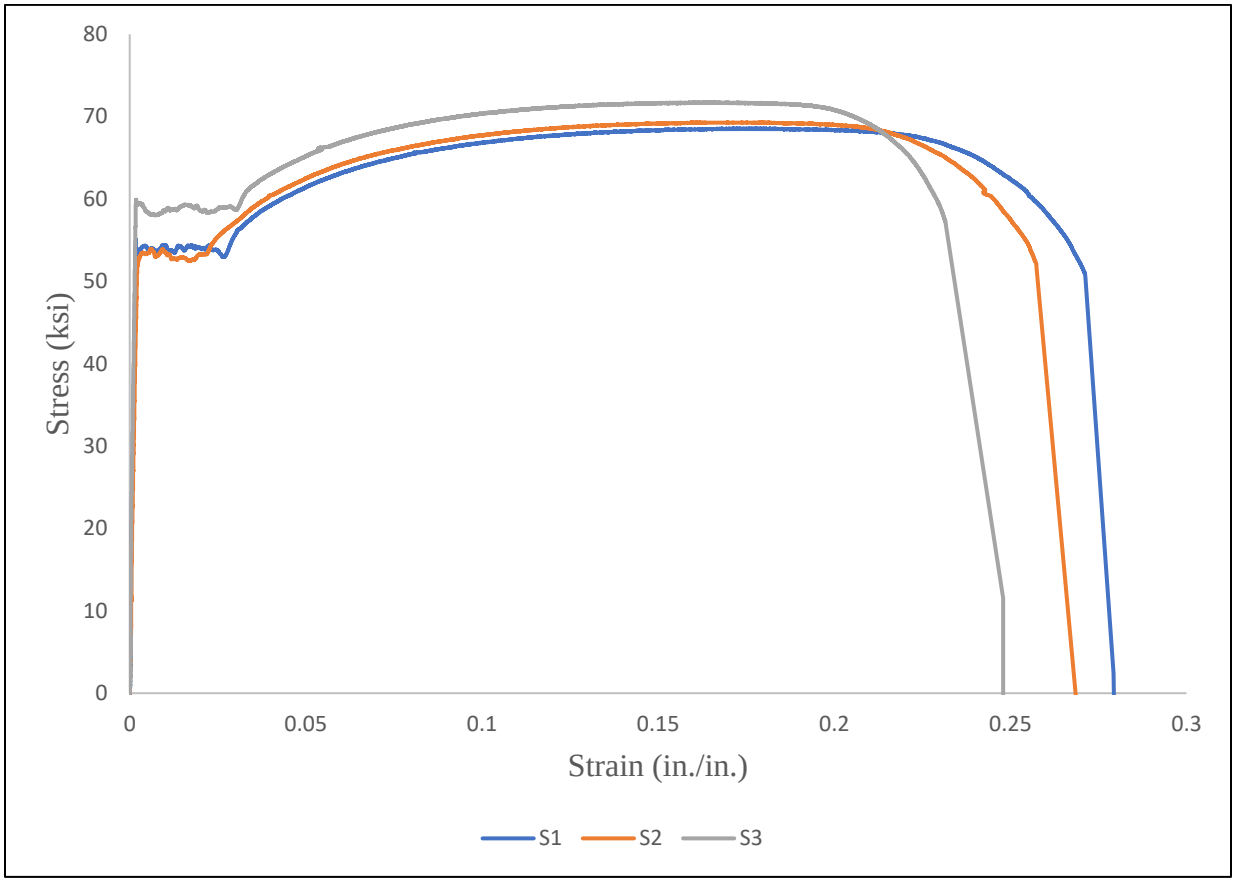

Fig. C.7 Stress-Strain Plots for WT 6 x 17.5

C.3 Steel Deck

TZ1 Steel Deck

Table C.8 TZ1 Steel Deck Properties

	Modulus of Elasticity, E (ksi)	Yield Stress, f_y (ksi)	Ultimate Strength, f_u (ksi)	Elongation, in./in. (%)
S1	38656	54.5	66.6	25.6
S2	37819	56.5	66.9	25.2
S3	37413	56.9	67.2	27.0
Average	37963	56.0	66.9	25.9

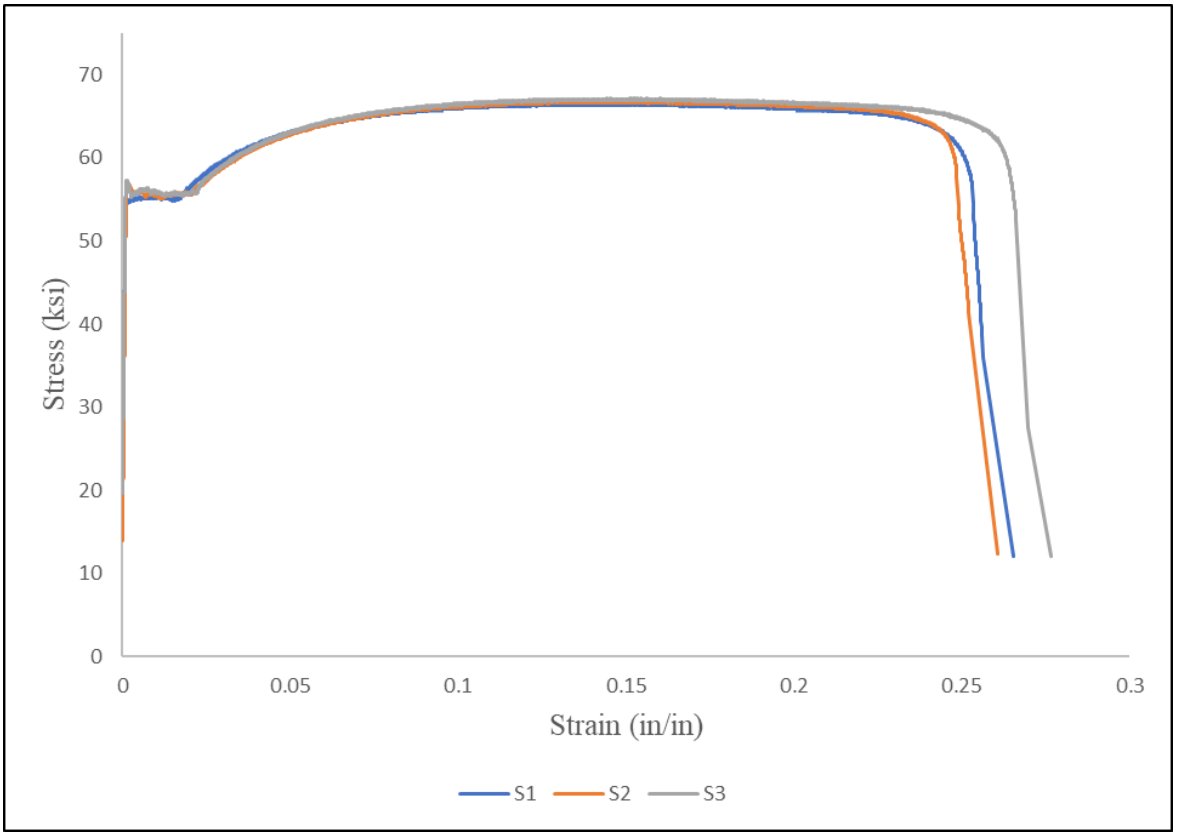

Fig. C.8 Stress-Strain Plots for Steel Deck (TZ1)

TZ2 Steel Deck

Table C.9 TZ2 Steel Deck Properties

	Modulus of Elasticity, E (ksi)	Yield Stress, f_y (ksi)	Ultimate Strength, f_u (ksi)	Elongation, in./in. (%)
S1	23586	62.4	83.7	18.8
S2	31935	63.7	85.4	19.5
S3	33574	64.2	83.3	19.1
Average	29698	63.4	84.1	19.1

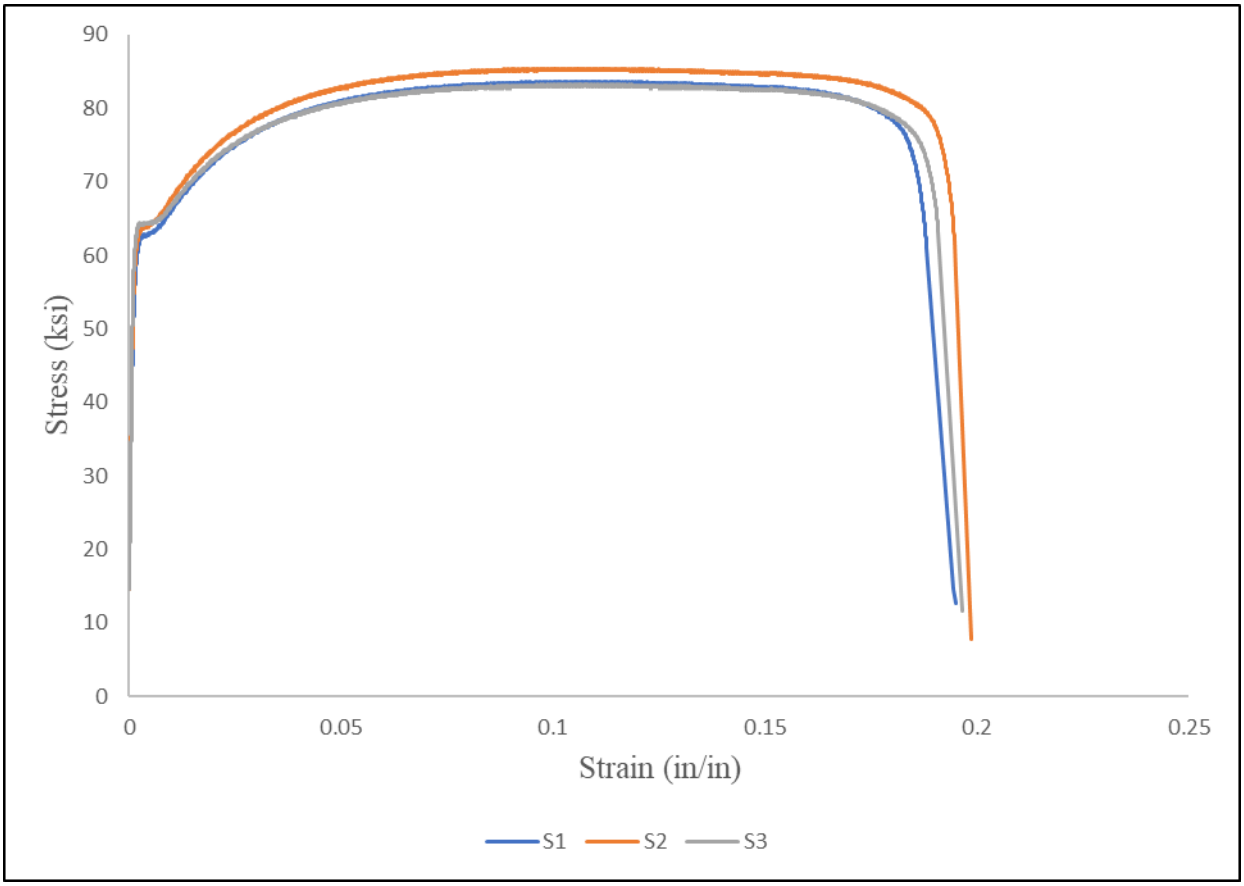

Fig. C.9 Stress-Strain Plots for Steel Deck (TZ2)

DT1 Steel Deck

Table C.10 DT1 Steel Deck Properties

	Modulus of Elasticity, E (ksi)	Yield Stress, f_y (ksi)	Ultimate Strength, f_u (ksi)	Elongation, in./in. (%)
S1	24788	56.1	67.6	24.7
S2	39122	57.3	67.7	25.9
S3	44898	59.4	69.7	26.0
Average	36269	57.6	68.3	25.5

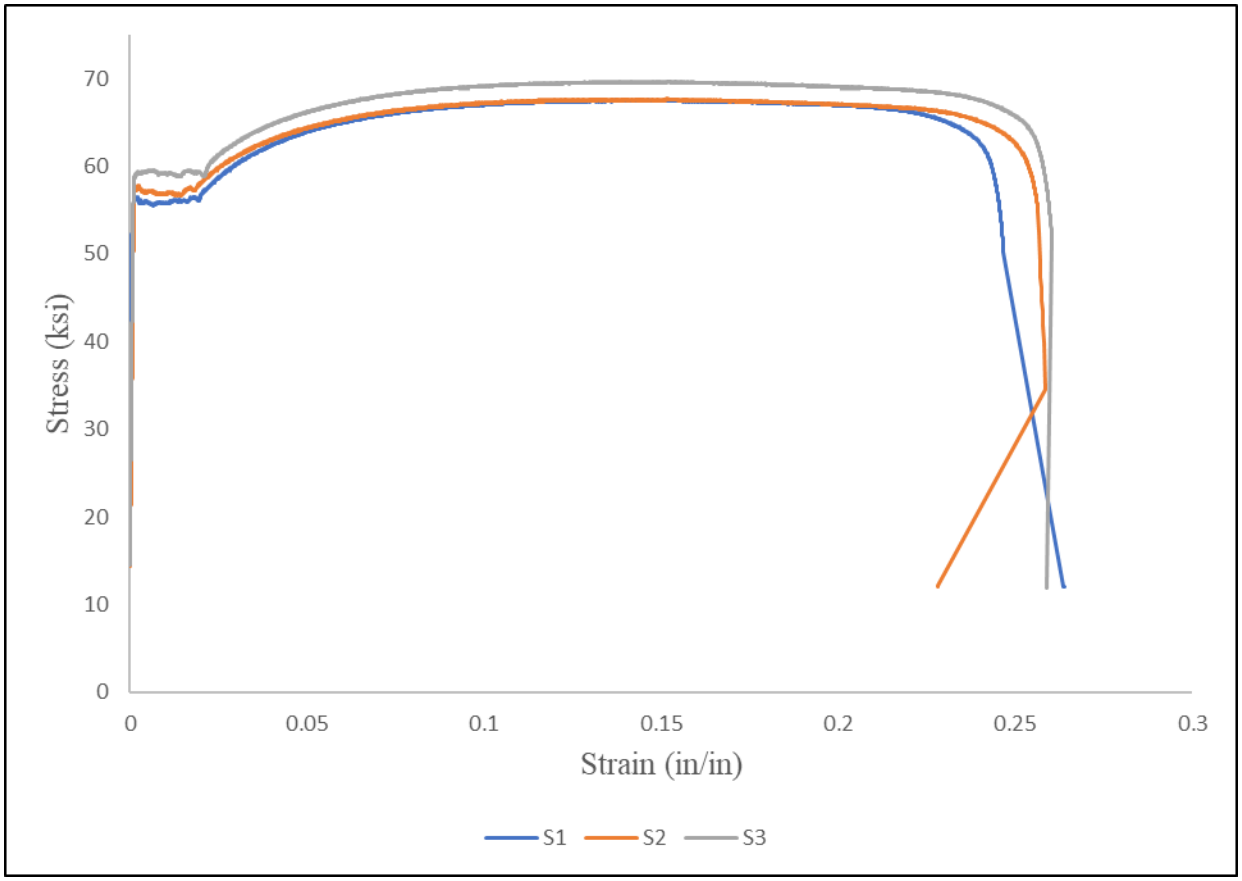

Fig. C.10 Stress-Strain Plots for Steel Deck (DT1)

DT2 Steel Deck

Table C.11 DT2 Steel Deck Properties

	Modulus of Elasticity, E (ksi)	Yield Stress, f_y (ksi)	Ultimate Strength, f_u (ksi)	Elongation, in./in. (%)
S1	36762	64.8	71.1	20.0
S2	38944	64.7	71.6	20.4
S3	33449	64.0	70.4	20.9
Average	36385	64.5	71.0	20.4

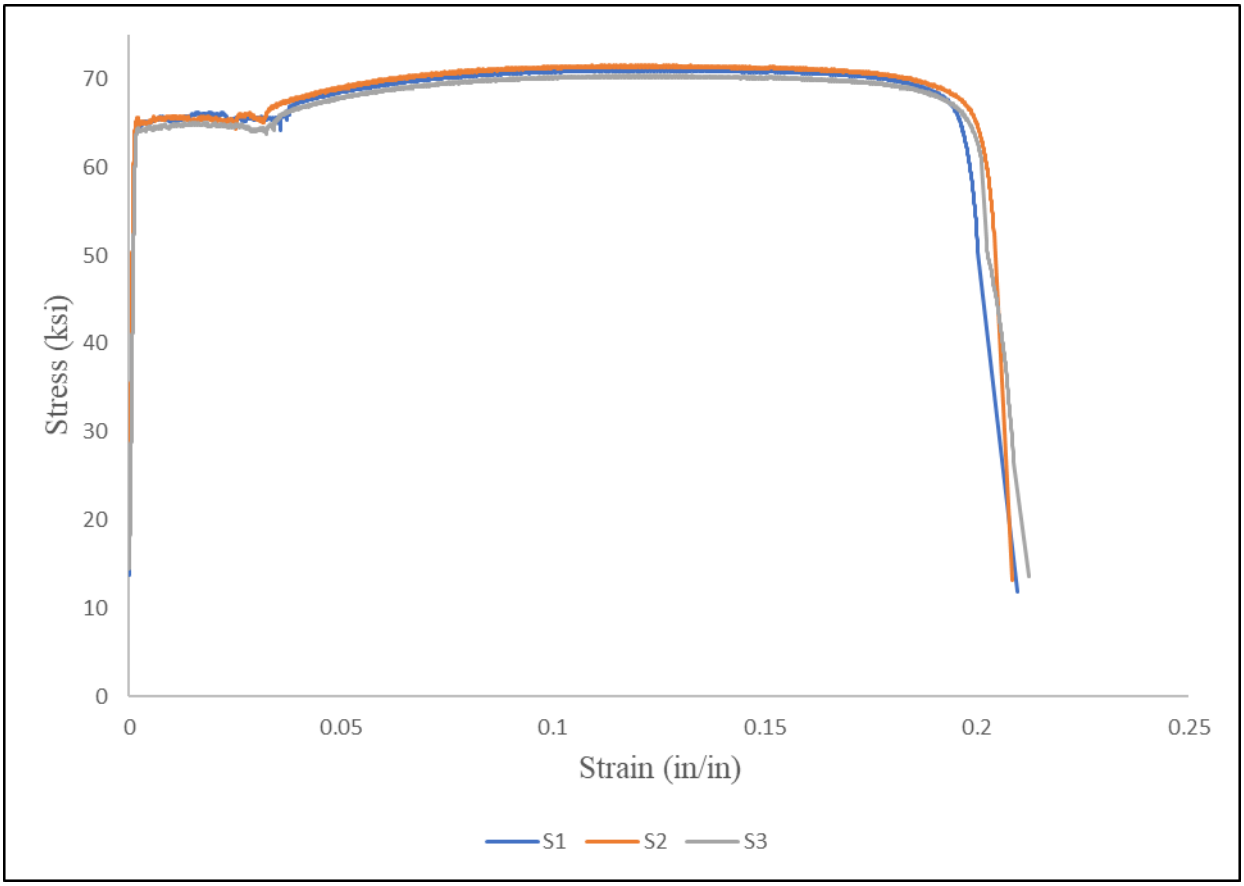

Fig. C.11 Stress-Strain Plots for Steel Deck (DT2)

C.4 Headed Shear Studs

¾ Dia. Headed Shear Studs

Table C.12 S3L 3/4 X 4-7/8 MS Stud Properties

	Ultimate Strength, f_u (psi)	Shear Strength, V_e (kip)	V_e/A_sF_u
S1	75200	21.3	0.64
S2	75200	22.1	0.67
S3	75200	21.7	0.66
Average	75200	21.7	0.65

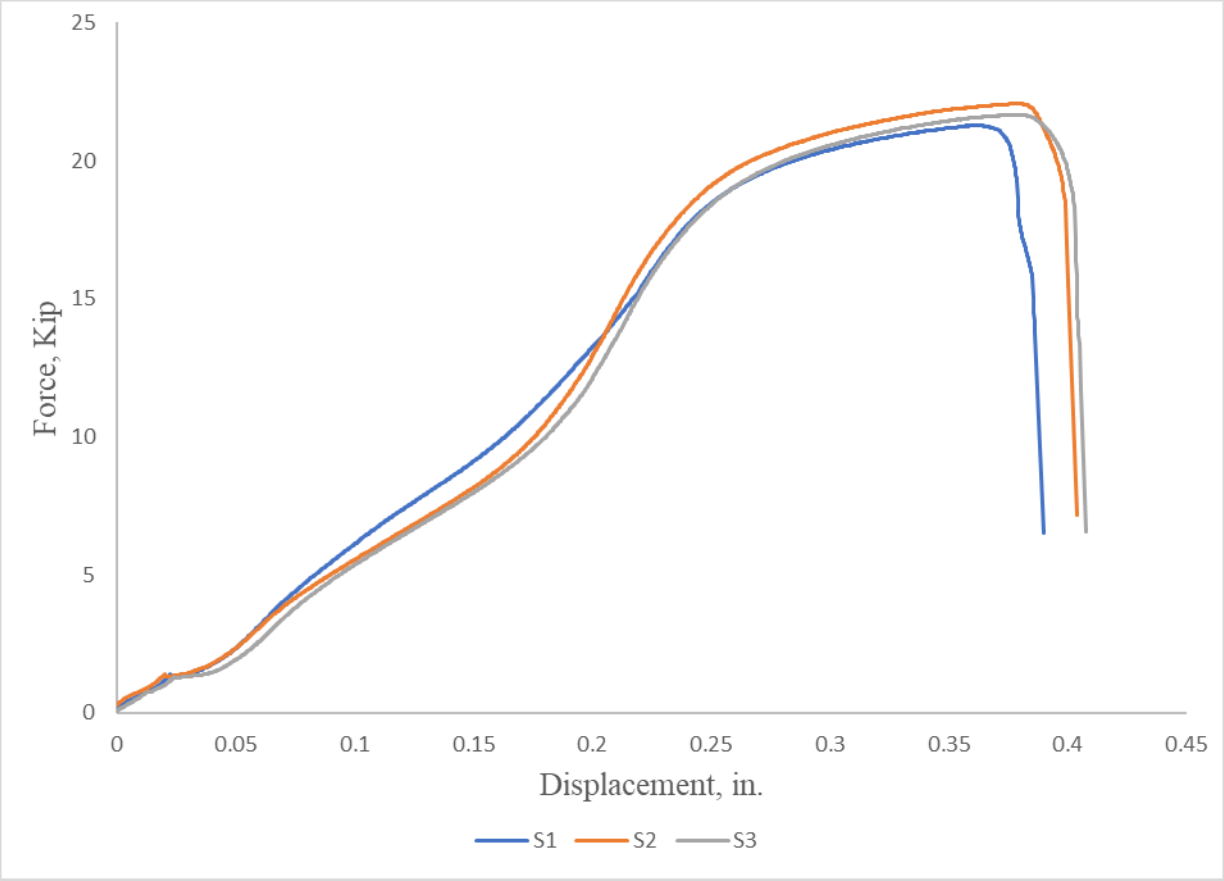

Fig. C.12 Force vs Displacement Plots for Headed Shear Studs (S3L 3/4 X 4-7/8 MS)

Table C.13 S3L 3/4 X 5-3/16 MS Stud Properties

	Ultimate Strength, f_u (psi)	Shear Strength, V_e (kip)	V_e/A_sf_u
S1	74000	22.4	0.69
S2	74000	22.4	0.69
S3	74000	22.2	0.68
Average	74000	22.3	0.69

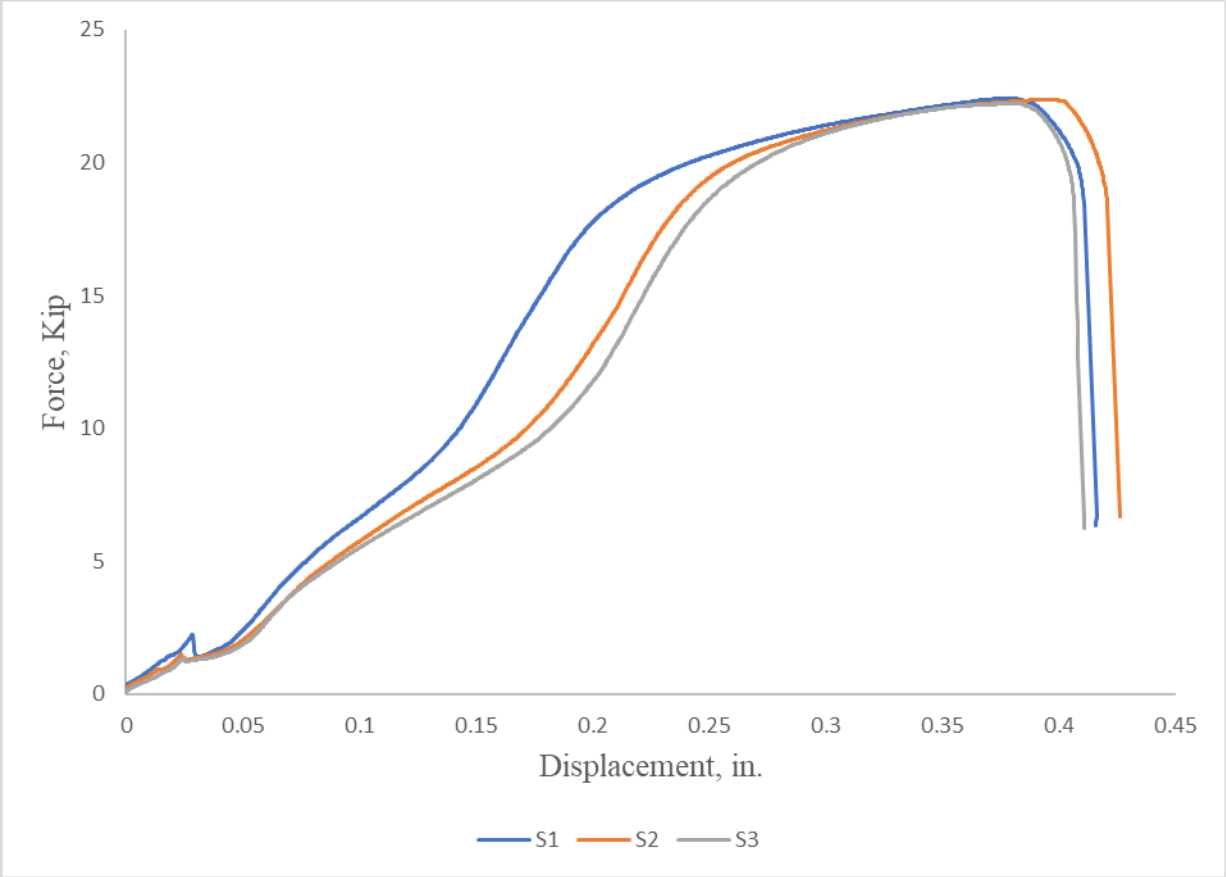

Fig. C.13 Force vs Displacement Plots for Headed Shear Studs (S3L 3/4 X 5-3/16 MS)

Table C.14 S3L 3/4 X 5-7/8 MS Stud Properties

	Ultimate Strength, f_u (psi)	Shear Strength, V_e (kip)	V_e/A_sf_u
S1	78300	21.8	0.63
S2	78300	22.0	0.64
S3	78300	22.4	0.65
Average	78300	22.1	0.64

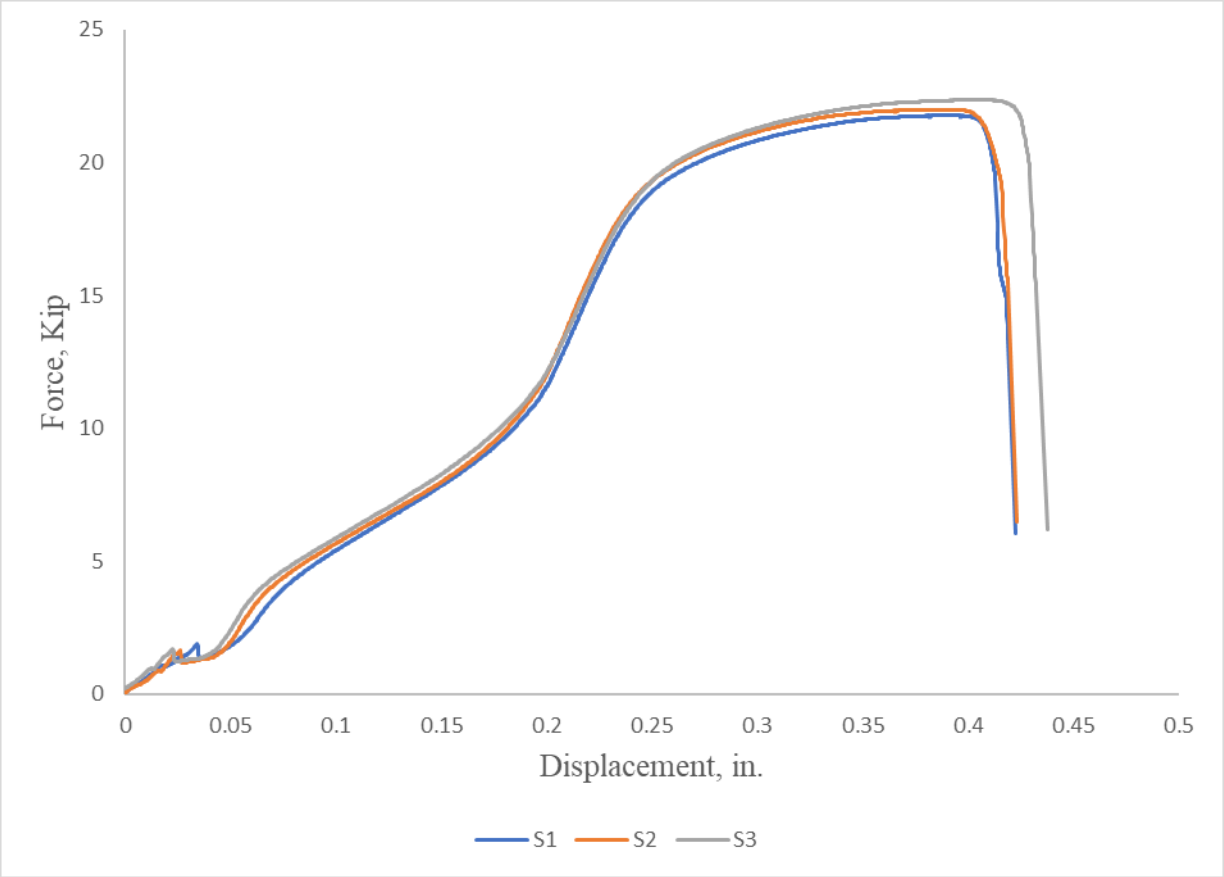

Fig. C.14 Force vs Displacement Plots for Headed Shear Studs (S3L 3/4 X 5-7/8 MS)

Appendix D: Mill Certificates

D.1 Specimen Steel

W 12 x 50

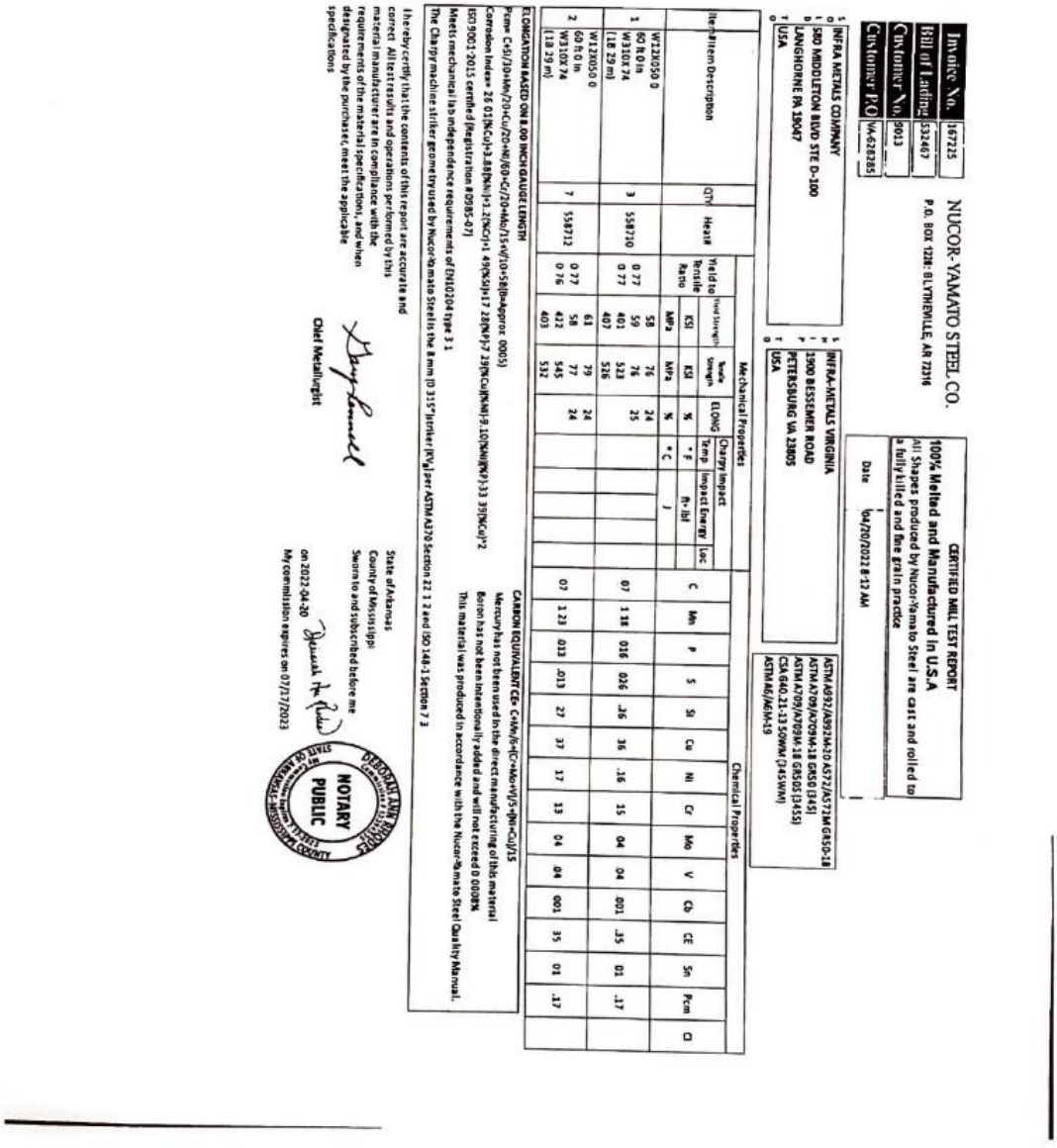

Customer Name	Customer PO#	Shipper No	Heat Number
AMERICAN INSTITUTE OF STEEL	ENG071822B	2026908	558710

NUCOR-YAMATO STEEL CO.
P.O. BOX 1228 BLYTHEVILLE, AR 72316

CERTIFIED MILL TEST REPORT
100% Melted and Manufactured in U.S.A.
All Shapes produced by Nucor-Yamato Steel are cast and rolled to a fully killed and fine grain practice

Invoice No. 167225
Bill of Lading 532467
Customer No. 8013
Customer P.O. W-628285
Date 04/20/2022 8:12 AM

SOLD TO: INFRA METALS COMPANY
580 MIDDLETON RIDD STE D-100
LANGHORNE PA 19047
USA

SHIP TO: INFRA-METALS VIRGINIA
1900 BESSEMER ROAD
PETERSBURG VA 23805
USA

ASTM A992/A992M-20 A572/A572M GR50-18
ASTM A709/A709M-18 GR50 (345)
ASTM A709/A709M-18 GR50S (345S)
CSA G40.21-13 50WW (345WW)
ASTM/AE/AEM-19

Mechanical Properties

Item	Pieces	Heat	Yield to Tensile Ratio	Yield Strength		Tensile strength		ELONG	Charpy Impact Temp		Impact Energy		Loc
				KSI	MPa	KSI	MPa	%	°F	°C	ft-lbf	J	
1 W12X50 0 60 ft 0 in W310X74 (18 29 m)	3	558710	0 77	58	401	76	523	25					
			0 77	59	407	76	526	24					
2 W12X50 0 60 ft 0 in W310X74 (18 29 m)	7	558712	0 77	61	422	79	545	24					
			0 76	58	403	77	532	24					

Chemical Properties

Item	C	Mn	P	S	Si	Cu	Ni	Cr	Mo	V	Cb	CE	Sn	Pcm	CI
1	07	1 18	016	026	.26	36	.16	15	04	04	001	.35	01	.17	
2	07	1 23	.013	.013	.27	37	17	13	04	04	001	35	01	.17	

ELONGATION BASED ON 8.00 INCH GAUGE LENGTH

Penn: C45/30+Mn/20+Cu/20+Ni/60+Cr/20+Mo/15+V/10+5B(Approx 0005)

Corrosion Index= 26 01(%Cu)+3 88(%Ni)+1 27(%Cu)+1 49(%Si)+17 28(%P)-7 29(%Cu)(%Ni)-9 10(%Ni)(%P)-33 39(%Cu)^2

CARBON EQUIVALENT CE= C+Mn/6+(Cr+Mo+V)/5+(Ni+Cu)/15

Mercury has not been used in the direct manufacturing of this material

Boron has not been intentionally added and will not exceed 0 0008%

ISO 9001:2015 certified (Registration #0985-07)

This material was produced in accordance with the Nucor-Yamato Steel Quality Manual.

Meets mechanical lab independence requirements of EN10204 type 3 1

The Charpy machine striker geometry used by Nucor-Yamato Steel is the 8 mm (0 315") striker (KV$_8$) per ASTM A370 Section 22 1 2 and ISO 148-1 Section 7 3

I hereby certify that the contents of this report are accurate and correct All test results and operations performed by this material manufacturer are in compliance with the requirements of the material specification, and when designated by the purchaser, meet the applicable specifications

Chief Metallurgist

State of Arkansas
County of Mississippi
Sworn to and subscribed before me
on 2022-04-20
My commission expires on 07/17/2023

NOTARY PUBLIC

Customer Name	Customer PO#	Shipper No	Heat Number
AMERICAN INSTITUTE OF STEEL	ENG071822B	2026908	558712

Invoice No.	167215
Bill of Lading	532467
Customer No.	8013
Customer P.O.	VA632885

NUCOR-YAMATO STEEL CO.
P.O. BOX 1228 BLYTHEVILLE, AR 72316

CERTIFIED MILL TEST REPORT

100% Melted and Manufactured in U.S.A

All Shapes produced by Nucor-Yamato Steel are cast and rolled to a fully killed and fine grain practice

Date 04/06/2022 12 AM

Sold To: INFRA METALS COMPANY
1580 MIDDLETON BLVD STE D-100
LANGHORNE PA 19047
USA

Ship To: INFRA-METALS VIRGINIA
1900 BESSEMER ROAD
PETERSBURG VA 23805
USA

ASTM A992/A992M-20 A572/A572M GR50-18
ASTM A709/A709M-18 GR50 (345)
ASTM A709/A709M-18 GR50S (345S)
CSA G40.21-13 50WM (345WM)
ASTM A6/A6M-19

Item	Item Description	QTY	Heat#	Mechanical Properties								Chemical Properties												
				Yield to Tensile Ratio	Yield Strength	Tensile Strength	ELONG	Charpy Impact			Loc	C	Mn	P	S	Si	Cu	Ni	Cr	Mo	V	Cb	CE	Sn	Pcm	Cl
								Temp	Impact Energy																	
					KSI	KSI	%	°F	ft-lbf																	
					MPa	MPa	%	°C	J																	
1	W12X50 0 60 ft 0 in W310X74 (18 29 m)	3	558710	0 77 0 77	58 59 401 407	75 75 523 526	24 25					07	1 18	016	026	.26	36	.16	15	04	004	.001	.35	01	.17	
2	W12X50 0 60 ft 0 in W310X74 (18 29 m)	7	558712	0 77 0 76	61 58 422 403	79 77 545 532	24 24					07	1 23	013	013	.27	37	.17	13	04	004	001	35	01	.17	

ELONGATION BASED ON 8 00 INCH GAUGE LENGTH

CARBON EQUIVALENT Cbe C+Mn/6+(Cr+Mo+V)/5+(Ni+Cu)/15

Pcm= C+Si/30+Mn/20+Cu/20+Ni/60+Cr/20+Mo/15+V/10+5B [B=Approx 0005]

Mercury has not been intentionally added and will not exceed 0 0008%

Corrosion Index= 26 01(NiCu)+3 88(NiCu)+1 20(Cr)+1 49(Si)+17 28(P)*2 29(NiCu)(PCr)+9 10(Ni)(P)*2+33 39(Cu)*2

Boron has not been intentionally added and will not exceed 0 0008%

ISO 9001:2015 certified (Registration # 0985-07)

This material was produced in accordance with the Nucor-Yamato Steel Quality Manual.

Meets mechanical lab independence requirements of D1D1204 type 3 1

The Charpy machine striker geometry used by Nucor-Yamato Steel is the 8 mm (0 315") striker (R) per ASTM A370 Section 22 1 2 and ISO 148-1 Section 7 3

I hereby certify that the contents of this report are accurate and correct All test results and operation performed by this material manufacturer are in compliance with the requirements of the material specifications, and when designated by the purchaser, meet the applicable specifications

Chief Metallurgist

State of Arkansas
County of Mississippi
Sworn to and subscribed before me
on 2022-04-20
My commission expires on 07/17/2023

NOTARY PUBLIC

WT 6 x 17.5

Customer Name	Customer PO#	Shipper No	Heat Number
AMERICAN INSTITUTE OF STEEL	ENG071822A	2026840	556446

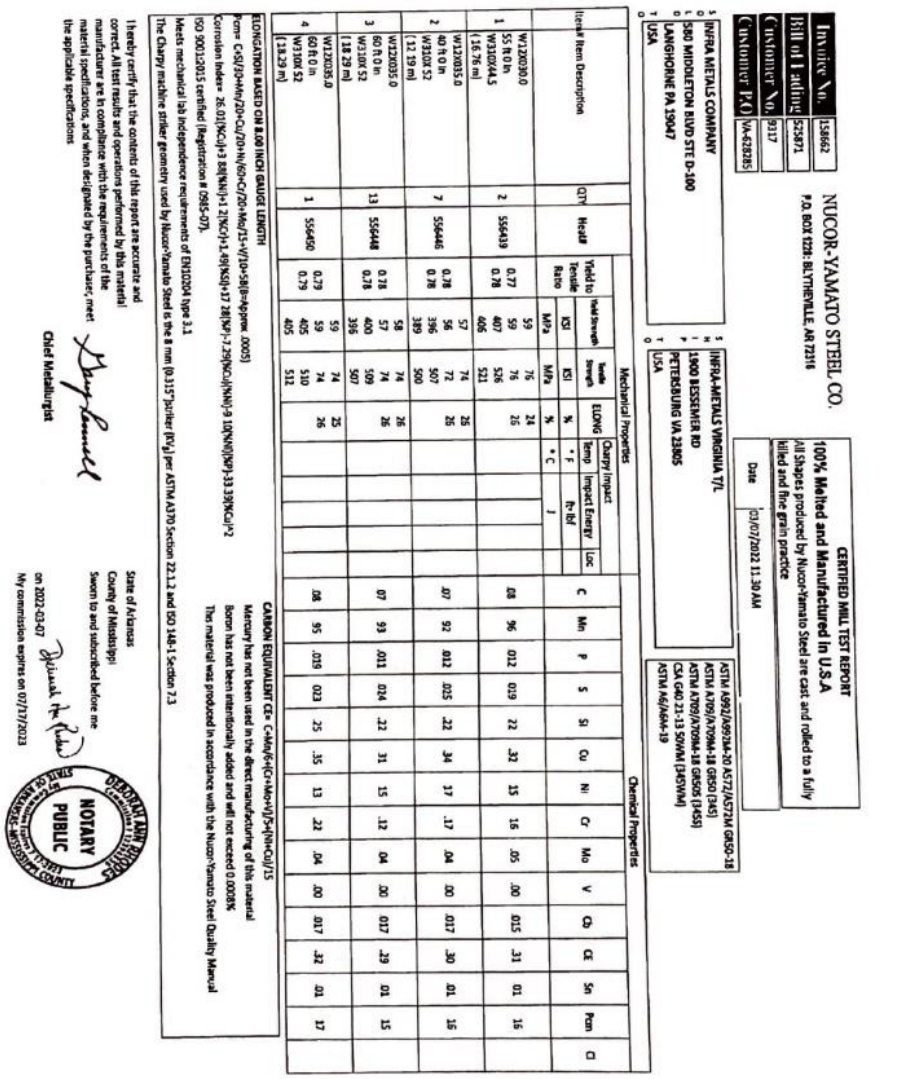

NUCOR-YAMATO STEEL CO.
P.O. BOX 1228 BLYTHEVILLE, AR 72316

CERTIFIED MILL TEST REPORT
100% Melted and Manufactured in U.S.A
All Shapes produced by Nucor-Yamato Steel are cast and rolled to a fully killed and fine grain practice

Invoice No. 158662
Bill of Lading 525971
Customer No. 9317
Customer P.O. VA-628285
Date 03/07/2022 11:30 AM

SOLD TO: INFRA-METALS COMPANY
580 MIDDLETON BLVD STE D-100
LANGHORNE PA 19047
USA

SHIP TO: INFRA-METALS VIRGINIA T/L
1900 BESSEMER RD
PETERSBURG VA 23805
USA

ASTM A992/A992M-20 A572/A572M GR50-18
ASTM A709/A709M-18 GR50 (345)
ASTM A709/A709M-18 GR50S (345S)
CSA G40.21-13 50WW (345WW)
ASTM A6/A6M-19

Item#	Item Description	QTY	Heat#	Mechanical Properties: Yield to Tensile Ratio	Yield Strength MPa	Yield Strength KSI	Tensile Strength MPa	Tensile Strength KSI	ELONG %	Charpy Impact Temp °F	Charpy Impact Temp °C	Charpy Impact Energy ft-lbf	Charpy Impact Energy J	Loc	Chemical Properties: C	Mn	P	S	Si	Cu	Ni	Cr	Mo	V	Cb	CE	Sn	Pcm	Cl
1	W12X30.0 55 ft 0 in W310X44.5 (16.76 m)	2	556439	0.77 0.78	59 407	76 59 526 407	76 59 526 407	24 26							.08	.96	.012	.019	.22	.32	.15	.16	.05	.00	.015	.31	.01	.16	
2	W12X35.0 60 ft 0 in W310X52 (18.29 m)	7	556446	0.78 0.78	56 389	72 507 500 507	74 396	28 28							.07	.92	.012	.025	.22	.34	.17	.17	.04	.00	.017	.30	.01	.16	
3	W12X35.0 60 ft 0 in W310X52 (18.29 m)	13	556448	0.78 0.78	57 400	74 509	74 509	26 26							.07	.93	.011	.024	.22	.31	.15	.12	.04	.00	.017	.29	.01	.15	
4	W12X35.0 60 ft 0 in W310X52 (18.29 m)	1	556450	0.79 0.79	59 405	74 510	74 510	25 26							.08	.95	.019	.023	.25	.35	.13	.22	.04	.00	.017	.32	.01	.17	

ELONGATION BASED ON 8.00 INCH GAUGE LENGTH

Pcm= C+Si/30+Mn/20+Cu/20+Ni/60+Cr/20+Mo/15+V/10+5B(If>.Approx .0005)

Corrosion Index= 26.01(%Cu)+3.88(%Ni)+1.2(%Cr)+1.49(%Si)+17.28(%P)-7.29(%Cu)(%Ni)-9.10(%Ni)(%P)+33.39(%Cu)^2

ISO 9001:2015 certified (Registration # 0985-07).

Meets mechanical lab independence requirements of EN10204 type 3.1

The Charpy machine striker geometry used by Nucor-Yamato Steel is the 8 mm (0.315") striker (K) per ASTM A370 Section 22.1.2 and ISO 148-1 Section 7.3

CARBON EQUIVALENT CE= C+Mn/6+(Cr+Mo+V)/5+(Ni+Cu)/15

Mercury has not been used in the direct manufacturing of this material

Boron has not been intentionally added and will not exceed 0.0008%

This material was produced in accordance with the Nucor-Yamato Steel Quality Manual

I hereby certify that the contents of this report are accurate and correct. All test results and operations performed by this material manufacturer are in compliance with the requirements of the material specifications, and when designated by the purchaser, meet the applicable specifications

Chief Metallurgist

State of Arkansas
County of Mississippi
Sworn to and subscribed before me
on 2022-03-07
My commission expires on 07/17/2023

NOTARY PUBLIC

Customer Name	Customer PO#	Shipper No	Heat Number
AMERICAN INSTITUTE OF STEEL	ENG071822A	2026840	542804

NUCOR-YAMATO STEEL CO.

P.O. BOX 1228 BLYTHEVILLE, AR 72316

CERTIFIED MILL TEST REPORT

100% Melted and Manufactured in U.S.A

All Shapes produced by Nucor-Yamato Steel are cast and rolled to a fully killed and fine grain practice

Invoice No.	98561
Bill of Lading	483763
Customer No.	9013
Customer P.O.	VA-61897

Date 06/28/2021 0 48 AM

SOLD TO: INFRA METALS COMPANY
580 MIDDLETON BLVD STE D-100
LANGHORNE PA 19047
USA

SHIP TO: INFRA-METALS VIRGINIA
1800 BESSEMER ROAD
PETERSBURG VA 23805
USA

ASTM A992/A992M-20 A572/A572M GR50-18
ASTM A709/A709M-18 GR50 (345)
ASTM A709/A709M-18 GR50S (345S)
CSA G40 21-13 50WM (345WM)
ASTM A6/A6M-19

Mechanical Properties

Item	Item Description	QTY	Heat#	Yield to Tensile Ratio	Yield Strength		Tensile Strength		ELONG	Charpy Impact Temp		Charpy Impact Energy		Loc.
					KSI	MPa	KSI	MPa	%	° F	° C	ft-lbf	J	
1	W14X043.0 40 ft 0 in (12.19 m) W360X64	12	542804	0.73	54	374	74	510	25					
				0.72	53	371	72	497	26					
2	W14X043.0 60 ft 0 in (18.29 m) W360X64	12	542811	0.71	53	360	74	497	25					
				0.75	55	364	72	512	24					
					57	376	72	498						

Chemical Properties

Item	C	Mn	P	S	Si	Cu	Ni	Cr	Mo	V	Cb	CE	Sn	Pcm	CI
1	08	1 29	.014	028	.23	35	18	17	06	.04	001	38	02	19	
2	06	1 26	.014	028	25	26	12	16	04	04	001	34	02	16	

ELONGATION BASED ON 8.00 INCH GAUGE LENGTH

CARBON EQUIVALENT CE= C+Mn/6+(Cr+Mo+V)/5+(Ni+Cu)/15

Pcm= C+Si/30+Mn/20+Cu/20+Ni/60+Cr/20+Mo/15+V/10+5B(If>Approx .0005)

Mercury has not been used in the direct manufacturing of this material

Boron has not been intentionally added and will not exceed 0.0008%

Corrosion Index= 26 01(%Cu)+3 88(%Ni)+1 2(%Cr)+1 49(%Si)+17 28(%P)-7 29(%Cu)(%Ni)-9 10(%Ni)(%P)+33 39(%Cu)^2

This material was produced in accordance with the Nucor-Yamato Steel Quality Manual

ISO 9001 2015 certified (registration #0085-07).

Meets mechanical lab independence requirements of EN10204 type 3 1

Meets mechanical lab independence requirements of EN10204 type 3 1

The Charpy machine striker geometry used by Nucor-Yamato Steel is the 8 mm ID 315° Striker (KV) per ASTM A370 Section 22 1.2 and ISO 148-1 Section 7.3

I hereby certify that the contents of this report are accurate and correct. All test results and operations performed by this material manufacturer are in compliance with the requirements of the material specification(s), and when designated by the purchaser, meet the applicable specifications.

Chief Metallurgist

State of Arkansas
County of Mississippi
Sworn to and subscribed before me
on 2021-06-28
My commission expires on 07/17/2023

NOTARY PUBLIC

WT 7 x 21.5

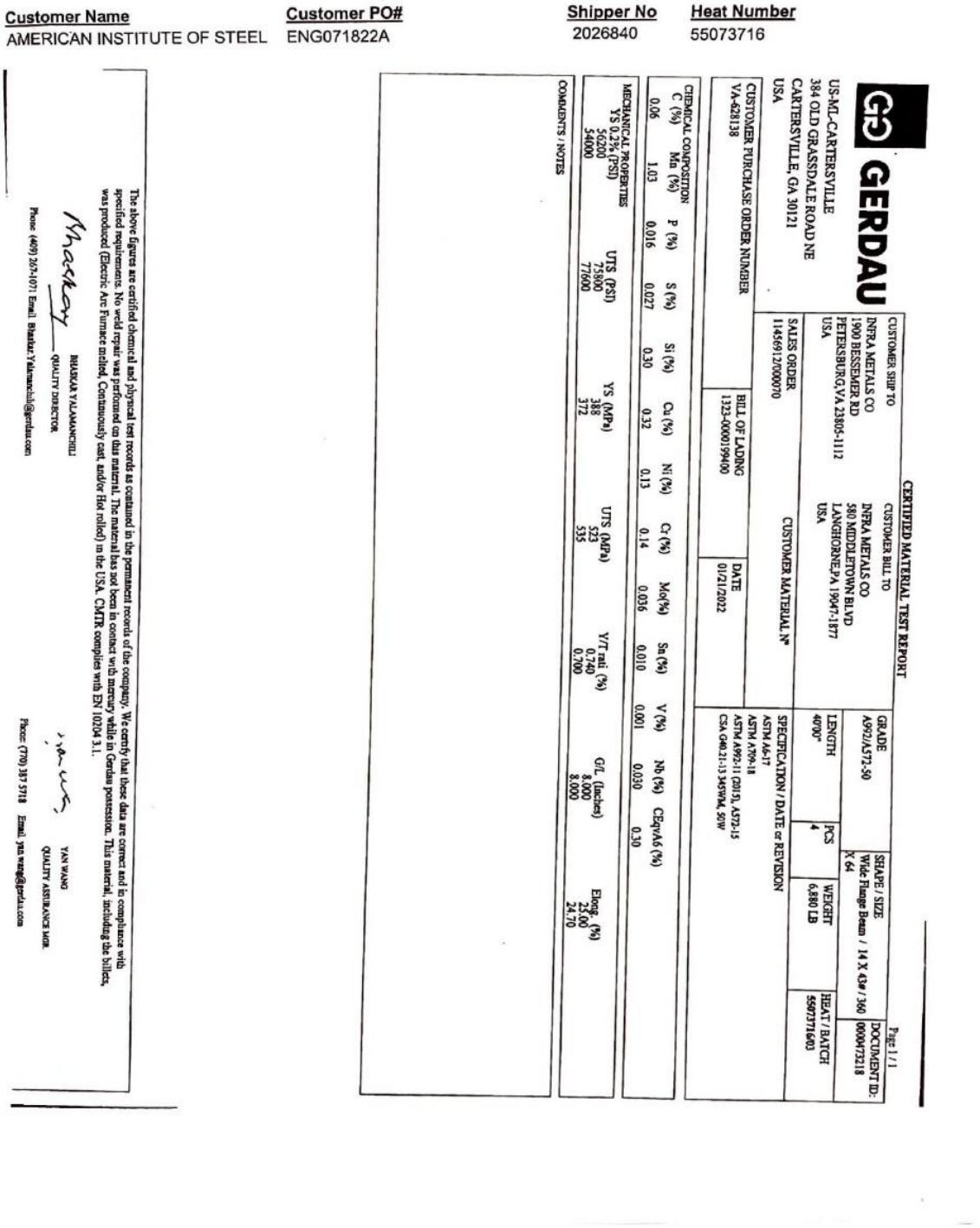

Customer Name
AMERICAN INSTITUTE OF STEEL

Customer PO#
ENG071822A

Shipper No
2026840

Heat Number
55073716

GERDAU

CERTIFIED MATERIAL TEST REPORT

Page 1 / 1

CUSTOMER SHIP TO
INFRA METALS CO
1900 BESSEMER RD
PETERSBURG,VA 23805-1112
USA

CUSTOMER BILL TO
INFRA METALS CO
580 MIDDLETOWN BLVD
LANGHORNE,PA 19047-1877
USA

GRADE
A992/A572-50

SHAPE / SIZE
Wide Flange Beam / 14 X 43# / 360 X 64

DOCUMENT ID:
0000473218

US-MI-CARTERSVILLE
384 OLD GRASSDALE ROAD NE
CARTERSVILLE, GA 30121
USA

SALES ORDER
1145691/2/0000070

CUSTOMER MATERIAL N°

LENGTH
40'00"

PCS
4

WEIGHT
6.880 LB

HEAT / BATCH
55073716/03

CUSTOMER PURCHASE ORDER NUMBER
VA-628138

BILL OF LADING
1323-0000199400

DATE
01/21/2022

SPECIFICATION / DATE or REVISION
ASTM A6-17
ASTM A709-18
ASTM A992-11 (2015), A572-15
CSA G40.21-13 345WWA, 50W

CHEMICAL COMPOSITION

C (%)	Mn (%)	P (%)	S (%)	Si (%)	Cu (%)	Ni (%)	Cr (%)	Mo(%)	Sn (%)	V (%)	Nb (%)	CEqvA6 (%)
0.06	1.03	0.016	0.027	0.30	0.32	0.13	0.14	0.036	0.010	0.001	0.030	0.30

MECHANICAL PROPERTIES

YS 0.2% (PSI)	UTS (PSI)	YS (MPa)	UTS (MPa)	Y/T ratio (%)	G/L (inches)	Elong. (%)
56200	75800	388	523	0.740	8.000	25.00
54000	77600	372	535	0.700	8.000	24.70

COMMENTS / NOTES

The above figures are certified chemical and physical test records as contained in the permanent records of the company. We certify that these data are correct and in compliance with specified requirements. No weld repair was performed on this material. The material has not been in contact with mercury while in Gerdau possession. This material, including the billets, was produced (Electric Arc Furnace melted, Continuously cast, and/or Hot rolled) in the USA. CMTR complies with EN 10204 3.1.

BHARKAR YALAMANCHILI
QUALITY DIRECTOR
Phone: (469) 267-1071 Email: Bharkar.Yalamanchili@gerdau.com

YAN WANG
QUALITY ASSURANCE MGR.
Phone: (770) 387 5718 Email: yan.wang@gerdau.com

Customer Name
AMERICAN INSTITUTE OF STEEL

Customer PO#
ENG071822A

Shipper No
2026840

Heat Number
60137693

GERDAU

CERTIFIED MATERIAL TEST REPORT

US-ML-PETERSBURG 2580 HOFHEIMER WAY PETERSBURG, VA 23803-8905 USA	CUSTOMER SHIP TO INFRA METALS CO 1900 BESSEMER RD PETERSBURG, VA 23805-1112 USA	CUSTOMER BILL TO INFRA METALS CO 580 MIDDLETOWN BLVD LANGHORNE PA 19047-1877 USA	GRADE A992/A572-50	SHAPE / SIZE Wide Flange Beam / 14 X 43# / 360 X 64	DOCUMENT ID 0000326614
	SALES ORDER 10774222/000230	CUSTOMER MATERIAL N°	LENGTH 40'00"	PCS 8	WEIGHT 13,760 LB
	BILL OF LADING 1330-0000164215	DATE 08/19/2021	SPECIFICATION / DATE or REVISION ASTM A6-17 ASTM A709-18 ASTM A992-11 (2015), A572-15 CSA G40.21-13 345WM, 50W		HEAT / BATCH 60137693002
CUSTOMER PURCHASE ORDER NUMBER VA-618771					

CHEMICAL COMPOSITION	C (%)	Mn (%)	P (%)	S (%)	Si (%)	Cu (%)	Ni (%)	Cr (%)	Mo(%)	Sn (%)	V (%)	Nb (%)	Al (%)	CEqvA6 (%)
	0.08	0.98	0.010	0.023	0.23	0.33	0.14	0.09	0.040	0.008	0.002	0.015	0.003	0.30

MECHANICAL PROPERTIES	UTS (PSI)	YS (MPa)	UTS (MPa)	Y/T ratio (%)	G/L (inches)	G/L (mm)	Elong. (%)
YS 0.2% (PSI)							
53900	70500	372	486	0.760	8.000	200.0	25.80
53400	69700	368	481	0.770	8.000	200.0	26.30

COMMENTS / NOTES

The above figures are certified chemical and physical test records as contained on file permanent records of the company. We certify that these data are correct and in compliance with specified requirements. No weld repair was performed on this material. The material has not been in contact with mercury while in Gerdau possession. This material, including the billets, was produced (Electric Arc Furnace melted, Continuously cast, and/or Hot rolled) in the USA. CMTR complies with EN 10204 3.1

Bhaskar Yalamanchili
QUALITY DIRECTOR
Phone (469) 267-1071 Email Bhaskar.Yalamanchili@gerdau.com

Alice K. Pitchford
ALICE PITCHFORD
QUALITY ASSURANCE MGR
Phone (804) 524-2851 Email Alice.pitchford@gerdau.com

D.2 Steel Deck Mil Certificates

United States Steel Corporation
Fairless Plant
Fairless Hills, PA 19030-5099

METALLURGICAL TEST REPORT

ORDER: GD76193-01 SALES NUM: 2004298083 PART:
LOAD: 640380 INVOICE: 146-297324 SHIP DATE: 11/18/21
PO NBR: 39575 VEH ID: SSL17 TX8215

--- SOLD TO: ---
EPIC METALS CORP
11 TALBOT AVE
RANKIN, PA 15104-1113

--- SHIP TO: ---
EPIC METALS CORP
C/O PLUM CORP
1534 WOODWARD DR EXT
GREENSBURG, PA 15601-6418

MATL ID: 9751878 HEAT: F24217 TEST OR PIECE IDENTITY: 7777150
GAUGE: .0360 IN WIDTH: 52.7500 IN LENGTH: COIL 1 PC WEIGHT: 23190 LBS
GAUGE: .9144 MM WIDTH: 1339.8500 MM LENGTH: COIL 1 PC WEIGHT: 10518 KGS

SPEC: GALVANIZE CARBON ASTM A653-20 GR 40 APPROVED SS MINIMUM SPANGLE C .10 MAX EXPOSED PRIME SIDE OUT G90 MIN SPANGLE CHEM TREAT DRY NO PICKLE WELDS YS MIN 40 KSI .2% OFFSET TS MIN 55 KSI EL MIN 16% EL DIST 2 INCHES LONGITUDINAL ASTM STD TENS

INSP: 01 MILL INSPECTION RA/SN ALSO RA/LT REPORT CHEMISTRY TENSILE-KSI

HEAT: F24217 - MELTED AND MANUFACTURED IN THE USA
C=.11 MN=.35 P=.009 S=.011 SI=.008 CU=.04 NI=.02 CR=.04 MO=.005 SN=.007 AL=.033 N=.004
V=.000 B=.0001 TI=.001 CB=.000
Chemical analysis in weight %.

TEST RESULT - F24217	VALUE	DIRECTION	LOCATION
Yield strength - 0.2% offset	42.6 KSI	Longitudinal	
Tensile strength (UTS)	55.8 KSI	Longitudinal	
2" Elongation	39%	Longitudinal	
N Value	.208	Longitudinal	
Yield strength - 0.2% offset	42.7 KSI	Longitudinal	
Tensile strength (UTS)	56.3 KSI	Longitudinal	
2" Elongation	39%	Longitudinal	
N Value	.207	Longitudinal	

END OF TEST RESULT DATA

THE MATERIAL CHEMICAL ANALYSIS WAS PERFORMED AT MON VALLEY WORKS, BRADDOCK, PA 15104.
THIS TEST REPORT IS IN COMPLIANCE WITH SPECIFICATION EN 10204 SECTION 4.1 Inspection Certificate 3.1 (Type 3.1)
THIS REPORT SHALL NOT BE REPRODUCED OR ALTERED WITHOUT THE PRIOR WRITTEN APPROVAL OF UNITED STATES STEEL.
TESTING IS CONDUCTED IN ACCORDANCE WITH METHODS ASTM E8, ASTM A370, ASTM E18, ASTM E646, ASTM E415 and JIS Z2241.
TEST DATES FROM RETAINED RECORDS CAN BE PROVIDED UPON CUSTOMER REQUEST.
THE ABOVE RESULTS RELATE ONLY TO THE ITEMS TESTED, CALIBRATED OR SAMPLED.

THIS IS TO CERTIFY THAT THE PRODUCT DESCRIBED HEREIN WAS MANUFACTURED, TESTED AND/OR INSPECTED IN ACCORDANCE WITH THE SPECIFICATION AND FULFILLS REQUIREMENTS IN SUCH RESPECT. PREPARED BY THE OFFICE OF JOSHUA SHAFFER,

QA MANAGER. BY:

DATE:11/18/2021

*0311 NCNNF 0 0 0 0065252016Z JMS 0 0 1 PAGE 1 OF 1

METALLURGICAL CERTIFICATION

2027 East State Highway 198
Osceola, AR 72370
www.bigriversteel.com

Sold To: EPIC METALS
RANKIN, PA 15104

Ship To: EPIC METALS - GREENSBURG P
GREENSBURG, PA 15601

Certificate #: 242819
Load Number: 225054

Material Weight: 23,325 LBS
Heat Number: 20071601

Part No.:

Description: COLD ROLLED GALVANIZED-CARBON STEEL COILS
0.0360X54.4370 (MIN)

Ship Date: 05/15/2020
Material ID: 20071601-05100
Linear Ft: 3,403 ft

Customer PO: 38955
Order #: 36589

Spec: A653 SS GRADE 40

CHEMICAL ANALYSIS

C	Mn	P	S	Si	Al	Cu	Ni	Cr	Mo	Sn	Ti	V	Nb	N	B	Ca	C(eq)
.06	.35	.006	.003	.04	.030	.10	.04	.03	.022	.0045	.001	.002	<.001	.0079	.0001	.0025	.141

BRS RESULTS

0.2% Yield Strength	52 ksi	360 MPa
Direction	Longitudinal	
Tensile Strength	62 ksi	426 MPa
Total Elongation	35 %	35 %
Actual Gauge	0.0370 in	.94 mm
Coating Weight	G90	
Surface Treatment	Chrome 6	

BRS RESULTS

We hereby certify the above is correct as contained in the records of the company. All tests performed according to ASTM standard E8, A370, E18, E415 and E1019.

This product was melted and manufactured in the USA.

The value of the material is not portrayed in this document due to confidential clauses.

Certified By: Denis Hennessy
E-mail: dhennessy@bigriversteel.com
Main: 870-819-3031

Certificate Date: 05/15/2020

D.3 Headed Shear Studs Mil Certificates

4/12/23 Certificate of Compliance 08

VIRGINIA TECH
300 TURNER STREET NW
BLACKSBURG VA
24061

NELSON STUD WELDING, INC.
7900 WEST RIDGE ROAD
P.O. BOX 4019
ELYRIA, OH 44036 2019

Material Description/Part Numbers	Quantity	Heat Number	Lab Number
S3L 3/4 X 5 7/8 MS	700	10792770	
101098138			27326

Nelson Order Number: 1308329 Customer P.O.: P4127752

The product supplied under the contract or purchase order number shown is certified to comply with the latest revision of one or more of the applicable product specifications therein; AWS D1.1, AWS D1.5, AWS D1.6, ISO 13918, BS 5950, ASTM A108, ASTM A29, ASTM A276, ASTM A493, ASTM A1064, ASTM A496, ASTM A479, ASTM A1022.

The chemical analysis reported below was extracted from the certified mill test report. This report will be supplied when specified in the customer order or upon request. The physical properties reported were determined to be in conformance using ASTM A370 testing procedure.

Nelson Stud Welding is an IATF 16949:2016 certified supplier. This material is free from mercury contamination and is RoHS compliant. This product is melted and manufactured in the USA. No weld repair was performed on the raw material or the studs. Parts are manufactured from cold drawn bar.

Grade	C-1015
Heat Number	10792770
Ultimate PSI	78,300
Yield PSI	63,900
% Reduction of Area	62.0
% Elong. (in 2"or4D)	22.0
% Elong. (in 5D)	18.000
Carbon	.160
Manganese	.530
Phosphorous	.007
Sulphur	.010

I hereby certify that the data listed in this Certificate of Compliance is true and correct as as contained in the company test records and that it complies with the specifications shown.

Authorized by: _____

4/12/23

Certificate of Compliance

NELSON STUD WELDING

VIRGINIA TECH
300 TURNER STREET NW
BLACKSBURG VA 24061

56 Pelham Davis Circle
Suite A
Greenville, SC 29615
Tel: 864-967-9267

Material Description/Part Numbers	Quantity	Heat Number	Lot Number
S3L 3/4 X 4 7/8 MS 101098131	80	10785720	27268
S3L 3/4 X 4 7/8 MS 101098131	80	1000215983	27211
S3L 3/4 X 5 3/16 MS 101098011	1040	1000115471	702757

Nelson Order Number: 1308320 Customer P.O.: P4127752

The product supplied under the contract or purchase order number shown is certified to comply with the latest revision of one or more of the applicable product specifications therein; AWS D1.1, AWS D1.5, AWS D1.6, ISO 13918, BS 5950, ASTM A108, ASTM A29, ASTM A276, ASTM A493, ASTM A1064, ASTM A496, ASTM A479, ASTM A1022.

The chemical analysis reported below was extracted from the certified mill test report. This report will be supplied when specified in the customer order or upon request. The physical properties reported were determined to be in conformance using ASTM A370 testing procedure.

Nelson Stud Welding is an IATF 16949:2016 certified supplier. This material is free from mercury contamination and is RoHS compliant. This product is melted and manufactured in the USA. No weld repair was performed on the raw material or the studs. Parts are manufactured from cold drawn bar.

Grade	C-1015	C-1018	1018
Heat Number	10785720	1000215983	1000115471
Ultimate PSI	78,200	75,200	74,000
Yield PSI	64,700	67,200	56,300
% Reduction of Area	61.0	61.0	63.0
% Elong. (in 2"or4D)	23.0	23.0	26.0
% Elong. (in 5D)		20.000	23.000
Carbon	.150	.150	.160
Manganese	.590	.690	.690
Phosphorous	.005	.009	.009
Sulphur	.011	.007	.004
Silicon			.080
Chromium			.090
Nickel			.040
Copper			.120

I hereby certify that the data listed in this Certificate of Compliance is true and correct as as contained in the company test records and that it complies with the specifications shown.

Authorized by: Jan Foster

Appendix E: Reinforcement Calculations

Assuming the specimen to be a deep beam of 6 ft length with pin supports at 1ft from each end.

The beam will have a depth equal to the width of the specimen and width can be average concrete thickness of the specimen

So for Specimen D3.5A-3N-C

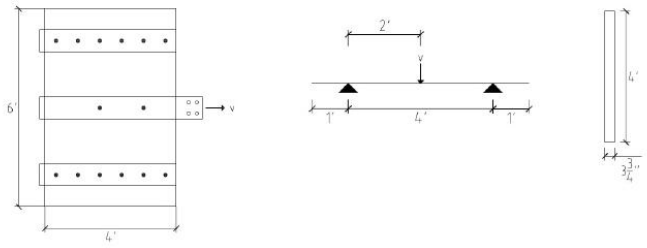

$h := 4\ ft = 48\ in$

$d_d := 3.5\ in$

$d_c := 2\ in$

$b := d_c + \frac{d_d}{2} = 3.75\ in$

The amount of load V appiied will be equal to the predicted strength the headed shear studs in the specimen will take

considering all the nominal properties

$f'_c := 3\ ksi$ $\qquad w := 145\ \frac{lbf}{ft^3}$

$E := w^{1.5} \cdot \sqrt{\frac{f'_c}{ksi}}\ ksi = 3024.2148\ ksi$

Headed shear stud in strong position

$A_s := 0.44\ in^2$ $\qquad f_u := 65\ ksi$

$R_g := 1$ one stud per rib

$R_p := 0.75$ strong position

$n := 2$ no. of headed shear studs to be tested in the specimen

$Q_n := \min\left(\left[\ 0.5 \cdot A_s \cdot \sqrt{f'_c \cdot E}\ \ R_g \cdot R_p \cdot A_s \cdot f_u\ \right]\right)$

$Q_n = 20.9551\ kip$

$V := n \cdot Q_n = 41.9102\ kip$

$M_u := \frac{\frac{V}{2} \cdot 4\ ft}{2} = 41.9102\ kip\ ft$

FLEXTURE REINFORCEMENT

now assuming tesnion yielding

Whitney Stress Block

$c := 1.945\ in$

$\beta_1 := 0.85$

$A_s := 0.31\ in^2$ assuming one #5 bar

$F_y := 60\ ksi$

$d := h - 2\ in = 46\ in$

$C := 0.858 \cdot f'_c \cdot b \cdot c = 18.7741\ kip$

$T := A_s \cdot F_y = 18.6\ kip$

$\varepsilon_c := 0.003$ $\varepsilon_y := \frac{F_y}{29000\ ksi} = 0.0021$ $a := \beta_1 \cdot c = 1.6532\ in$

$\varepsilon_t := \left(\frac{d - c}{c}\right) \cdot \varepsilon_c = 0.068$ $\blacksquare > \varepsilon_y$ steel is yielding

$\blacksquare > \varepsilon_y + 0.003$ Tension controlled

$\Phi := 0.9$ Tension control

$M_n := A_s \cdot F_y \cdot \left(d - \frac{a}{2}\right) = 70.0187\ kip\ ft$

$\Phi \cdot M_n = 63.0169\ kip\ ft$ $\blacksquare > \blacksquare$ M_u OKAY

Provide one #5 bar

REINFORCEMNT TO LIMIT TRANSVERCE CONCRETE CRACKING

$$S_n = k_c \lambda_{LW} b t_e \sqrt{f'_c} + A_v F_{ys} \le (7.5/1000) b t_e \sqrt{f'_c} \qquad (Eq.\ D4.1.1\text{-}1)$$

$f'_c := 3000\ psi$

$\Phi := 0.8$

$k_c := \frac{3.2}{1000}$ For U.S customary units

$\Lambda := 1.0$ For normalweight concrete

$b := 12\ in$

$t_a := d_c + \frac{d_d}{2} = 3.75\ in$

$n_{sc} := \frac{29000\ ksi}{E} = 9.5893$

$t := 0.0359\ in$

$d := 8\ \text{in}$

$e := 3.5\ \text{in}$

$w := 3.5\ \text{in}$

$f := 3\ \text{in}$

$s := 2 \cdot (e + w) + f = 17\ \text{in}$

$t_e := t_a + n_{sc} \cdot t \cdot \frac{d}{s}$

$t_e = 3.912\ \text{in}$

considering 6x6 W1.4 x W1.4 welded wire reinforcemnt

$A_v := 0.028\ \text{in}^2$

$f_{ys} := 60\ \text{ksi}$

$S_n := \min\left(\left[\ k_c \cdot \Lambda \cdot b \cdot t_e \sqrt{\frac{f'_c}{\text{ksi}}}\ \text{ksi} + A_v \cdot f_{ys}\ \frac{7.5}{1000} \cdot b \cdot t_e \sqrt{\frac{f'_c}{\text{ksi}}}\ \text{ksi}\ \right]\right)$

$S_n := \min\left(\left[\ 9.91\ \frac{\text{kip}}{\text{ft}}\ 19.3\ \frac{\text{kip}}{\text{ft}}\ \right]\right)$

$S_n = 9.91\ \frac{\text{kip}}{\text{ft}}$ ▮ < ▮ $\frac{\left(\frac{V}{2}\right)}{4\ \text{ft}} = 5.2388\ \frac{\text{kip}}{\text{ft}}$ OKAY

The shear force in the concrete would be divided on both sides of the headed shear studs so $\frac{V}{2}$ is considered

so providing the following reinforcemnt,

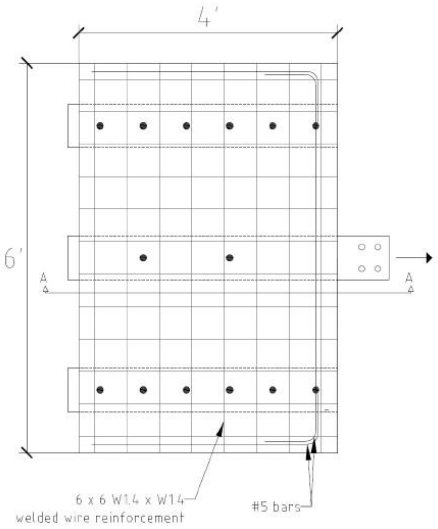

Calculations are all other shear test specimens are given in Table E.1 and E.2

Table E.1 Flexure Reinforcement Summary

Group	F'c, Ksi	Ec, Ksi	Stud Configuration	Predicted force V, Kip	Tension Cord							
					Mu, kip-ft	Whitney Stress block, c, in	β1	b, in	As, in2		Mn, Kip-ft	Mn/Mu
D3.5A-3-C	3	3024.21	Centered	41.910	50.29	1.945	0.85	3.75	No.5	0.31	66.92	1.33
D3.5A-3-2S	3	3024.21	Two studs	72.930	87.52	3.890	0.85	3.75	two No.5	0.62	131.27	1.50
T3.5A-3-S	3	3024.21	Strong	41.910	50.29	1.945	0.85	3.75	No.5	0.31	66.92	1.33
T3.5A-3-W	3	3024.21	Weak	34.320	41.18	1.945	0.85	3.75	No.5	0.31	66.92	1.62
T3.5A-3-2ST	3	3024.21	Two Staggered	65.637	78.76	3.890	0.85	3.75	two No.5	0.62	131.27	1.67
D3.5B-3-C	3	3024.21	Strong	41.910	50.29	1.945	0.85	3.75	No.5	0.31	66.92	1.33
D3.5B-3-2S	3	3024.21	weak	34.320	41.18	3.890	0.85	3.75	two No.5	0.62	131.27	3.19
T3.0A-3-W	3	3024.21	Weak	34.320	41.18	1.945	0.85	3.75	No.5	0.31	48.32	1.17

Table E.2 Shear Reinforcement Summary

Group	F'c, Ksi	Ec, Ksi	Stud Configuration	Predicted force V, Kip	Welded Wire Mesh					
					Av, in2/ft		Sn, Kip/ft	Sn, Kip	Sn/Qn	Sn/(V/2)
D3.5A-3-C	3	3024.21	Centered	41.910	6x6 W1.4 xW.14	0.028	9.91	39.63	0.95	1.89
D3.5A-3-2S	3	3024.21	Two studs	72.930	6x6 W1.4 xW.14	0.028	9.91	39.63	0.54	1.09
T3.5A-3-S	3	3024.21	Strong	41.910	6x6 W1.4 xW.14	0.028	10.07	40.28	0.96	1.92
T3.5A-3-W	3	3024.21	Weak	34.320	6x6 W1.4 xW.14	0.028	10.07	40.28	1.17	2.35
T3.5A-3-2ST	3	3024.21	Two Staggered	65.637	6x6 W1.4 xW.14	0.028	10.07	40.28	0.61	1.23
D3.5B-3-C	3	3024.21	Strong	41.910	6x6 W1.4 xW.14	0.028	9.91	39.63	0.95	1.89
D3.5B-3-2S	3	3024.21	weak	34.320	6x6 W1.4 xW.14	0.028	9.91	39.63	1.15	2.31
T3.0A-3-W	3	3024.21	Weak	34.320	6x6 W1.4 xW.14	0.028	10.07	30.21	0.88	1.76

Since all the values of M_n/M_u and $S_n/(V/2)$ are greater than one so the reinforcement will be sufficient.